The University of Nottingham

UNITED KINGDOM · CHINA · MALAYSIA

Investigating the immunomodulatory properties of *Nippostrongylus brasiliensis; a potential model for Necator americanus*

Tahani H. Alharbi

Supervised by

PROFESSOR AMIR M. GHAEMMAGHAMI

PROFESSOR DAVID I. PRITCHARD

Abstract

Introduction: *Necator americanus* infection is a significant public health concern, particularly in developing countries. Dendritic cells (DCs) are considered as sentinels of the immune system and act as a link between innate and adaptive immune systems. Following antigen uptake in peripheral tissues, DCs migrate into the regional lymph nodes, where they present peptide antigens derived from pathogens into naïve T cells and guide T cell differentiation towards distinct inflammatory or regulatory phenotypes. The fundamental information about how *N. americanus* interfaces with immune cells such as DCs and how *N. americanus* secretions affect DC function and downstream immune responses such as T cell polarisation are still under intensive research. Despite relative successes with the drugs used in treating hookworm infection, there is a high rate of reinfection, and the immune response against hookworms is typically not protective. Therefore, there is a need for a better understanding of the early events involved in the interface between the hookworm and the immune system, which could pave the way for the design of more efficient therapies and vaccines. In a recent study our group have shown exsheathment of *N. americanus* L3 upon interaction with human immature dendritic cells (iDCs). Intriguingly, these cells did not interact with the exposed infective third-stage larvae (L3) cuticle. However, the exact mechanism underlying such immune evasion has remained elusive. Therefore, characterisation of *N. americanus* L3 interaction with DCs could provide invaluable insight into mechanism that underpin *N. americanus* immune evasion and its immune modulatory effects, which could in turn help in the design of new therapeutic strategies. However, a major limitation of working with *N. americanus* is the availability of viable L3, as they require a human host. Thus, identifying other more readily accessible nematode species that can be used as a surrogate model system for studying human immune responses would greatly facilitate such studies. In this study I used *Nippostrongylus brasiliensis* parasite as a laboratory model system to investigate physical interaction of *N. brasiliensis* infective larvae L3 with human DCs and investigated the surface chemical signatures of *N. brasiliensis* L3 cuticle and its sheath to determine any similarities or differences with *N. americanus* and whether such molecular signatures could explain the interaction between larvae and DCs. I also investigated the immune modulatory properties of *N. brasiliensis*

infective larvae L3 and their secretion on DCs phenotype and function as well as how these conditioned DCs could influence downstream T cell polarisation. Furthermore, I identified some sugar moieties in the *N. brasiliensis* L3 secretion similar to those expressed on the surface of larval cuticle and investigated their impact on DCs phenotype and on T cell polarisation.

Results: Our data showed that the exsheathment of *N. brasilienis* L3 upon the interaction with human iDCs with minimal physical interaction between DCs and the exposed cuticles. I then characterised the chemical composition of larvae sheath and cuticle using Time-of-Flight Secondary Ion Mass Spectrometry (TOF-SIMS). Interestingly, our TOF-SIMS data revealed differences between the surface chemistries of larvae sheath and the cuticle which might be of biological relevance and explain immune evasion by larvae cuticle. For example, the surface of larval cuticle contains phosphatidylglycerol which may inhibit aggregation of DC around larval cuticle and support the migration of infective stage, while the surface of larval sheath express heparan sulphate which could result in the aggregation of DCs and diverse immune defences. Our finding confirm that chemical signatures expressed on *N. brasiliensis* larval cuticle and its sheath are similar to those signatures expressed on *N. americanus* larvae previously reported using TOF-SIMS.

Furthermore, DC co-cultured with *N. brasiliensis* larvae cuticle induced a regulatory DC phenotype characterised by significant production of IL-10, suppression of IL12p70 production in response to LPS as well as induction of regulatory T (Treg) cell differentiation in coculture experiments between conditioned DC and autologous naïve T cells. Given the very limited physical interaction between DCs and larvae, it was reasonable to assume that the observed immune modulatory effects are potentially driven by larvae secretion. To test this hypothesis, similar experiments were carried out using larvae secretions which showed similar effect as infective larvae on DC phenotype, function as well as on T cell polarisation. Further characterisation of larval secretions revealed the presence of sugars moieties such as galactose and N-acetylgalactosamine similar to sugars previously observed on the surface of larval cuticle that could impact DC functions. Intriguingly, this finding highlights the potential role of C-type lectin ligands in mediating the observed immune regulatory effects. Together,

these results demonstrate the strong immune regulatory effects of *N. brasiliensis* infective larvae and their secretions on human DCs and T cells as well as the potential role of CLRs in the process.

Galactose and N-acetylgalactosamine (GalNAc) purified from larval secretion induce regulatory DC phenotype as evidenced by a significant downregulation of LPS induced HLA-DR, CD80, CD86 and CD40 expression compared to LPS alone as well as significant upregulation of PDL-1 expression. This was accompanied by significant increase in production of prototypic regulatory cytokine IL-10 and a significant decrease of signature pro-inflammatory cytokine IL-12. Together, these data suggest a regulatory phenotype for DCs treated with galactose and GalNAc in larvae secretions. Furthermore, DCs conditioned with these sugars induced naïve T cell polarisation towards regulatory phenotype that clearly showing the potential role of galactose and GalNAc in immunomodulation.

Conclusion: Taken together, these observations are in line with previous observations showing similar effects as *N. americanus*, highlighting the suitability of *N. brasiliensis* as a model system for investigating early events between human DCs and infective hookworm larvae. In addition, our findings show the potential immunomodulatory properties of *N. brasiliensis* infective larvae and their secretion in regulating DCs phenotype and skewing immune responses towards regulatory phenotypes. It also provides in understanding of how some sugars present in larval secretion have the ability to modulate immune system. This understanding could pave the way for utilising parasite-derived products in the development of potent treatment for autoimmune or autoinflammatory conditions.

Publication

Nippostrongylus brasiliensis larvae induce a regulatory phenotype in human dendritic cells that support Treg differentiation; the critical role of monosaccharides (in preparation).

Tahani Alharbi, David Pritchard, Claire Ciancia, Nicola Britton, Anne Marie Donachie, Amir M Ghaemmaghami.

Presentations

1. Immunomodulatory properties of hookworms on dendritic cells (poster), Life Sciences Symposium, 24th July 2019, University of Nottingham, UK.
2. Immunomodulatory properties of hookworms on dendritic cells (poster), British Society for Immunology, 4th December 2019, Liverpool, UK.
3. Immunomodulatory properties of *Nippostrongylus brasiliensis* larval secretion on human dendritic cells (Talk), Life Sciences Symposium, 22nd July 2020, University of Nottingham, UK.
4. Immune modulatory properties of hookworms on human dendritic cells using *Nippostrongylus brasiliensis* as a model (poster), British Society for Immunology, 30th November 2021, Edinburgh, UK.

Dedication

To my father’s soul

Who wished to see my thesis

Acknowledgements

First and foremost, I would like to praise and thank God, the Almighty and Merciful, for His countless blessings given to me throughout my studies to complete my PhD journey.

Second, I would like to express my sincere gratitude and greatest thanks to my supervisor, Prof. Amir Ghaemmaghami, for everything he has taught me; for his continuous guidance and the immense knowledge provided to me throughout my PhD study. I would also like to thank Prof. David Pritchard for his great support and helpful suggestions for my research.

My appreciation extends to our collaborators at the University of Glasgow, Prof. Maizels, Claire Ciancia, Nicola Britton, and Anne-Marie Donachie, for their efforts in supporting parasites despite very difficult times. Special thanks to Dr. David Scurr, Dr. Nichola Starr, and Dr. Stefanie Kern for their help with TOF-SIMS measurements. Further great thanks to Dr. David Onion and Miss. Nicola Croxall for their assistance with flow cytometry.

Words could never express how grateful I am to my husband Bandar for his incredible support and for staying by my side, and for my children (Abdullah and Laith)—I could not have enjoyed my PhD without them being with me throughout this journey.

My deepest thanks go to my mother for always encouraging me towards my goals and achievements. I have gratitude for my brothers and sisters for their endless love, for contributing their support, and for believing in me during my PhD journey.

I would like to thank Albaha University and the Saudi Ministry of Higher Education for sponsoring my scholarship to achieve this degree.

Table of contents

List of figures

Chapter 1

Chapter 2:

Chapter 3

Chapter 4

Chapter 5:

List of tables

Chapter 3

Abbreviations

AChE acetylcholinesterase

AhR Aryl hydrocarbon receptor

APCs Antigen presenting cell

BSA Bovine serum albumin

Con-A concanavalin A

CpG Cytidine-phosphate guanosine

CRD carbohydrate recognition domain

CTL C-Type lectins

DAMPs Damage-associated molecular patterns

DBA Dolichos biflorus agglutinin

DCs Dendritic cells

DC-SIGN Dendritic cell-specific intercellular adhesion molecule-3-grabbing non-integrin

DNA Deoxyribonucleic Acid

dsRNA double-stranded RNA

ER Endoplasmic reticulum

FBS Foetal bovine serum

FOXP3 Forkhead box P3

GalNAc N-acetylgalactosamine

GM-CSF Granulocyte macrophage colony-stimulating factor

GST glutathione-S-transferases

HDM House dust mite

HEPES Hydroxy-ethyl-piperazine

HLA Human leukocyte antigen

IDO Indoleamine 2,3-dioxygenase

IFN-γ Interferon gamma

IL Interleukin

iL3 infective stage larvae

IRAK Interleukin 1 receptor associated kinase

IRFs interferon regulatory factors

LAL Limulus amoebocyte lysate

LRR leucine-rich repeats

LPS Lipopolysaccharide

MACS Magnetic cell separation system

MAPKs mitogen-activated protein kinases

mDCs Myeloid dendritic cells

MFI Median fluorescence intensity

MHC major histocompatibility complex

MR Mannose receptor

MRI magnetic resonance imagining

MS multiple sclerosis

MVA multivariate analysis

MyD88 myeloid differentiation 88

NIF neutrophil inhibitory factor

NK Natural Killer

NF-κB nuclear factor kappa-B

PAMPs Pathogen associated molecular patterns

pDCs Plasmacytoid dendritic cells

PBA Phosphate-buffered albumin

PBMCs Peripheral blood mononuclear cells

PBS Phosphate buffer saline

PCA principal component analysis

PCR Polymerase chain reaction

PD-L Programmed death ligand

PNA peanut agglutinin

PRRs Pattern recognition receptors

RCA Ricinus communis agglutinin

RNA Ribonucleic Acid

ROS reactive oxygen species

SBA soybean agglutinin

SDS-PGE Sodium dodecyl-sulfate polyacrylamide gel electrophoresis

SOD superoxide dismutase

ssRNA single-stranded RNA

TAK transforming growth factor-activated protein kinase

TCR T cell receptor

TGF-β transforming growth factor β

Th T helper

TIR Toll-interleukin-1 receptor

TLRs Toll like receptors

TNF Tumour necrosis factor

TOF-SIMS time-of-flight secondary ion mass spectrometry

TRAF Tumour necrosis factor receptor-associated factor

TRIF Toll-interleukin-1 receptor-domain-containing adaptor inducing IFN-β

T-reg T regulatory cell

UEA Ulex europaeus agglutinin

WCA water contact angle

WGA wheat germ agglutinin

WHO World Health Organization

Chapter 1:

General introduction

1.1 Introduction

1.1.1. Human immune system

The human environment contains many microbes that are either pathogenic or non-pathogenic. The human body is continuously exposed to these foreign substances, resulting in the eradication of the organisms via a complex protective mechanism known as the immune system. The immune system is a fundamental defensive system that contains an intricate network of cells and humoral factors (e.g., proteins and enzymes) that are used to identify and eradicate these organisms and maintain body's homeostasis [1,2]. These immune cells are distributed in different areas of the human body, including the skin, blood, spleen, mucosal barriers, thymus, lymph nodes, and bone marrow. The human immune system can be categorised into two components based on their reaction time, memory and specificity: the non-antigen-specific immune component, known as innate immunity, and the antigen-specific immune component, which is also referred to as adaptive immunity. Both parts of the immune system work closely together to establish a protective spectrum of immune responses against invading pathogens while maintaining tolerance to self-antigens [3].

1.1.1.1. Innate immunity

Innate immunity, also known as natural immunity, provides the host with immediate protection against microbial invasion. It is considered the first line of defence against invading pathogens that enter the human body and may lead to tissue damage. Innate immunity provides a non-specific immune response which acts by removing microbes and stopping their attempt to invade the host tissue. This system has different components that work together to establish an initial protective mechanism [4]. These components can be divided into physical and chemical barriers (e.g., epithelial tissue present in the skin, and respiratory and gastrointestinal [GI] tracts), soluble plasma proteins, such as cytokines of the complement system, and leukocyte, such as neutrophils, macrophages, natural killer (NK) cells, and dendritic cells (DCs) [5,6]

Neutrophils originate from myeloid progenitors in the bone marrow, while macrophages are differentiated from monocytes that are generated from myeloid progenitors in the bone marrow (Fig. 1.1). Neutrophils are found in peripheral blood in large numbers and can quickly migrate to any injury

site whereas microphage can be found in all tissues throughout the human body such as spleen, lymph nodes, and lung, where they act as phagocytic cells. Under infectious and inflammatory conditions, these cells are involved in the eliminating invading pathogens through a process known as phagocytosis [7,8]. Phagocytosis is the process of engulfing and internalising foreign bodies into intracellular vesicles to neutralise and destroy them. It begins with the migration of phagocytes through the extracellular matrix towards the site of infection in response to chemokines which are secreted within the infected or injured tissue. Once the cells reach the infected tissue, the encounter between the neutrophils and macrophages and the invading pathogen, likely to be already opsonised with complement factors results in extension of phagocytic cell plasma membrane around invading pathogen forming of pseudopodia. These pseudopodia enhance internalisation and engulfment of the pathogen into a phagocytic vesicle—known as a phagosome—which then fuses with an intracellular lysosome to form a phagolysosome. Within the phagolysosome, the invading pathogen is destroyed by enzymes and substances such as reactive oxygen species (ROS) within the phagolysosome [9].

Another important component of innate immunity are the dendritic cells (DCs). DCs are specialised antigen presenting cells that act as sentinels of the immune system that are highly efficient in antigen uptake and presentation to T cells; therefore, they play a key role in linking innate and adaptive immunity [10]. These cells are originated from the bone marrow and can be found in many organs such as the peripheral blood, barrier tissues, lymph nodes and spleen [11].

1.1.1.2. Adaptive immunity

Adaptive immunity, also defined as acquired immunity and is responsible for developing a specific immune response against a targeted pathogen. This antigen-specific immunity, as specified by the name, demonstrates specific affinity for the evoking pathogen in combination with the development of a memory that has an expedited and potent response against specific pathogens in case of re-exposure. Lymphocytes are immune cells involved in mediating the immune response in adaptive immunity. Lymphocytes originate from lymphoid progenitor cells that arise from the bone marrow and become differentiated in primary lymphoid organs (thymus and bone marrow). In the thymus, lymphoid cells differentiate into T cells whereas in the bone marrow they become B cells. After

differentiation, they migrate into secondary lymphoid organs, such as lymph nodes and the spleen, where they provide two types of immune response: cellular immunity, provided by T cells, and antibody-mediated immunity, provided by B cells [12,13].

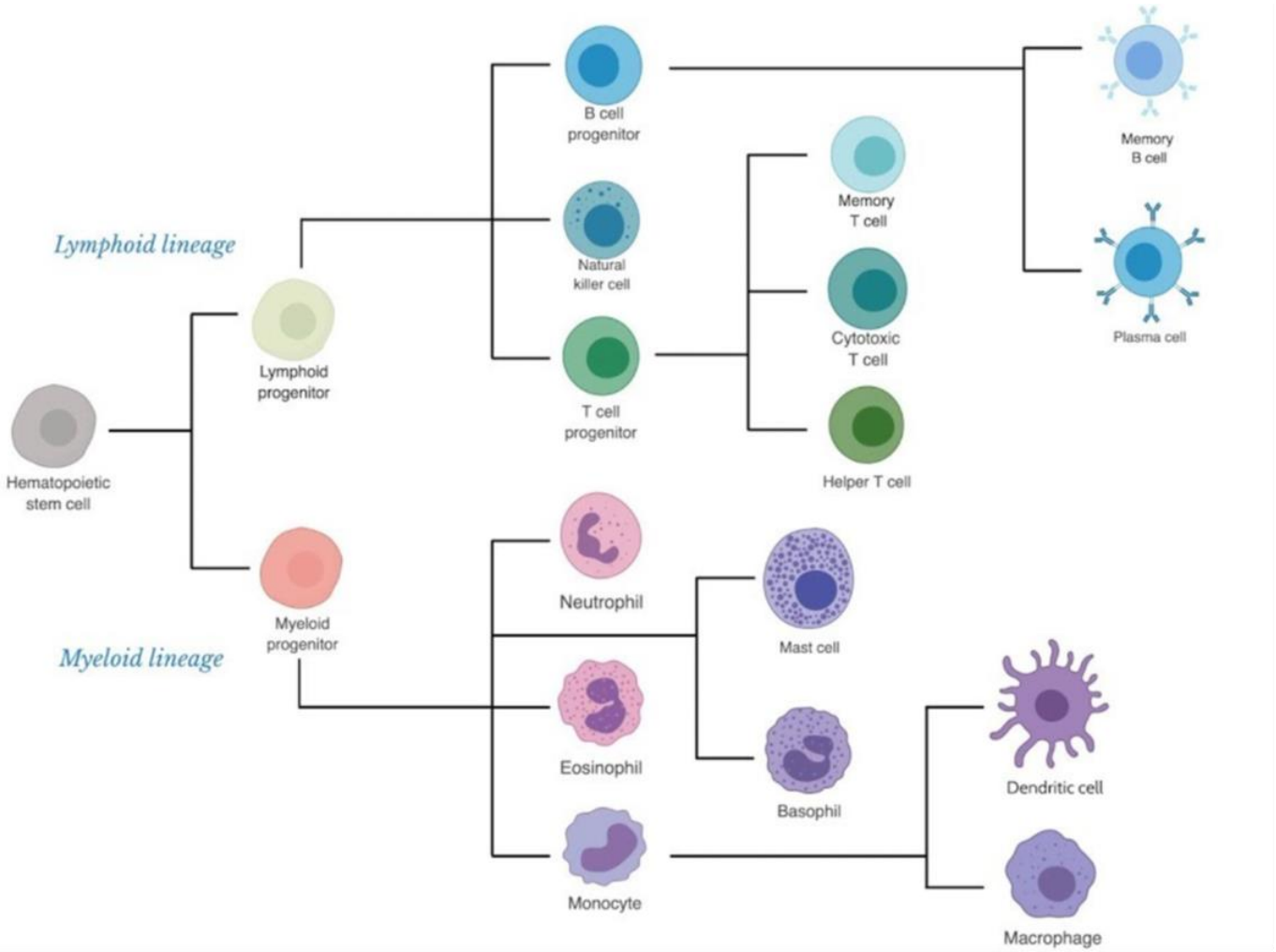

Figure 1.1: Immune-cell lineages derived from bone marrow. Bone marrow-derived cells give rise to myeloid and lymphoid progenitor cells. Leukocytes (e.g., basophils, eosinophils, neutrophils, and monocytes) are differentiated from myeloid cells; T cells, B cells, and natural killer cells originate from the lymphoid linage. Dendritic cells (DCs) originate from lympho-myeloid progenitors and can be differentiated from peripheral blood monocytes, similar to macrophages. Adopted from [12]

1.1.2. Antigen-presenting cells act as a link between the innate and adaptive immune systems

While DCs are major antigen-presenting cells (APCs) that act as a link between the innate and adaptive immune systems, other cell types such as macrophages, and B cells can also act as antigen presenting cells. These cells are sentinels of the immune system; they present antigens to T cells in the context of major histocompatibility complex (MHC) molecules. DCs are considered the most potent APC of the immune system as they can migrate to lymph nodes to promote primary activation of naïve T cells [14-16].

1.1.2.1. Dendritic cells

DCs arise from haematopoietic precursors in the bone marrow that gives rise to both lymphoid and myeloid progenitor precursors. DCs can be divided into two subsets namely plasmacytoid DCs (pDCs) and myeloid DCs (mDCs) based on their origin and function. Both populations are characterised by phenotypic markers and can be found in lymphoid tissue (e.g., spleen and blood) and non-lymphoid tissue (e.g., lung and skin). pDCs are characterised by the expression of CD123 (IL-3R), CD303 (BDCA-2), and CD304 (BDCA-4) antigens and the absence of CD11c expression. In contrast, mDCs—also known as classical or conventional DCs (cDCs)—are characterised by the expression of CD11c, CD11b, CD13, and CD33 [17-19]. DCs circulate in the blood or reside in barrier tissues as immature cells characterised by low-level expression of MHC II and co-stimulatory molecules, including CD80, CD86, and CD40. Once DCs encounter a pathogen, they are activated and matured, resulting in upregulation of MHC II and co-stimulatory molecule expression; this enhances the migration of activated DCs through lymph vessels into lymph nodes to present antigens to naïve T cells [20].

1.1.2.1.1. Antigen recognition and presentation by dendritic cells

DCs can monitor the microenvironment against danger signals using pattern recognition receptors (PRRs) [21]. Foreign antigens and tissue damage can be recognised by DCs through either pathogen-associated molecular patterns (PAMPs) or damage-associated molecular pattern (DAMPs). PAMPs are conserved molecular signatures of pathogens, including viruses, bacteria (or their products), fungi, and protozoa, while DAMPs are molecules such as intracellular protein, DNA or RNA that are

constitutively released by dying/damaged tissues or tumour cells [22,23]. Once DCs capture foreign antigens via their PRRs, they begin to process the antigens into small peptides either by the endosomal pathway or proteolytic pathway to initiate an adaptive immune response [24]. These two pathways involve processing antigens from different compartments. For example, exogenous antigens (i.e., antigens present in the extracellular environment) are processed and degraded into small peptides through the endosomal pathway; the ingested antigens enter a phagosome which then fuses with a lysosome to form a phagolysosome, which breaks the antigens down into small peptides. The phagolysosome delivers the peptides to MHC II molecules that are synthesised in the endoplasmic reticulum (ER). Peptides that bind to MHC II will then be transported to the cell surface to be presented to $CD4^+$ T cells upon DCs migration to the T cell area of a draining lymph node. In contrast, endogenous antigens (i.e., antigens present in the intracellular environment) are processed through the proteolytic pathway. After antigen uptake, the antigen enters a proteasome which degrades it into peptides; the peptides produced by proteasomal digestion are attached to MHC I molecules and transported to the cell surface for presentation to $CD8^+$ T cells [25-28].

1.1.2.1.2. Dendritic cell receptors involved in pathogen recognition

DCs are responsible for continuously sensing their surroundings using PRRs that are capable of recognising PAMPs and DAMPs. PRRs can be divided into several families, including Toll-like receptors (TLRs), C-type lectin receptors (CLRs), Nod-like receptors (NLRs), and RIG-I-like receptors (RLRs) [29]. Each receptor is essential for identifying a group of molecular signatures which are found on pathogen but not host cells. (Fig. 1.2) shows a summary of main extra and intra cellular PAMP and their PRRs counterparts [30].

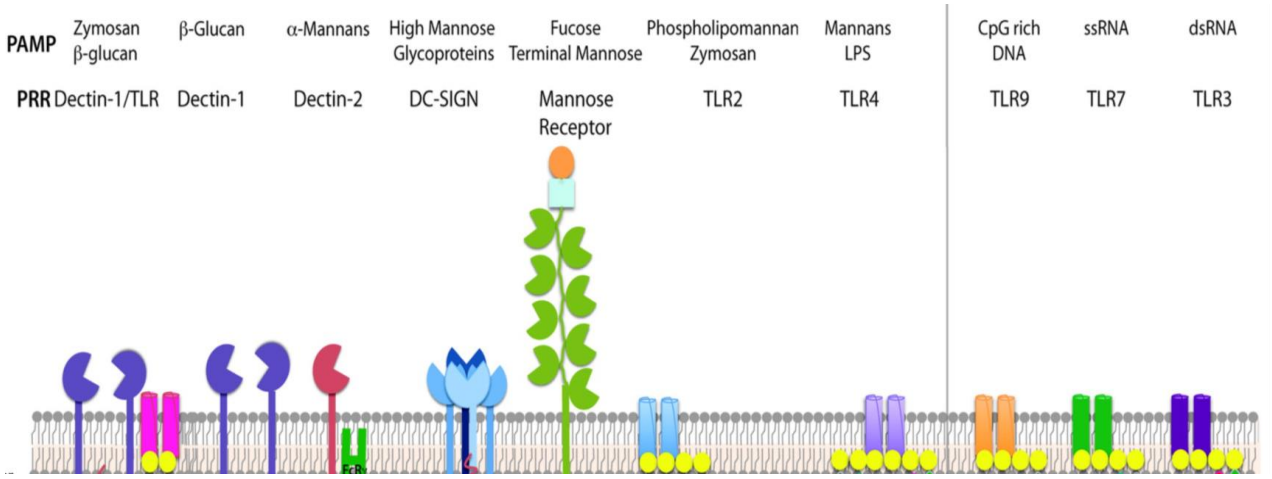

Figure 1.2: Families of pattern recognition receptors (PRRs) expressed on DCs and their ligands. Toll-like receptors (TLRs) and C-type lectin receptors (CLRs) recognise different antigenic determinants to promote cell activation. Adopted from [31].

1.1.2.1.2.1. Toll-like receptors in pathogen recognition

1.1.2.1.2.1.1. Classification of Toll-like receptors

TLRs are a type of PRR that play a fundamental role in recognising the components of PAMPs and DAMPs leading to activation of DCs and triggering a plethora of signalling pathways. TLRs in human comprises of 10 members (TLR1–10) [32]. TLRs are categorised into two groups depending on their localisation and binding ligands (Fig. 1.3). The first group consist of TLR1, TLR2, TLR4, TLR5, TLR6, and TLR10, which are expressed on the cell surface. Each receptor in this family can recognise and bind to specific PAMPs derived from different pathogens [33]. For example, TLR2 recognises a wide range of PAMPs, such as lipopeptides derived from bacteria, zymosan derived from fungi, tGPI-micin derived from parasites, and haemagglutinin protein derived from the measles virus. There are also instances that two different TLRs are involved in recognition of a group of PAMPs. For example, TLR2 and TLR1 recognise triacylated lipopeptides derived gram-negative bacteria and mycoplasma, while TLR2 and TLR6 bind to diacylated lipopeptides derived from gram-positive bacteria and mycoplasma. TLR4 is involved in the recognition of bacterial lipopolysaccharide (LPS) [34], whereas TLR5 recognises bacterial flagellin [35]. TLR10 on the other hand acts together with TLR2 to

recognise ligands from *Listeria* and can also respond to influenza A virus infection [36,37]. The second group comprises TLR3, TLR7, TLR8, and TLR9 thar are expressed in intracellular compartments, such as the ER, endosomes, and lysosomes [33]. TLR3 can recognise double-stranded RNA (dsRNA) [38,39] while TLR7 and TLR8 recognise single-stranded RNA (ssRNA) [40,41]. Cytidine-phosphate guanosine (CpG) is considered as ligand for TLR9 [35].

Structurally, TLRs consist of two domains: the extracellular binding domain and the cytoplasmic signalling domain, also known as the Toll-interleukin-1 receptor (TIR). The extracellular binding domain contains leucine-rich repeats (LRRs) that are involved in the recognition of PAMPs, while the TIR domain contains adaptor molecules responsible for downstream signal transduction [42]. Adaptor molecules involved in intracellular signal transduction for TLRs include myeloid differentiation 88 (MyD88), MyD88 adaptor-like protein (Mal, also known as TIR domain-containing adaptor protein [TIRAP]), TIR-domain-containing adaptor-inducing IFN-β (TRIF), TRIF-related adaptor molecule (TRAM), and sterile-alpha- and armadillo-motif-containing protein (SARM) (Fig. 1.4) [43]. Following interaction of TLRs with their respective ligands these adaptor molecules are capable of inducing signalling pathways in by activating nuclear factor kappa-B (NF-κB) that in turn activates additional signalling components, including mitogen-activated protein kinases (MAPKs) and interferon regulatory factors (IRFs). The activation of MAPKs results in the production of pro-inflammatory cytokines, while IRFs induce the production of type I interferons (IFNs) [44,45]. All TLRs depend on the MyD88 pathway for signal transduction, except for TLR3, which depends on TRIF. However, some TLRs utilise more than one adaptor molecule for activation of downstream signalling pathways, such as TLR-4, which has four different adaptor molecules for signal triggering (MyD88, TRIF, Mal, and TRAM), while TLR2/TLR1 and TLR2/TLR6 require Mal with MyD88 for signal stimulation [46-51].

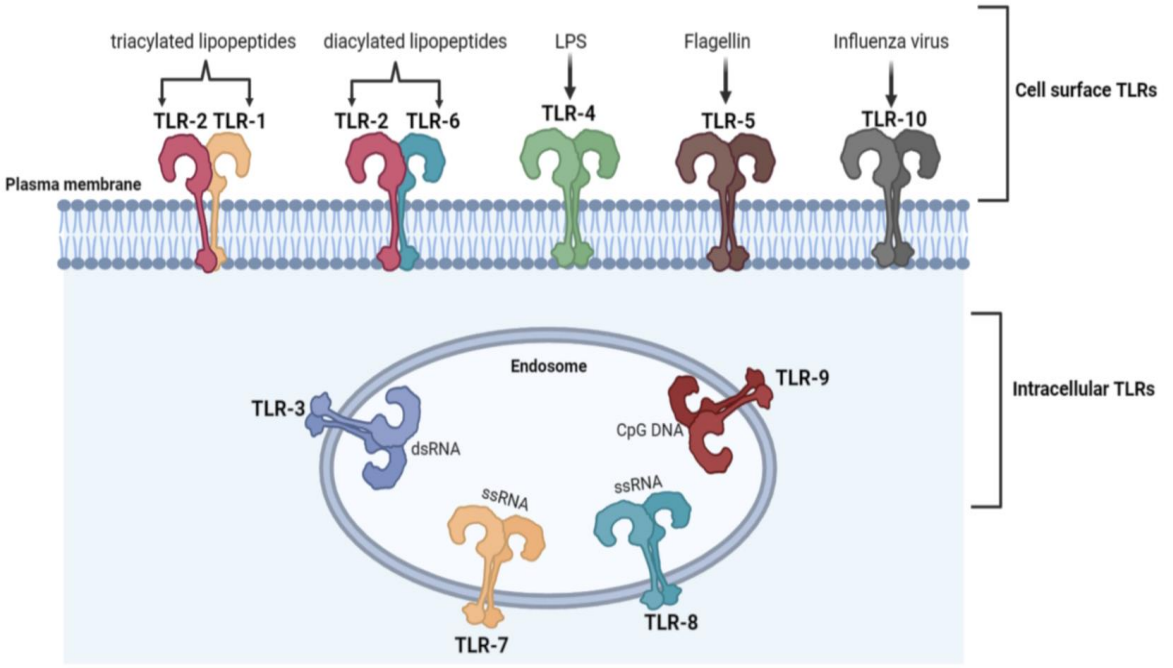

Figure 1.3: Families of TLRs and their corresponding ligands. TLRs can be divided into the cell-surface family (TLR1, TLR2, TLR4, TLR5, TLR6 and TLR10) and intracellular family (TLR3, TLR7, TLR8, and TLR9). Each TLR binds to a specific ligand to be activated.

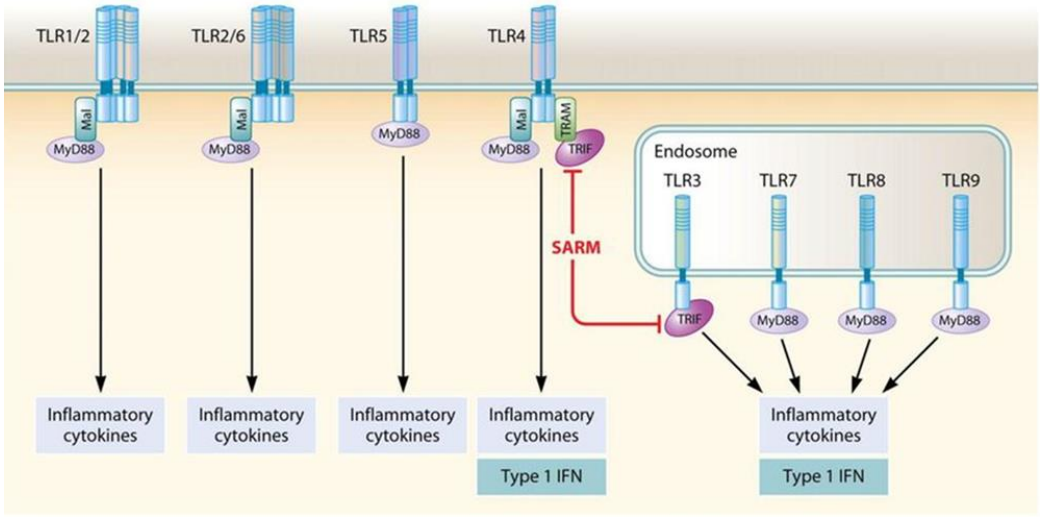

Figure 1.4: TLRs and their intracellular domains containing adaptor molecules. TLR1/2 and TLR2/6 depend on MyD88 and Mal as adaptor molecules, whereas TLR5, TLR7, TLR8, and TLR9 depend only on MyD88. TLR4 utilises four adaptor molecules (MyD88, Mal, TRAM and TRIF), while TLR3 depends only on TRIF. Adopted from [43].

1.1.2.1.2.1.2. Toll-like receptors mediate intracellular signalling pathways in dendritic cells

1.1.2.1.2.1.2.1. MyD88-dependent pathway

Upon engagement of TLRs, such as in the case of TLR4 with an appropriate PAMP, the MyD88 adaptor molecule promotes the recruitment of IL-1 receptor (IL-1R)-associated kinase (IRAK) members, including IRAK1 and IRAK4, resulting in the formation of the Myddosome [52] (Fig. 1.5). During formation of the Myddosome, IRAK4 sequentially activates IRAK1, resulting in the phosphorylation of IRAK1 [53], which leads to its dissociation from MyD88 [54]. IRAK1 activation induces activation of TNF receptor-associated factor 6 (TRAF6), which acts as a ubiquitin ligase (E3) [55]. TRAF6, along with enzyme complex E2, promotes polyubiquitination of K63 on TRAF6 and on another protein complex called transforming growth factor-activated protein kinase 1 (TAK1). Further step is the recruitment of TAK1-binding protein 2 (TAB2) and TAB3 to ubiquitinated leading to TAK 1 activation [56]. TAK1 then stimulates two different pathways involved in the activation of the IκB kinase (IKK) complex and MAPK pathway [57]. The IKK complex is composed of IKKα, IKKβ, and the NF-κB essential modifier (NEMO, also called IKKγ). TAK1 binds to the IKK complex, resulting in activation of IKKβ; activation of IKKβ induces phosphorylation of IκB, which is then ubiquitinated and degraded by the proteasome to allow activation and translocation of NF-κB to the nucleus, where it enhances pro-inflammatory cytokine production [58-61].

1.1.2.1.2.1.2.2. TRIF-dependent pathway

The TRIF-dependent pathway initiates downstream signalling through the binding of TRIF (associated with TRAM in case of TLR4) to either TRAF3 or TRAF6. TRIF interaction with TRAF6 and subsequent TRAF6-mediated recruitment of receptor-interacting protein 1 (RIP 1) results in the activation of TAK1. Activation of TAK1 leads to NF-κB activation through the IKK complex and activation of the MAPK pathway, thereby inducing the production of inflammatory cytokines [62]. In the case of TRIF interaction with TRAF3, the latter recruits the IKK-related kinases TBK1 (TRAF-binding kinase 1) and IKKε, which then induce phosphorylation and subsequent translocation of IRF3 to the nucleus where it induces expression of type I IFN genes [63] (Fig. 1.5).

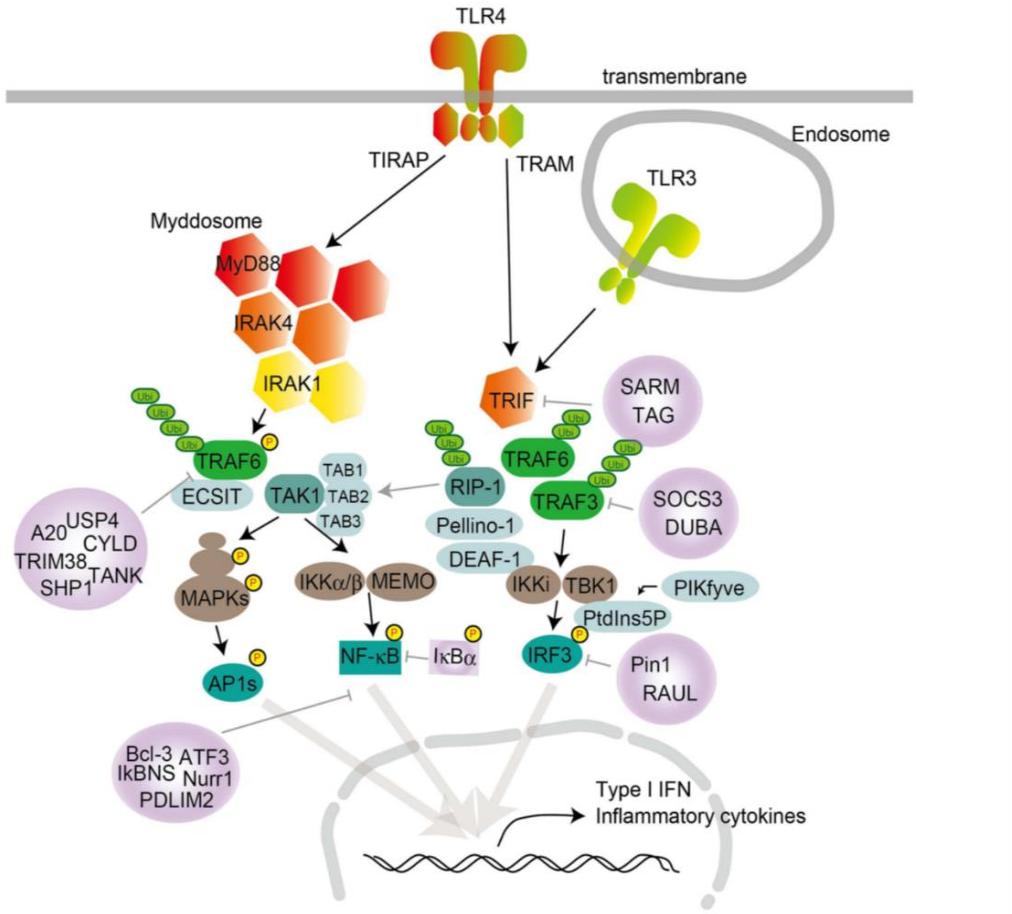

Figure 1.5: TLR intracellular signalling. TLR4 localises to the cell surface while TLR3 localises in the endosomal compartment. MyD88 and TRIF are the two major adaptor molecules that initiate signalling in TLRs. TLR4 can activate both MyD88 and TRIF pathways, while TLR3 activates only TRIF. In the MyD88-dependent pathway, upon engagement of TLR4 with the appropriate pathogens, TIRAP mediates signalling from TLR4 to MyD88. Activation of MyD88 leads to the recruitment of IRAK1 and IRAK4, resulting in the formation of the Myddosome. Subsequent activation of IRAK1 induces activation of TRAF6, which leads to activation of TAK1, which further activates the IKK complex and MAPKs, promoting the production of inflammatory cytokines. In the MyD88-independent pathway (TRIF-dependent pathway), TRAM mediates signalling from TLR4 to the TRIF adaptor protein, resulting in the activation of TRIF, which leads to recruitment of TRAF6 and TRAF3. TRAF6 then recruits RIP-1, which induces activation of the TAK1 complex and MAPK, resulting in activation of NF-κB to induce the production of pro-inflammatory cytokines. TRAF3 recruits TBK1,

which induces activation of IRF3. IRF3 induces expression of type-I IFN genes and contributes to inflammatory responses. Adopted from [33].

1.1.2.1.2.2. C-type lectin receptors in pathogen recognition

CLRs are another family of PRRs that are responsible for pathogen recognition; they are involved in the recognition of glycosylated antigens. This family of PRRs contains a carbohydrate recognition domain (CRD) that is essential for carbohydrate ligand binding, a process that also requires calcium (Ca^{2+}) ions [64,65]. Ca^{2+} ions are crucial for the binding of CRDs to their corresponding monosaccharide ligands. CLRs can be found as cell surface receptors or soluble receptors, depending on their role [66,67].

An example of a CLR is the mannose receptor (MR, also known as CD206). MR is a type I transmembrane CLR, and it contains both an extracellular and intracellular domain. The extracellular region of MR contains eight CRDs involved in the recognition of monosaccharides (e.g., mannose moiety antigens) in the presence of Ca^{2+}. The intracellular region contains a tyrosine-based motif that plays a role in receptor internalisation and recycling. MR is an endocytic receptor that mediates the internalisation and release of binding ligands into endosomal compartments via the clathrin-dependent pathway. The receptors are then recycled and returned to the cell surface to mediate further ligand internalisation [68-70]. DC-ICAM3-grabbing non-integrin (DC-SIGN, also known as CD209), is another example of a CLR. DC-SIGN is a type II transmembrane receptor; its extracellular domain contains a single CRD, while its intracellular domain contains an internalisation motif. DC-SIGN is involved in the recognition of ligands that contain mannose and fucose. Like MR, it can be involved in the internalisation of binding ligands through the clathrin-dependent pathway and functions as an endocytic receptor [71,72].

1.1.2.1.2.2.1. C-type lectin receptors mediate intracellular signalling in dendritic cells

Intracellular signalling initiated by activated CLRs is dependent on carbohydrate residues expressed on pathogens [73]. For example, the intracellular domain of DC-SIGN is bound to the adaptor protein leukocyte-specific protein 1 (LSP-1), which is associated with a signalosome complex consisting of CNK1, KSR1, and RAF1. Upon recognition of mannose moieties, such as ManLam expressed by

mycobacterium or HIV-1, RAF-1 is activated and subsequently phosphorylated. The activation of RAF-1 results in the acetylation and phosphorylation of the p65 subunit. This pathway is crucial for DC-SIGN to modulate TLR-induced NF-κB activation, which results in modulation of immune responses [74,75]. Upon recognition of fucose on *Helicobacter pylori*, the signalosomes dissociate from the intracellular domain of DC-SIGN, while LSP-1 remains attached. This modulates TLR4-induced NF-κB activation and leads to suppression of the pro-inflammatory responses mediated by TLR4 [76].

1.1.2.1.3. Immune modulatory properties of dendritic cells

DCs use various pathways to fine-tune immune responses and thus play a potential role in determining the outcome of immune responses against different antigens and pathogens [77,78]. For example, the crosstalk between CLRs and PRRs (such as TLRs) represents an immunomodulatory pathway that can guide the DC response. One scenario involving this pathway is the ligation of MR to modulate activation of TLR4, which results in modulation of the aryl hydrocarbon receptor (AhR) and indoleamine-2,3-dioxygenase (IDO) [79,80]. Other scenarios, as mentioned previously, include the ligation of mannose or fucose with DC-SIGN to modulate activation of TLR4 in DCs and suppression of pro-inflammatory responses [75,76]. Furthermore, DCs can use immunomodulatory enzymes, such as IDO, to modulate the immune response. IDO is a rate-limiting enzyme that catabolises tryptophan into kynurenine metabolite, which acts as a ligand to activate AhR to promote metabolic changes in the cells [81,82]. Under inflammatory conditions, IDO activity contributes to limiting the inflammatory response by increasing consumption of tryptophan in the microenvironment, increasing kynurenine metabolite levels to attenuate inflammation caused by infectious microorganisms [83,84]. For example, activated DCs induce high IDO enzyme levels to control inflammatory responses and suppress pathogen replication [85-87]. Some pathogens, such as parasites, can modulate IDO activity to promote their survival inside a host [88].

1.1.3. T-cell subtypes

T cells originate from the lymphoid lineage in bone marrow and migrate to the thymus for maturation and positive selection. After T cells undergo positive selection, they migrate through the bloodstream into lymph nodes, where they reside to support the initiation of the adaptive immune response [89]. T cells can be classified into two main types: $CD4^+$ T cells, also known as T-helper (Th) cells; and $CD8^+$ T cells, also known as T-cytotoxic (Tc) cells. $CD4^+$ T cells can be categorised into different subtypes: Th1 Th2, Th17, Th9, T-follicular (Tfh) and regulatory (Treg). Each type of Th cell has a role in the immune response and can be recognised based on its cytokine secretion profile and expression of transcription factors (Fig. 1.6) [90].

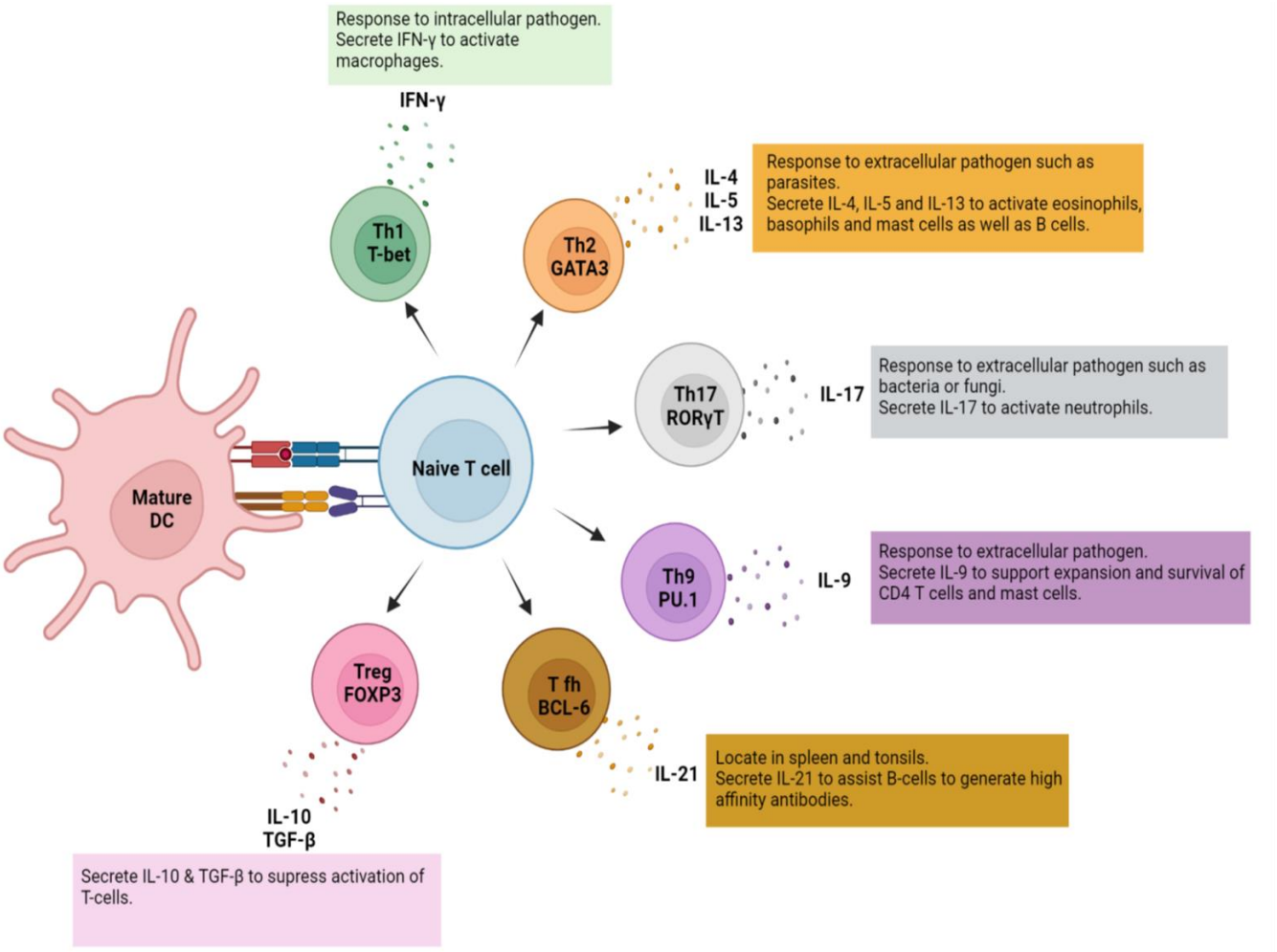

Figure 1.6: Subsets of T-helper cells. Each type of cell has a specific function in the immune response and can be identified by its cytokine production and transcription factor expression.

1.1.4. Helminthic parasites overview

The term helminth generally refers to parasitic worms, which can be classified into four phyla: flatworms (Platyhelminthes), including trematodes (flukes) and cestodes (tapeworms); hairworms (Nematomorpha); thorny-headed worms (Acanthocephala); and roundworms (Nematoda) [91,92]. Nematodes can be classified into five clades (I–V) based on morphological similarities between species within each subgroup, in addition to similarities in their DNA and ribosomal RNA sequences (Fig. 1.7) [93, 94].

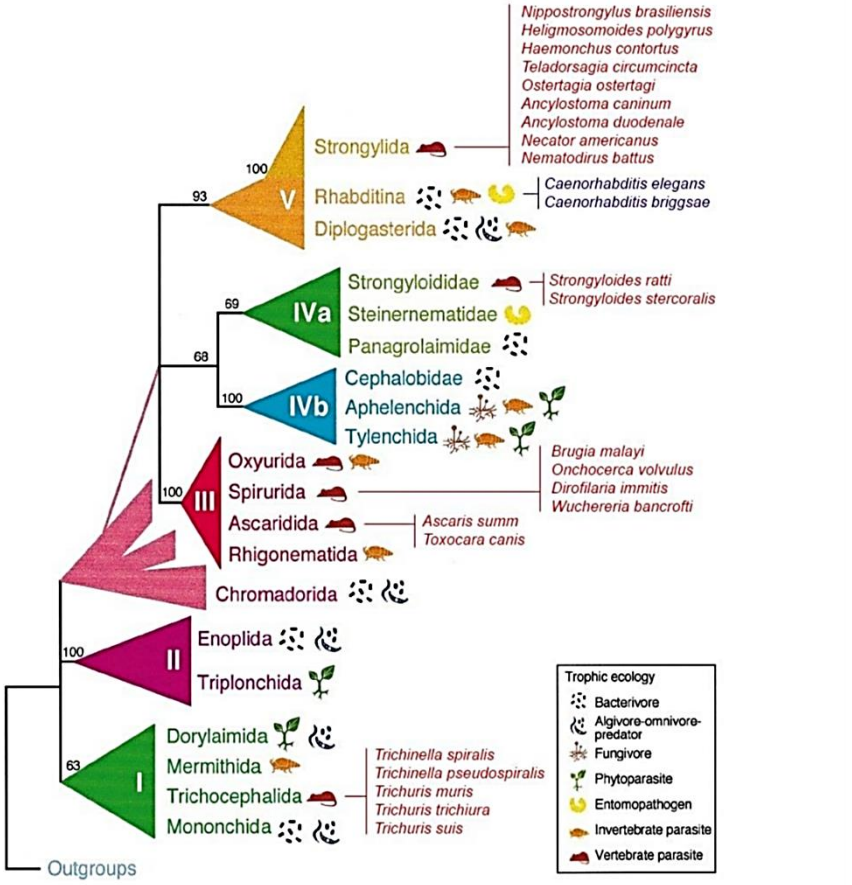

Figure 1.7: The classification of the phylum Nematoda. Nematodes are classified into five clades (I–V) based on their DNA and RNA sequences. *Necator americanus* and *Nippostrongylus brasiliensis* belong to the same clade. Adopted from [93].

As shown in the illustration in Figure 1.7, human hookworm parasites such as *Necator americanus* belong to the Strongylida family (clade V). *Nippostrongylus brasiliensis*, which is commonly used in research as a model system, also lies in the same clade as *N. americanus*, showing high similarity in the genomic sequences of theses nematodes [93-95].

1.1.4.1. Human hookworms

1.1.4.1.1. *Necator americanus*

Hookworm infection caused by nematode parasites is one of the most clinically important soil-transmitted infections that affects 1 billion people in tropical and sub-tropical regions [96,97]. *Ancylostoma duodenale* and *N. americanus* are the two main hookworm species that cause infection in humans [98]; the latter is more prevalent in human and has thus been more widely studied [99]. *N. americanus* infection occurs primarily in warm climates, with the highest prevalence in sub-Saharan Africa and Papua New Guinea [100]. *N. americanus*, "American murder", is an obligate blood-feeding parasite that causes rash, fever, abdominal pain, vomiting, iron deficiency anaemia, and growth retardation in hosts with high hookworm burden; it is asymptomatic in hosts with a low hookworm burden. As *N. americanus* hookworms do not replicate in humans due to the natural of their life cycle, hookworm infection intensity is usually estimated by counting faecal eggs. As defined by the World Health Organization (WHO), moderate hookworm-infected individuals produce 2,000–3,999 eggs per gram (epg) of faeces, whereas individuals with heavy hookworm burdens produce more than 4,000 epg. [101].

1.1.4.1.1.1. Life cycle of *N. americanus*

N. americanus is an obligate blood feeder skin-penetrating parasite that resides in the small intestine. Typically, the infective larvae L3 (iL3) mature into adult worms 42–94 days post-infection [102-104]. When adult hookworms reach sexual maturity, the female worm begins to produce unembryonated eggs that are passed in the faeces. Within 1–2 days, and under specific temperature and moisture conditions, the eggs undergo several cellular divisions and become embryonated eggs that hatch into first-stage rhabditiform larvae (L1). The L1 feed on faecal microflora and organic debris in the faeces to continue their development (~10 days), and they moult twice to form infective, third-stage filariform

larvae (iL3), which are characterised by the presence of a cuticle sheath that forms from the second moult in the L2 developmental stage; its function is to protect iL3 from desiccation and to support L3 survival in tropical climates [105-108, 98,103].

Under the presence of favourable conditions, such as warmth, humidity, and shade, iL3 increase their search for a new host by altering their crawl movement in multiple ways, referred as 'questing behaviour' (109,110, 97). When iL3 come in contact with the skin of the target host, they burrow into the skin by pressing and pushing their anterior sections against the skin [111]. The presence of key molecules, including chloroform-soluble lipids and receptors on the skin, stimulates iL3 to release enzymes that digest skin macromolecules to reach the bloodstream [112,113]. Numerous studies have observed exsheathment of the *N. americanus* infective stage before and after skin penetration [113,114]. iL3 normally goes through exsheathment before penetrating human skin however exsheathment during skin penetration has also been reported implying that exsheathment may not be essential for iL3 penetration through the skin [115].

N. americanus iL3 remain within the skin for approximately 48 hours, as reported in animal models [116]. It has been suggested that during this period, larvae resume feeding before they migrate to the lung where they possibly evade the host immune response. Once the invading larvae successfully enter the bloodstream through the capillaries, they migrate to the lung and enter the alveolar spaces, migrate into the tracheae where they are coughed up and swallowed into the GI tract [117,102]. Estimated migratory periods following skin penetration into either the lung or the small intestine is 2–4 or 4–5 days, respectively [104]. Once the larvae reach the small intestine, they undergo further development and moult into the L4 stage and, ultimately into adult worms.

Approximately >42 days after infection, adult hookworms reach full sexual maturity at a length of about 1 cm (female adults are larger than males). They are cylindrical in shape and characterised by the formation of cutting plates located on the anterior of the hookworm. These cutting plates allow adult hookworms to attach to the intestinal wall and feed on the intestinal mucosa and blood. The worms are estimated to cause blood loss of 40 µl per worm daily. Adults mate and start laying eggs that pass into the host faeces, completing the life cycle of *N. americanus* (Fig. 1.8) [104-106, 117].

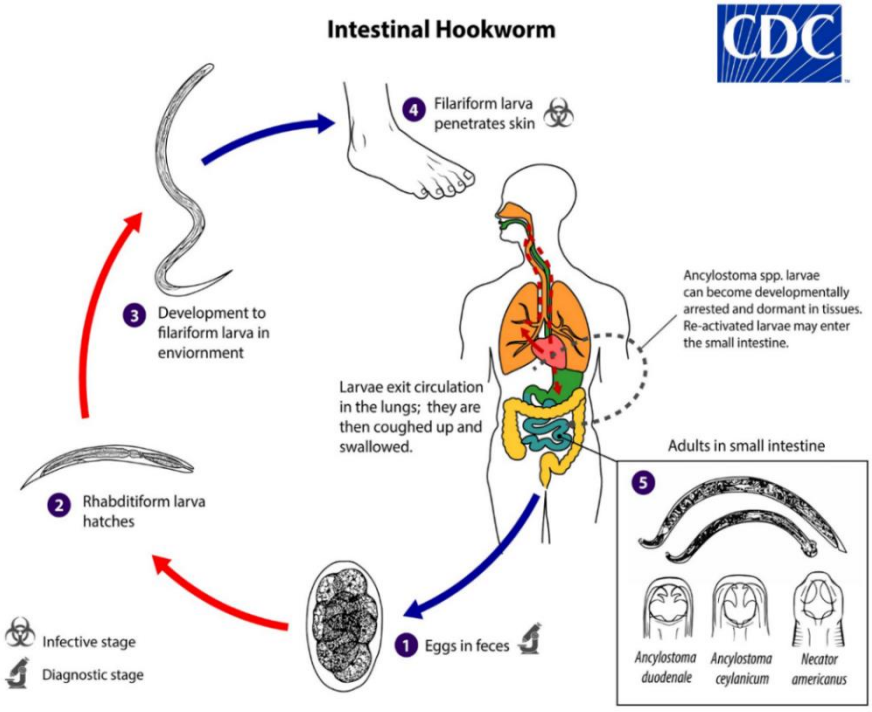

Figure 1.8: Life cycle of *N. americanus:* Unembryonated eggs are passed in the stool from the infected individual ❶. Following 1–2 days and under specific conditions, rhabditiform larvae hatch and grow in the faeces to become infective-stage larvae ❷. Larvae continue growing in the faecal material and soil for ~10 days and moult twice to develop into infective third-stage filariform larvae (iL3) ❸. Upon contact with the human host, they penetrate and burrow into the skin ❹. Once they successfully penetrate the skin, they migrate to the lung through capillaries, migrate further into the pulmonary alveoli, ascend the bronchial tree to the pharynx, and are finally swallowed into the GI tract. When they reach the small intestine, the larvae anchor and develop into mature adults. Adult hookworms attach to the intestinal epithelium and feed on intestinal mucosa and blood. Female adults start laying eggs that pass in the host faeces ❺. Adopted from [118]

1.1.4.1.1.2. Immune responses to invading larvae of *N. americanus*

Various experimental and clinical data have indicated that most of the host immune activation and modulation following *N. americanus* infection happen in different tissues including the skin, lungs, and intestine, where migration and development of *N. americanus* takes place [107,119]. When *N. americanus* larvae penetrate human skin, it causes in itching, skin redness, and migratory creeping, which are likely associated with the inflammatory responses [97,120]. *N. americanus* iL3 deposit their sheath during skin penetration to allow the exsheathed larvae to remain unrecognised. Interestingly, during this invasive stage, antibodies fail to recognise exposed L3 cuticles (exsheathed L3), whereas they successfully detect antigens on the ensheathed L3 surface. The larval cuticle secretes a variety of immune diversionary molecules to facilitate their migration through tissues [106,107,115]. When invading larvae successfully penetrate the host skin, they are confronted with a first line of immune defence represented by innate immune cells. However, the role of the innate immune response against hookworms has received less attention than the adaptive immune response and is yet to be fully elucidated [121]. Innate immunity generated against parasitic invasion includes soluble factors, such as the complement system, and cells, such as mast cells, DCs and macrophages. Upon larval penetration of human skin, mast cells residing in the tissue degranulate to release the inflammatory mediator such as histamine into the local microenvironment. Histamine acts as an endothelial vasodilator to facilitate vascular permeability, enabling other immune cells to migrate to inflamed tissues and trigger local oedema, redness, swelling, and itching [107, 122, 123]. Furthermore, tissue-resident macrophages become activated and produce a wide range of cytokines and chemokines, including IL-1β and TNF-α, which enhance expression of cellular adhesion molecules, including P-selectins on the endothelium of blood vessels at the infection site. Once P-selectin is expressed on endothelial cells, leukocytes expressing P-selectin glycoprotein 1 ligand (PSGL-1) can bind to Endothelial P-selectin, followed by expression of E-selectin on endothelial cells and its ligand E-selectin ligand-1 (ESL-1) on leukocytes. These events permit rolling of leukocytes to the site of infection. Endothelial cells also express further adhesion molecules, including intracellular adhesion molecule 1 (ICAM-1) and vascular cell adhesion molecule 1 (VCAM-1) that bind to β2 integrin

expressed on leukocytes; this tight binding enables immune cells, such as monocytes, present in circulation to move across the blood vessel endothelium and into inflamed tissues [124,125].

Complement is a part of innate immunity that also acts as a first line of defence against many invading pathogens by inducing the opsonisation and lysis of pathogens. However, parasites have a strategy to overcome complement attack and inhibit formation of the membrane attack complex (MAC) via the secretions of proteins. Studies have shown that *N. americanus* secretes calreticulin, which acts as an inhibitor of C1q that eventually blocks activation of the classical pathway involved in pathogen clearance and recruitment of neutrophils, eosinophils, and macrophages to the site of infection [126-128].

Eosinophils and neutrophils are among the cells involved in innate immunity that play a role against *N. americanus* infection. Human studies have shown that eosinophilia is a common characteristic of *N. americanus* infection; peripheral blood eosinophils from infected individuals show that eosinophils are highly activated, evidenced by an increase in their surface receptor IgG, whereas no changes are seen in neutrophils regarding their number, morphology, or immune response [129]. Evidence suggests that eosinophils bind *N. americanus* larvae in the presence of the complement system and antibodies [120]; however, this interaction is poorly understood [130], and it is not known whether this interaction has any larvicidal effect [107]. Not surprisingly, the presence of immunomodulator proteins in *N. americanus* secretions—such as neutrophil inhibitory factor (NIF)—inhibit adherence of activated neutrophils to vascular endothelial cells at the infection site [131,132]. Moreover, *N. americanus* is a highly adapted pathogen, with secretions that can cleave IgA and produce Fab fragments that combine with NIF to block IgG- or IgM-mediated phagocytosis and complement activation [133].

The other arm of innate immunity that plays an important role against parasites and aids in the activation of adaptive immunity is DCs [134]. DCs are professional APCs that are amongst the first immune cells to interact with pathogens; they act as a crucial link between innate and adaptive immune responses. These cells collectively express a range of PRRs, such as TLRs and CLRs. Once they have received ‘danger signals’ associated with different pathogens via these receptors, they undergo

maturation through a series of morphological changes, including the loading of antigenic peptides into MHC II and upregulation of co-stimulatory molecules (e.g., CD86/CD80). Activated DCs migrate to regional lymph nodes where they present antigen-derived peptides to naïve T cells, leading to the differentiation of T cells to different functional phenotypes (Th1, Th2, or Treg). Human studies on hookworm infections found that DCs demonstrated a different phenotype as they failed to induce maturation, downregulated expression of co-stimulatory molecules (CD86 and HLA-DR) and polarised to drive development of Treg cells [135-137]. This phenomenon is thought to be caused by the highly glycosylated proteins secreted by hookworms, which are recognised and internalised by CLRs on DCs. These carbohydrates play an important role in modulating DC function towards a regulatory response via induction of the anti-inflammatory cytokine IL-10 [138], as there is significant evidence supporting the role of parasite glycans in the modulation host immunity towards a regulatory response [139-145]. Interestingly, numerous studies have observed that parasitic secretions suppress the ability of TLRs to induce DC activation and pro-inflammatory cytokine production. The reasons underlying this inhibition are still poorly understood; however, it is believed that pathogens target CLRs that could result in modulation of downstream TLR signalling. Therefore, it is reasonable to hypothesise that CLRs on DCs play a role in the recognition of glycans and mediation of the immunomodulatory effect.

1.1.4.1.1.3. Immune response to adult hookworms

Upon arrival of the *N. americanus* larvae to the intestine, they mature into adult worms, whose presence is usually associate with nausea, abdominal pain, and intestinal bleeding [97,120]. The survival of *N. americanus* adult worms in humans over long periods (on average 5–7 years) is believed to occur through modulation of the host immune system [138,146]. *N. americanus* secretes a wide range of immunomodulatory molecules that play a fundamental role in modulation and suppression of the immune response during hookworm infection [96,100]. An in vitro study showed that NK cells from *N. americanus*-infected individuals were unable to interact with the secreted products of adult worms [146]. Furthermore, *N. americanus* infection had the capacity to elicit a Th2 response, which was associated with the production of cytokines, such as IL-4, IL-5, and IL-13 [147]. However, the

mechanism by which DCs respond to parasite antigens for priming naïve T cells towards a Th2 response is still not fully understood [148]. Previous observations suggested that DCs failed to induce maturation in response to parasite secretions, and that these secretions could modulate TLR signalling pathways [149]. Moreover, *N. americanus* infection induces expansion of Treg cells to increase their chance of survival. The induction of this regulatory response is likely independent from parasitic secretions, and cytokines produced by DCs, such as IL-10, play a fundamental role in induction of Tregs through DCs priming [150,151].

1.1.4.1.1.4. *N. americanus*-secreted products and their role in immunomodulation

N. americanus secretes molecules into the host environment that are defined as excretory-secretory products [152]. A hallmark function of theses secretions is that they permit the survival of live parasites in the host for extended periods through evasion and suppression of host immune responses [153]. Numerous studies have reported on downregulation of the host immune response caused by hookworm secretions. Some of these studies revealed a common set of proteins secreted by *N. americanus,* including NIF, antioxidants, proteases, protease inhibitors, acetylcholinesterase (AChE), glycolytic enzymes, and C-type lectins [107, 154, 155]. The presence of NIF has been reported in *N. americanus* secretions. NIF plays a role in immune evasion by interfering with recruitment of activated neutrophils to the vascular endothelium by releasing hydrogen peroxide that blocks essential integrins for neutrophil migration, including CD11c and CD18 [131,156].

N. americanus also secretes antioxidants that are thought to provide protection to the exposed larval cuticle surface by counteracting the effects of host free radicals, with enzyme such as superoxide dismutase (SOD), and neutralising lipid hydroperoxide by glutathione-S-transferases (GSTs) [107,110,157]. Studies suggest that *N. americanus* larvae secrete a mixture of hydrolytic enzymes to facilitate skin digestion, larval migration through tissues, and intestinal attachment [158-160]. These enzymes include metalloproteases, cysteine proteases, serine and aspartyl proteinases, and evidence

suggests that these enzymes are stored in secretory granules localised in the oesophageal glands of *N. americanus* larvae [161-163]. The metalloproteases secreted by *N. americanus* play an important role in immunomodulation by inhibiting eosinophil recruitment to sites of infection through blockage of eotaxin [164]. In addition, the aspartic protease Na-APR-1 and the cysteine protease Na-CP-3 are among of immunomodulator enzymes secreted by *N. americanus*. These enzymes are involved in the hydrolysis of human haemoglobin from consumed erythrocytes and the promotion of parasite feeding [165,166].

Previous studies have identified the presence of different carbohydrate moieties, such as galactose, mannose, fucose, heparan sulphate, and N-acetylgalactosamine (GalNAc), on the surface of *N. americanus* larvae [167]. These carbohydrates are abundant on the parasite surface and in their secretions, and they thus have a role in fine-tuning the host immune response. Interestingly, these carbohydrates are believed to be analogous in both structure and function to human glycans and thus evade recognition by host immune responses [138]. Numerous studies have shown that the interaction of these carbohydrates with DCs can interfere with effective induction of host immune responses [168-172]

1.1.4.1.1.5. Treatment of *N. americanus* infection

Four anthelmintic drugs have been approved by the WHO to treat hookworm infection: albendazole, mebendazole, pyrantel pamoate, and levamisole. These drugs have been used effectively against a broad spectrum of parasites for more than 30 years; they have high affinity for eliminating helminths and excreting them swiftly, without undesired effects on host tissues [173-176].

Albendazole and mebendazole are derivatives of the benzimidazole class. These two drugs bind hookworm beta-tubulins and prevent polymerisation of microtubules inside the worm. Recent reviews have investigated the efficacy of albendazole and mebendazole in the treatment of hookworm infection. The results found that a 400-mg dose of albendazole was associated with a cure rate of 66%, whereas 500 mg of mebendazole had an effective cure rate of 31% [177,178]. Albendazole and mebendazole are the most common anthelminthic drugs used to control intestinal nematode infection due to their high efficacy and low cost; however, there are increasing concerns regarding drug

resistance. To date, mebendazole resistance has been reported in human hookworm infections in Australia and Africa [179,180]. Recent clinical trials demonstrated the promising effect of tribendimidine against *N. americanus* at a dose of 400 mg, reporting an 86% cure rate, which could indicate that this drug may represent an alternative treatment choice [175,176]. However, anthelmintic drugs do not provide long-lasting protection as there is an increased rate of re-infection for individuals living in endemic areas, and the infection can endure throughout a lifetime [181,182]. Therefore, developing an effective vaccine is an alternative method to preventing this disease and may provide long-lasting protection against *N. americanus.*

1.1.4.1.1.6. Therapeutic potential for hookworm infection in treating autoimmune and inflammatory diseases

The hookworm *N. americanus* resides in humans for long periods due to its secretion of a wide range of immunomodulator proteins that play a fundamental role in suppressing the production of pro-inflammatory cytokines and inducing anti-inflammatory processes [96]. Interestingly, numerous studies have reported that hookworm infection can protect against allergies and several autoimmune conditions, such as rheumatoid arthritis, multiple sclerosis (MS), and inflammatory bowel disease [183,184]. Furthermore, epidemiological studies suggested that there was a decreased prevalence of allergies and autoimmune diseases in helminth carriers [185-187]. From an immunological point of view, autoimmune diseases appear to have Th1-mediated pathology involving the production of pro-inflammatory cytokines IL-12 and IFN-γ. In contrast, hookworm infections regulate the immune response and promote balance in the immune system [188].

N. americanus is considered a favourable parasite to treat those diseases as it does not replicate within the human host and adult worms can live for many years in the GI tract [189,184]. Infection with *N. americanus* at low numbers is safe and tolerable, with no documented serious adverse effects. In 2006, it was demonstrated that infection with approximately 10–50 infective *N. americanus* larvae was safe and well-tolerated, with no significant induction of anaemia; the number of eggs recovered was 50 epg. However, eosinophilia, IgG, and IgE were detected in the blood, even with the low degree of infection [190,191].

The immune-suppressive properties of *N. americanus* have been demonstrated in different autoimmune and autoinflammatory diseases, including asthma, Crohn's disease, coeliac disease, and MS. In an asthma study, 32 patients were each infected with 10 infective *N. americanus* larvae and followed up for 16 weeks. This study reported no significant improvement in airway responsiveness. The possible reason for the failure of this trial was thought to be because patients were undergoing corticosteroid treatment, which may have impaired the immune response during *N. americanus* infection [192]. In a study on Crohn's disease, a type of inflammatory bowel disease, 9 patients were infected with 25–50 infective larvae and followed up for 20 weeks. The Crohn's disease activity index (CDAI) showed improvement for 7 of the patients, with no anaemia reported during the infection period. These results suggest that *N. americanus* infection could prove more beneficial for diseases that occur in the same location where the mature worms reside [193].

The benefit of *N. americanus* was also demonstrated in coeliac disease, which is an autoimmune disease that occurs when genetically susceptible people consume a gluten-containing diet. In this study, 20 patients were treated with 5–10 infective larvae for period of 20 weeks. Patients demonstrated decreased levels of the inflammatory cytokines IFN-γ and IL-17A after a gluten challenge [194,195].

Interestingly, *N. americanus* may also alter immune reactivity in MS patients. MS is an inflammatory disorder that affects the central nervous system, inducing myelin injury [196]. Previous studies revealed a relationship between parasite infection and the course of MS. In a study, 24 volunteers (12 uninfected MS patients and 12 parasite-infected MS patients) were evaluated to compare the effects of parasitic infection on MS progression over 4.5 years. During the 4.6-year follow-up period, parasite-infected MS patients showed significantly decreased magnetic resonance imagining (MRI) activity as compared with uninfected MS patients; furthermore, the peripheral blood of parasite-infected MS patients showed a significant increase in IL-10 and TGF-β levels and a decrease in IL-12 and IFN-γ levels as compared with uninfected patients. These observations suggest the possibility of using *N. americanus* and its protein secretions as a therapeutic tool for autoimmune and inflammatory diseases in clinical trials [197,198].

1.1.4.1.2. *Nippostrongylus brasiliensis* as a model parasitic nematode

N. brasiliensis is widely used as an experimental model in the study of GI nematode infection and immunity. This parasite is studied because it has a similar life cycle and skin-penetrating third larval infective stage as the human hookworm. *N. brasiliensis* belongs to the same clade as the human hookworm species *N. americanus*. In addition, *N. brasiliensis* has a short life cycle, allowing it to be easily maintained in a laboratory. Rodents, such as rats and mice, are the specific hosts of *N. brasiliensis*, making it easy to obtained large quantities of worms at different stages. The life cycle of the parasite begins with eggs that hatch in faecal material through two moult stages, from L1 stage to L3 stage. The infective third-stage L3 invade the host by penetrating the skin to initiate infection, followed by migration of L3 from the skin to the lungs through the circulatory system. Upon arrival in the lungs, they moult into L4 stage; this migration occurs between 24 and 32 hours post-infection. L4 then migrates up the trachea to be coughed up into pharynx and swallowed into the GI tract. Upon arrival in the GI tract, the larvae attach to the intestinal wall and undergo further development to become fully matured adult worms. The adult worms mate and eggs start to appear in the rodent faeces. The eggs then undergo two further moults to become infective L3 [199,200]. (Fig. 1.9) illustrate life cycle of *N. brasiliensis*.

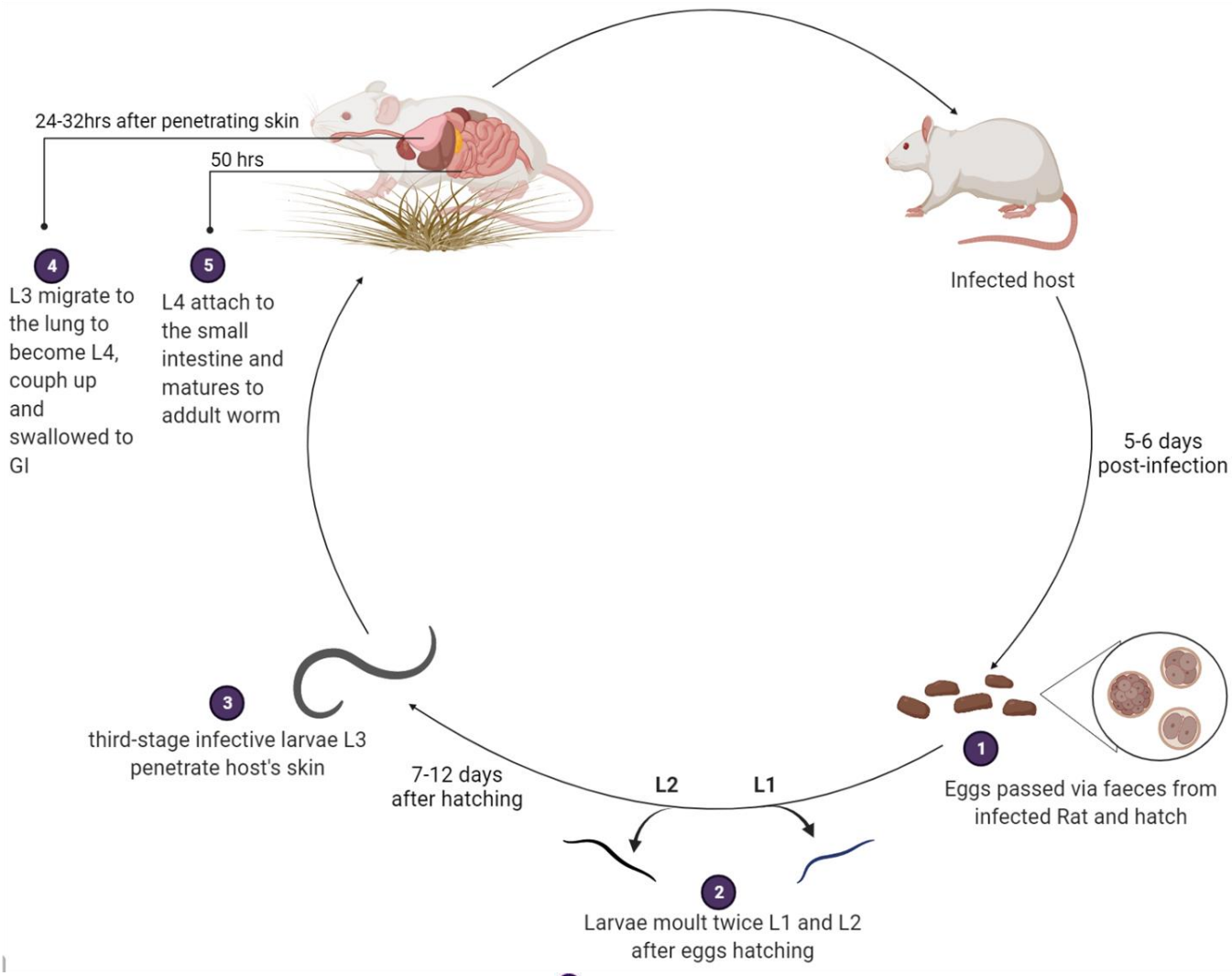

Figure 1.9: Life cycle of *N. brasiliensis*. ❶ Unembryonated eggs are passed in the faeces of an infected rodent. ❷ Eggs hatch and undergo two moults as L1 stage and L2 stage. ❸ Infective L3 emerge 7–12 days after hatching. ❹ Infective L3 penetrate the host's skin and migrate via the circulatory system to the lungs where they moult into L4 stage. This occurs between 24 and 32 hours post-infection. L4 migrate to the trachea and are coughed up and swallowed into the GI tract. ❺ When they reach small intestine, the larvae develop into mature adults. Adult worms mate and start to produce eggs, which pass into the host's faeces.

1.2. Research objectives

N. americanus infection is a significant public health concern, particularly in developing countries. However, fundamental information about how this parasite initially interface with immune cells and how their secretions affect DC function and downstream T cell responses is the subject of intensive research. Despite relative success with drugs used in treating hookworm infections, there is a high rate of re-infection, and the immune response against hookworms is typically not protective. Therefore, there is a need for better understanding of the early events involved in the interface between the hookworm and the immune system, which could pave the way for the design of more effective therapies and vaccines.

Given that the infective larvae of *N. americanus* requires human host, limits access to this worm for mechanistic studies. Moreover, working with *N. americanus* larvae in the laboratory is quite challenging due to the high infection rate of this parasite in humans and the complexity of its life cycle, which takes around 5–7 weeks to develop an infective stage. Therefore, the main aim of this was to investigate whether other more readily accessible *N. brasiliensis* can be used as a model system to investigate the immune modulatory properties of infective larvae and their secretions on human immune cells. Here, we hypothesised that *N. brasiliensis* infective larvae has modulate human DC functional properties similar to those reported for *N. americanus*. Furthermore, we aimed to characterise the surface chemistries of infective larvae and identify carbohydrate components within larval secretions that could help us to understand the immune modulatory strategies used by the parasites to modulate the immune system adding more mechanistic insight on how the infective larvae interacts with the immune system. These findings may contribute to the design of therapeutic tools to treat autoimmune and autoinflammatory conditions.

Chapter 2:

Investigating the physical interaction of *Nippostrongylus brasiliensis* infective larvae with dendritic cells and surface chemistry analysis of infective larvae

2.1 Introduction

N. americanus larvae are believed to establish a number of successful immune evasion strategies to evade immune recognition and eradication [119]. Studies have observed that antibodies from individuals infected with *N. americanus* could recognise antigens on ensheathed larvae but failed to recognise antigens on the exposed larval cuticle [106,115]. Therefore, it has been hypothesised that the L3 larvae shed their sheath (exsheathment) during percutaneous infection to diverts the immune system to allow successful infection and reinfection in endemic areas [102]. DCs are professional antigen presenting cells (APCs) and among the first immune cells that interact with pathogens, acting as a crucial link between the innate and adaptive immune responses [21]. A recent study by our group showed exsheathment of *N. americanus* L3 upon interaction with human immature dendritic cells (iDCs). Intriguingly, these cells did not interact with the exposed third-stage larvae (L3) cuticle [201]. However, the exact mechanism underlying such immune evasion has remained elusive. Therefore, characterisation of *N. americanus* L3 interaction with DCs could provide invaluable insight into mechanism that underpin *N. americanus* immune evasion and its immune modulatory effects, which could in turn help in the design of new therapeutic strategies. However, a major limitation of working with *N. americanus* is the availability of viable L3, as they require a human host. Thus, identifying other nematode species that can be used as a model system for studying human immune responses would greatly facilitate such studies.

N.brasiliensis is an intestinal nematode parasite that infects rodents; it has been widely used as an experimental model for studying gastrointestinal nematodes that infect humans because it has a similar life cycle and skin-penetrating L3 infective stage to *N. americanus* [202]. However, the physical interaction of *N. brasiliensis* with human DCs and the chemical properties of the L3 cuticle and their sheath have not yet been studied.

Therefore, in this chapter we aimed to investigate the possibility of using *N. brasiliensis* as a laboratory model system by elucidating its physical interaction with human DCs in the presence or absence of larval sheath. Furthermore, we aimed to investigate the surface chemical signatures of *N. brasiliensis* L3 cuticle and the sheath using time-of-flight secondary ion mass spectrometry (TOF-SIMS) to

determine similarities or differences with *N. americanus* and whether such molecular signatures could explain immune evasion by larvae cuticle.

2.2 Materials and methods

2.2.1 Preparation of *N. brasiliensis* infective larvae

A faecal culture containing *N. brasiliensis* infective L3 larvae was sourced from our collaborator (Maizels laboratory, University of Glasgow, United Kingdom), where they collected faecal material from infected rodents and mixed it with charcoal and antibiotics, including penicillin and streptomycin. The stock of *N. brasiliensis* has been tested and shown to not carry any pathogenic micro-organisms. L3 were isolated from faecal material via the Baermann technique, as previously described [202]. Briefly, the faecal culture was applied onto gauze padding into the Baermann apparatus (containing ~15 ml of tap water) and left overnight. The water containing larvae was collected in a 15-ml centrifuge tube; the larvae were allowed to settle on the bottom of the tube for 30 minutes before the excess water was drawn off. The concentrated larvae were washed extensively with sterile deionised water containing 100 IU/ml penicillin, 100 µg/ml streptomycin, and 1% gentamicin, and were allowed to settle by gravity after each wash for ~30 minutes. Following washes, the larvae were counted and stored at room temperature in the dark until use.

2.2.2 Generation of human dendritic cells from peripheral blood mononuclear cells

Whole blood samples were obtained from healthy donors (National Blood Service, Sheffield, UK) following approval of the ethics committee (Faculty of Medicine and Health Sciences, Research Ethics Committee, University of Nottingham). Peripheral blood mononuclear cells (PBMCs) were isolated from the whole blood using Histopaque (Sigma-Aldrich, UK) by density gradient centrifugation. $CD14^+$ monocytes were purified from PBMCs by positive selection using a magnetic cell separation system (Miltenyi Biotech, UK). The purity of the purified monocytes was tested using flow cytometry. Purified monocytes were counted using a Countess™ II FL Automated Cell Counter (Thermofisher, UK) and supplemented in RPMI 1640 medium (Sigma-Aldrich) containing 10% heat-inactivated fetal bovine serum (FBS), 100 U/ml penicillin, 100 µg/ml streptomycin, and 2 mM L-glutamine (all from Sigma-Aldrich); this supplemented culture medium will referred to as ‘complete medium’. For immature DC generation, 10^6 cells/well of monocytes were seeded into a 24-well plate (Corning Life Science, NY, USA) in the presence of 50 ng/ml GM-CSF and 250 U/ml IL-4 (both from Miltenyi

Biotech) and incubated for 6 days at 37°C and 5% CO_2. Fresh complete medium was added on day 3 and supplemented with the same concentration of GM-CSF and IL-4 as on day 0 [203].

2.2.3 Incubation of *N. brasiliensis* infective larvae with human immature dendritic cells

Human immature DCs (iDCs) (2.5 x 10^5 cells/well) were seeded in a 24-well plate in complete RPMI 1640 medium and treated with mixed number of ensheathed and exsheathed L3 (~50 larvae), followed by incubation of the cells for 24 hours at 37ºC with 5% CO_2. During the incubation period, cells were imaged using a Fluorescent Cell Imager (Etaluma).

2.2.4 Quantification of DCs viability assay

2.2.4.1 Trypan blue

The number of viable cells was primarily determined using Trypan blue (Sigma-Aldrich). Briefly, the cell suspension was stained with 0.4% Trypan blue at a 1:20 dilution factor. Cells were then counted using Countess™ II FL Automated Cell Counter (Thermofisher, UK).

2.2.4.2 LIVE/DEAD stain

Cell viability was evaluated using LIVE/DEAD stain (Thermo Fisher Scientific) according to the manufacturer's protocol. Briefly, cell supernatants were removed, stained with 250 µl of LIVE/DEAD stain, then incubated for 20 minutes in the dark at 37°C before analysis. Cells were imaged using the Fluorescent Cell Imager (Etaluma) and data analysis was conducted either by counting fluorescent cells using ImageJ software or using flow cytometry.

2.2.5 Characterisation of *N. brasiliensis* larvae surface chemistry

2.2.5.1 Poly-L-lysine-coated slide preparation

Microscopy glass slides (76 x 26 x 1.0–1.2 mm), methanol (HPLC grade), and acetone (HPLC grade) were purchased from Thermo Fisher Scientific, UK. Poly-L-lysine (70–150 kDa) was purchased from Sigma-Aldrich, UK. The microscopy slides were cleaned using deionised water, methanol, and acetone. Poly-L-lysine was prepared in deionised water at a concentration of 0.1%, and then 100 µl of 0.1% poly-L-lysine solution was pipetted onto the centre of the cleaned microscopy glass slide. To distribute the poly-L-lysine over the slide, another cleaned microscopy slide was placed on top of the

poly-L-lysine drop. Then, the slides were incubated for 5–10 minutes at room temperature, separated carefully, and washed with deionised water.

2.2.5.2 Preparation of *N. brasiliensis* slides

N. brasiliensis L3 (n>100) were washed extensively with sterile deionised water (10 times). The larvae were allowed to settle by gravity to the bottom of a 15-ml centrifuge tube for approximately 15–30 minutes, and the excess water was drawn off. After the washing step, 100 µl (n~10) of *N. brasiliensis* suspension was pipetted onto poly-L-lysine-coated slides, and the larvae were allowed to settle on the slides. The slides were examined using an optical microscope before the excess water was aspirated to dry the slides. Next, the slides were stored at -20°C in an airtight sealed container to maintain the integrity of larval morphology.

2.2.5.3 Time-of-flight secondary ion mass spectrometry (TOF-SIMS)

TOF-SIMS experiment was carried out to detect the surface chemistries of larvae surface on poly-lysin coated slides. The experiment was done with the help of David Scurr and Nichola Starr. An IONTOF GmbH TOF-SIMS instrument equipped with a metal ion gun producing a Bi3+ primary ion source (25 keV) and a single-stage reflection analyser to collect positive and negative secondary ion data. An electron flood gun producing a low energy (20 eV) was used to compensate for positive ions generated by sample surface charging. To ensure static SIMS conditions, the dose of the primary ion beam was maintained at $1 \times 10^{12}/cm^2$ throughout the measurement. Slides containing *N. brasiliensis* larvae were measured using this instrument. A total of six larvae—three replicates of the L3 cuticle and three replicates of the larval sheath—were scanned at the region of interest (500 µm × 500 µm) at a resolution of 256 × 256 pixels in both positive and negative polarity. TOF-SIMS produces spectral datasets and images, and each pixel on the image relates to a specific mass spectrum. Therefore, to identify the masses that differentiated the larval sheath from its cuticle, multivariate analysis (MVA) was applied.

2.2.5.4 Multivariate analysis

To identify differences between the surface chemistries of the L3 cuticle and the sheath, principal component analysis (PCA) was performed using simsMVA software [204]. The peak list was

generated for a single L3 cuticle and sheath, and that peak list was applied to the mass spectra of all L3 cuticles and sheaths. In total, 100 m/z peaks for negative ion polarity and 100 m/z peaks for positive ion polarity were examined. The peak list intensities were normalised to the total ion count and exported to simsMVA software, and PCA was performed to assess the differences in the spectra between the L3 cuticle and sheath. The data from the PCA are presented as score plots and loading plots; the score plots were generated to determine the correlation between selected variables on the cuticle and sheath, while the loading plots were generated to visualise mass ions that were expressed on the larval cuticle and sheath individually.

2.3 Results

2.3.1 Characterising the *N. brasiliensis* infective larvae

Length measurement of *N. brasiliensis* L3 was performed and calculated using ImageJ software (Fig. 2.1A&B), while structural characterisation was performed using a Fluorescent Cell Imager (Etaluma) (Fig. 2.2). Analysis of the length measurements of the infective L3 stage (ensheathed L3 and L3 cuticle) was conducted on ~10 larvae; the length varied among these larvae. The ensheathed L3 length ranged between 600–690 μm; in contrast, L3 cuticle length ranged between 500–600 μm (Fig. 2.1C). This assessment was followed by identification of the external morphology of the infective stage, include the sheath, oesophagus, and tail structures. *N. brasiliensis* L3 retained its cuticle by a sheath, which developed from the second stage (Fig. 2.2A). The oesophagus of the infective L3 was slightly enlarged, tubular in shape, and located at one-quarter of *N. brasiliensis* larval length. In addition, *N. brasiliensis* L3 had a short tail and a ventral protuberance (arrowhead) (Fig. 2.2 B). These characterisations proved that the larvae employed in this study were the infective stage of *N. brasiliensis* [198].

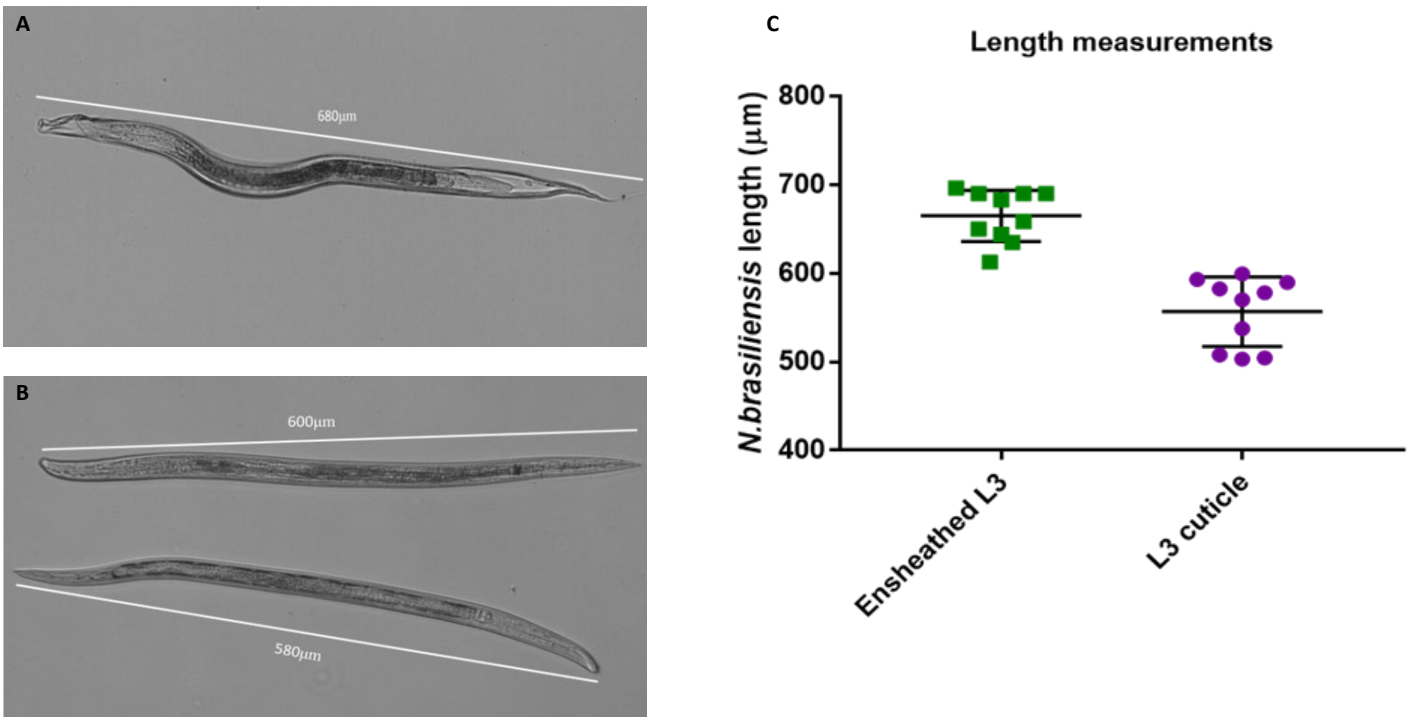

Figure 2.1: **A) & B) The determination of length measurement of *N. brasiliensis* infective stage L3 using ImageJ software.** In ImageJ software: open image > drawing a straight line over larvae starting from mouth to tail > analyse > set scale > change length unit to µm > analyse > measure. **C)** The measurement of ensheathed L3 (n=10) ranged between 550–600 µm, while L3 cuticle length (n=10) was approximately 550–600 µm.

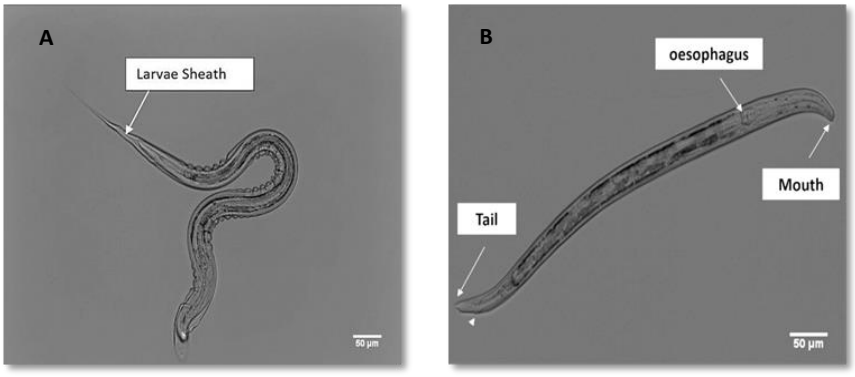

Figure 2.2: Structural characterisation of the ensheathed infective L3 (EnL3) and the ex-sheathed L3 (ExL3). A) EnL3 is enclosed in the sheath, which contains the cuticle for L3. **B)** The L3 cuticle has a short tail with a ventral protuberance (arrowhead) and a tubular oesophagus located at about one-third of the larval length.

2.3.2 The physical interaction between *N. brasiliensis* iL3 and dendritic cells

The physical interaction between *N. brasiliensis* infective larvae and human DCs was examined by incubation of *N. brasiliensis* L3 (ensheathed and exsheathed L3) with immature monocyte derived DCs. The interactions were observed for up to 24 hours using the Fluorescent Cell Imager (Etaluma). After one hour of incubation time between the ensheathed L3 with iDCs, the microscopy data showed that DCs bound or aggregated to the ensheathed *N. brasiliensis* larvae. The ensheathed larvae moved dynamically for 2-3 hours after start of incubation with DCs, which promoted which promoted exsheathing of the larvae. The exsheathing process can take up to 4 hours after incubation and no exsheathing was noticed within 2 hours of incubation with DCs. Consequently, the exposed larvae cuticle migrated away from the sheath, while DCs continued to sequester onto the discarded sheath and formed aggregates, without binding to the exposed larval cuticle (Fig. 2.3 A). In contrast, when exsheathed larvae (L3 cuticle only) were incubated with iDCs, the iDCs exhibited no binding or aggregation to the L3 cuticle in the absence of the cuticle sheath. The L3 cuticle moved dynamically and freely, without any aggregation of DCs around it at different time points (Fig. 2.3 B). After 24 hours of incubation, the L3 cuticle—in the presence or absence of the sheath—moved freely, without attracting DCs, while aggregation of DCs was observed around the discarded larval sheath (Fig. 2.3A $_{(vii,\ viii)}$, 2.3B $_{(viii)}$). Full-length videos of the interaction between DCs and either ensheathed or L3 cuticles are available in (supplementary video 1 and 2).

Furthermore, to investigate whether or not ensheathed and exsheathed L3 larvae could impact on iDCs viability, Live/Dead assay was used. Our data showed that ~90% of cells were viable after co-culture with L3 larvae (Fig. 2.4).

A

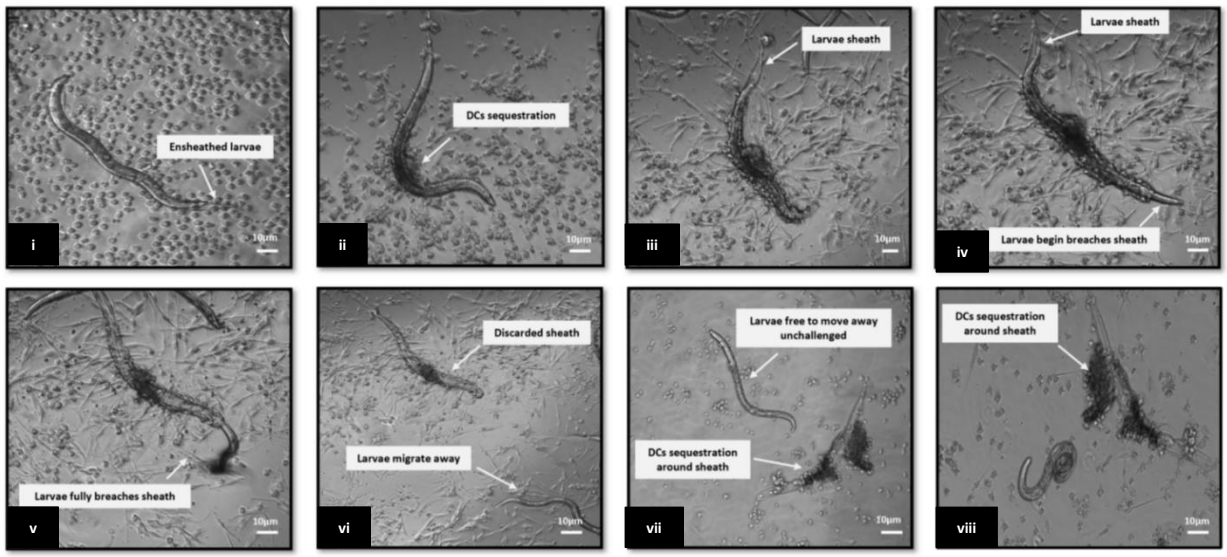

Figure 2.3: A) Time-lapse images show the physical interaction of ensheathed *N. brasilienis* L3 with iDCs. A-i, A-ii and A-iii) At initial incubation of the ensheathed L3 and up to 2 hours, the larva moves dynamically and remains hidden in its sheath, while DCs continue to sequester around the sheath. **A-iv, A-v, A-vi)** Ensheathed L3 initially begins to puncture the sheath (first visualisation of the ex-sheathing process) and continues moving dynamically until L3 is completely exsheathed. The exposed L3 cuticle migrates independently of the sheath. **A-vii, A-viii)** After 24 hours of incubation, sequestration of DCs around the discarded sheath is observed, while the exposed L3 cuticle remains unchallenged. Data show representative images of two independent experiments (n=2).

B

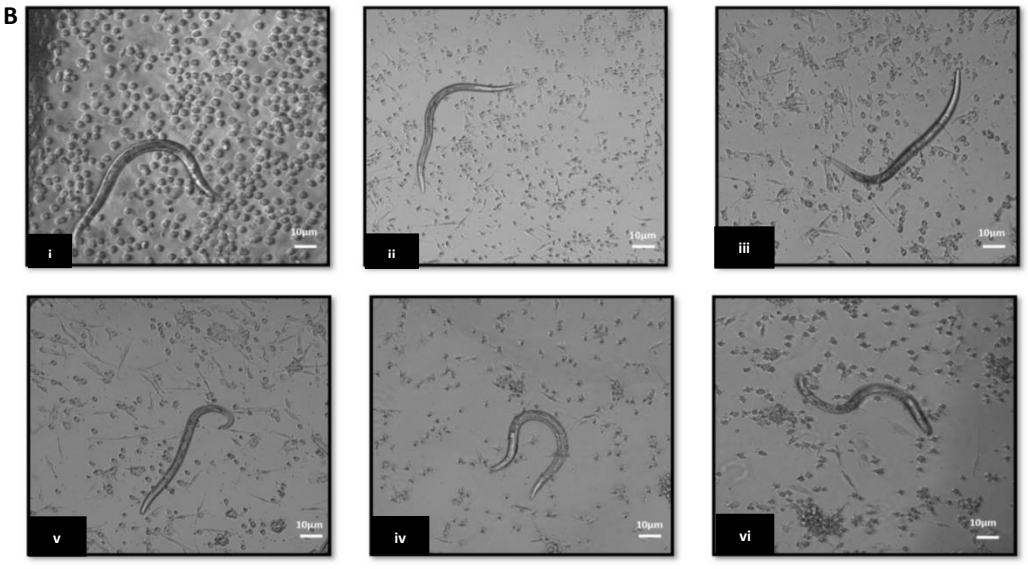

Figure 2.3: B) Time-lapse images showing the physical interaction of *N. brasiliensis* L3 cuticle with iDCs. B-i–B-iv) At initial incubation of the exsheathed L3 and up to 4 hours, the larvae are free to move without any attraction to DCs. **B-v, B-vi)** After 24 hours of incubation, the DCs showed no interest in binding to the L3 cuticle, and the larvae continue to move freely. Data show representative images of three independent experiments (n=3).

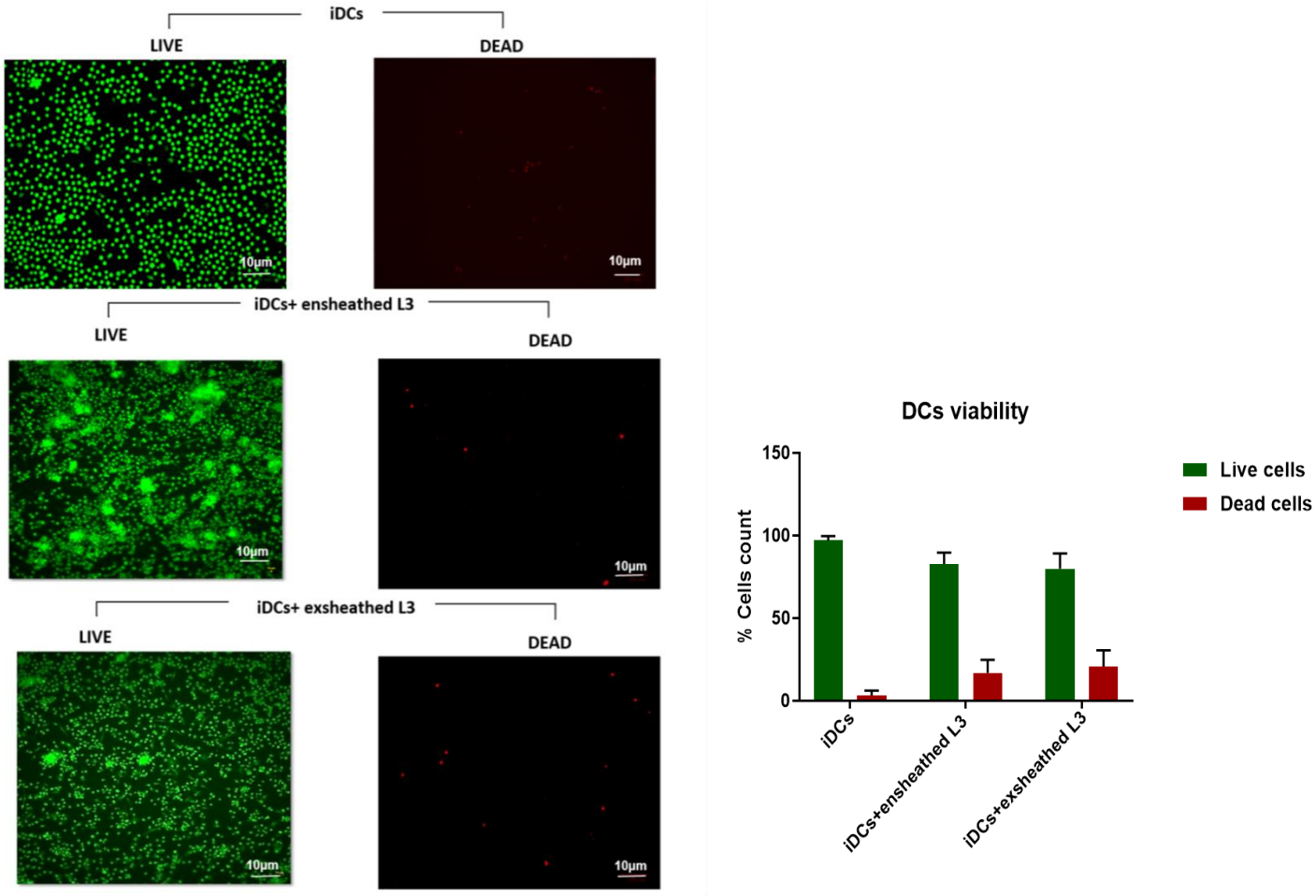

Figure 2.4: The viability of DCs after 24 hours of treatment with *N. brasiliensis* L3. Quantification of LIVE/DEAD fluorescent cells was performed using ImageJ software. Briefly, in ImageJ software: open image > change image type to 8-bit > adjust threshold to highlight cells to be counting, process > binary > convert to mask, analyse > analyse particles to count all cells. The results showed that >90% of DCs were alive after treatment with L3. Data are representative of three independent experiments using DCs from three different donors (n=3).

2.3.3 Chemical characterisation of *N. brasiliensis* L3 larvae

Our previous observation showed the differential ability of iDCs to interact with ensheathed larvae and the cuticle; therefore, we hypothesised that the surface of the L3 cuticle could be chemically differentiated from the larval sheath. We used TOF-SIMS to test our hypothesis. PCA of the data generated from negative-polarity TOF-SIMS of the larval cuticle (n=3) and larval sheath (n=3) was performed using sims-MVA to assess key differences across the datasets. A peak list was generated for a single larval cuticle and larval sheath (supplementary figure 1), that peak list was then applied for all larvae cuticles and sheaths. Data obtained was applied to the sims-MVA software to determine whether the larval cuticle and sheath could be chemically differentiated. The score plots generated from PCA clustered the data into two distinct populations based on chemical similarity. All L3 cuticle samples were separated from sheath samples using the ions included in PC1, whereas PC2 contained ions specific to the sheath. Our data showed that the L3 cuticle PC1 group contained 64.72% of the selected m/z peaks within the dataset, while the larval sheath PC2 group contained 30.18% (Fig. 2.5).

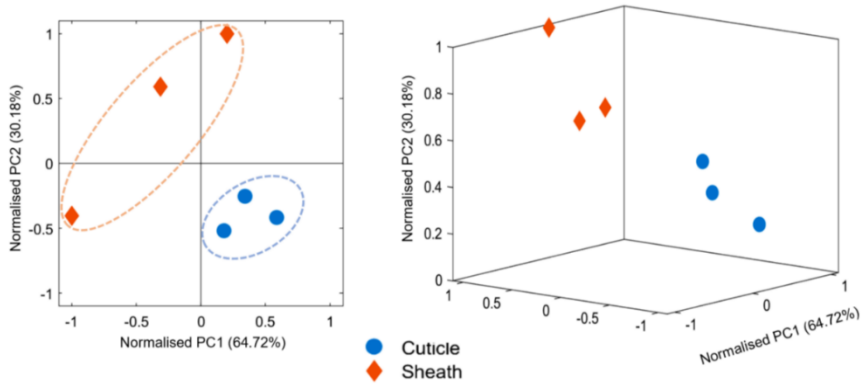

Figure 2.5: 2D and 3D PCA score plots showing PC1 (L3 cuticle) and PC2 (sheath) from data generated from negative-polarity TOF-SIMS. PC1 contained 64.72% of the variables within the dataset, while PC2 contained 30.18% of the variables within the dataset (L3 cuticle n=3, sheath n=3).

The loadings for PC1 and PC2 were identified to determine the mass ions specific to the larval cuticle and larval sheath (Fig. 2.6 A&C), and chemical assignment of highly loaded mass ions for PC1 and PC2 was performed (Fig. 2.6 B&D).

A

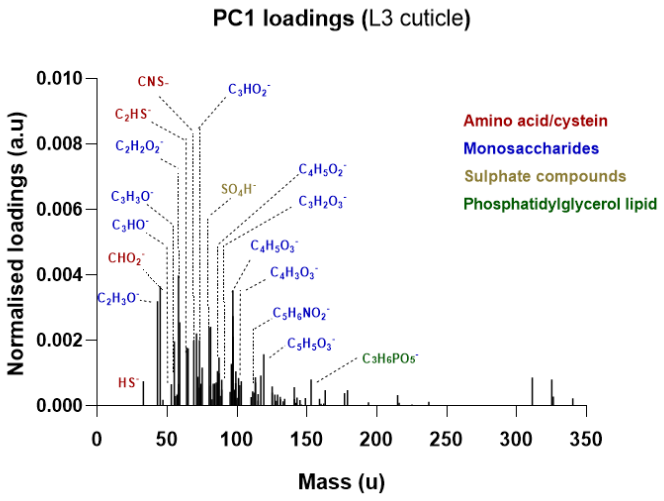

B

Rank	Mass	Assignment	Peak most prominent in
1	45.00	CHO_2^-	All amino acids
2	58.00	$C_2H_2O_2^-$	Galactose, fucose, L-rhamnose
3	73.00	$C_2H_3O^-$	Fucose, L-rhamnose
4	68.99	$C_3HO_2^-$	Galactose, fucose, L-rhamnose
5	55.01	$C_3H_3O^-$	Galactose, fucose, L-rhamnose
6	96.96	SO_4H^-	Sulphate
7	100.00	$C_4H_5O_3^-$	Galactose
8	57.97	CNS^-	Cysteine
9	46.99	C_2HS^-	Cysteine
10	43.02	$C_2H_3O^-$	N-acetylgalactosamine
11	53.00	C_3HO^-	Galactose
12	99.01	$C_4H_3O_3^-$	N-Acetylgalactosamine
13	86.01	$C_3H_2O_3^-$	Galactose
14	85.03	$C_4H_5O_2^-$	Galactose, fucose, L-rhamnose
15	112.00	$C_5H_6NO_2^-$	N-acetylgalactosamine
16	113.00	$C_5H_5O_3^-$	Galactose
17	152.99	$C_3H_6PO_5^-$	phosphatidylglycerol

C

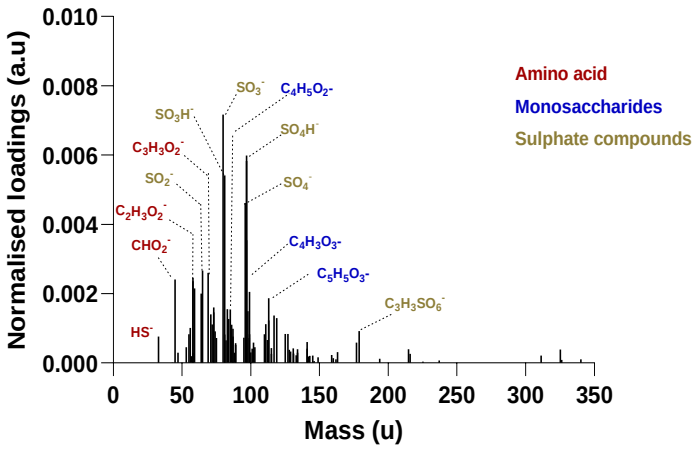

D

Rank	Mass	Assignment	Peak most prominent in
1		SO_3^-	Sulphate
2		SO_4H^-	Sulphate
3		SO_4^-	Sulphate
4		SO_3H^-	Sulphate
5		CHO_2^-	All amino acids
6		SO_2^-	Sulphate
7		$C_3H_3SO_6^-$	Heparan sulphate
8		$C_4H_5O_2^-$	Galactose, fucose, L-rhamnose
9		$C_4H_3O_3^-$	N-acetylgalactosamine
10		$C_5H_6NO_2^-$	N-acetylgalactosamine

Figure 2.6: A) & B) Normalised loading plots for the L3 cuticle (n=3) and chemical assignment of highly loaded ions on the L3 cuticle. C) & D) Normalised loading plots for the sheath (n=3) and chemical assignments of major loaded ions for the larval sheath.

Cuticle. The PC1 loadings elucidated that the L3 cuticle surface contained mass ions at 44.99 u, identified as CHO_2^- (Fig. 2.6B), which is a generic fragment associated with most amino acids [205]. CHO_2 was distributed on both the L3 cuticle and sheath; however, it was more highly expressed on the L3 cuticle surface than on the sheath. Interestingly, the surface of the L3 cuticle contained secondary ions associated with characteristic monosaccharide fragments, including fucose, galactose, L-rhamnose, and GalNAc (Fig. 2.7 A) [206]. The chemical assignment for each monosaccharide is provided in (Fig. 2.7 B). Further analysis, the surface of L3 cuticle elucidated expression of $C_3H_6PO_5^-$ ion, which indicates a phosphatidylglycerol head group and is located specifically on the L3 cuticle surface (Fig. 2.7 B). Through further analysis of ions loaded specifically on the L3 cuticle revealed the presence of secondary ions associated with cysteine amino acids, including HS^- (32.98 u), CH_3S^- (46.99 u), C_2HS^- (56.98 u), CNS^- (57.97 u), S_2^- (63.94 u) and HS_2^- (64.95 u) (Fig. 2.7 C). However, the L3 cuticle surface demonstrated a lower abundance of secondary ions associated with sulphated compounds than the sheath, including SO_2^- (63.96 u), SO_3^- (79.96), SO_3H^- (80.97 u), SO_4^- (95.96 u), and SO_4H^- (96.96 u) (Fig. 2.7 D).

Sheath. The loadings for PC2 demonstrated that the larval sheath was highly loaded with secondary ions associated with sulphated compounds, including SO_2^- (63.96 u), SO_3^- (79.96), SO_3H^- (80.97 u), SO_4^- (95.96 u), and SO_4H^- (96.96 u) (Fig. 2.8D). These compounds were distributed over the larval sheath and L3 cuticle surfaces; however, they were observed in greater density on the sheath. In contrast to this observation, the larval sheath contained characteristic monosaccharide fragments (Fig. 2.8A); however, they were more highly expressed on the L3 cuticle than the sheath. Interestingly, the sheath surface contained secondary ions specific to heparan sulphate $C_3H_3SO_6^-$ (Fig. 2.8D) [207] but do not contain a phosphatidylglycerol head group and secondary ions associated with cysteine amino acids (Fig. 2.8 B&C). Differences between chemicals found on the surface of cuticle and sheath are illustrated in (Fig. 2.9)

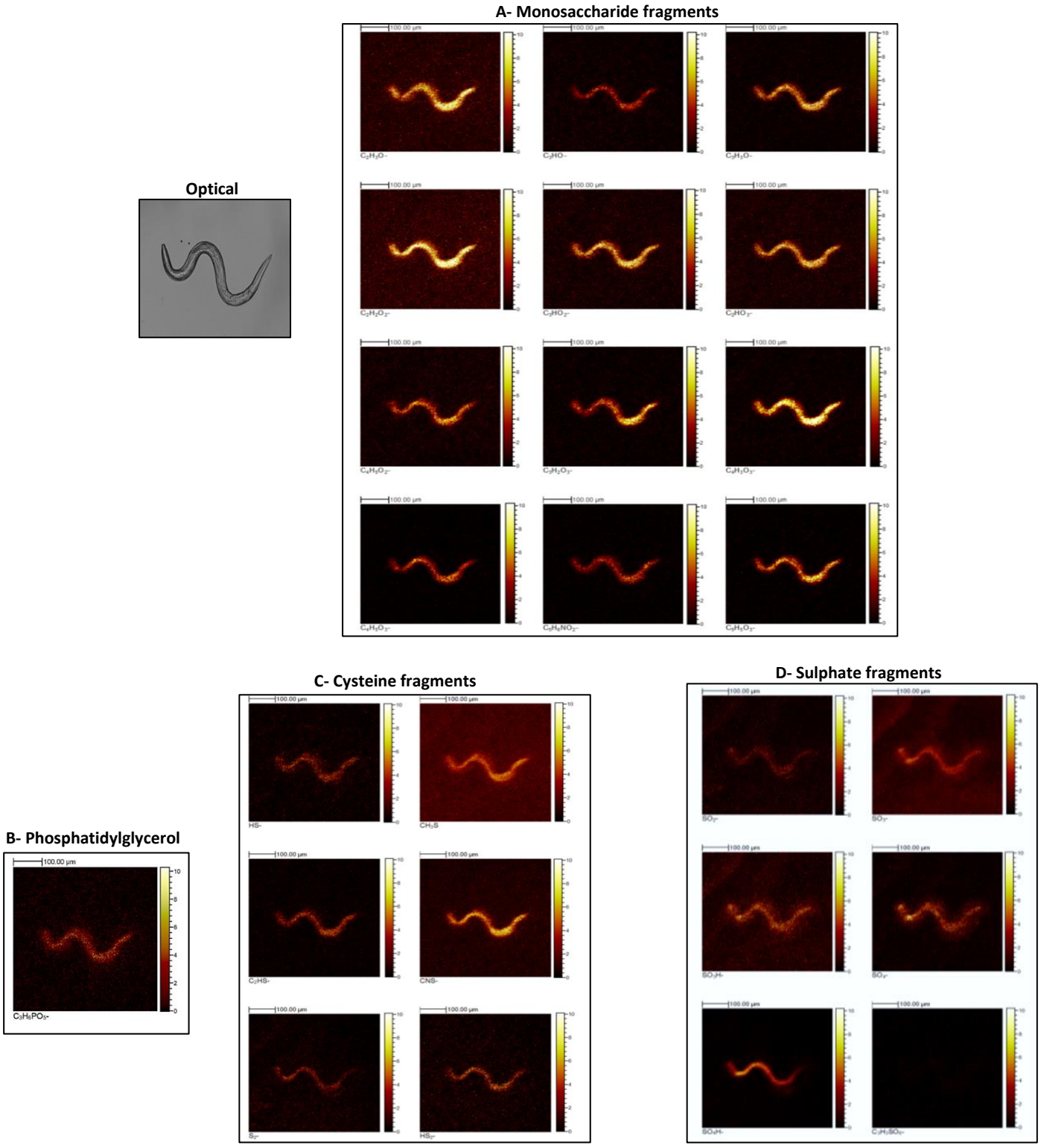

Figure 2.7: Ion images for the L3 cuticle. A) The L3 cuticle surface exhibited monosaccharide secondary ions. **B)** In addition, it contains phosphatidylglycerol head group. **C)** The surface of L3 elucidate expression of secondary ions associated with cysteine amino acids **D)** The L3 cuticle contained probable sulphate compounds, but not heparan sulphate. (n=3). Total loaded ions expressed on the larval cuticle are illustrated in (supplementary figure 2), while ion images for other L3 cuticles are illustrated in (supplementary figure 3&4).

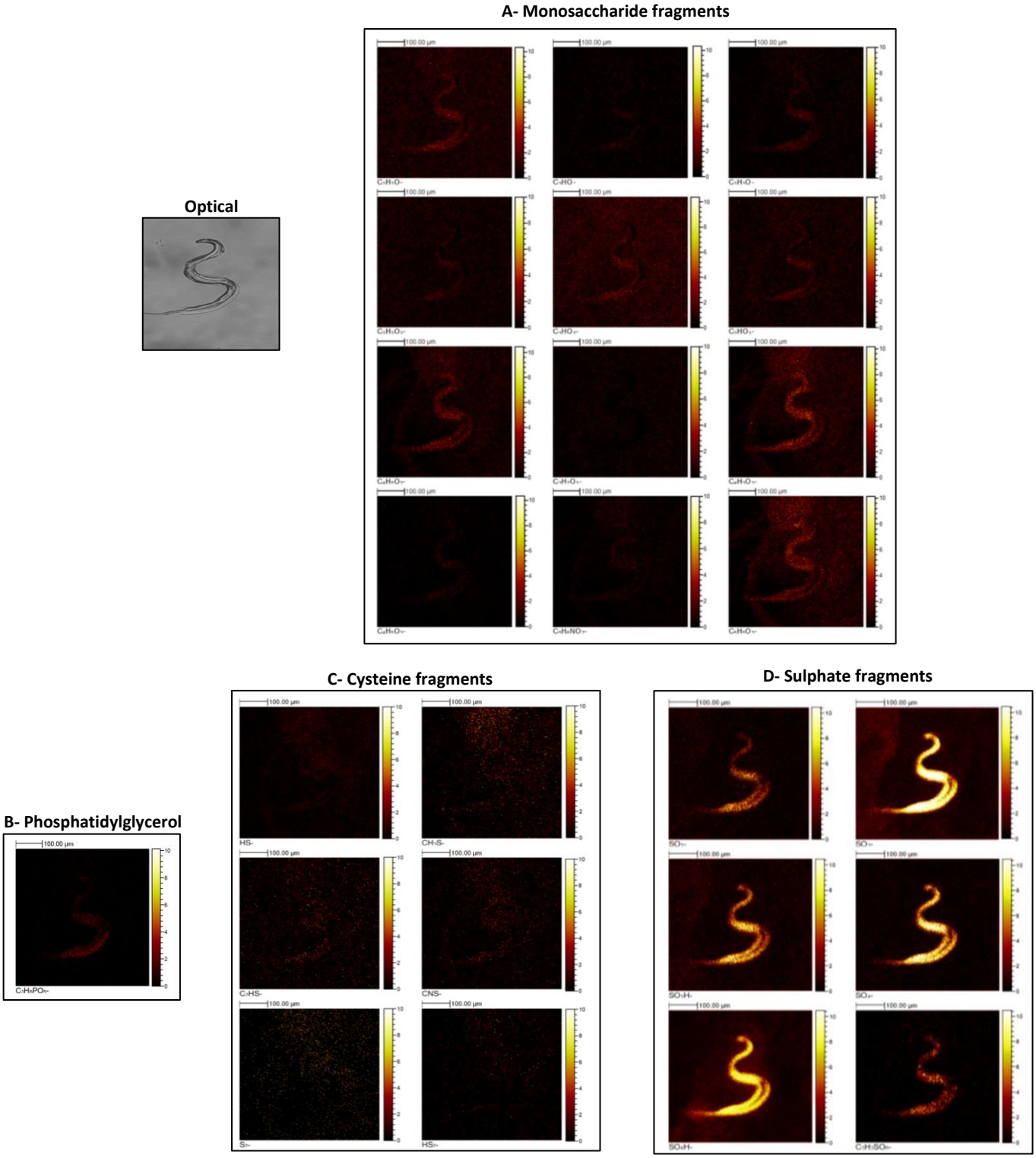

Figure 2.8: Ion images for the larval sheath. A) The surface of larval sheath exhibited no monosaccharide secondary ions**. B and C)** The sheath surface did not contain cysteine subunits and phosphatidylglycerol head group. **D)** The larval sheath surface exhibited sulphate-containing compounds and heparan sulphate. (n=3). Total loaded ions expressed on the larval cuticle are illustrated in (supplementary figure 2), while ion images for other larval sheaths are illustrated in (supplementary figure 5&6).

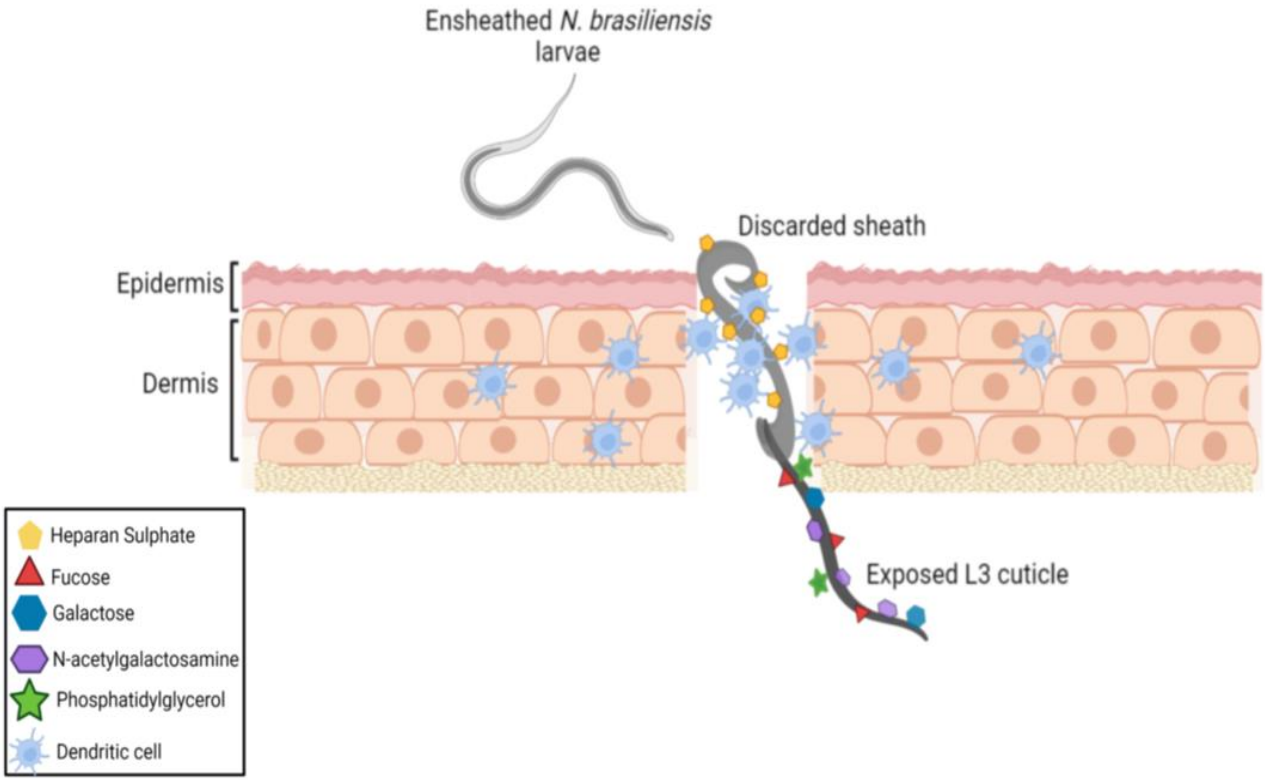

Figure 2.9: Schematic diagram showing the immune evasion strategy of *N. brasiliensis* infective larvae. DCs bind to ensheathed *N. brasiliensis* L3 and result in exsheathment of larvae. DCs aggregate to the discarded larval sheath due to the presence of heparan sulphate, providing an escape mechanism for the larval cuticle.

2.4 Discussion

The *N. americanus* hookworm infects 576–740 million people worldwide. Infection mainly occurs in impoverished rural areas and in tropical regions in individuals who inhabit endemic areas where they encounter soil containing the faecal material of infected individuals. Chronic infection can cause long-term consequences, including chronic iron deficiency anaemia. The consequences of chronic iron deficiency anaemia include physical and cognitive disabilities. Even though hookworm infection can be controlled effectively with anthelmintic drugs, reinfection after treatment is common and leads to the serious problem of drug resistance. Despite the chronicity of the infection, widespread prevalence, and the potential development of drug resistance, very little is known about how this parasite interacts in the early phase with the immune system. Therefore, there is an urgent needed to interrupt transmission of the parasite and thus control the infection [96,208,209].

N. americanus infective larvae are characterised by a non-notched pointed tail with an oesophageal bulb located at one-third of the length of the hookworm; infective L3 length ranges from 300–400 μm [210]. In contrast, the morphological features of *N. brasiliensis* L3 are a tube-shaped (enlarged) oesophagus that is located slightly posterior from the mouth. Furthermore, *N. brasiliensis* L3 have a short tail with a ventral protuberance, and the infective larval length ranges from 594–668 μm. Our findings are in line with those of Kassai [198] and confirm that the larvae used in the present study are the infective stage of *N. brasiliensis*.

The infective stage of *N. americanus* is surrounded by a sheath to protect the larval cuticle from desiccation in warm conditions, thus allowing larvae to survive long enough to encounter human host. Moreover, it is believed that the ensheathed larvae play a role in immune evasion during transdermal invasion through the exsheathment process [113,115]. *N. brasiliensis* infective stage retains its cuticle by a sheath that is discarded during skin penetration [211].

DCs are sentinels of immune system that constantly sense their surrounding environment using PRRs. They are abundant in barrier tissues and act as link between the innate and adaptive immune systems. Different pathogens and parasites have been shown to modulate DC function and therefore modulate the adaptive immune response. Therefore, given the potential role of DCs in shaping adaptive immune

responses, better understanding of mechanisms that modulate DC function could make them ideal for developing new treatment strategies against infectious or autoimmune diseases [212-214].

A previous study in our group showed that human DCs bind to ensheathed *N. americanus* infective larvae, initiating the exsheathment of *N. americanus* and exhibiting no interest in binding to the exposed L3 cuticle [201]. However, interaction of human DCs with the *N. americanus* L3 cuticle in the absence of the cuticle sheath has not yet been investigated. Therefore, we aimed to investigate whether human DCs were capable of interacting with the L3 cuticle in the absence of the larval sheath by using *N. brasiliensis* as a model system. Furthermore, we investigated the physical interaction between the ensheathed larvae of *N. brasiliensis* and DCs to determine whether *N. brasiliensis* infective larvae could behave similarly to *N. americanus*. Our results showed that iDCs exhibited no preference to interact with the *N. brasiliensis* L3 cuticle in the absence of the cuticle sheath after a 24-hour incubation period. iDCs aggregated and bound to the ensheathed L3, which promoted the exsheathment of larvae and subsequent movement away of the exposed larval cuticle. The latter were free to move without any aggregation of DCs around them, while DCs continuously sequestered onto the discarded sheath. It is reasonable to postulate that chemical structures are fundamentally different between the L3 cuticle and the sheath, which contributes to the observed immune evasion. Interestingly, our findings were in line with a study by Hassan et al.; confirm that *N. brasiliensis* behaves similarly to human *N. americanus*. In addition, our results were consistent with the observation of the diversionary activity of *N. americanus* larvae bypassing immune responses when penetrating host skin via exsheathment. It is remarkable that antibodies from infected individuals with *N. americanus* infection can bind to antigens on the surface of ensheathed larvae but fail to recognise antigens on the larval cuticle [106,114].

Given that there was minimal physical interaction between DCs and the *N. brasiliensis* L3 cuticle, and that they were attracted to the larval sheath, we hypothesised that the surface chemistries between the larval sheath and cuticle were different. To test our hypothesis, we aimed to identify antigenic molecules that may act as differential markers of the immune system using TOF-SIMS. Our data obtained from TOF-SIMS confirmed that ion assigned to lipid (such as phosphatidylglycerol), was

more highly expressed on the L3 cuticle than on the sheath. In contrast, ions assigned to sulphur-containing compounds and heparan sulphate were more prevalent on the larval sheath than on the cuticle. Our observation is in line with research showing that L3 cuticle of *N. americanus* infective contained phosphatidylglycerol whereas larval sheath exhibited heparan sulphate. Our finding confirm that chemical signatures express on *N. brasiliensis* larval cuticle and its sheath are similar to those signatures expressed on *N. americanus* larvae previously reported using TOF-SIMS [215]. These results provide additional support for the notion that *N. brasiliensis* could be a good experimental model to investigate the modulation of the immune response to a human hookworm. Interestingly our TOF-SIMS data elucidated that ion assigned to monosaccharides (such as galactose, GalNAc, fucose and L-rhamnose) and amino acids (such as cysteine) were more highly expresses on the L3 cuticle than on sheath. This observation in the line with studies showing that *N. americanus* contained a variety of carbohydrate moieties while that cysteine was present in many parasite species [167,197]. However, despite this rather detailed understanding of the surface chemistry of both *N. brasiliensis* and *N. americanus* the exact mechanism by which they modulate the immune response through these chemical signatures have yet to be explored. A study has shown that ability of phosphatidylglycerol lipid on inhibiting aggregation of pseudomonas aeruginosa to respiratory epithelial cell [216]. In addition, in vitro studied has shown that phosphatidylglycerol has a potent activity against respiratory syncytial virus in the way it can inhibit viral attachment to epithelial cells which in turn supress viral infection [217]. Considering the data obtained for exhibited phosphatidylglycerol ion on the *N. brasiliensis* larval cuticle (Fig. 2.8), it is reasonable to suggest that the presence of that ion could inhibit DCs aggregation around the L3 cuticle.

An intriguing observation was the presence of a cysteine protease enzyme secreted from the *N. americanus* L3 cuticle but not from ensheathed larvae. This finding suggests that enzymes might play a role in the exsheathment process, providing an escape for the L3 cuticle [218]. This is consistent with our finding where *N. brasiliensis* larval cuticle express cysteine secondary ions indicating that *N. brasiliensis* larvae have similar chemical signatures as *N. americanus* that play a role in evading immune system.

Several studies have demonstrated the biological relevance of monosaccharides in the modulation of the immune system and in the control of inflammation. An example, a study by Tohru et al. showed that various monosaccharides, namely fucose, L-rhamnose, and GalNAc, could suppress the immune response by inhibiting macrophage migration and leukocyte activity [219]. Furthermore, some pathogens that contain carbohydrates have an immunomodulatory effect on DCs and the activation of adaptive immune responses [220,221]. Therefore, the next chapter will explain in more detail the biological relevance of monosaccharides chemical signatures expresses on *N. brasiliensis* larval in modulating immune responses.

Heparan sulphate- and sulphur-containing compounds were more abundant on the larval sheath than on the cuticle. The sulphur-containing compounds present on nematodes are responsible for the formation of collagen cuticles, as reported by Kim et al. [222]. Interestingly, it has also been shown that expression of heparan sulphate on endothelial cells played an important role in the recruitment of DCs from peripheral tissues, while decreased expression of heparan sulphate reduced recruitment of DCs [223]. Therefore, our findings provide a rationale for why DCs bind to and sequester the larval sheath but not the L3 cuticle. More importantly, our results are in line with those showing that the *N. americanus* sheath exhibits heparan sulphate compounds [215].

2.5 Conclusion

The data presented in this chapter describe the physical interaction between *N. brasiliensis* infective L3 and iDCs that follows a similar pattern to what has been previously described for *N. americanus* namely induction of L3 exsheathment and aggregation of DCs around larval sheath. Moreover, examining the surface chemistry of *N. brasiliensis* cuticle and larval sheath revealed marked similarities to those of *N. americanus* which could also, at least partly, explain the differential interaction between DCs and cuticle versus larval sheath, Nevertheless, to understand the immunomodulatory properties of *N. brasiliensis* on immune cells, it is important to investigate the effect of the *N. brasiliensis* L3 cuticle on DC phenotype and function, and on T-cell activation. Therefore, co-culturing of *N. brasiliensis* L3 with human DCs was carried out and is detailed in the next chapter.

Chapter 3:

Investigating the impact of *Nippostrongylus brasiliensis* infective larvae on human dendritic cells and T-cell polarisation

3.1 Introduction

DCs are professional APCs and are amongst the first immune cells that interact with pathogens and act as a crucial link between the innate and adaptive immune responses [224]. These cells efficiently recognise and encounter antigens via PRRs in peripheral tissues [225]. Once DCs are activated, they undergo maturation through expression of co-stimulatory molecules and the production of cytokines. Mature DCs migrate to lymph nodes where they present peptide antigens derived from pathogens to naïve T cells and instruct their differentiation [226,227]. However, in the absence of maturation signals from DCs, they induce immune tolerance through the expression of co-inhibitory molecules, including programmed death ligand (PDL), and production of immunoregulatory cytokines (e.g., IL-10) that inhibit the activation and proliferation of T cells and promote generation of Tregs [228-230]. Therefore, the outcome of immune responses induced by DCs depends on the activation status of DCs, which determines their expression of surface markers and cytokine production. DCs can instruct the differentiation of naïve $CD4^+$ T cells into functional Th-cell phenotypes, which can be either pro-inflammatory (Th1, Th2, Th9, Th17) or anti-inflammatory (Treg) [231,232]. Each of the T-h-cell populations have a distinct function and role in the immune response to fight against a specific type of pathogen. For example, Th1 cells are responsible for inducing immunity against intracellular pathogens, resulting in the production of Th1 cytokines, such as IFN-γ whereas Th2 cells are involved in immune responses against allergens and extracellular pathogens, such as parasites, resulting in the production of Th2 cytokines, such as IL-4, IL-5, and IL-13 [233,234]. Furthermore, DCs can promote generation of Treg cells by inducing IL-10 to inhibit effector T-cell responses [235].

CLRs are a family of PRRs that are expressed on iDCs and play a role in the capture and internalisation of antigens for presentation to T cells to initiate adaptive immune responses. Among the CLRs expressed on DCs are MR and DC-SIGN; they are involved in the recognition of different carbohydrate moieties [236]. DC-SIGN recognises mannose and fucose structures on glycosylated pathogens, while MR recognises sulphated and mannosylated sugars [237]. Studies have shown that galactose and GalNAc can bind to CLRs, where 3- and 4-hydroxyl groups of galactose and GalNAc bind to the calcium ion in the CRD [238-241]. Engagement of CLRs with their specific glycosylated

ligands could influence immune modulatory properties of DCs, and downstream events leading to T-cell polarisation [237,242].

For example, ligation between CLRs and glycosylated antigens has been shown to modulate IDO activity in DCs. IDO is a tryptophan-degrading enzyme that is produced by immune cells upon stimulation with different stimuli [243]. A previous study has shown the relationship between IDO enzyme activity and CLR activation, where ligation of glycosylated allergens containing mannan to MR on DCs resulted in downregulation of IDO activity and generation of the Th2 phenotype [244]. Other studies have been reported that in vitro induction of IDO can control growth of various pathogens, including bacteria (e.g., group B streptococci) and parasites (e.g., *Toxoplasma gondii*) [245,246].

Studies have shown that some pathogens (e.g., parasites) and certain infections can utilise their carbohydrate moieties to engage CLRs on DCs to evade immune system surveillance. For example, *N. americanus* iL3 have been shown to evade immune detection and surveillance through a mechanism involving DC-SIGN and MR [201]. Another study showed that mycobacterial ManLAm, which contains mannose, was able to inhibit IL-12 production by DCs via MR ligation that in turn resulted in contribution to the persistence of *Mycobacterium tuberculosis* [247]. Moreover, human immunodeficiency virus (HIV) contains high levels of mannose moieties (gp120) on its envelop, which bind to DC-SIGN on DCs, thereby facilitating efficient transfer of the virus into T cells; the virus can subvert DC-SIGN function to evade immune detection [248,249].

Having shown the lack of physical interaction between *N. brasiliensis* infective L3 larvae and DCs, in this chapter I investigate any potential paracrine effect of L3 on DC phenotype, cytokine profile and IDO activity. In addition, we used DC-T-cell co-culture experiment to understand how this parasite shapes the outcome of adaptive immune response.

3.2 Materials and methods

3.2.1 Preparation of *N. brasiliensis* infective larvae

The infective larvae were prepared by the method described in Chapter 2 section 2.2.1.

3.2.2 Generation of human dendritic cells from peripheral blood mononuclear cells

Human DCs were generated by the method described in Chapter 2 section 2.2.2

3.2.3 Incubation of *N. brasiliensis* infective larvae with human immature dendritic cells

Human iDCs (2.5×10^5 cells/well) were seeded in a 24-well plate in complete RPMI 1640 medium and treated with ~50 exsheathed L3 (L3 cuticle), followed by incubation of the cells for 24 hours at 37ºC with 5% CO_2. For the positive control, iDCs stimulated with LPS from *E. coli* (10 ng/ml), and unstimulated DCs were used as controls.

3.2.4 Incubation of *N. brasiliensis* infective larvae with human mature dendritic cells

Human iDCs (2.5×10^5 cells/well) were seeded in a 24-well plate in complete RPMI 1640 medium, stimulated with LPS from *E. coli* (10 ng/ml), followed by treatment of the cells with 50 exsheathed L3. Cells were then incubated for 24 hours at 37ºC with 5% CO_2. iDCs stimulated with LPS from *E. coli* (10 ng/ml), and unstimulated DCs were used as controls.

3.2.5 Quantification of DCs viability assay

DC viability was quantified according to the method described in Chapter 2 section 2.2.4.

3.2.6 Flow cytometric analysis

Antibodies against DC-SIGN (clone DCN47.5), MR (clone DCN228), HLA-DR (clone RE A805), CD80 (clone RE A661), CD86 (clone RE A968), CD40 (clone REA733), PDL1 (clone REA1197) (all purchased from Miltenyi Biotec, UK), antibodies against AhR (clone FF3399) (eBioscience, UK) were used as DC markers, and non-reactive isotype-matched antibodies were used as controls. Antibodies against CD3 (clone BW264/56), CD45RA (clone T6D11), CD4 (clone REA623), CD25 (clone 4E3) (all from Miltenyi Biotec, UK), and FOXP3 (clone 236AE7) were used as T-cell markers. Non-reactive isotype-matched antibodies were used as controls.

3.2.6.1 Extracellular surface marker staining

Surface staining was performed. Briefly, cells were harvested from a well plate to FACS tubes and washed with cold PBS containing 0.5% bovine serum albumin and 0.1% sodium azide, which was named PBA (all from Sigma-Aldrich). Cells were stained by the addition of 2 µl of labelled antibody and incubated for 20 minutes at 4°C in the dark, then washed with cold PBA and fixed with 4% paraformaldehyde (Sigma-Aldrich). The samples were measured using an FC500 flow cytometer (Beckman Coulter, UK) and the resulting data were analysed using Kaluza software.

3.2.6.2 Intracellular surface marker staining

For intracellular staining, cells were harvested to FACS tubes and fixed with 4% paraformaldehyde for 10 minutes at room temperature, then washed twice with permeabilisation solution (PBS containing 0.5% bovine serum albumin, 0.1% sodium azide, and 0.5% saponin). Cells were then stained with labelled antibody for 30 minutes at 4°C in the dark, followed by washing twice with cold PBA, and the samples were measured using the FC500 flow cytometer (Beckman Coulter). The resulting data were analysed using Kaluza software.

3.2.7 Cytokine expression measurements

Following culture for 24 hours, the supernatant from the cells was collected and stored at -20°C until analysis. The concentrations of cytokines (IL-12p70, IL-10, TGF-β, IL-4, and IFN-γ) were measured using the DuoSet ELISA system (R&D System), according to the manufacturer's guidelines. The absorbance for each cytokine was measured at 450 nm using a Glomax Promega plate. Cytokine concentration levels were analysed using GraphPad Prism 7 from a standard curve.

3.2.8 Quantification of indoleamine-2,3-dioxygenase enzyme activity

This was done as previously described in our laboratory [203]. Briefly, human iDCs (2.5×10^5 cells/well) were seeded in a 24-well plate in complete RPMI 1640 medium, treated with exsheathed L3 (~50 larvae) in the presence or absence of LPS. The cells were supplemented with 100 µM L-tryptophan (Sigma-Aldrich). Cells were then incubated for 24 hours at 37°C with 5% CO_2. The cell supernatant was collected from each condition to determine IDO enzyme activity by measuring L-kynurenine (KYN) levels using a colourimetric assay. This step was performed by adding 50 µL of

30% trichloroacetic acid to 100 μL of cell supernatant in a microcentrifuge tube (Fisher Scientific) and centrifuging samples for 5 minutes at 13,000 rpm to separate the protein component from the KYN metabolite so that the protein component precipitated in the bottom of the tube, while KYN remained on top. After centrifugation, KYN was collected in a new microcentrifuge tube and 150 μL of Ehrlich reagent is added to each tube (5 ml of glacial acetic acid [Fisher Scientific] in 100 mg of 4-dimethylaminobenzaldehyde [Sigma]). We pipetted 200 μL of each condition into a well of a 96 well-plate and the absorbance was measured at a wavelength of 490 nm using a Promega GlowMax plate reader. The KYN standard absorbances were plotted against their corresponding known concentrations, from 0 μM to 200 μM; the sample KYN concentration was calculated from the standard curve by a linear equation.

3.2.9 Isolation of naïve CD45RO$^-$ T cells and dendritic cell-T-cell co-culture

Isolation of human naïve T cells was conducted according to established protocols in our laboratory [203]. Briefly, PBMCs were isolated from the buffy coat samples and counted to determine their number, and T cells were isolated using a pan-T-cell isolation kit (Miltenyi Biotec). Naïve CD45RO$^-$ T cells were depleted from the pan-T-cell population by applying negative selection using immunomagnetic beads (Miltenyi Biotec). The purity of the naïve T-cell population was confirmed by staining cell samples (2.5×10^5) with PE fluorescence antibody against human CD45RA. Then, autologous naïve T cells were co-cultured with DCs primed by infective larvae at a ratio of 1:10 (DC:T cell) in RPMI media supplemented with 5% human AB serum, 100 U/ml penicillin, 100 mg/ml streptomycin, and 2 mM L-glutamine. On day 3 after co-culture, fresh media was supplemented with 2 ng/ml of IL-2 (Miltenyi Biotec). On day 6, cells were harvested, counted, re-stimulated with 2 ug/ml of anti-CD3 (clone OKT3) and anti-CD28 (clone 28.2) and 1×10^5 cells/well were seeded in a flat-bottom 96-well plate and incubated for 24 hours. The cells were then stained for phenotypic identification, and the cell supernatants were collected for cytokine analysis.

3.2.10 RNA isolation, endpoint-PCR, and quantitative real-time PCR

To identify and quantify FOXP3 transcription factor expression, end-point polymerase chain reaction (PCR) and quantitative real-time PCR (qRT-PCR) were performed, respectively. Briefly, after 6 days of DC-T-cell co-culture, T cells were harvested, washed with PBS, and stored at -80˚C until RNA extraction. The RNA extraction was purified using the RNeasy kit (Qiagen) according to the manufacturer's protocol. We measured the concentration of the isolated RNA using a Nanodrop 1000 Spectrophotometer (Thermo Fisher Scientific, Pierce). cDNA was synthesised using a PCRBIO synthesis kit according to the manufacturer's instructions. Endpoint-PCR and real-time PCR were performed using Taq mix and SYBR Green qPCR Master Mix, respectively (PCR Biosystems). For the RT-PCR, the heat cycle reaction was started at 95°C for 2 minutes, 40 cycles at 95°C for 5 s, and 65°C for 25 s, followed by 95°C for 1 minute, 55°C for 30 s, and 95°C for 30 s. All sample values were normalized to GAPDH and were run in duplicate. The heat cycle for the end-point PCR was initiated at 95°C for 1 minute, followed by 40 cycles at 95°C for 15 s, 55°C for 15 s, 72°C for 30 s, and 72°C for 3 minutes. To inspect the size and integrity of the PCR product, samples were run on 2% agarose gel using an E-gel system with ethidium bromide (Invitrogen). Forward and reverse primers were used (Merck, UK) (Table 1).

Genes	Primer	Sequence (5`-3`)
GAPDH	Forward	5`-GAGTCAACGGATTTGGTCGT-3`
	Reverse	5`-GACAAGCT TCCCGTTCTCAG-3`
FOXP3	Forward	5`- GTGGCCCGGATGTGAGAA-3`
	Reverse	5`- GGAGCCCTTGTCGGATGATG-3`

Table 3.1: Forward and reversed primers used in PCR experiments.

3.2.11 Isolation of naïve CD45RO$^+$ T cells and suppression assay

CD45RO$^+$ memory T-cell isolation was performed by isolating pan-T cells from PBMCs, as described previously (see section 3.2.9). CD54RO$^+$ memory T cells were separated from the pan-T-cell population by applying positive selection using immunomagnetic beads (Miltenyi Biotec). A suppression assay was performed via co-culture of naïve T cells primed by DCs stimulated with L3

using CD54RO$^+$ autologous memory T cells isolated from the buffy coat. Briefly, CD45RO$^+$ autologous memory T cells were removed from liquid nitrogen, washed, and counted. Prior to seeding, cells were incubated for 20 minutes in the dark at 37˚C with 1 ml (5 μM) of CFSE cell proliferation solution (Thermo Fisher Scientific, U.K.). Cells were then washed, suspended in complete culture media (5% human AB serum, 1% penicillin/streptomycin, and 1% L-glutamine), and incubated for 5 minutes in the dark at 37˚C. The cells were then washed and suspended in complete culture media. Then, unlabelled T cells from the DC-T-cell co-cultures were harvested on day 6, counted, and co-cultured with CFSE-labelled CD45RO$^+$ autologous memory T cells in 96-well round-bottom plates (Corning Life Sciences) at a ratio of 1:8 (CD4$^+$CD25$^+$FOXP3$^+$: CD45RO$^+$) in complete RPMI media (5% human AB serum, 1% penicillin/streptomycin, and 1% L-glutamine) for 72 hours. T cells were harvested, stimulated with anti-CD3 antibody and anti-CD28 antibody, seeded in flat-bottom 96-well plates (1×10^5 cells/well), and incubated for 24 hours. The cells were then harvested, washed, and fixed using 4% paraformaldehyde solution. Flow cytometry was performed on the FC500 (Beckman Coulter), and cell proliferation and data analysis were determined using Kaluza software (version 2.1).

3.2.12 Statistical analysis

Data were analysed and evaluated using GraphPad Prism version 7.02 (GraphPad Software, San Diego, CA). Values are presented as mean ± SEM, and statistical significance was determined by one-way ANOVA when comparing two groups. A p-value <0.05 was considered statistically significant.

3.3 Results

3.3.1 Dendritic cells adopt a tolerogenic phenotype following exposure to *N. brasiliensis* infective third-stage larvae

iDCs were generated from monocytes that were isolated from PBMCs, as described previously see section (2.2.2). The purity of the monocytes was tested using flow cytometry, data showed 97% viability for isolated monocyte (Fig. 3.1). To confirm differentiation of monocytes to iDCs, iDCs generation on day 6 was analysed for expression of CD11c and CD14 using flow cytometry. Results in (Fig. 3.2) show that iDCs expressed 99.5% of CD11c and almost no CD14, indicating the successful generation of iDCs on day 6.

To investigate the effect of *N. brasiliensis* L3 on DC phenotype, iDCs (2.5×10^5 cells/well) were coculture with exsheathed L3 larvae (n=50) and incubated for 24 hours at 37°C in 5% CO_2. In a parallel positive-control sample, cells were stimulated with 10 ng/ml of LPS, and untreated cells were used as a negative control. DC phenotype was assessed by quantifying expression of cell-surface markers, including DC-SIGN (CD209), MR (CD206), HLA-DR, CD80, CD86, and PDL-1. Data obtained from flow cytometry showed no significant increase in the expression of maturation markers, including HLA-DR, CD86, CD80, and CD40 in L3-treated cells compared with iDCs (Fig. 3.3). In addition, MR (CD206) and DC-SIGN (CD209) expression were significantly downregulated in DCs primed with infective larvae compared with untreated cells. Interestingly, expression of programmed death-ligand-1 (PDL-1) was significantly increased following exposure to L3 compared with untreated cells (Fig. 3.3). Collectively, these results support the generation of a regulatory DC phenotype after treatment with *N. brasiliensis* L3. All data are shown on a histogram (supplementary figure 7). Additionally, DC viability was monitored following these experiments using LIVE/DEAD staining, and the data showed that ~90% of DCs were viable after co-culture with L3 (Fig. 3.4).

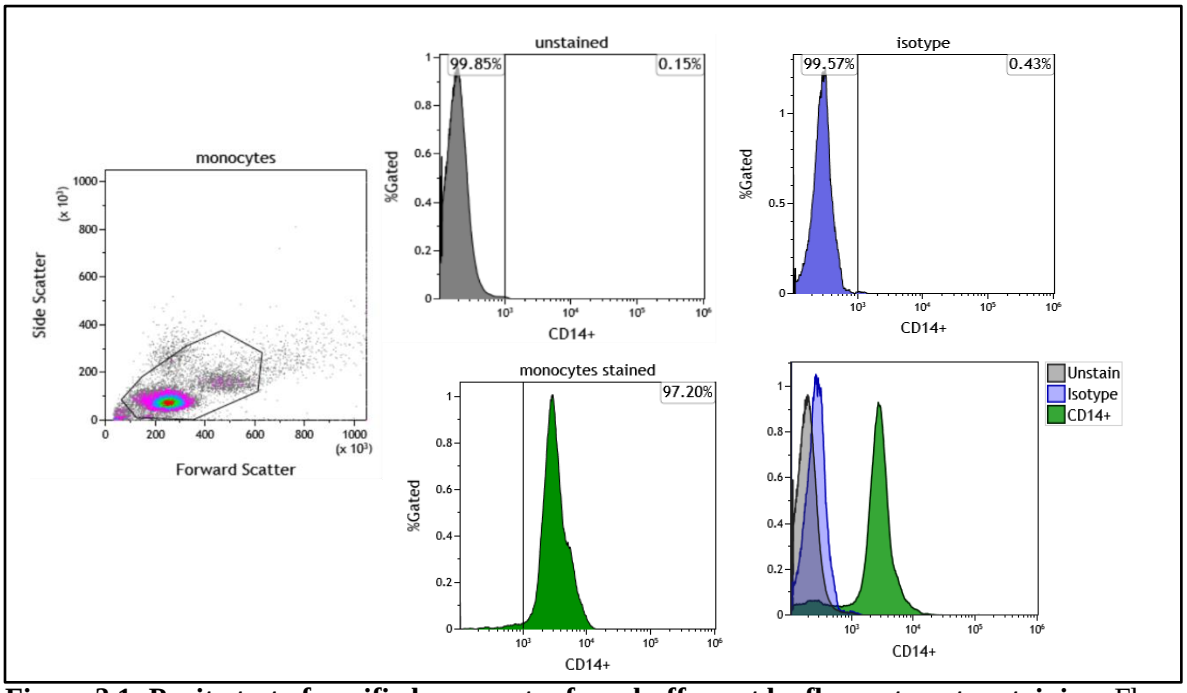

Figure 3.1: Purity test of purified monocytes from buffy coat by flow cytometry staining. Flow cytometry data showed that 97% $CD14^+$ monocytes were successfully isolated from the buffy coat. Quadrants were set according to unstained cells in a way that 99% of the cells were in the left quadrants. Data from three independent donors (n=3).

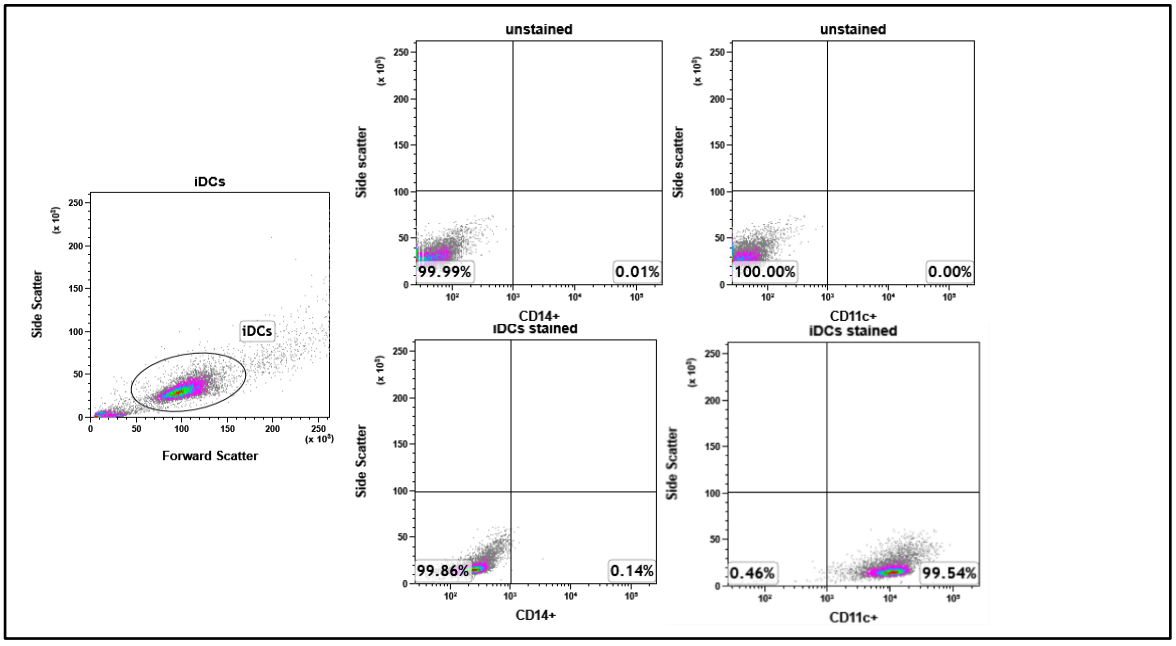

Figure 3.2: Flow cytometry staining for immature DCs. Flow cytometry data shows that generated iDCs expressed 93% CD11c with no expression of CD14, indicating the generation of iDCs. Quadrants were set according to unstained cells in a way that 99% of the cells were in the left or bottom quadrants. Data from of three independent donors (n=3).

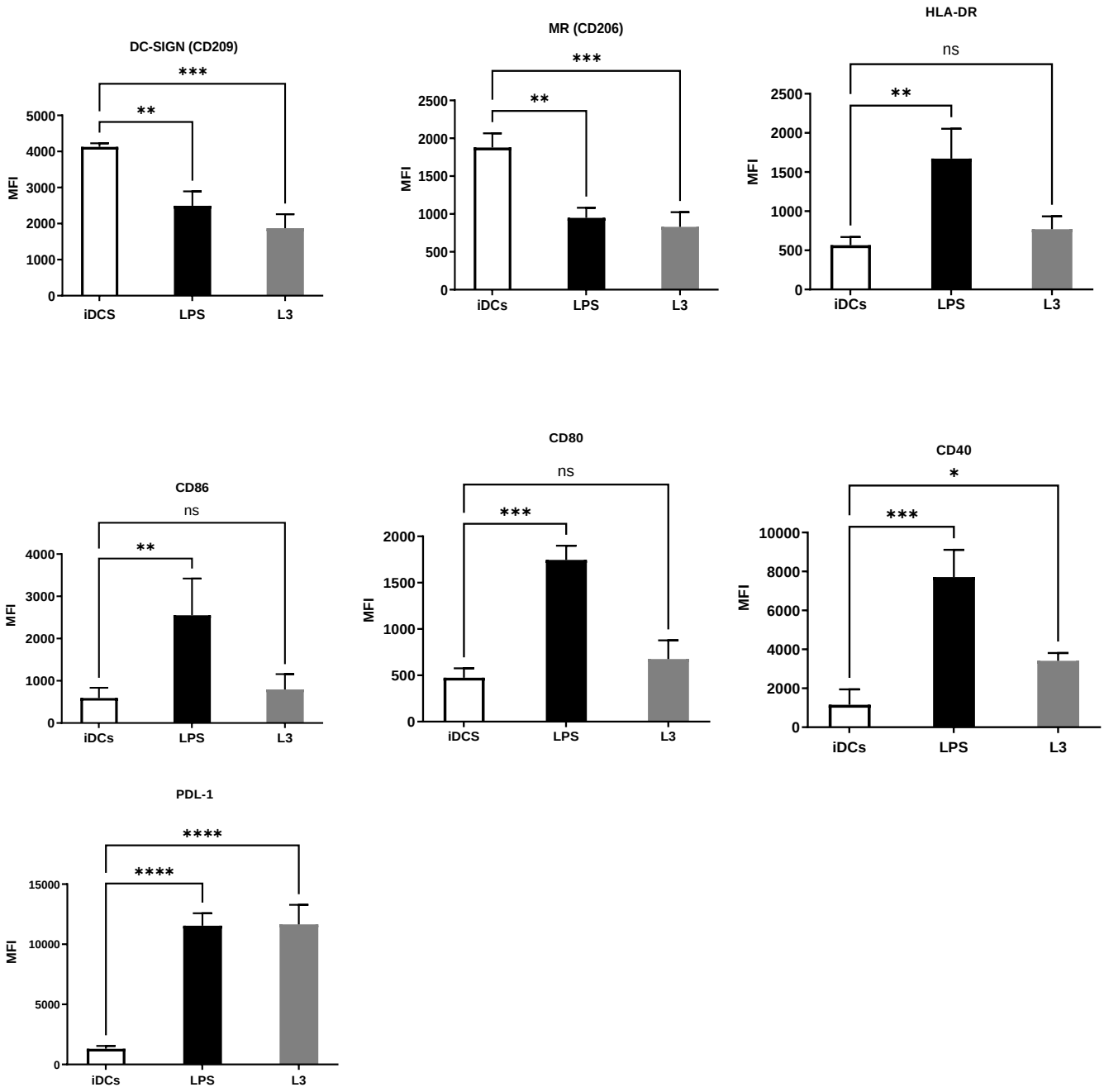

Figure 3.3: The expression of DC receptor molecules in response to stimulation with infective L3 or LPS. Median fluorescence intensity was obtained from flow cytometry data and analysed. All data are shown as mean ± SD for three independent donors (n = 3). *p<0.05, **p<0.01, ***p< 0.001, ****p <0.0001. Data from three independent experiments using DCs from three different donors (n=3).

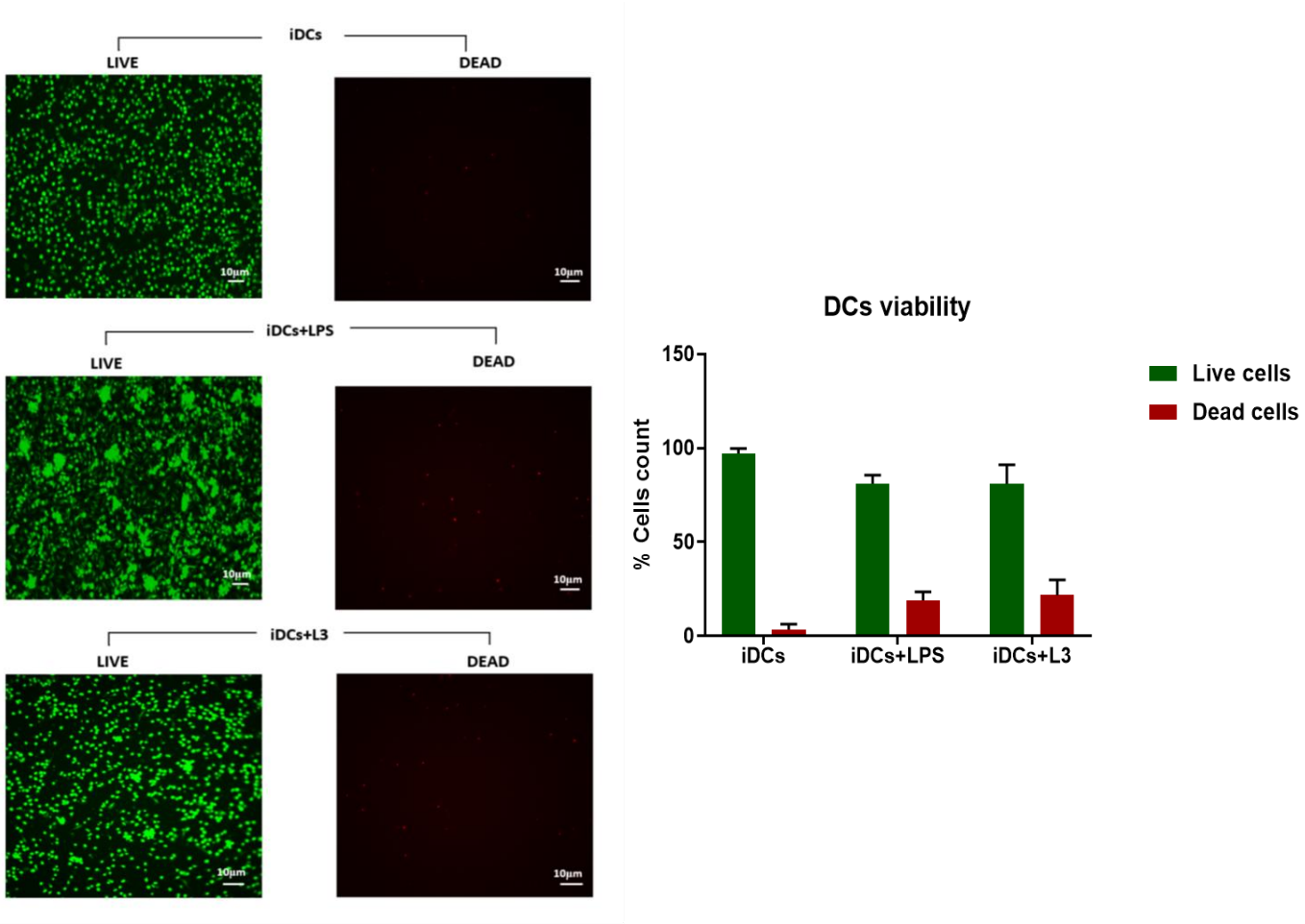

Figure 3.4: The viability of DCs 24 hours after treatment with *N. brasiliensis* L3. Quantification of LIVE/DEAD fluorescence cells was performed using ImageJ software. Briefly, in ImageJ software: open image > change image type to 8-bit > adjust threshold to highlight cells to be counted, process > binary > convert to mask, analyse > analyse particles to count all cells. The results showed that >90% of DCs were alive after treatment with L3. Data from three independent experiments using DCs from three different donors (n=3).

3.3.2 Effects of *N. brasiliensis* L3 on cytokines production by dendritic cells

DC phenotype was further characterised by assessing the production of cytokines, including IL-12p70 and IL-10 as signature pro and anti-inflammatory cytokines respectively. A cytokine assay was performed using cell-free supernatants collected following DC stimulation with either LPS or *N. brasiliensis* L3 after 24 hours. The results showed significant induction of IL-10 in DCs stimulated with *N. brasiliensis* L3 compared with untreated cells (Fig. 3.5A), whereas no significant increase was observed in IL-12p70 expression (Fig. 3.5B). These findings indicated that DCs treated with L3 released high levels of a potent anti-inflammatory cytokines, which together with their low expression of maturation markers could support priming naïve T cells towards Tregs.

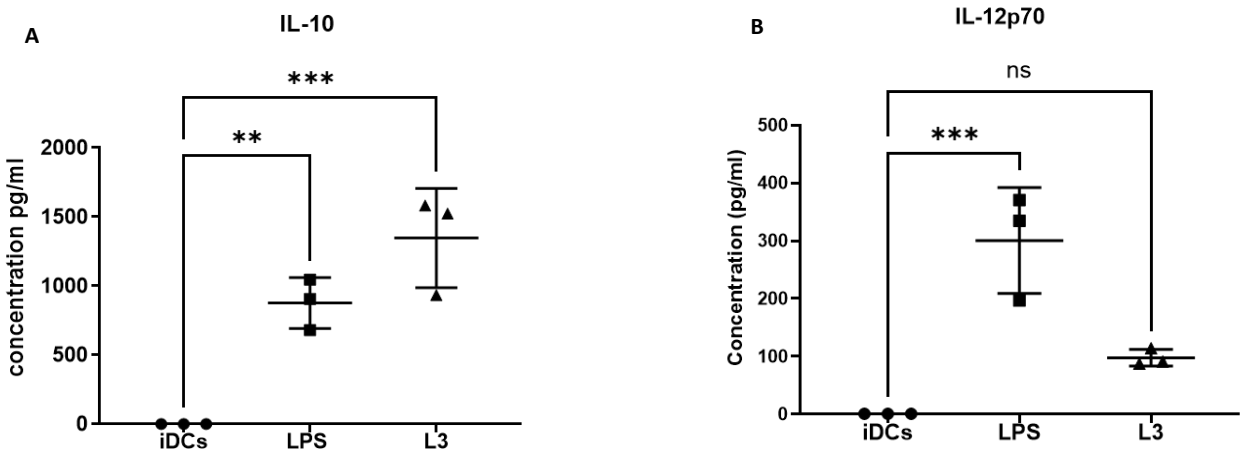

Figure 3.5: Cytokine production by DCs in response to stimulation with either LPS or *N. brasiliensis* infective larvae. A) & B) The culture supernatant was analysed for cytokine production by ELISA. DCs stimulated with infective larvae induced high levels of IL-10 but not IL-12. In contrast, cells stimulated with LPS produced high levels of pro-inflammatory cytokine IL-12. All data are shown as mean ± SD for three independent donors (n = 3). *p<0.05, **p<0.01, ***p< 0.001, ****p <0.0001. Data from three independent experiments using DCs from three different donors (n=3).

3.3.3 Indoleamine-2,3-dioxygenase activity in response to *N. brasiliensis* L3

Activated DCs have increased IDO enzyme levels, which converts L-tryptophan into KYN metabolites that contribute to a pro-inflammatory response. In addition, the AhR is a ligand-dependent transcription factor that has been shown to be involved in IDO activity, where a change in IDO enzyme is directly proportional to AhR expression [78]. Therefore, to investigate whether L3 produce an anti-inflammatory environment, IDO activity and AhR expression were analysed. Results showed that no significant induction of IDO enzyme was seen in DCs after L3 stimulation compared with untreated DCs; however, there was a significant increase in IDO activity in LPS-stimulated DCs compared with unstimulated DCs as expected (Fig. 3.6A). Next, we studied potential impact of L3 on AhR expression in iDCs and again not surprisingly we observed no induction of AhR expression followed L3 stimulation. In contrast, AhR expression significantly increased upon LPS stimulation compared with unstimulated cells (Fig. 3.6B) (supplementary figure 8). This finding was consistent with our IDO activity data, where AhR expression was directly correlated with IDO induction. Collectively, these results indicated that *N. brasiliensis* L3 increased the production of IL-10 by iDCs, which is in line with previous observations using *N. americanus* in a similar experimental set up [201].

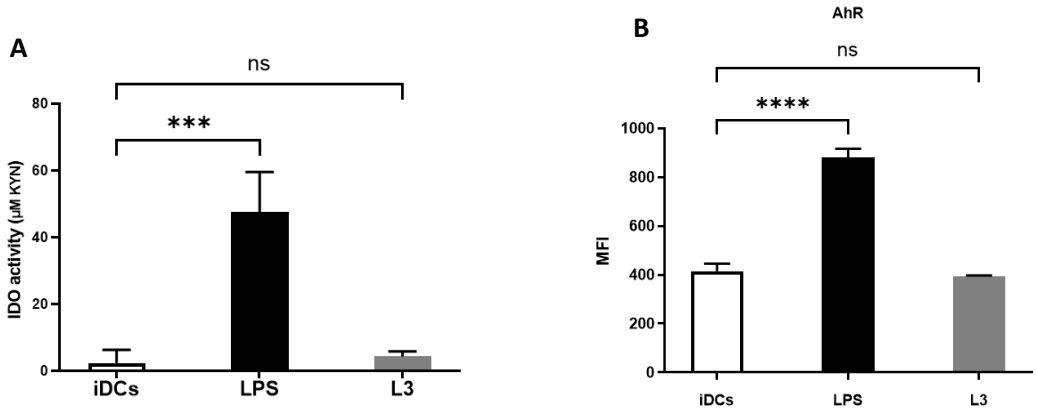

Figure 3.6. Induction of indoleamine-2,3-dioxygenase (IDO) activity in response to *N. brasiliensis* L3 secretion in human DCs. (A) IDO activity in DCs was stimulated with either LPS or L3 secretions. **(B)** Flow cytometry analysis of aryl hydrocarbon receptor (AhR) expression in the DCs stimulated with either LPS or L3 larvae. Data are shown as mean ± SD of three independent donors (n = 3).

3.3.4 *N. brasiliensis* L3 suppressed the immune stimulatory effects of LPS

As shown in this study, iDCs readily undergo maturation upon exposure to LPS. To further investigate the modulatory effect of the *N. brasiliensis* larvae, we assessed the influence of L3 on DC maturation, in response to LPS stimulation. DCs were treated with infective larvae in the presence of 10 ng/ml LPS. Data showed that DCs exhibited decreased expression of maturation markers, including HLA-DR, CD86, CD80, and CD40, in response to LPS in the presence of L3 compared with LPS alone (Fig. 3.7). Similarly, L3 significantly suppressed LPS-induced IL-12 production (Fig. 3.8A) and IDO activity (Fig. 3.8B). Together, these data showed that the infective larvae of *N. brasiliensis* negatively modulated the immune response through TLR4 signalling, which could alter the immune function of DCs.

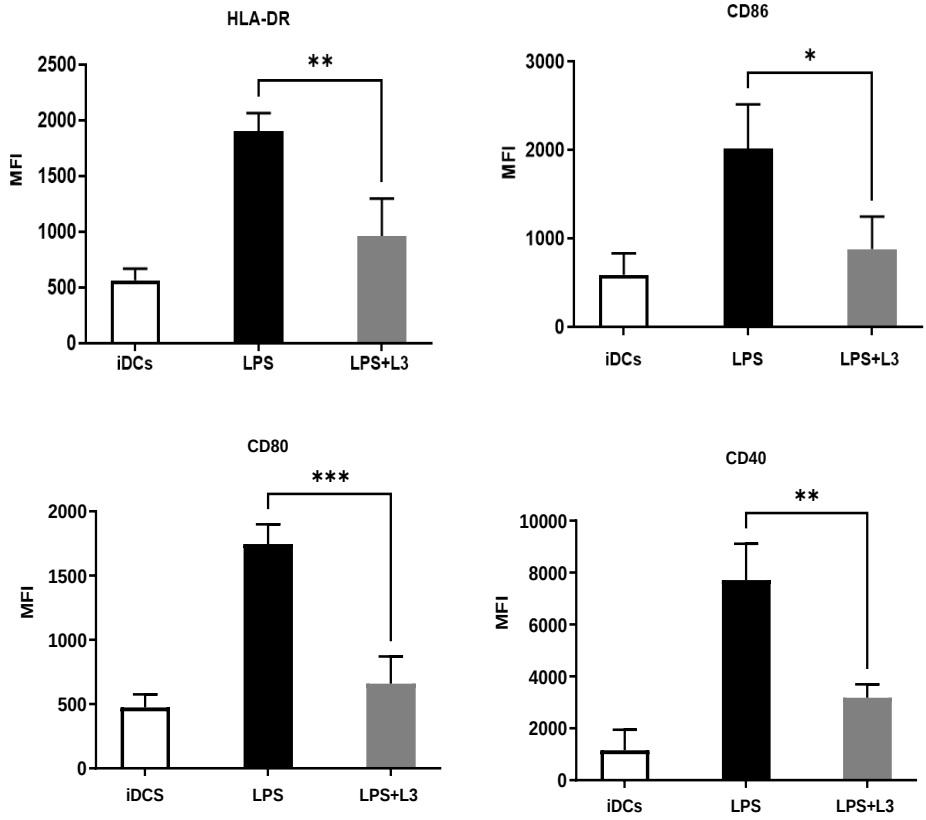

Figure 3.7: TLR-induced signalling is negatively regulated by *N. brasiliensis* L3. Flow cytometry data of DC surface marker expression after stimulation with LPS in the presence of infective larvae were obtained and analysed for median fluorescence intensity. Data are shown as mean ± SD of three independent donors (n = 3).

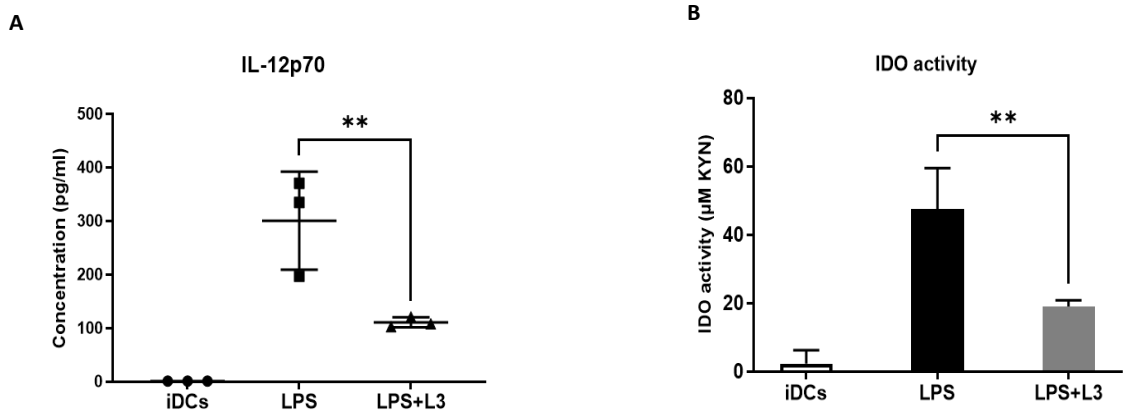

Figure 3.8: *N. brasiliensis* L3 modulates LPS-induced cytokine production and IDO activity. A) LPS-induced IL-12 production was suppressed in the presence of iL3. **B)** IDO activity decreased in DCs stimulated with LPS in the presence of L3. Data are shown as mean ± SD of three independent donors (n = 3). *p<0.05, **p<0.01, ***p< 0.001, ****p <0.0001.

3.3.5 *N. brasiliensis* infective larvae modulate dendritic cell-induced T-cell polarisation

Naïve CD45RA^{+} T cells were isolated from PBMCs, as described previously see section 3.2.9. After the isolation process, the purity of the purified naïve T-cell population was assessed using flow cytometry. Fig. 3.9 shows the expression of CD45RA in naïve T cells, which confirmed the isolation of the target cells from PBMCs.

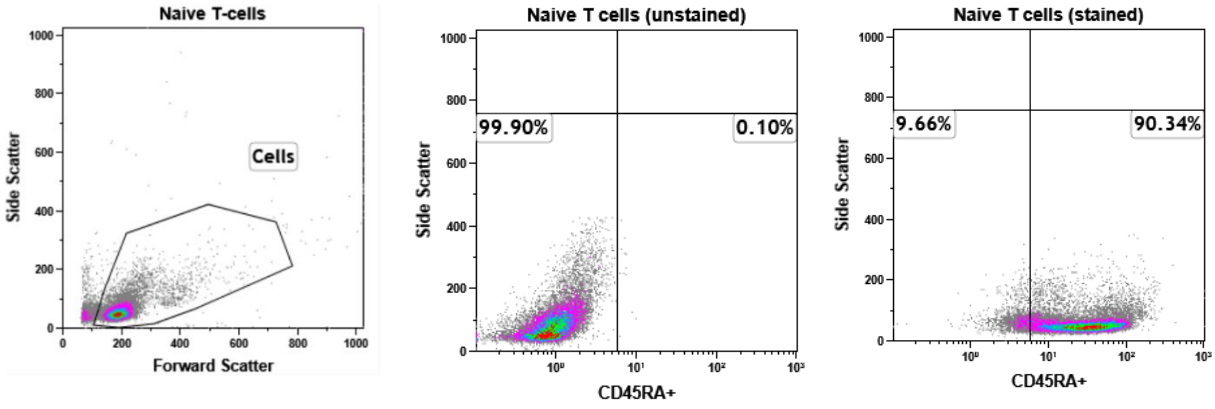

Figure 3.9: Analysis of isolated naïve T cells using flow cytometry. The population of naïve T cells showed 90% expression of CD45RA, which indicated successful isolation of the target cells. Data are from three independent experiments using naïve T cells from three different donors (n=3).

Then purified naïve T cells were preserved in liquid nitrogen for 7 days while iDCs were generated from autologous monocytes isolated from PBMCs (Fig. 3.10). On co-culture day and after thawing naïve T cells from liquid nitrogen, cells were assessed for their viability and activation status. Viability assays were performed using LIVE/DEAD staining and a Countess™ II FL Automated Cell Counter (see section 2.2.4). Activation status for naïve T cells was assessed by observing CD25 as an indicator for activation. Fig. 3.11 demonstrates that liquid nitrogen preservation did not affect naïve T-cell viability, as 92% of the cells were living after liquid nitrogen preservation. We then evaluated CD25 marker expression on naïve T cells to confirm steady state after defrosting from liquid nitrogen. Fig. 3.12 shows that naïve T cells did not express the CD25 activation marker, indicating that the cells were not activated maintaining their naïve status. Collectively, these data confirm the quality of cells generated after the isolation and preservation process, which allowed us to move forward to perform the autologous co-culture experiments.

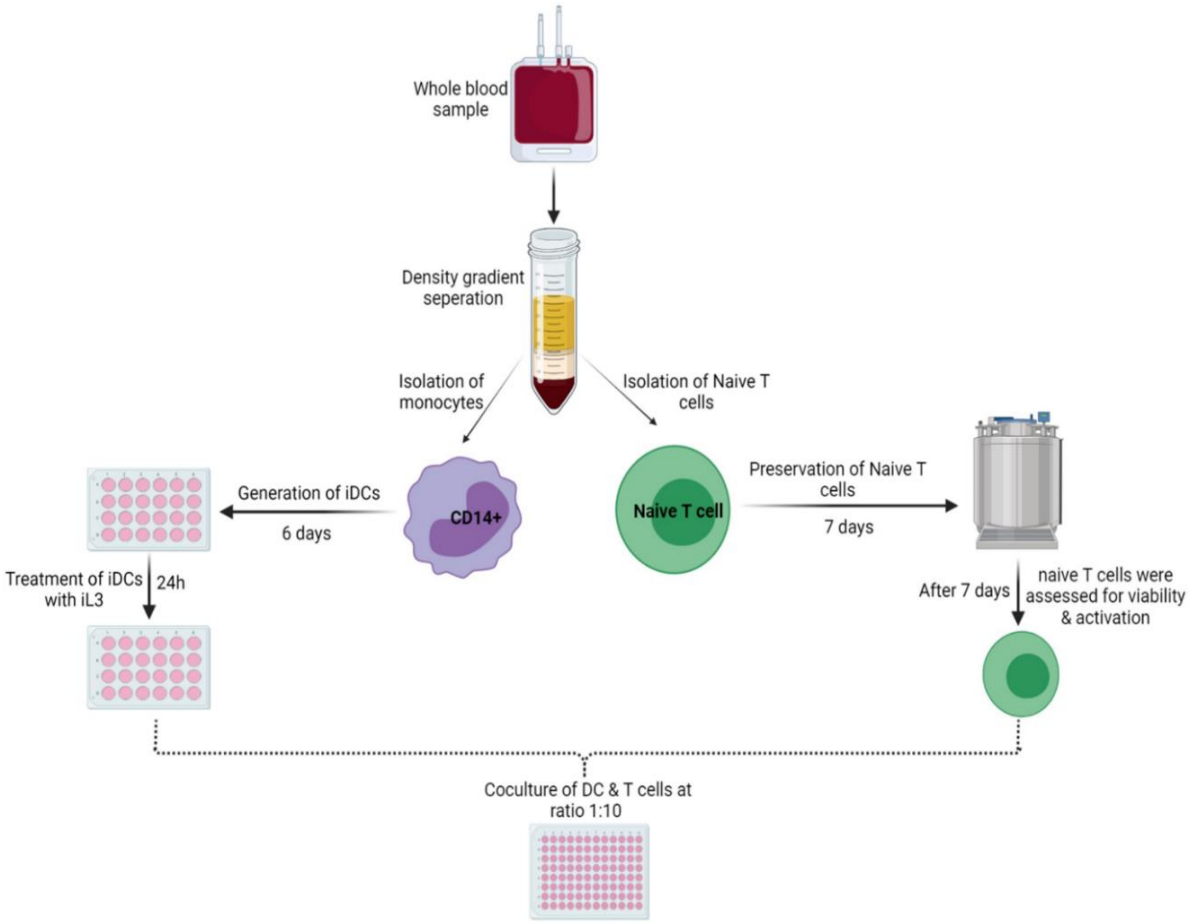

Figure 3.10: Schematic method of T-cell preservation in liquid nitrogen and autologous co-culture. The process shows isolation of monocytes and naïve T cells from a buffy coat sample by gradient separation using magnetic beads. After isolation of both populations, monocytes underwent a differentiation process into iDCs for 6 days, followed by treatment of the generated iDCs with iL3 (24 hours), while the naïve were preserved in liquid nitrogen. The naïve T cells were then defrosted, assessed for their viability and activation, and then co-cultured with pre-treated DCs at ratio or 1:10 (DCs:T cells) for 6 days. Co-culture cells were supplemented with IL-2 on day 3 and stimulated with anti-CD3 and anti-CD28 on day 6. Cell phenotype was assessed using flow cytometry, cytokine secretion by ELISA, and gene expression using PCR experiments.

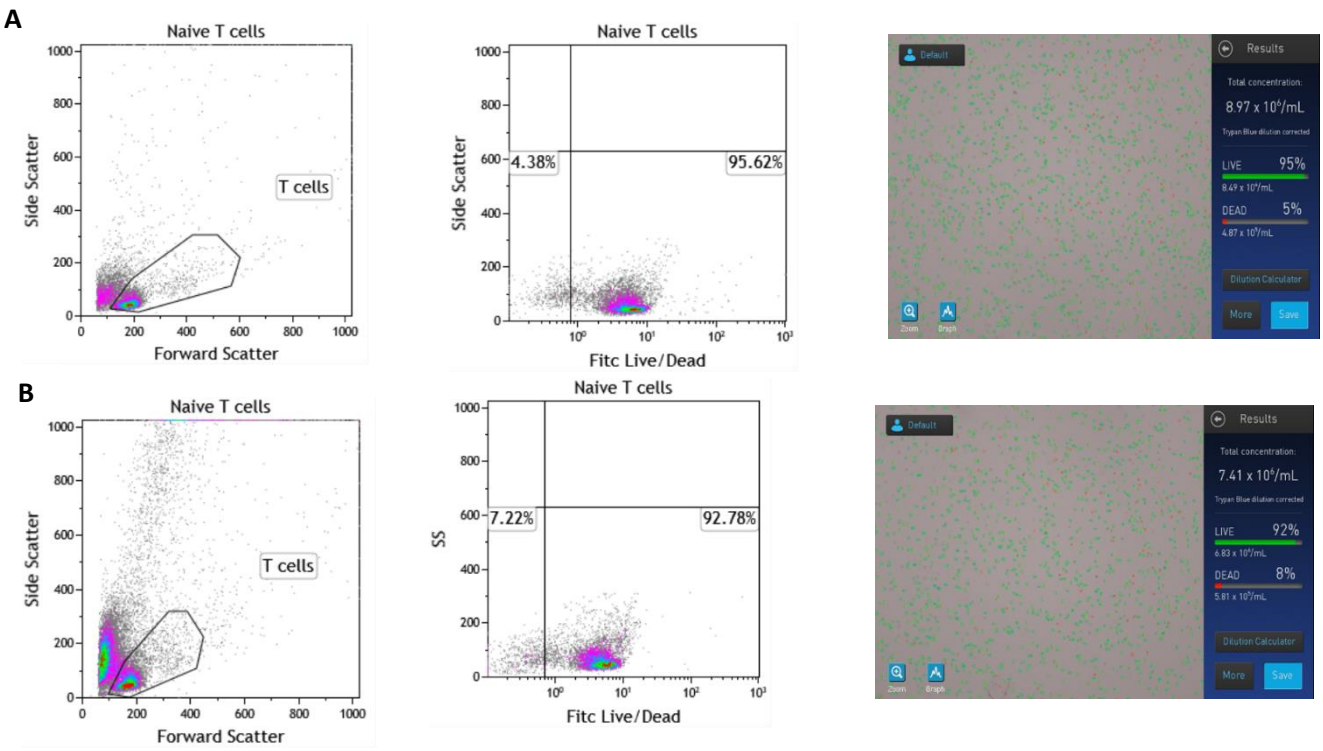

Figure 3.11: Viability of naïve T cells using LIVE/DEAD flow cytometry staining and Countess™ II FL Automated Cell Counter after isolation and liquid nitrogen preservation. A) Data show that 95% of naïve T cells were alive after isolation from PBMCs by using LIVE/DEAD flow staining; similar viability was observed using a Countess™ II FL Automated Cell Counter. **B)** There was no marked reduction in live cell numbers after liquid nitrogen thawing comparing to the naïve T cell numbers after the isolation process. Data are from three independent experiments using naïve T cells from three different donors (n=3).

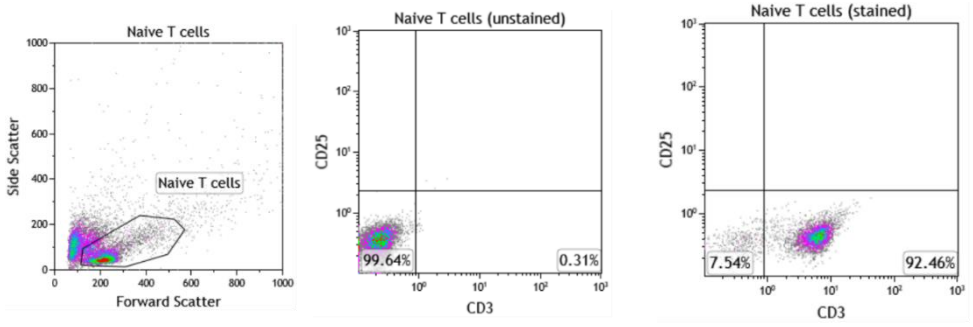

Figure 3.12: CD25 expression in CD3⁺ T cells after preservation in liquid nitrogen. Naïve T cells showed no expression of CD25 activation marker after storage in liquid nitrogen. Data are from three independent experiments using naïve T cells from three different donors (n=3).

Considering the noticeable effect of the L3 on DC surface phenotypic markers and cytokine profile, we investigated the impact of L3 primed DCs on downstream T-cell differentiation by performing co-culture studies where naïve T cells were co-cultured with DCs pre-stimulated with L3 in the presence or absence of LPS for 6 days. In parallel, DCs pre-treated with 10 ng/ml LPS co-cultured with naïve T cells were used as a positive control, while untreated iDCs co-cultured with naïve T cells were used as a negative control. On day 3, co-culture cells were supplemented with IL-2, and on day 6, cells were stimulated with anti-CD3 and anti-CD28 for 24 hours followed by analysing T-cells phenotype and cytokine profile. Phenotypic analysis of T cells was performed by measuring FOXP3 and CD25 expression in CD4+ cell population. Representative data shown in Fig. 3.13 show that L3 primed DCs support a marked increase in the number of CD25+/FOXP3+ cells indicating differentiation of naïve T cells towards a Treg phenotype (64%) that was greater than the impact of LPS stimulated DCs which also supported Treg phenotype (47%).

We also measured the level of key cytokines in the co-culture supernatant, including IL-10 and TGF-β as prototypic Treg cytokines. Data presented in Figure 3.14 shows increased IL-10 and TGF-β production in T cells co-cultured with L3-treated DCs in the presence or absence of LPS. Overall, the co-culture results indicated that L3 modulated DC function, which led to the induction of CD4+FOXP3+CD25high Tregs.

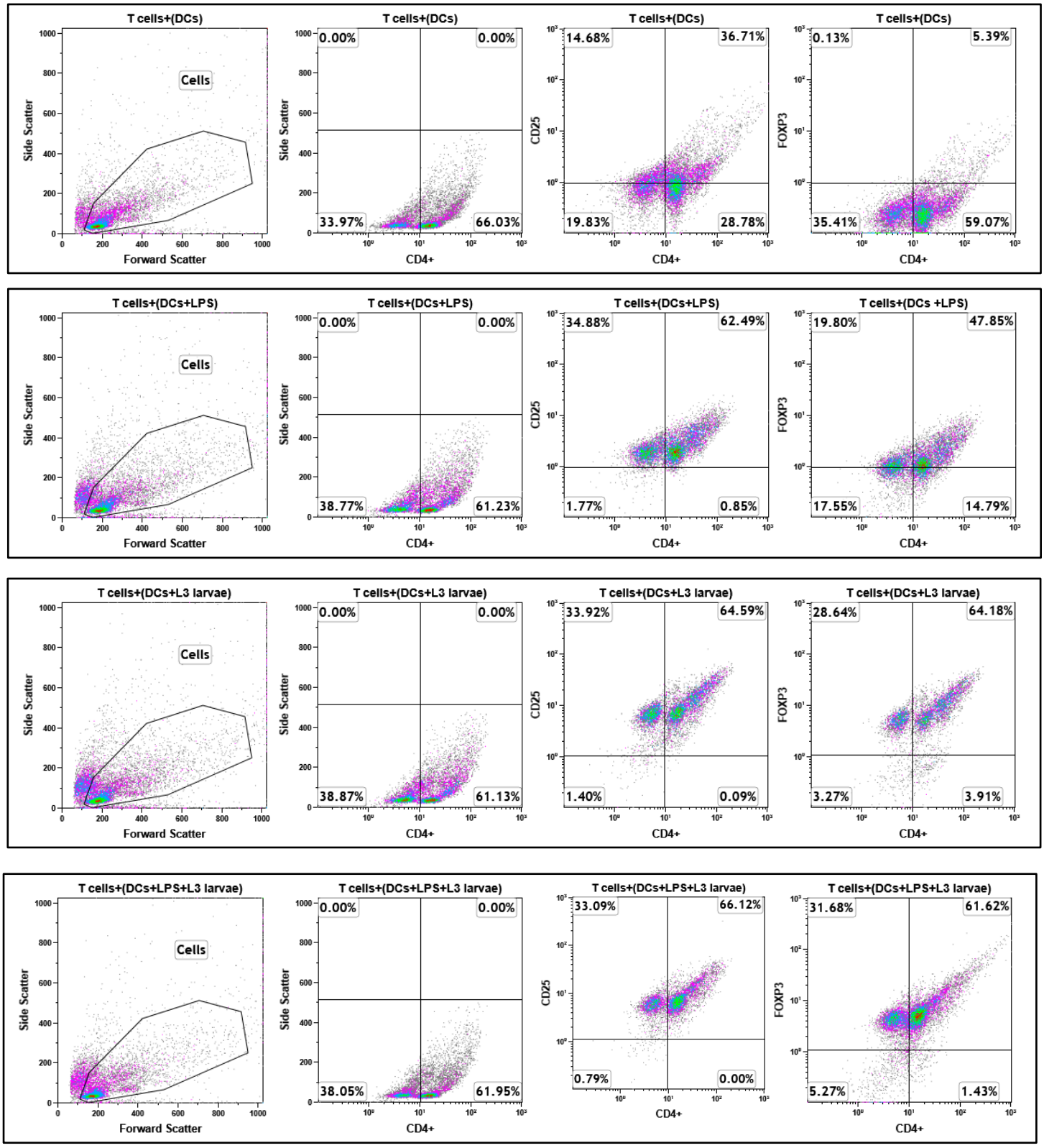

Figure 3.13: Flow cytometry phenotypic analysis of naïve T cells co-cultured with primed DCs. Dot plot data confirms expression of $CD4^+$ cell populations under all conditions. The presence of CD25 and FOXP3 expression in the $CD4^+$ T-cell population can be seen under L3 conditions in the presence and absence of LPS. Data are from three independent experiments using naïve T cells from three different donors (n=3).

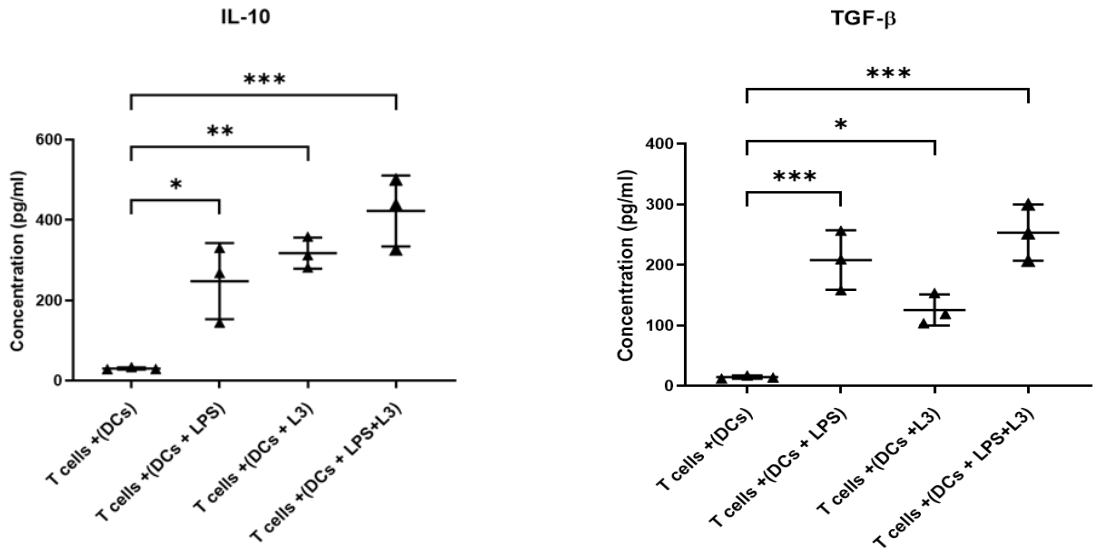

Figure 3.14: Investigation of the effect of infective larvae on T-cell differentiation using cytokine production. Marked increase in IL-10 production was observed in all conditions compared with the control. Intriguingly, an increase in TGF-β was noted under the same conditions. Data are reported as mean ± S.D of three independent experiments using cell supernatants from three different donors (n=3).

3.3.6 Quantification of FOXP3 expression using polymerase chain reaction

The increased production of IL-10 and TGF-β that we observed in T cells co-cultured with DCs pre-stimulated with infective larvae was similar to findings that have been reported in the context of *N. americanus* [271]. Based on this observation, we hypothesised that the naïve T cells had acquired the anti-inflammatory/regulatory phenotype; therefore, to further confirm we investigated FOXP3 mRNA expression using end-point and RT-PCR. The data obtained from end-point PCR indicated an increase in the level of FOXP3 expression in T cells co-cultured with infective L3-primed DCs compared to compared with the control (LPS only or no-stimulation). (Fig. 3.15A). To further determine the levels of FOXP3 expression in these cells we used RT-PCR that showed a significant increase in FOXP3 expression in T cells co-cultured with DCs primed with infective L3, indicating that Treg cells were generated under these conditions (Fig. 3.15B). More importantly, these findings support that *N. brasiliensis* infective larvae can regulate the human immune system and suggests the use of these larvae as a model to investigate the modulation of the immune response by the human hookworm.

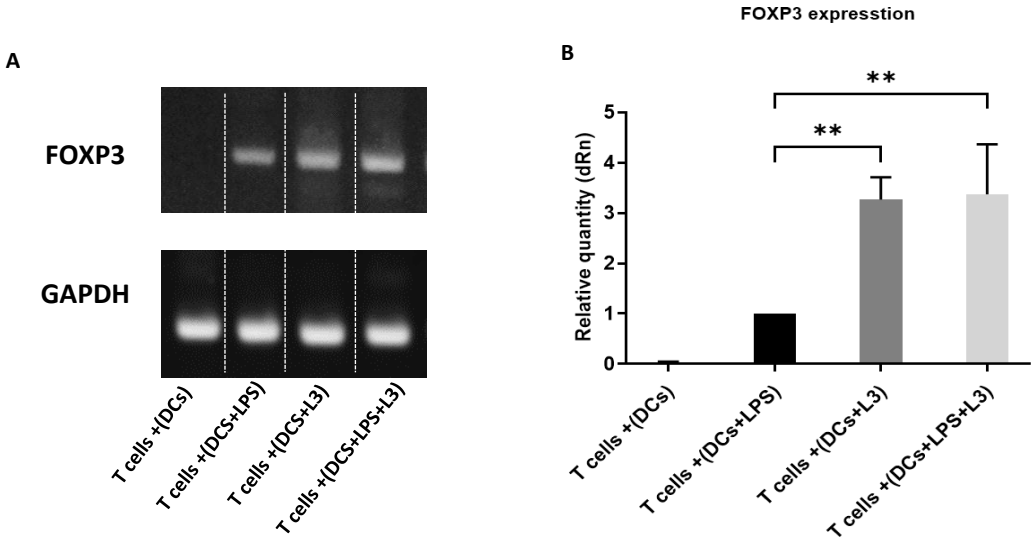

Figure 3.15: PCR experiments were conducted to confirm the T-cell phenotype generated by DCs treated with *N. brasiliensis* infective larvae. A) End-point PCR data show the induction of the FOXP3 gene in infective larvae alone and in the presence of LPS (n=3). **B)** RT-PCR data is consistent with end-point PCR data showing significant increases in FOXP3 gene expression compared with LPS only, indicating the generation of a Treg phenotype in the population of infective larvae. Data are reported as mean ± SD of three independent donors (n=3).

4.3.8 T cells differentiation in co-cultures with *N. brasiliensis* iL3 primed DCs suppress activation of memory T cells

To further ascertain the functional properties of Tregs differentiated in co-cultures with L3 primed DCs we investigated their inhibitory potential on memory T cells. In these experiments CD45RA- memory T cells were isolated from PBMCs, as described previously (see section 3.2.12). After the isolation process, the purity of the purified isolated cell population was assessed for the lack of CD45RA expression marker (Fig. 3.16). Then purified memory T cells were preserved in liquid nitrogen for 14 days until they were co-cultured with T cells primed by stimulated DCs (Fig. 3.17). Before conducting the suppression assay co-culture, defrosted memory T cells were assessed for viability using LIVE/DEAD flow cytometry staining and a Trypan blue automated cell counter (see Materials and Methods). Figure 3.18 illustrates that ~90% of the memory T cell were alive after storage in liquid nitrogen, indicating that the method used to store cells did not affect cell viability. The suppression assay experiment was performed using autologous memory T cells and naïve T cells, where the naïve T cells were primed by stimulated DCs with either L3 alone or in the presence of LPS for 7 days and then co-cultured with CFSE-labelled memory T cells for 96 hours (see materials and methods section 3.2.11). After 96-hour culture, effector T cells were harvested and analysed by flow cytometry. CFSE-labelled effector T cells showed a clear reduction in proliferation in the presence of L3 but not in the presence of LPS. These data are consistent with our previous observations, which indicated that L3 drove most of the T cell differentiation towards Tregs and that these Tregs contributed suppressive activity (Fig. 3.19).

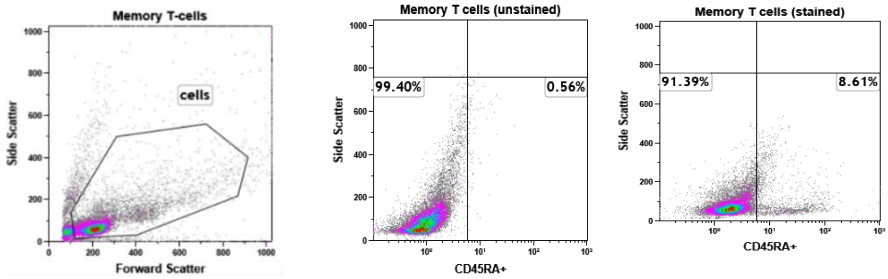

Figure 3.16: Flow cytometry staining of isolated memory T cells. Isolation of memory T cells from pan T cells after successful depletion of CD45RA+ as evidenced by low level of CD45RA^{+} cells. Data are from three independent experiments using naïve T cells from three different donors (n=3).

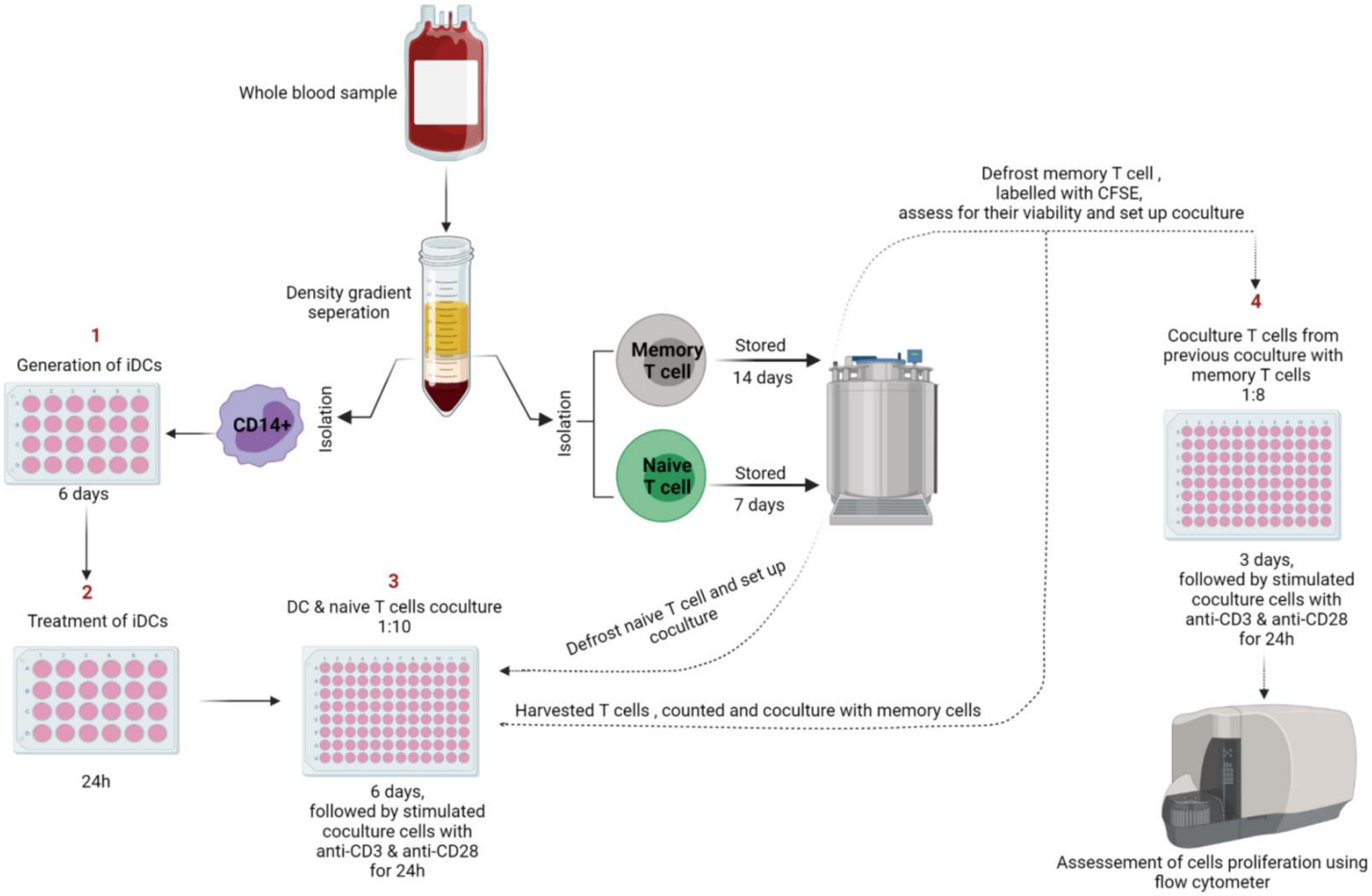

Figure 3.17: Schematic process for memory T-cell isolation, preservation, and suppression assay co-culture. In this process, $CD14^+$ monocytes, naïve T cells, and memory T cells were purified from a buffy coat by gradient separation using magnetic beads. **1*** $CD14^+$ monocytes were differentiated into iDCs for 6 days, while naïve and memory T cells were stored in liquid nitrogen for 7 days and 14 days, respectively. **2*** The generated iDCs population was treated with L3 for 24 hours. **3*** Autologous DC-T-cell co-culture was carried out by co-culturing pre-treated DCs with naïve T cells at a ratio of 1:10 for 7 days. After 7 days of co-culture, T cells were harvested and prepared for co-culture with autologous memory T cells. **4*** The suppression assay was conducted by co-culturing autologous memory T cells and naïve T cells, where naïve T cells were primed with stimulated DCs for 7 days and then co-cultured with CFSE-labelled memory T cells.

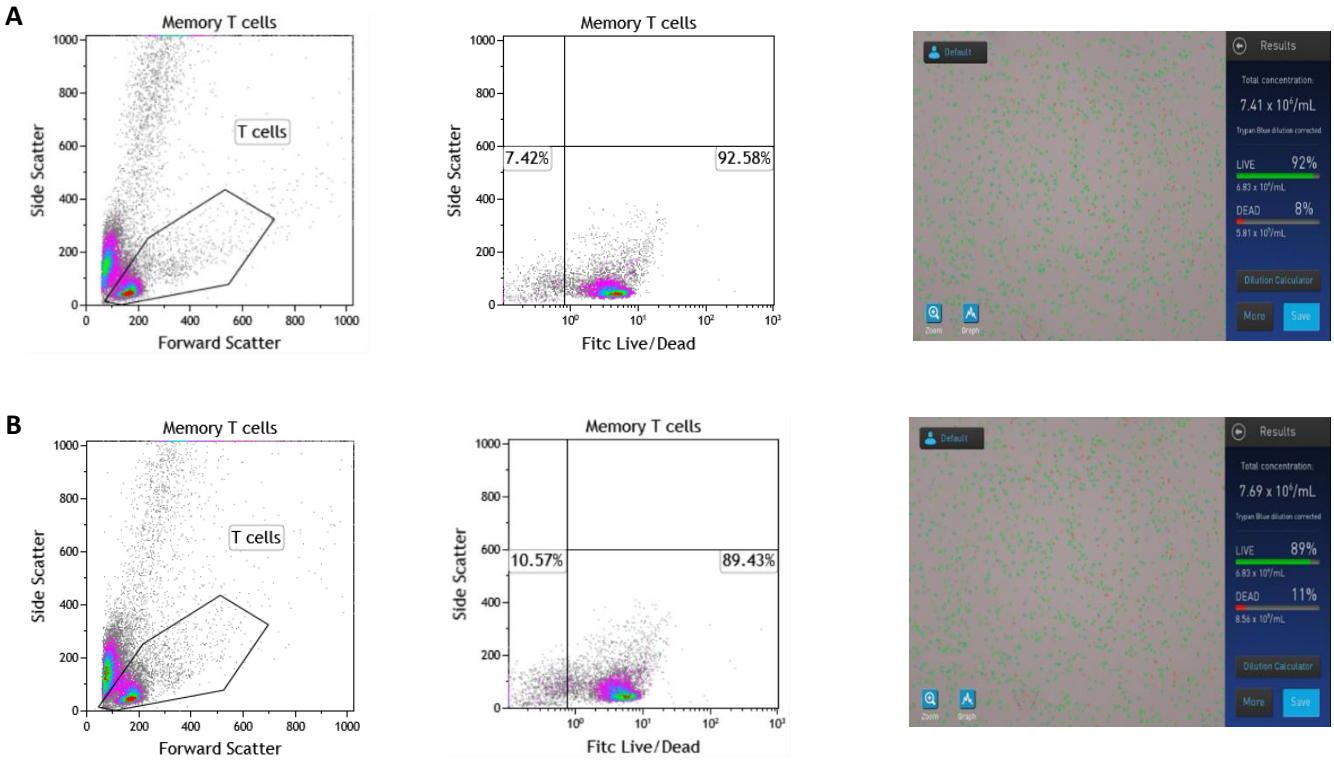

Figure 3.18: Memory T-cell viability analysis using LIVE/DEAD flow cytometry staining Countess™ II FL Automated Cell Counter after isolation and liquid nitrogen preservation. A) The data show that 95% of the naïve T cells are alive after isolation from PBMCs by using LIVE/DEAD flow staining, showing similar viability using a Trypan blue automated counter. **B)** Naïve T cell viability showed no marked reduction in live cell number after liquid nitrogen thawing compared to naïve T cell numbers after the isolation process. Data are from three independent experiments using naïve T cells from three different donors (n=3).

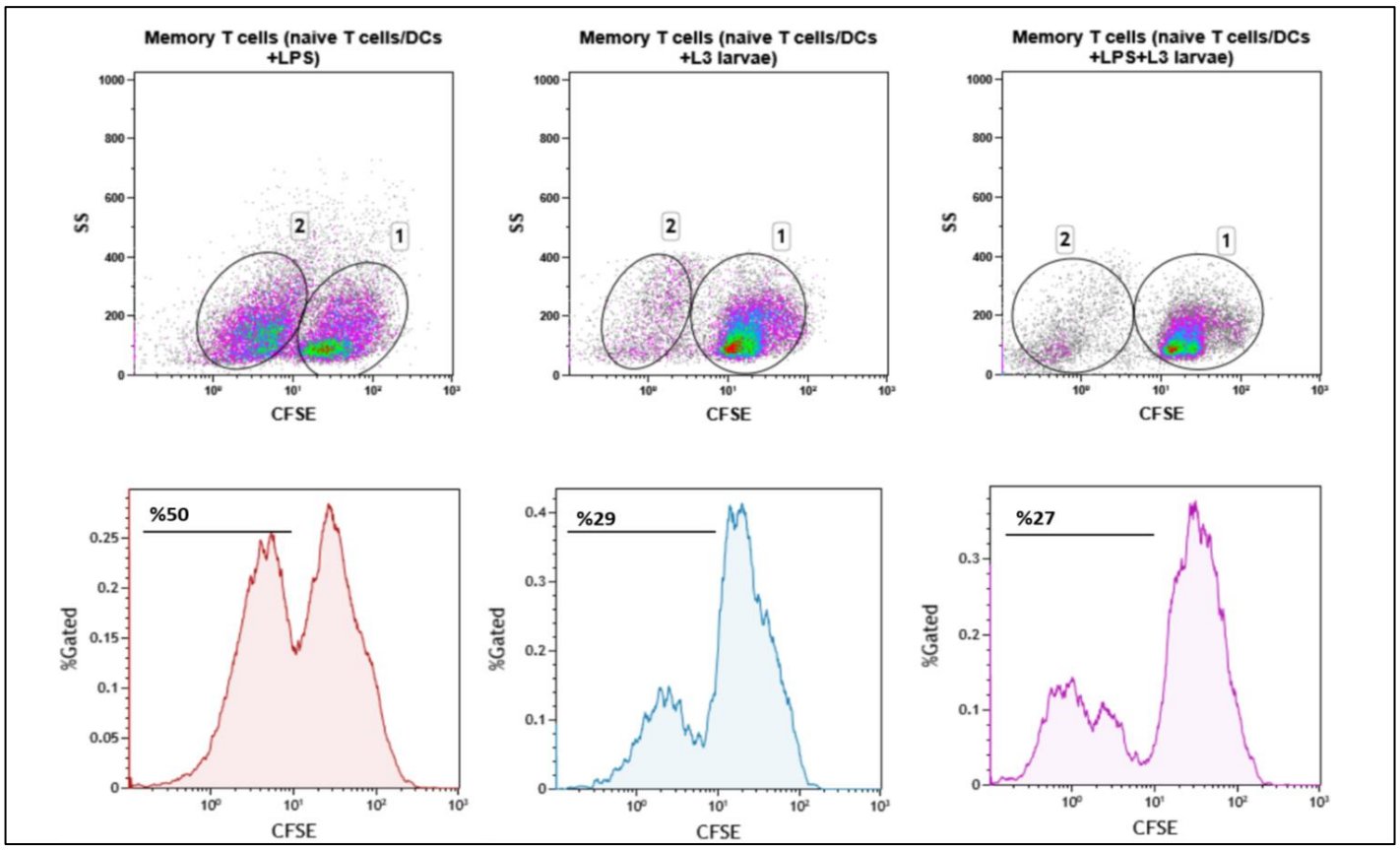

Figure 3.19: T-cell suppression assay. Histograms show the percentage of dividing CFSE-labelled effector T cells co-cultured with Tregs. Effector T cells show increased proliferation under the LPS condition and reduced proliferation under the L3 condition. Data shown are of three independent experiments (n=3).

3.4 Discussion

Hookworm infection is a significant public health concern, particularly in developing countries; however, the fundamental mechanism of how parasites initially modulate DC function is not fully understood [250]. There is intensive interest in understanding host these parasites modulate the immune system leading to their long-term survival in the host. Furthermore, there is also interest in harnessing immune regulatory properties of parasites as potential therapeutic tools for autoimmune and inflammatory diseases [197]. In this chapter I investigated immune modulatory properties of *N. brasiliensis* iL3 on human DCs to see if they align with previously reported effects of *N. americanus* larvae.

The maturation status of DCs plays a key role in their ability to initiate T-cell activation. Other co-stimulatory molecules found on DCs, such as CD40, are necessary for DC activation and priming of Th1-cell differentiation through induction of IL-12 production by DCs [251,252]. However, the lack of upregulation of DC co-stimulatory molecules, such as CD80/86, prevents the effective activation of T cells, as these bind to TCR and CD28 [253]. Furthermore, a lack of HLA-DR upregulation in response to foreign antigens prevents further activation of Th cells and the production of antibodies against pathogens [254]. Cytokine production is present during any in vivo exposure and plays a crucial role in the migration of DCs to the lymphoid organs for T-cell priming [255]. IL-10 is an anti-inflammatory cytokine; it has a crucial role in inhibiting and downregulating Th1 cytokines, including IFN-γ, TNF-α, IL-2, and IL-3 [256]. While IL-12 is a pro-inflammatory cytokine, it has a role in inducing Th1 cells to secrete IFN-γ [257].

We started by evaluating the DC phenotype following treatment with *N. brasiliensis* L3 cuticle by analysing DC surface markers. The data showed a significant reduction in MR and DC-SIGN expression following treatment of iDCs with the larval cuticle. This is likely due to the presence of glycosylated ligands on the L3 cuticle that might bind to CLRs. In contrast, there was no observed change in the expression of other surface markers (CD80, CD86, HLA-DR, and CD40) and DCs maintained an immature phenotype. However, DCs maintained their ability to respond to LPS stimulation in the experiment, as evidenced by upregulation in maturation markers. In addition, when

assessing the cytokine production by DCs following treatment with larval cuticle, there was a significant increase in the anti-inflammatory cytokine IL-10 and no significant production of pro-inflammatory cytokine IL-12. DC viability was analysed in all experiments using the LIVE/DEAD staining, most of DCs were alive upon treatment with *N. brasiliensis* larvae. These findings indicated the generation of a regulatory DC phenotype after treatment with *N. brasiliensis* infective larvae compared with the control. A previous study reported that impaired of DC maturation following treatment with *N. americanus* infective larvae caused no significant increase in pro-inflammatory cytokine secretion by DCs in individuals with necatoriasis [120]. This finding was in line with our findings indicating that *N. brasiliensis* behaves similarly to the human hookworm. More importantly, carbohydrate-containing pathogens or allergens have been shown to have an immunomodulatory effect on DCs. Studies have shown that glycosylated allergens that contain different carbohydrate moieties are able to bind to MR on DCs and modulate the immune system [258,269]. A similar study showed that allergens from house dust mites mediated uptake by DC-SIGN and modulated the immune response [260]. These findings suggest that *N. brasiliensis* larvae could utilise monosaccharides expressed on its cuticle surface to modulate immune cells.

IDO is a tryptophan-degrading enzyme that is produced by immune cells upon stimulation by the pro-inflammatory cytokine IFN-γ. IDO mediates catabolism of the essential amino acid tryptophan, leading to the production of KYN, which can activate AhR. AhR is a ligand-dependent transcription factor that has been shown to be involved in IDO induction [261,262].

Interestingly, addition of L3 to LPS stimulated DCs led to a significant reduction in IDO activity further highlighting the immune suppressive potential of L3. Research has shown that increased IDO activity can be seen under production of inflammatory cytokines; in contrast, a lack of IDO activity or reduced tryptophan levels in the microenvironment suppresses immune cells [263-265]. These observations are in line with our findings, where a reduction in IDO activity in DCs treated with *N. brasiliensis* infective larvae corresponded to a regulatory phenotype, as evidenced by decreased IL-12 production and increased IL-10 production.

PRRs expressed on DCs include TLRs and CLRs. Activation of TLRs, particularly TLR4, leads to upregulation of maturation markers and secretion of inflammatory cytokines; CLR ligation results in processing of the antigen into peptides, which are presented via MHC II and induce the production of anti-inflammatory cytokines [71,170]. For induction of the optimal immune response, both TLRs and CLRs need to be involved in antigen recognition. Several studies have suggested that pathogens exploit the interplay between the receptors and interfere with TLR signalling, thereby inducing immune tolerance [73,266]. In our study, we investigated how *N. brasiliensis* infective larvae modulated TLR4 signalling induced by LPS in the context of cell phenotype, cytokine profile, and IDO activity. Our previous results showed that LPS induced DC maturation, enhancing the production of pro-inflammatory cytokines; this activity was suppressed in the presence of L3, indicating that L3 can modulate LPS-induced TLR4 signalling.

Considering the effect of *N. brasiliensis* infective larvae on DC phenotype, cytokine profile, and IDO activity, we further investigated whether DCs primed with infective L3 could modulate T-cell priming by DCs in autologous DC-T cell co-cultures. The data indicated the presence of a $CD4^+CD25^+FOXP3^+$ population of T cells when they were co-cultured with DCs pre-treated with L3 either in the presence or absence of LPS compared with the control (LPS only or no-stimulation). This finding indicated the generation of a regulatory T-cell phenotype, which is in line with our previous finding where DCs treated with infective L3 expressed a regulatory phenotype through expression of PDL-1 and increased IL-10 production. Several studies have demonstrated that tolerogenic DCs, which are characterised by increased IL-10 secretion and the expression of PDL-1, play a key role in promoting immune tolerance through induction of Tregs [267-269].

To better understand the T-cell phenotype, the level of key cytokines, such as IL-10, TGF-β, IL-4, and IFN-γ, were measured in the co-culture supernatants. Interestingly, the results showed increase IL-10 and TGF-β production in T cells co-cultured with DCs that were primed with infective larvae in the presence or absence of LPS compared with the control; however, no statistically significant increase was detected in the production of IFN-γ and IL-4 under these conditions. Overall, the co-culture results indicated that *N. brasiliensis* larvae modulated DC function, leading to induction of Tregs. In

agreement with Matoso et al. [270], *N. americanus* infection was associated with the induction and expansion of Tregs, which leads to enhanced pathogen survival and promotes long-term persistence. Regulatory T cells play a key role in maintaining peripheral tolerance and controlling the immune response; they are characterised by expression of CD4, CD25, and FOXP3. This T-cell population produces suppressive cytokines, such as IL-10 and TGF-β, to exert its regulatory activity. Infection with *N. americanus* is associated with the induction and expansion of Tregs; however, the mechanism underlying this process needs to be further investigated [271]. The presence of regulatory monosaccharides on the surface of the larval cuticle has been demonstrated, which might play a role in generating regulatory cells. Different studies have shown that pathogens containing carbohydrates have an immunomodulatory effect on DCs and downstream effects on the activation of adaptive immunity. For example, a study showed the ability of *F. hepatica* glycoconjugates, which contain mannose and fucose residues, to induce of regulatory DCs by binding to DC-SIGN [221]. Another study reported that expression of fucosylated antigens on the envelope of *H. pylori* can interact with DCs and modulate host immune responses [220]. Furthermore, Tn antigens expressed on malignant cells that contain galactose and GalNAc can induce an immunosuppressive response from DCs, thereby evading the immune system [272]. These studies show the importance and biological relevance of glycosylated antigens in modulating or suppressing DC function.

We evaluated the expression of the regulatory gene FOXP3 in each condition to confirm the immune regulatory effect that was generated by *N. brasiliensis* larvae. The PCR results showed significant increases in FOXP3 expression in larval conditions, which have previously been shown to increase IL-10 production. This finding supports the consistency of our observations for the larval condition and confirms the presence of Tregs in these conditions compared with the control. Our findings are consistent with studies showing that *N. americanus* had similar effects on the generation of FOXP3 Tregs, suggesting that *N. brasiliensis* induced similar immunomodulatory effects as the human hookworm [271]. Chronic human *N. americanus* infection is classically associated with a profound ablation of cell proliferation, but the role of Tregs in human hookworm infection is still poorly understood. To determine the possible role of Tregs in hookworm infection, a suppression assay was

designed to evaluate whether $CD4^+CD25^+FOXP3^+$ Treg cells could modulate the in vitro cellular proliferation of effector T cells following parasite antigen stimulation. Our data showed that $CD4^+CD25^+FOXP3^+$ cells suppressed the activation and proliferation of effector T cells by direct contact with effector T cells or secretion of immunoregulatory cytokines, such as IL-10 and TGF-β. These data are in line with studies that have investigated the immunomodulatory hallmarks of *N. americanus* infection involving induction of Tregs, latter which plays a fundamental role in downregulating the responses of effector T cells [273-275].

3.5 Conclusion

The data presented in this chapter describe the impact of *N. brasiliensis* infective larvae on pivotal cells of the immune system. DCs treated with infective larvae were able to modulate DC phenotype and function and could generate regulatory cells through co-culture experiments. These data clearly show that L3 larvae from *N. brasiliensis* impact human DC phenotype and cytokine profile similar to effects previously shown to be induced by *N. americanus* infective larvae highlighting the possibility of using *N. brasiliensis* as an experimental model for *N. americanus* in in vitro functional studies. Furthermore, given that such potent immune modulatory effects and lack of any stable physical interaction between DCs and exsheathed larvae as we have seen it previously in the chapter 2 highlight the possibility that L3 cuticle could insert immune modulatory effects in a paracrine manner via its secretion. Therefore, to fully understand the immunomodulatory effects of *N. brasiliensis* infective larvae, we aimed to investigate the immunomodulatory properties of parasite secretions on immune cells, which is described in detail in Chapter 4.

Chapter 4:

Investigating the impact of *Nippostrongylus brasiliensis* infective larvae secretions on human dendritic cells and T-cell polarisation

4.1 Introduction

Despite the chronicity of infections caused by *N. americanus*, little is known about how this parasite interacts with the host immune system to arrive in the gut and survive for long-term besides the complex immune responses generated against it [276]. This is likely due to various immune evasion and immune regulatory features of *N. americanus* arising from its complex antigenic structure as well as secreting a wide range of glycoproteins [151,218]. These secretions are mostly glycosylated in nature with potential immune regulatory properties [106,154]. However, the mechanism through which these secretions could influence different immune cells, particularly DC functions, is not completely understood [250]. Therefore, understanding the regulatory effect of parasites and how it might result in a dampened host immune system is a subject of intense research [152]. Glycoprotein and glycan decoration of pathogens has proven to be important in understanding the relationship that develops between parasites and their hosts, including recognition by the innate immune system and the immunomodulatory effects caused by these glycoproteins [70, 141, 277]. For example, it has been shown that O-methylated glycans of *Toxocara canis* contain fucose and galactose residues that mimic mammalian blood group antigen H, making them able to interact with DC-SIGN on DCs and cause regulation of immune responses [278]. *Schistosoma mansoni* fucosylated glycoproteins can interact with DC-SIGN on DCs and subsequently inhibit maturation of DCs [279]. Little is known about the presence of monosaccharides in *N. americanus* secretions, and the mechanisms by which these molecules interfere with the host immune system [250, 280]. Therefore, investigating monosaccharides in *N. americanus* secretions is of major importance in determining their involvement in modifying DC function and understanding the possible mechanisms involved that could help us to design novel therapeutic strategies.

In the previous chapters we have shown the immunomodulatory effect of *N. brasiliensis* infective larvae on human immune cells and the ability of L3 larvae to skew DC immune responses into an anti-inflammatory phenotype and modulate adaptive immune responses. Given the short term and unstable physical interaction between DCs and L3, it is reasonable to suggest that the observed immune regulatory effects are mediated through L3 secretions. To examine this hypothesis, in this chapter, we

aim to collect *N. brasiliensis* larvae secretion in order to evaluate the impact of larval secretions on DCs and T-cell polarisation as well as to investigate whether larval secretions have similar effects on modulating immune responses as infective larvae. Moreover, we aimed to investigate presence of monosaccharides that have been previously identified on larvae cuticle and whether these monosaccharides could be found in the larval secretions.

4.2 Materials and methods

4.2.1 Preparation of *N. brasiliensis* infective larvae

Infective larvae were prepared as described in Chapter 2.

4.2.2 Preparation of *N. brasiliensis* infective larval secretions

N. brasiliensis L3 were cultured in RPMI 1640 medium supplemented with 100 IU/ml penicillin, 100 µg/ml streptomycin, and 1% gentamicin, then incubated for 24 hours at 37°C in 5% CO_2. We collected larval secretions and concentrated them using Vivaspin2 centrifugal concentrator unit MWCO 3 kDa (purchased from Sigma-Aldrich) via centrifugation at 3000 g for 20 minutes. The proteins and endotoxins of the concentrated secretion were quantified using the protein assay (BCA) and Limulus amoebocyte lysate (LAL) assay kits, respectively (both were purchased from Thermo Fisher Scientific, UK). The standard and test samples were prepared according to the manufacturer's protocols. Protein absorbance was measured at 562 nm, while endotoxin absorbance was measured at 405 nm using the SpectraMax Paradigm spectrophotometer. Absorbance of protein and endotoxin standards were plotted against their corresponding known concentrations for the determination of the unknown sample concentrations. Concentrated larval secretions were stored at -80°C until use (Fig. 4.1)

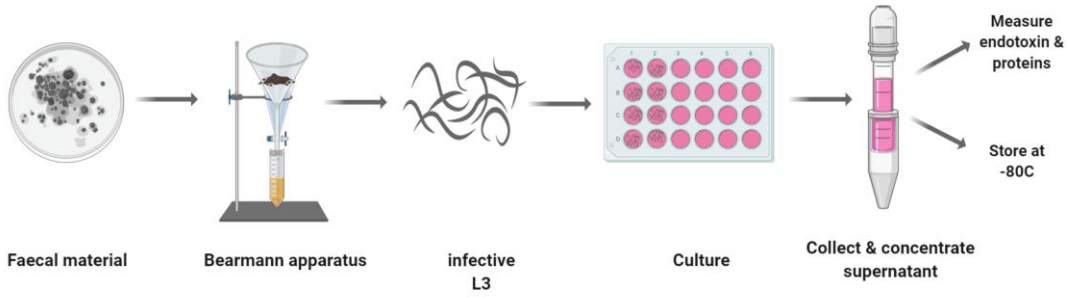

Figure 4.1: Process for collection of *N. brasiliensis* larval secretions. L3 are isolated from faecal material using a Baermann apparatus. The isolated larvae were washed extensively with sterile deionised water containing 100 IU/ml penicillin, 100 µg/ml streptomycin, and 1% gentamicin and cultured in RPMI medium supplemented with the same concentrations of antibiotics as used for the washing solution for 24 hours at 37°C in 5% CO_2. After 24h, the media containing the larval secretions was collected, concentrated using MWCO 3kDa filters, and the protein and endotoxin concentrations were measured.

4.2.3 Measurement of protein concentration

The protein concentrations of the larval secretions were measured using a BCA protein assay, according to the manufacturer's recommendations. Briefly, a solution of 2 mg/ml bovine serum albumin (BSA) standard was used to prepare a set of protein standards at range of 20–2000 µg/ml. BSA dye reagent was prepared at ratio of 50:1 (BCA reagent A:BCA reagent B). Then, 25 µl of BSA standards and samples were pipetted into 96-well plate (in duplicate) followed by addition of 200 µl of prepared dye reagent into each well. After mixing, the well plate was incubated for 30 minutes at 37°C and the absorbance was measured at a wavelength of 562 nm using Promega GlowMax plate reader. The concentration of the protein samples was determine using the equation of standard curve obtained from the BSA standard concentration.

4.2.4 Generation of human dendritic cells from peripheral blood mononuclear cells

Human DCs were generated as described in Chapter 2 see section 2.2.2.

4.2.5 Incubation of *N. brasiliensis* larval secretions with immature dendritic cells

Human iDCs (2.5×10^5 cells/well) were seeded in a 24-well plate in complete RPMI 1640 medium and treated with 20 ug/ml of larval secretions, followed by incubation of the cells for 24 hours at 37^{o}C with 5% CO_2. iDCs stimulated with LPS from *E. coli* (10 ng/ml), and unstimulated DCs were used as controls.

4.2.6 Incubation of *N. brasiliensis* larval secretions with mature dendritic cells

Human iDCs (2.5×10^5 cells/well) were seeded in a 24-well plate in complete RPMI 1640 medium, stimulated with LPS from *E. coli* (10 ng/ml) and treated with 20 ug/ml of larval secretions. The cells were incubated for 24 hours at 37^{o}C with 5% CO_2.

4.2.7 Quantification of DCs viability assay

DC viability was assayed as described in Chapter 2 section 2.2.4.

4.2.8 Flow cytometric analysis and cytokine expression measurement

Flow cytometry and cytokine expression measurement were conducted as described Chapter 3 section 3.2.6.

4.2.9 Quantification of indoleamine-2,3-dioxygenase enzyme activity

IDO expression was quantified as described in Chapter 3 section 3.2.8.

4.2.10 Characterisation of *N. brasiliensis* larval products using SDS-PAGE and silver staining

To run the protein gel, the running buffer was prepared before starting the experiment, according to manufacturer's instructions. Briefly, 1x running buffer was used, which was produced by diluting 100 ml of 10 x running buffer (250 mM Tris, 1.92 M glycine, 1% sodium dodecyl sulphate [SDS], pH 8.3) (Bio-Rad, UK) in 900 ml of distilled water. A Mini-protean precast gel 4–15% (Bio-Rad, UK) was placed in the electrophoresis cell after removing the comb and the tape from the gel, followed by assembly of the electrophoresis cell and filling the inner and outer chambers with 1 x of running buffer. The sample (20 ug/ml of larval secretions) was prepared in a reducing reagent by dissolving one part of sample to one part of Laemmli sample buffer (Bio-Rad, UK) followed by heating of the sample at 100^{o}C for 5 minutes and loading into the gel well. The protein ladder and sample were loaded into the gel lanes (50 ul per lane) and the electrophoresis cell was connected to the power supply and programmed with 200 V for 1 hour. After completing of electrophoresis, the gel was removed. To visualise the proteins in the larval product, the SDS-polyacrylamide gel electrophoresis (SDS-PAGE) gel was stained with silver (Vector laboratories, UK). Briefly, the gel was fixed with fixing solution I (methanol, acetic acid, and distilled water) for 10 minutes, followed by fixing solution II (methanol, acetic acid, fixing reagent I, and distilled water) for 15 minutes. The gel was then pre-treated with methanol, pre-treatment reagent, and distilled water for 10 minutes, and washed with distilled water for 5 minutes. Then gel was stained with silver staining solution I and II for 15 minutes and washed twice with distilled water for 2 minutes each time. To enhance the contrast of silver staining, 10% concentrator developer in distilled water was placed on the gel. The staining reaction was stopped by adding citric acid and agitating it for ~10 minutes. Finally, the gel was washed with distilled water and imaged.

4.2.11 Glycosylation analysis

Concentrated larval secretions (20 µg/ml per lane) were run on 4–15% SDS-PAGE, as described previously, and the SDS-PAGE gel was transferred onto a PVDF nitrocellulose membrane (Bio-Rad,

UK) to perform Western blotting. Briefly, after completing the transfer of the electrophoresis gel, the membrane was stained using biotinylated labelled lectin antibodies (Vector Laboratories, UK), according to the manufacturer's protocol. First, the membrane was incubated in Carbo-Free Blocking Solution (Vector Laboratories, UK) for 30 minutes at room temperature. Then, the membrane was incubated with 20 µg/ml of biotinylated lectin antibody* for 30 minutes at room temperature and washed with PBS containing 0.05% Tween 20. The membrane was then incubated in alkaline phosphatase conjugate enzyme for 30 minutes and washed with PBS containing 0.05% Tween 20. Finally, the membrane was incubated with Chemiluminescent/Fluorescent Substrate and imaged using a chemiluminescent imaging system.

* Biotinylated labelled lectin included concanavalin A (Con-A) specific for mannose, Dolichos biflorus agglutinin (DBA) specific for GalNAc, peanut agglutinin (PNA) specific for galactose, Ricinus communis agglutinin (RCA) specific for galactose, soybean agglutinin (SBA) specific for GalNAc, Ulex europaeus agglutinin (UEAI) specific for fucose, and wheat germ agglutinin (WGA) specific for GalNAc. The membrane was analysed using a LAS-400 imaging system.

4.2.12 Blocking of C-lectin receptors

Blocking antibodies for MR (clone 15.2) and DC-SIGN (clone H-200) were purchased from Santa Cruz Biotechnology. iDCs were treated with either MR-blocking antibody (100 µg/ml) or DC-SIGN-blocking antibody (20 µg/ml) and incubated at 37°C for 25 minutes. iDCs treated with the isotype control mouse IgG and untreated cells were used as control. Then, the cells were treated with larval secretions and incubated for 24 hours at 37°C with 5% CO_2.

4.2.13 Isolation of naïve CD45RO$^-$ T cells and dendritic cell-T-cell co-culture

Cell isolation and co-culture were performed as described in Chapter 3 section 3.2.9.

4.2.14 RNA isolation, endpoint PCR, and quantitative real-time PCR

RNA isolation, endpoint PCR, and qRT-PCR were performed as described in Chapter 3 section 3.2.10.

4.2.15 Isolation of naïve CD45RO$^+$ T cells and suppression assay

Cell isolation and suppression assay were performed as described in Chapter 3 section 3.2.11.

4.2.16 Statistical analysis

Data were analysed and evaluated using GraphPad Prism version 7.02 (GraphPad Software, San Diego, CA). Values are presented as mean ± SEM and statistical significance was determined by one-way ANOVA when comparing two groups. A p-value <0.05 was considered statistically significant.

4.3 Results

4.3.1 Effect of different concentrations of larval secretions on dendritic cell activation and cell viability

N. brasiliensis larval secretions were collected and concentrated using a 3KDa centrifugal concentrator unit, as described previously in the materials and methods section 4.2.2.

To understand the immunomodulatory properties of *N. brasiliensis* larval secretions on DC phenotype and function, larval secretion levels needed to be optimised while maintaining cell viability. To achieve this, we investigated the dose response of DCs with varying concentrations of larval secretions: 4 μg/ml, 20 μg/ml, and 100 μg/ml. Fig. 4.2 shows that different concentrations of larval secretions have different effects on cell viability: 4 μg/ml had no effect in cell viability or cell phenotype, as evidenced by no reduction in the expression of DC-SIGN or MR; 20 μ/ml had no toxic effect on DCs, with a slight effect on cell phenotype; and 100 μg/ml had a detrimental impact on cell viability, with similar effect as 20 μg/ml on cell phenotype. From this data, we decided to use the 20 μg/ml of larval secretions to stimulate DCs and study the immunomodulatory properties of *N. brasiliensis* larval secretions on DC phenotype and function, and to investigate the downstream effects of larval secretions on the adaptive immune system.

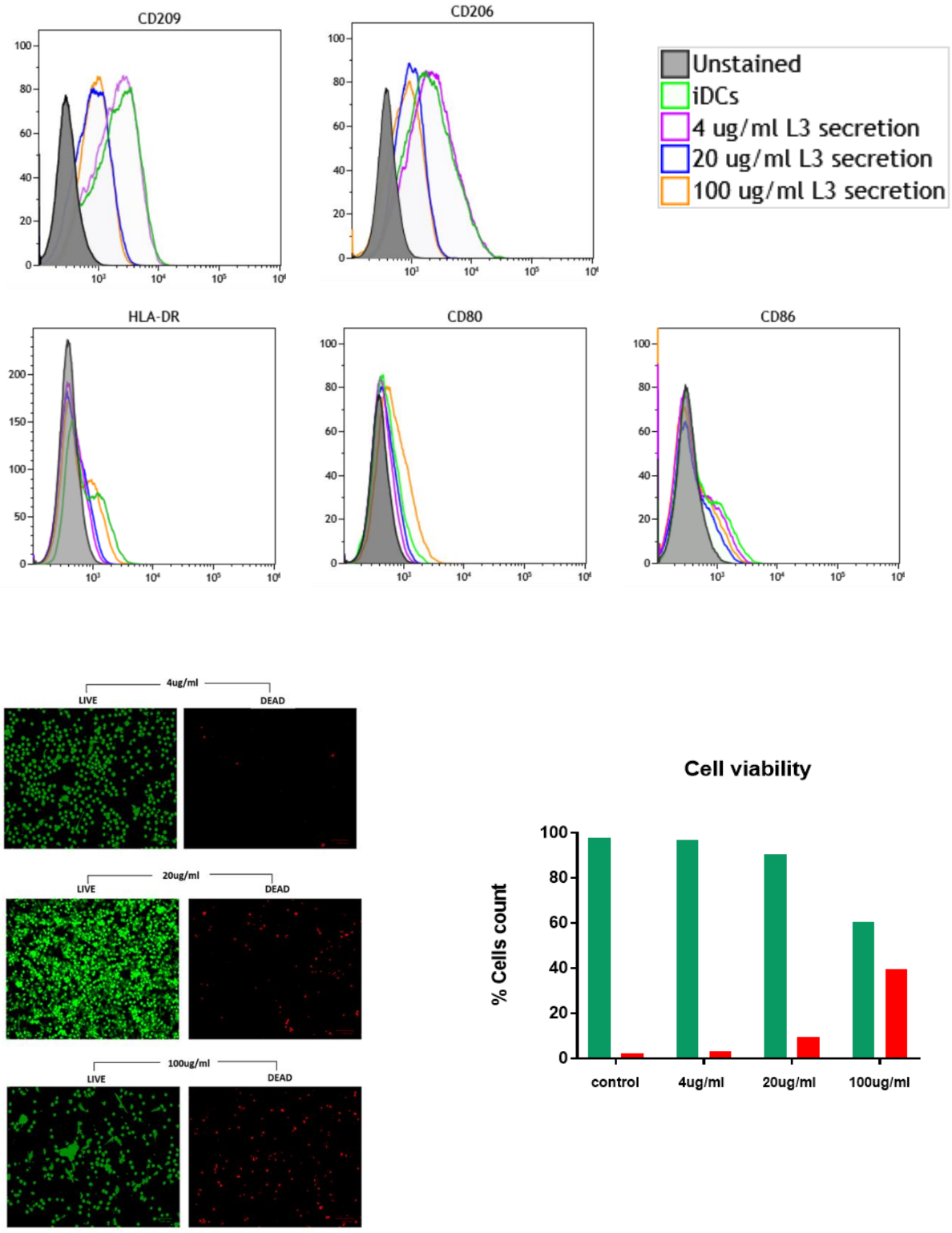

Figure 4.2: Dose-response effect of *N. brasiliensis* larval products on human DC phenotype and cell viability. Different concentrations of *N. brasiliensis* larval secretions had no effect on maturation marker expression in DCs, while 100 µg/ml negatively affected DCs viability compared with other doses. Data are representative of two independent experiments (n=2).

4.3.2 *N. brasiliensis* larval secretions induce tolerogenic dendritic cell phenotype and function

To investigate the effect of *N. brasiliensis* larval secretions on iDCs, these cells were treated with 20 μg/ml of larval secretions; cells stimulated with 10ng/ml of LPS alone and unstimulated cells were used as the positive and negative controls, respectively. After 24 hours of culture, DC surface markers were examined using flow cytometry to identify changes in DC phenotype, while pro-inflammatory (IL-12p40) and anti-inflammatory (IL-10) cytokines were measured in cell supernatants using ELISA. In addition, IDO activity was quantified as a surrogate for DC immunogenicity. Fig. 4.3 shows that DCs co-cultured with larval secretions retained the immature phenotype, as evidenced by low level expression of maturation markers, including HLA-DR, CD86, CD80, and CD40. However, an upregulation in PDL-1 expression was seen in DCs stimulated with larval secretions, suggesting a bias towards an anti-inflammatory phenotype under this condition. To confirm this observation, pro-inflammatory and anti-inflammatory cytokines were measured in cell supernatants. The data showed increased IL-10 production and decreased IL-12p40 secretion in DCs stimulated with larval secretions compared to unstimulated cells, which supports our observations of surface phenotype changes; this is also reflected in the no changes in IDO enzymatic activity in DCs stimulated with larval secretions compared with unstimulated DCs (Fig. 4.4). All data are shown as histograms (supplementary figure 9). Furthermore, DC viability was monitored following these experiments using LIVE/DEAD staining; ~90% of cells were viable after co-culture with L3 secretions (Fig. 4.5). Together, these data indicated that larval secretions had similar effects to infective larvae on DC phenotype.

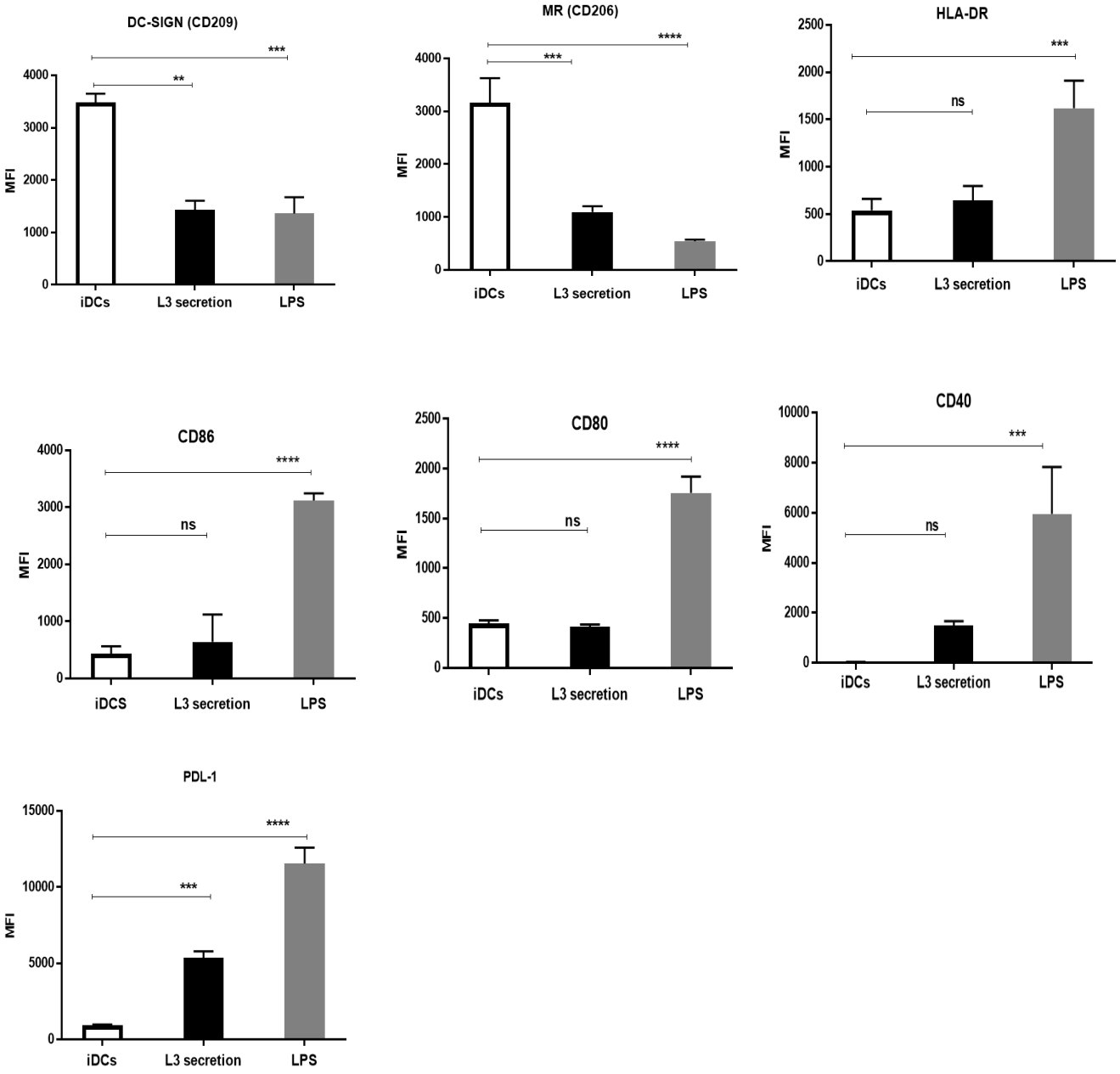

Figure 4.3: The expression of DC receptor molecules in response to stimulation with either 20 ug/ml of larval product or LPS. Median fluorescence intensity was obtained from flow cytometry data and analysed. All data are reported as mean ± SD for three independent donors (n = 3). *p<0.05, **p<0.01, ***p< 0.001, ****p <0.0001. Data are from three independent experiments using DCs from three different donors (n=3).

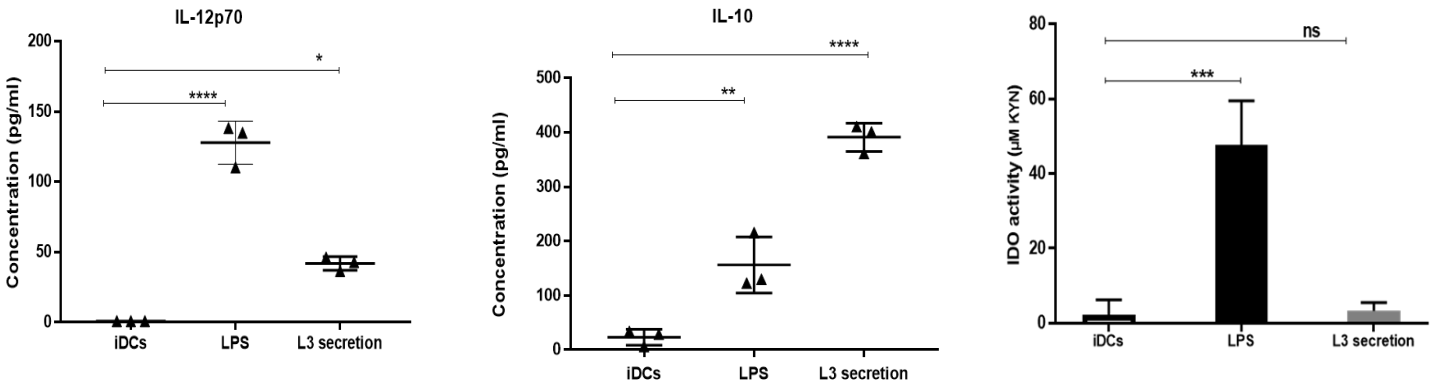

Figure 4.4: DC cytokine production and IDO activity in response to stimulation with either LPS or *N. brasiliensis* larvae secretions. A) & B) DCs treated with larval product had increased production of IL-10 but not IL-12. **C)** DCs treated with larval product show no significant induction of IDO activity compared with the control. All data are reported as mean ± SD for three independent donors (n = 3). *p<0.05, **p<0.01, ***p< 0.001, ****p <0.0001. Data are from three independent experiments using DCs from three different donors (n=3).

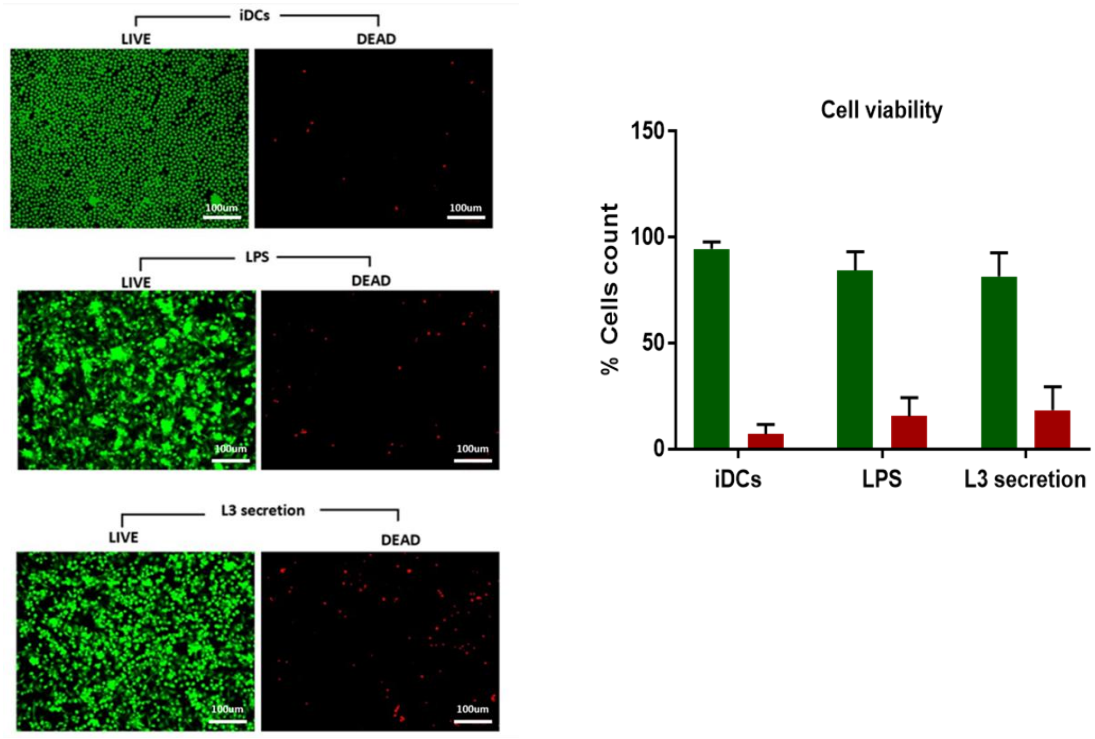

Figure 4.5: The viability of DCs 24 hours after treatment with *N. brasiliensis* L3 secretion. DCs treated with larval secretions showed >90% of viability. Data are from three independent experiments using DCs from three different donors (n=3).

4.3.3 *N. brasiliensis* larvae secretions modulate activated dendritic cell phenotype, cytokine secretion, and IDO activity

The ligation of LPS to TLR4 can induce DC activation and maturation, guiding a pro-inflammatory response. Research has shown that activation of CLRs can modulated TLR4 signalling [281]. To understand the immunomodulatory effect of larval secretions on CLR-TLR4 cross talk, we stimulated DCs with 20 μg/ml larval secretion and 10 ng/ml LPS. Figure shows that DCs exhibited lower expression of maturation markers, including HLA-DR, CD86, CD80, and CD40, in response to LPS in the presence of larval secretions compared with LPS alone (Fig. 4.6). Similarly, L3 secretions significantly suppressed LPS-induced IL-12 production (Fig. 4.7A) and IDO activity (Fig. 4.7C), with significant induction of IL-10 production (Fig. 4.7B). Collectively, these data confirmed that L3 secretions had a similar effect as infective L3 larvae in modulating the phenotype of LPS stimulated DCs.

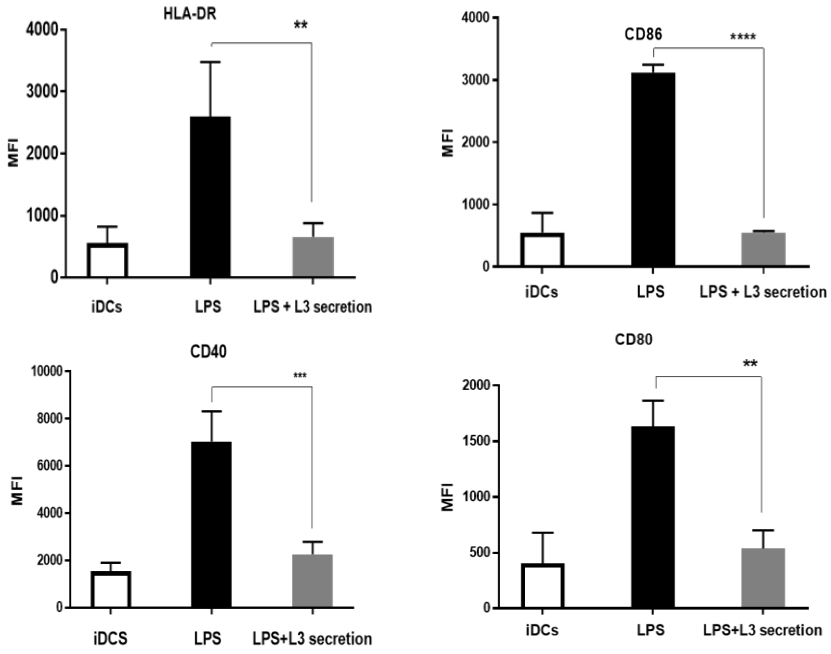

Figure 4.6: *N. brasiliensis* larvae secretions modulate TLR4 signalling. Flow cytometry data of the DC surface marker expression after stimulation with LPS in the presence of larval secretions. Data were obtained and analysed for median fluorescence intensity. Data are shown as mean ± SD of three independent donors (n = 3).

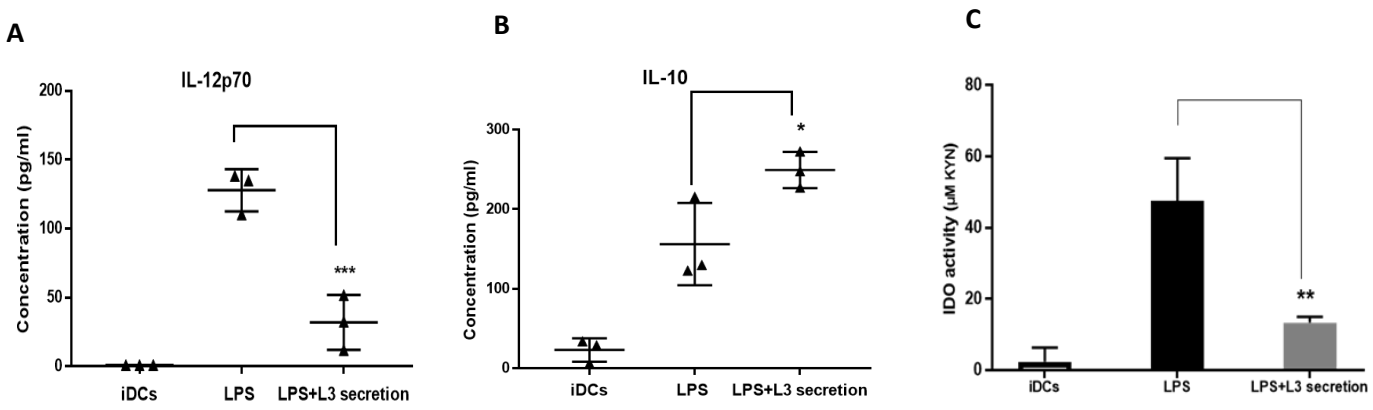

Figure 4.7: Larvae secretions modulate LPS-induced cytokine production and IDO activity. A) & **B)** DC cytokine production in response to L3 secretions with LPS. **C)** DC IDO activity and AhR expression after stimulation with L3 secretions in the presence of LPS. Data are shown as mean ± SD of three independent donors (n = 3). *p<0.05, **p<0.01, ***p< 0.001, ****p <0.0001.

4.3.4 *N. brasiliensis* larval secretions target C-lectin receptors on human dendritic cells

Our results have shown the suppression of DC maturation and pro-inflammatory responses by larval secretions. A possible explanation for the observed immunomodulatory effects could be the recognition of larval products by CLRs on DCs that interfere with TLR signalling and the presence of glycosylated antigens within larval secretions. According to this rationale, CLRs on DCs were blocked by specific antibodies prior to stimulation of DCs with L3 secretions. Briefly, iDCs were treated with either 20 µg/ml of MR-blocking antibody (clone 15.2) or 20 µg/ml of DC-SIGN-blocking antibody (clone H-200) (Santa Cruz Biotechnology). The cells were incubated for 25 minutes at 37°C with 5% CO_2. To confirm blocking of MR and DC-SIGN, the blocked cells were analysed using flow cytometry (supplementary figure 10). Then, 20 ug/ml of larval secretions in the presence or absence of LPS were added to blocked CLR-DCs, and the cells were incubated for 24 hours at 37°C with 5% CO_2. After 24 hours, cells were analysed regarding cytokine production and IDO enzymatic activity. Interestingly, data from these experiments illustrated a significant decrease in IL-10 production after MR and DC-SIGN were blocked in L3 secretion-treated cells compared with control DCs (CT-DCs) (Fig. 4.8B). Furthermore, there was a slight increase in IL-12p70 production following blockage of the CLRs (Fig. 4.8A). We did not observe a significant change in IDO activity in the DC-SIGN-blocked DCs treated

with L3 secretions; in contrast, there was significant induction of IDO activity in the DCs treated with larval products after MR blockage (Fig. 4.8C&D). Together, these data highlight that L3 secretions modulate the DC responses through the engagement of CLRs.

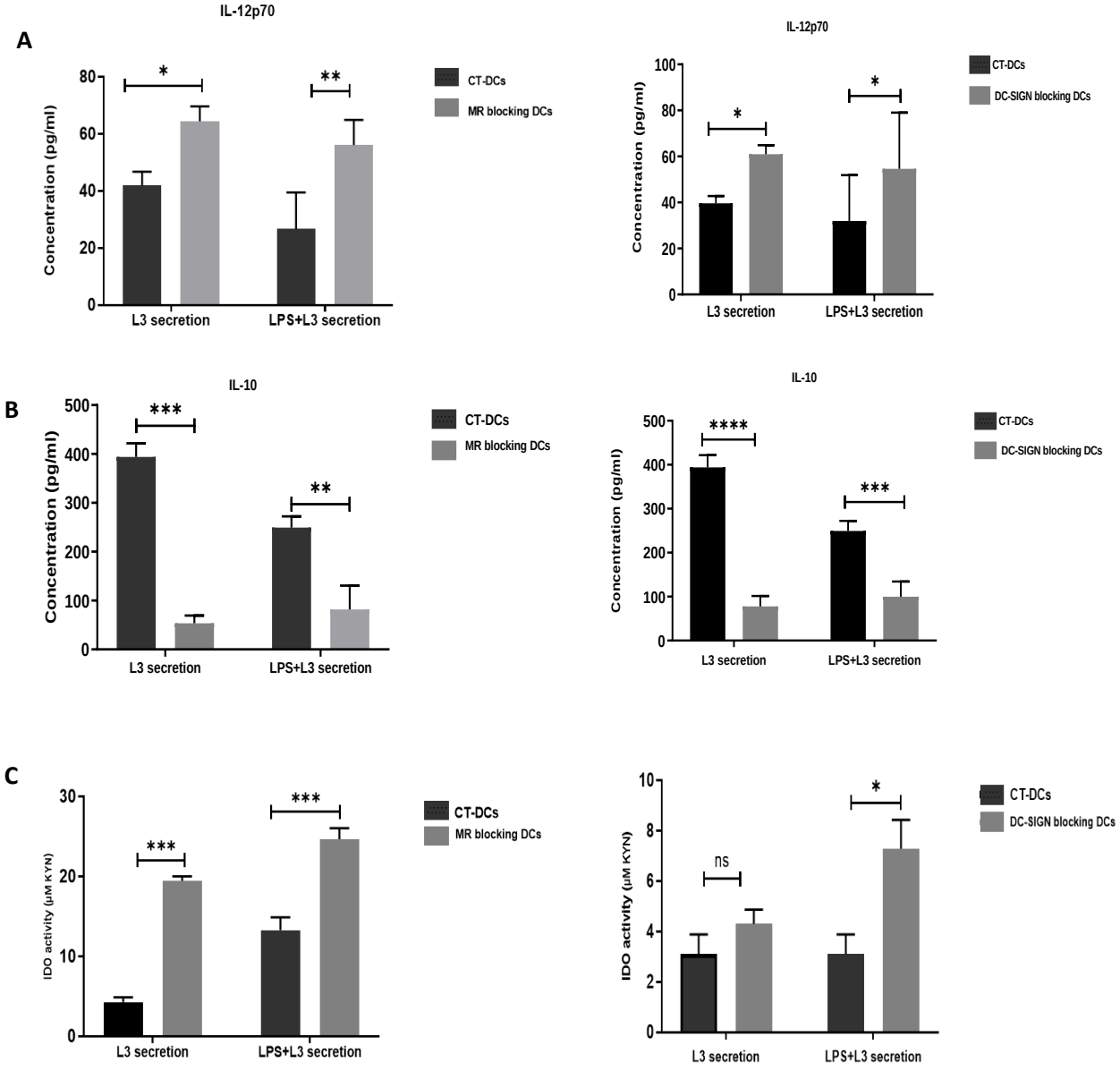

Figure 4.8: A) & B) Cytokine production in the CT-DCs and CLRs blocked cells stimulated by L3 secretions in the presence or absence of LPS for 24 hours. **C) and D)** IDO activity and AhR expression in CT-DCs and CLRs blocked cells stimulated by L3 secretions in the presence or absence of LPS for 24 hours. Data are expressed as mean ± SD of three independent donors (n = 3). *p<0.05, **p<0.01, ***p< 0.001, ****p <0.0001.

4.3.5 Characterisation of *N. brasiliensis* larval products and detection of the glycosylation pattern in larval secretions

N. brasiliensis larval secretions were initially analysed using protein gel electrophoresis (Fig. 4.9). Separated larval protein bands were not observed when staining gel with Coomassie blue stain; however, protein bands were detected following silver staining. Larval product proteins were observed at molecular weights ranging between 62–175 kDa.

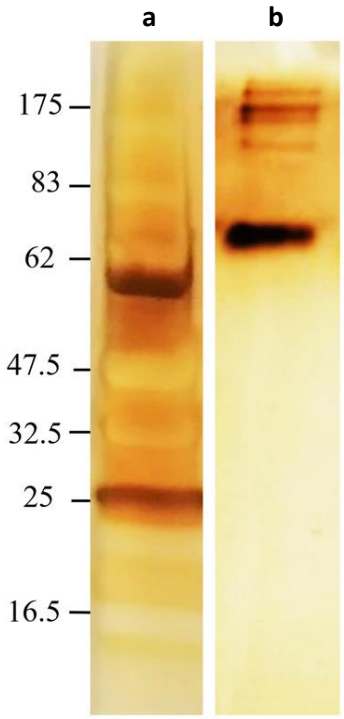

Figure 4.9: Separation of *N. brasiliensis* larval products on SDS-PAGE gel. After gel electrophoresis, gel was silver stained, as described previously. Protein ladder molecular weight is represented in (a), while larval separated protein molecular weight is represented in (b).

It is well known that CLRs on DCs, including DC-SIGN and MR, can recognise ligands that contain monosaccharides. Having investigated the potential role of DC CLRs for the recognition of larval products, the next step would be to investigate the different monosaccharide moieties present in the larval secretions. *N. brasiliensis* L3 secretions were examined for the presence of different sugars using biotinylated labelled lectin, which included Con-A, DBA, PNA, RCA_1, SBA, UEAI, and WGA. Our data revealed that different patterns of glycosylation were present in the L3 secretions; the larval product strongly reacted with RCA1 and SBA, which recognised galactose and GalNAc, respectively. Furthermore, L3 secretions also induced a positive reaction in the presence of UEA and Con-A, which recognised fucose and mannose residues, respectively. In contrast, L3 secretions failed to react with other biotinylated lectins, which suggested that the larval secretions might not contain sugars specific to those lectins (Fig. 4.10). These observations complement our finding of the reduction of IL-10 levels after blockage of CLR on DCs. This data is consistent with our previous observation in chapter 2 that showed the presence of these carbohydrates on the surface of larval cuticle.

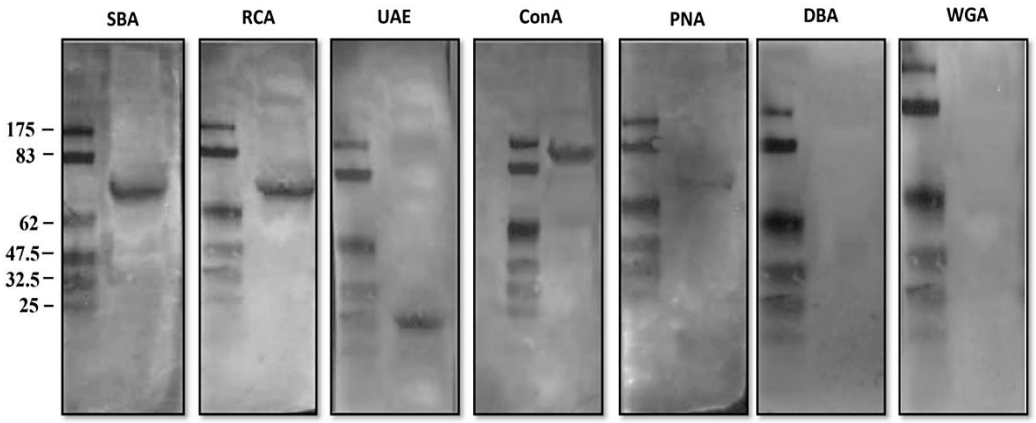

Figure 4.10: Analysis of L3 secretions in terms of glycosylation. L3 secretions are strongly glycosylated, containing galactose and GalNAc rich glycoproteins, as noted by the strong reaction with RCA and SBA compared with the other lectin. +++ strong reaction, ++ moderate reaction, + mild reaction, and – no reaction.

4.3.6 *N. brasiliensis* larval secretions modulate dendritic cell-induced T-cell polarisation

Our previous findings showed that *N. brasiliensis* larval secretions produced high levels of IL-10 by DCs while suppressing induction of IL-12 in the presence of LPS. Therefore, we next aimed to investigate the downstream effects of the larval secretions on T-cell differentiation through DC-T-cell co-culture studies. The co-culture experiment was conducted as described previously using autologous naïve T-cells and DCs. Briefly, DCs were treated with 20 μg/ml of larval secretions in the presence or absence of LPS for 24 hours. These stimulated DCs were harvested and co-cultured with naïve T cells for 7 days, where on day 6, the T cells were restimulated with anti-CD3 and anti-CD28 for 24 hours. The T cells were assessed for phenotype and cytokine profile. Fig. 4.11 confirms the presence of CD4 in all conditions. The data also show the presence of FOXP3 and CD25 within the $CD4^+$ cell population in larval conditions in presence or absence of LPS. This finding suggests the presence of T-cell populations expressing an anti-inflammatory phenotype similar to those that were observed in our previous findings (Chapter 3), where infective L3 conditioned DCs to express a regulatory phenotype.

To further confirm the phenotype of these cells, we assessed their cytokine profiles. As expected, Fig. 4.12 shows increase IL-10 and TGF-β production in T cells co-cultured with L3 secretion-treated DCs in the presence or absence of LPS. This finding is the line with our previous T-cell phenotype analysis data. Overall, the co-culture results indicated that larval secretions regulated DC function, which led to the induction of $CD4^+FOXP3^+CD25^+$ Tregs.

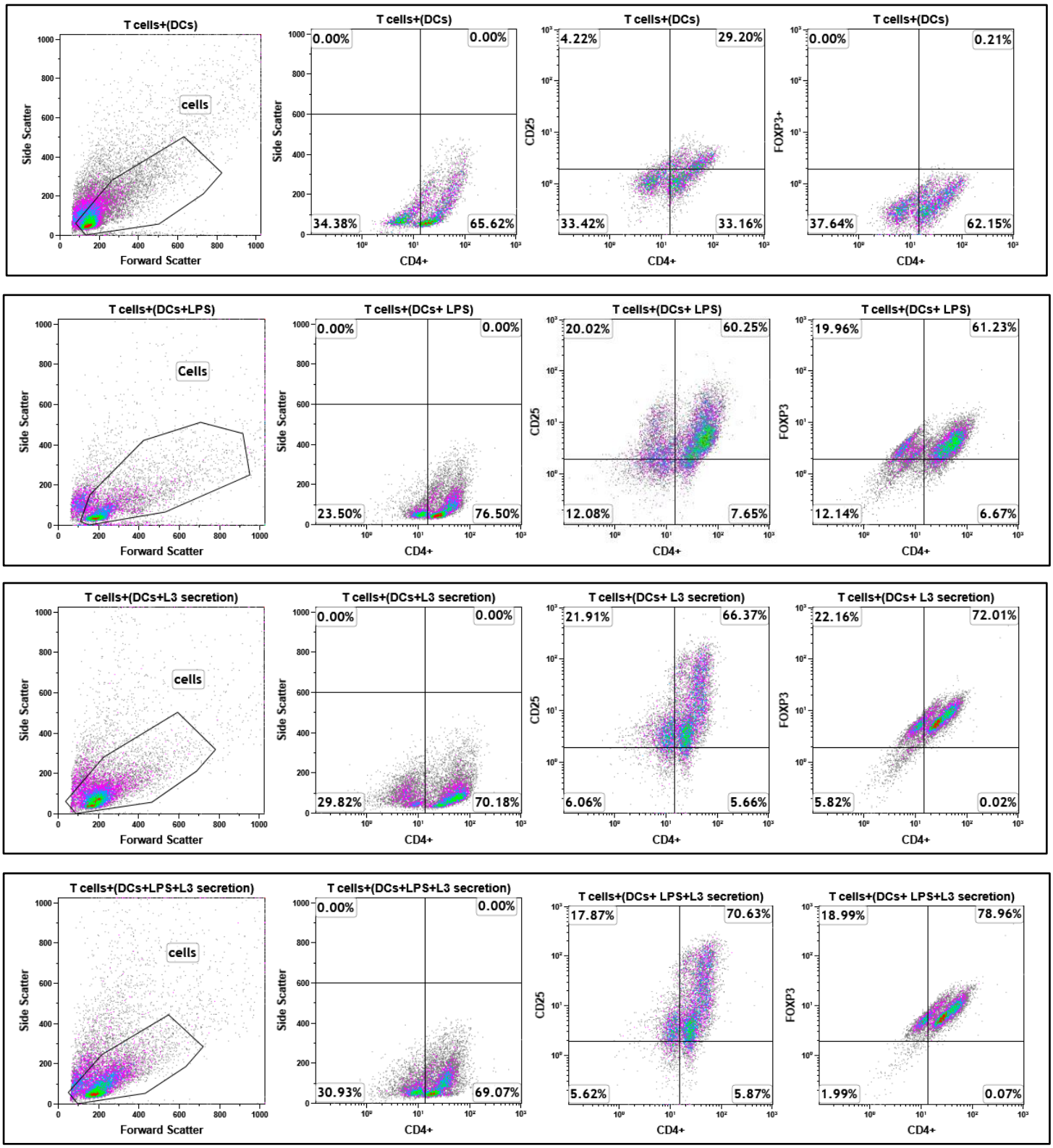

Figure 4.11: Flow cytometry phenotypic analysis of naïve T cells co-cultured with primed DCs. Dot plot data confirms expression of a $CD4^+$ cell population in all conditions. CD25 and FOXP3 expression in the $CD4^+$ T-cell population can be seen under larval secretion conditions in the presence or absence of LPS. Data are representative of three independent experiments using naïve T cells from three different donors (n=3).

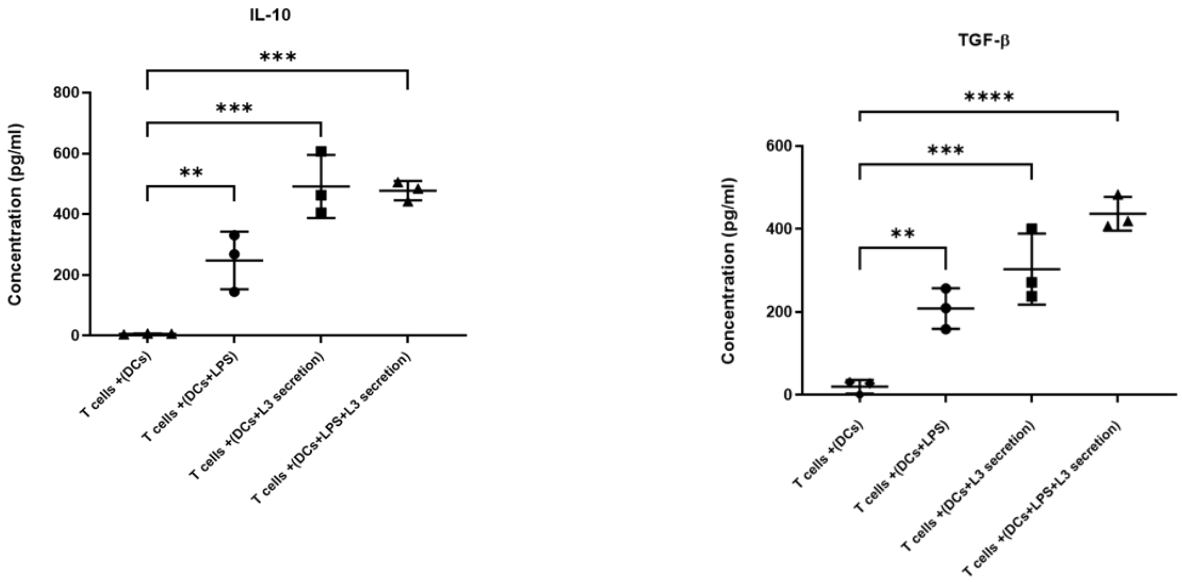

Figure 4.12: Cytokine production of T cells co-cultured with larval secretion-primed DCs. Marked increases in IL-10 and TGF-β production can be observed in T cells co-cultured with L3 secretion-treated DCs in the presence or absence of LPS. Data shown are means ± S.D of three independent experiments using cells supernatants from three different donors (n=3).

4.3.7 Quantification and quantitation of FOXP3 expression using polymerase chain reaction

To further confirm the generation of Tregs from T cells co-cultured with DCs pre-stimulated with larval secretions, we investigated FOXP3 expression as Treg transcription factor using end-point PCR and RT-PCR. The data obtained from end-point PCR and RT-PCR confirmed the expression of FOXP3 genes in T cells co-cultured with larval secretion-primed DCs in the presence or absence of LPS (Fig. 4.13A&B). This data was in line with our findings that showed that *N. brasiliensis* infective L3 was able to express FOXP3. Collectively, these findings indicated that *N. brasiliensis* infective larvae or their secretions could regulate the human immune system, which could suggest the potential role of L3 or their secretions in the treatment of autoimmune and inflammatory conditions.

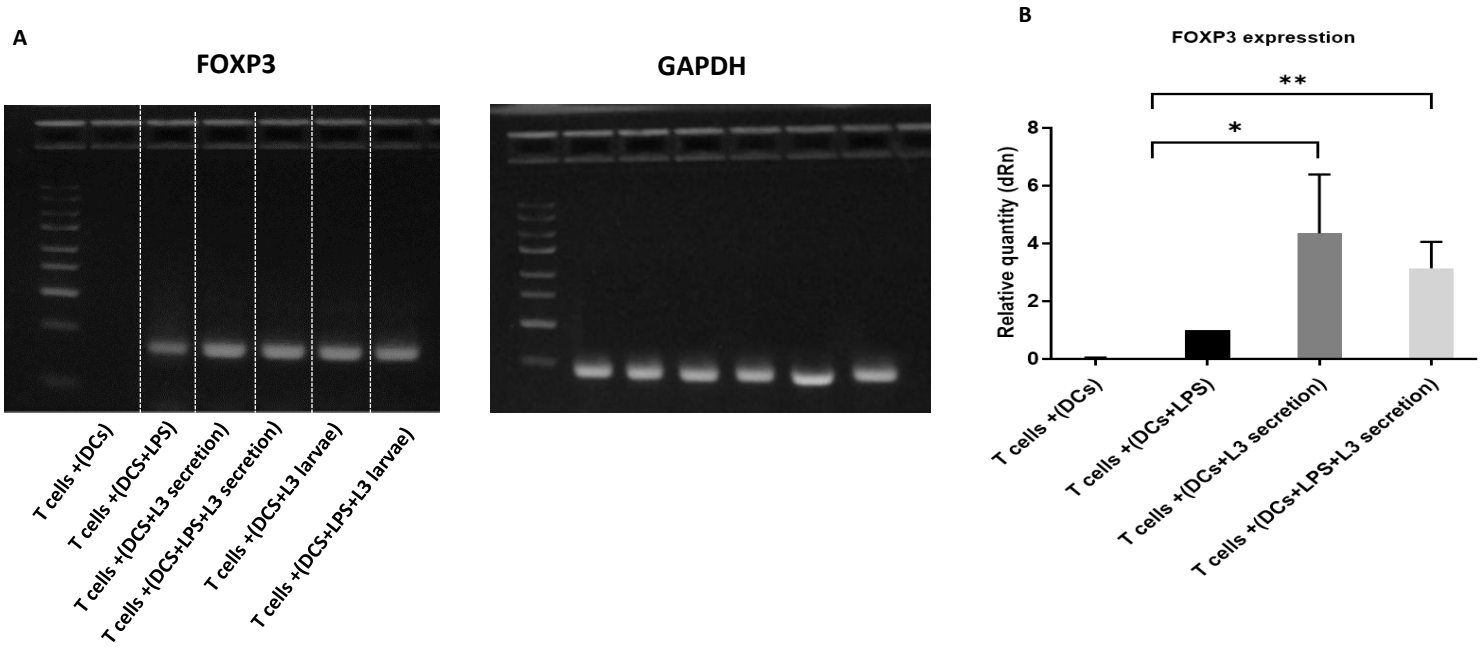

Figure 4.13: PCR to confirm T-cell phenotype generated by DCs primed with *N. brasiliensis* infective larvae. A) End-point PCR data show induction of FOXP3 in infective larvae alone and in the presence of LPS (n=3). **B)** RT-PCR data is consistent with end-point PCR data, showing significant increases in FOXP3 expression compared with LPS alone, indicating the generation of a Treg phenotype in the population for infective larvae. Data are shown as mean ± SD of three independent donors (n = 3).

4.3.8 T cell differentiation in co-cultures with *N. brasiliensis* larvae secretions primed DCs suppress activation of memory T cells

This assay was carried out to determine the influence of larval secretion-DC-primed T cells on effector T cells. T cells were co-cultured with DCs pre-treated with L3 secretion either in the presence or absence of LPS; the cells were harvested and co-cultured with CFSE-labelled effector T cells. After 96-hour culture, effector T cells were harvested and analysed by flow cytometry. CFSE-labelled effector T cells showed a clear reduction in proliferation in the presence of larval secretions, but not in the presence of LPS. These data are consistent with our previous observations, which indicated that larval products drove most of the T cells towards Tregs and that these Tregs contributed suppressive activity (Fig. 4.14).

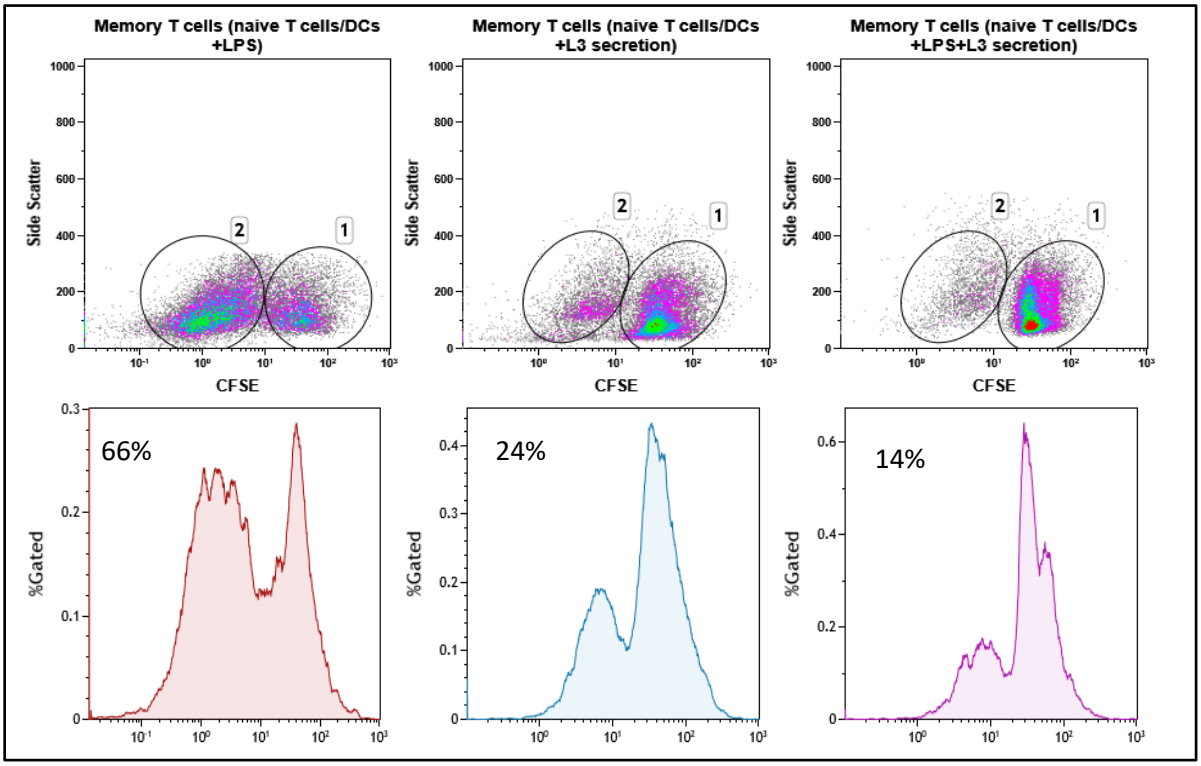

Figure 4.14: T-cell suppression assay. Histograms show the percentage of dividing CFSE-labelled effector T cells co-cultured with Tregs. Effector T cells show increased proliferation in the LPS condition decreased proliferation activity in larvae secretion condition. Data shown are of from three independent experiments (n=3).

4.4 Discussion

N. americanus larvae are believed to modulate the hots immune system both mechanically during penetration, but also by secreting a wide range of glycoproteins [152,218]. These glycoproteins can interact with TLRs and CLRs on host DCs, leading to immunomodulation. *N. americanus* larvae have been shown to secrete numerous glycoproteins that play a role in modulating the immune response [106,154]. Characterisation of these secretions is crucial to understand their impact in the context of immune regulation, which could help in the development of novel therapeutic strategies. Previous studies have indicated that secretions from *N. americanus* infective larvae modulated human DC phenotype and function; however, the exact mechanism involved in the immunomodulatory effects, the involvement of CLRs in the uptake of parasite secretions, and the downstream effect of larval secretions on shaping the adaptive immune response remains elusive [70]. Therefore, we aimed to investigate the influence of larval products on human DC phenotype and function, particularly within the context of cell-surface marker expression, production of cytokines, IDO activity, and downstream effects on T-cell polarisation.

We evaluated the impact of *N. brasiliensis* larval secretions on DC phenotype and function. The data showed that DCs maintained an immature phenotype following treatment with 20 µg/ml of larval secretions, as evidenced by a lack of maturation molecule expression, including HLA-DR, CD86, CD80, and CD40. In contrast, DCs expressed PDL-1 and overproduced IL-10. There was a significant reduction in DC-SIGN and MR expression following stimulating with larval products. In contrast, DCs maintained their ability to respond to LPS stimulation, as there was upregulation of maturation markers. These data indicated that the L3 secretions promoted tolerogenic DCs that could prime and induce the Tregs. Our data were similar to reports that suggested that PDL-1 plays a role in the expression and production of IL-10 during induction of immune tolerance [282-284]. The absence of maturation markers on the DCs could lead to the induction of Tregs [285]. Nevertheless, the downregulation of DC-SIGN and MR expression on DCs after stimulation with larval secretions highlights the presence of CLR ligands within larval products; these glycosylated antigens are investigated in this chapter.

As a result of the anti-inflammatory conditions induced by DCs after stimulation with *N. brasiliensis* L3 secretions, we further investigated how L3 secretions affect IDO activity. The data showed that DCs stimulated by larval secretions were unable to induce IDO activity. In contrast, IDO activity increased when the cells were exposed to LPS only. These results indicated that DCs had an anti-inflammatory role after they were exposed to L3 secretions due to a lack of IDO induction. Next, we investigated the process by which larval secretions modulated TLR4 signalling, which was induced by LPS within the context of the cell phenotype, cytokine production, and IDO activity. Our previous results showed that LPS induced DC maturation by enhancing production of pro-inflammatory cytokines and inducing a high level of IDO activity. Interestingly, these effects were absent in the presence of L3 secretions, which could indicate that larval secretions can modulate TLR4 and suppress the immune response. Research has shown that ligation of mannose or fucose with DC-SIGN on DCs can modulate TLR responses, as seen in *H. pylori* and *Mycobacterium* infection [286,287]. A study by Royer et al. reported that engagement of MR on iDCs with specific glycosylated antigens inhibited induction of IDO activity [258].

Amongst the CLRs expressed by DCs are MRs and DC-SIGN; both receptors recognise a wide range of glycosylated antigens, and they have a role in inducing inhibitory or stimulatory signals in DCs that result in modulation of DC function [288]. Given the high expression of DC-SIGN and MR on DCs and their role in the recognition of different pathogens, their potential role in DC interactions with larval products was investigated using antibodies to block MR and DC-SIGN. Our data demonstrated that DCs treated with blocking antibodies for either DC-SIGN or MR showed a significant decrease in induction of anti-inflammatory cytokines and reverted the observed suppression of IL-12 production compared with untreated DCs. Khoo et al., Cumming et al., and Hewiston et al. reported that glycosylated proteins, which were abundant on the parasite surface and within their secreted antigens, had a role in modulating host immunity [152,289,290]. This observation is in line with our findings, which showed downregulation of DC-SIGN and MR expression by DCs following treatment with the L3 secretions, indicating involvement of CLRs in the recognition of the L3 secretions. It was reasonable to assume that CLRs on human DCs acted as a main target in the recognition of these

secretions and presence of glycosylated protein within larval secretions. This clearly indicates the fundamental role of both DC-SIGN and MR in mediating interaction with glycosylated larval products. CLRs are key receptors targeted by larval products to modulate the innate immune response within a host.

Considering the noticeable immunomodulatory effect of the larval secretions on DCs, we examined the presence of glycosylated proteins within larval products. The initial examination of *N. brasiliensis* larval products by electrophoretic separation demonstrated the presence of most proteins with a molecular weight range of 62–175 kDa. Then, glycosylated proteins found in *N. brasiliensis* larval secretions were examined using biotinylated labelled lectins to identify carbohydrate moieties, as described previously. Carbohydrates are detected as dark bands against a clear background using Western blotting. Based on our findings, bands detected between 62–83 kDa were assigned to galactose and GalNAc containing glycoproteins; this was in line with a study that showed that galactose and GalNAc from mucin in bovine milk were located between 60–75kDa [291]. Bands detected between 100–175 kDa was assigned to mannose rich glycoproteins, while bands detected between 25–32 kDa were assigned to fucose rich glycoproteins; this was in line with a study that showed that mannosylated glycans of *Trypanosoma congolense* were detected between 100–130 kDa, while fucose in *Aspergillus fumigatus* was located between 23–30 kDa [292, 293]. These results highlighted the presence of a variety of carbohydrate moieties, including galactose, GalNAc, and fucose in the *N. brasiliensis* larval secretions, which could provide new insights into parasite secretion-mediated immune regulation. These insights could assist in the design of more efficient therapies and vaccines. More importantly, this finding is consistent with our previous finding that showed the presence of regulatory sugars on the *N. brasiliensis* infective larval cuticle and in larval secretions, indicating that L3 and their secretions have similar roles in regulating immune responses.

Several studies have demonstrated that tolerogenic DCs characterised by increased IL-10 secretion and expression of PDL-1 played a key role in promoting immune tolerance through induction of Tregs [267-269]. Therefore, we investigate the immunomodulatory effects of larval secretion-primed DCs on shaping the adaptive immune response using DC-T-cell co-culture experiments. Data obtained

from these experiments showed the presence of a $CD25^+FOXP3^+$ cell population within $CD4^+$ T cells that were co-cultured with L3 secretions in the presence or absence of LPS compared with the control. Level of key cytokines, such as IL-10, TGF-β, IL-4, and IFN-γ, were measured from the co-culture supernatants using ELISA. As expected, the results showed a significant increase in IL-10 and TGF-β production in T cells co-cultured with L3 secretion-treated DCs in the presence or absence of LPS. However, no statistically significant increase was detected in the production of IFN-γ and IL-4 under these conditions. Overall, the co-culture results indicated that the L3 secretions modulated DC function, leading to induction of $CD4^+CD25^+FOXP3^+$ Tregs. This finding is in line with a study that showed expansion of $CD4^+CD25^+FOXP3^+$ Tregs after infection with filarial parasites, such as *Brugia malayi*, which played an important role in evading host immunity [294]. We assessed T-cell proliferation after co-culture with larval secretion-conditioned or unconditioned DCs in the presence or absence of LPS. The data showed proliferation of T cells, which confirmed the potency and viability of T cells after the co-culture experiment. These findings confirmed that larval secretions had a similar role in regulating immune responses as infective larvae.

Next, we looked at FOXP3 gene expression to confirm our observation of the generated immune response. PCR data showed increased regulatory FOXP3 in larval secretions compared with the control, confirming the presence of a regulatory T-cell phenotype under that condition. This finding is consistent with our previous results, where infective larvae expressed the regulatory FOXP3 gene. These findings are in line with research that showed that parasites, such as *Entamoeba histolytica*, rely on galactose and GalNAc for survival [295]. Another study showed that a protein containing galactose from *Trypanosoma cruzi* bound to human erythrocytes and mediated host-cell invasion [296].

We designed a suppression assay to elucidate the effects of regulatory-phenotype cells generated after culturing larval secretion-treated DCs with naïve T cells. The data showed marked reduction in effector cell proliferation with larval secretions alone and in the presence of LPS, in which a $CD4^+CD25^+FOXP3^+$ cell population with production of IL-10 and TGF-β cytokines has previously been shown. This finding is in line with a study that showed that $CD4^+CD25^+$ Tregs suppressed effector T cells in leishmaniasis [297].

4.5 Conclusion

This chapter described the immunomodulatory properties of *N. brasiliensis* larval secretions that were able modulate DC immune responses, switching DCs to an anti-inflammatory phenotype through modulation of TLR–CTL crosstalk. First, we demonstrated that L3 secretions bound to CLRs, significantly downregulated the expression of these receptors, and induced a regulatory DC phenotype characterised by significant production of IL-10 and suppression of IL-12p70 production in response to LPS. Interestingly, blocking MR and DC-SIGN could—at least partially—revert the observed suppression of IL-12 production in the presence of larval secretions, which indicated that C-type lectin ligands might mediate the observed immunosuppressive effects. Furthermore, we noted that *N. brasiliensis* secretions suppressed IDO activity, which impacted downstream T-cell polarisation. Interestingly, we identified the presence of regulatory carbohydrates, including galactose and GalNAc containing glycoproteins within larval secretions, and discovered exciting new areas for further investigation. This study provides opportunities to understand the strategies used by parasites to modulate immune responses, which could help us to utilise these strategies for the treatment of autoimmune and inflammatory diseases. However, to fully understand the immune modulatory potential of these regulatory carbohydrates, it is important to deplete these sugars from larval secretions and investigate their impact on DCs and downstream on T-cell activation and polarisation following DC priming with depleted sugars. Depletion of target carbohydrates from larval secretions is detailed in Chapter 5.

Chapter 5:

Depletion of carbohydrates from *Nippostrongylus brasiliensis* infective larval secretions and investigation of their impact on immune cells

5.1 Introduction

Data presented in previous chapter illustrated the role of CLRs in mediating immune regulatory properties of *N. brasiliensis* infective larvae secretions on DC phenotype, cytokine profile, downstream effect on T-cell polarisation, highlighting the potential importance of carbohydrates, including galactose and GalNAc, in larvae secretions in these processes. It is therefore important to understand the biological relevance of these carbohydrates in modulating DCs phenotype and how these carbohydrates can shape the outcomes of adaptive immune responses.

Lectins are a group of proteins found in plants and in a diverse array of microorganisms; they can bind to specific carbohydrates [298]. Immune cells, such as DCs, express lectins on their surface, including PRRs, which can recognise carbohydrates and glycoproteins expressed on pathogen surfaces [299]. These lectins are either membrane-bound or soluble, depending on their role [300]. The interaction between these lectins and carbohydrate ligands have been the focus of increasing interest in recent years. The importance of this interaction is that it may aid in the understanding of the immunomodulatory role of pathogens in directing host immune systems to the tolerogenic pathway, thus allowing them to escape the immune system [301]. Many studies have shown that some carbohydrates—including those decorating pathogens—play a role in modulating the immune system by modulating DC function. For example, it has been shown that a synthetic immobilised galactose can induce a tolerogenic DC phenotype and skew T-cell responses towards the Treg phenotype [302]. Hamilton et al. showed that glyco-antigens of *F. hepatica* could bind to DC-SIGN on DCs and suppress DC maturation, which contributed to pathogen survival [303]. Furthermore, it has been shown that glycosylated allergens can modulate the immune system through binding to DC-SIGN [260].

It is well known that hookworms such as *N. americanus* can suppress production of pro-inflammatory cytokines and induce anti-inflammatory properties [95,96]. In addition, immunomodulatory molecules secreted by parasites can generate a regulatory or tolerogenic phenotype among immune cells, such DCs, that can influence T-cell differentiation [304]. There is a decline in the prevalence of allergies

and autoimmune diseases in helminth carriers [184-186]. Studies have shown that hookworm infection can protect against allergy and autoimmune conditions and has shown promising outcomes for the treatment of these conditions using parasite secretions [182,183]. For example, a study showed that ES-62 glycoprotein from *Acanthocheilonema viteae* had a protective effect on systemic lupus erythematosus (SLE) by downregulating MyD88 expression in B cells and kidney cells, therefore inhibiting production of IL-12 [305]. In another study, lacto-N-fucopentaose secreted by *S. mansoni* can bind to DC-SIGN on DCs thereby induce production of anti-inflammatory cytokines and it has been demonstrated to protect against type1 diabetes [306].

Much is known about how hookworms modulate immune responses, particularly through modulating DC phenotype and function, and these parasites have been studied as treatment for autoimmune diseases. However, the capacity for carbohydrates from larval secretions to modulate immune responses and using these carbohydrates as therapeutic tools has not been well studied. Therefore, this chapter investigates the effect of galactose and GalNAc depleted from *N. brasiliensis* larval secretions on DC phenotype and function. Accordingly, in this chapter, we depleted galactose and GalNAc from larval secretions and used RCA and SBA lectins to confirm their depletion to investigate whether these glycoproteins represent immunomodulator molecules in larval secretions. The ability of these carbohydrate-primed DCs to skew T-cell differentiation is investigated using DC-T-cell co-cultures. These findings will provide opportunities to use depleted carbohydrates from parasite secretions as immunomodulatory tools or as therapeutic agents for the treatment of autoimmune conditions and allergies.

5.2 Materials and methods

5.2.1 Preparation of *N. brasiliensis* infective larval secretions and measurement of protein concentration

As previously described in Chapter 4 see section 4.2.2 *N. brasiliensis* L3 were cultured in RPMI 1640 medium supplemented with 100 IU/ml penicillin, 100 µg/ml streptomycin, and 1% gentamicin, then incubated for 24 hours at 37°C in 5% CO_2. The larval secretions were then collected and concentrated using a Vivaspin2 centrifugal concentrator unit MWCO 3kDa. The protein concentration of the concentrated larval secretions was quantified using a protein assay (BCA). Then, the concentrated larval secretions were stored at -80ºC until carbohydrate depletion was carried out.

5.2.2 Enrichment of galactose and N-acetylgalactosamine

Pierce™ Disposable Columns were purchased from Thermo Fisher Scientific, UK. *Ricinus communis* agglutinin (RCA), an agarose-bound lectin specific for galactose depletion, was purchased from Vector Laboratories, UK. Soybean agglutinin (SBA), an agarose-bound lectin specific for GalNAc depletion, was purchased from Vector Laboratories, UK. Glycoprotein Eluting Solution for galactose/GalNAc-binding lectins was purchased from Vector Laboratories, UK. Hydroxy-ethyl-piperazine (HEPES) buffer solution was purchased from Sigma-Aldrich.

To deplete galactose and GalNAc from larval secretions, Pierce™ Disposable Columns were prepared before starting the experiment. Briefly, a porous filter disc was inserted into the column bottom and then the column was washed with 10 mM HEPES buffer to remove air bubbles from below the disc filter. We pipetted RCA and SBA agarose lectins into separated, prepared disposable columns and allowed the agarose to settle on the disc filter in the bottom of the tube by gravity. Then, 15-ml centrifugal tubes were placed under the columns, the columns were washed with 10 mM HEPES buffer and the flow-through was discarded. We placed new 15-ml centrifugal tubes under the columns, applied larval secretions into the first column containing RCA agarose lectin, and allowed the larval secretions to drain through the column by gravity. We retained the larval flow-through from the first column into the second column containing SBA agarose lectin, then allowed it to drain through the column by gravity. The larval secretion flow-through from the second column was referred to as

'depleted-sugars larval secretion' and stored at -20°C until use. The two columns were washed with 10-mM HEPES buffer solution to remove unbounded sugars before applying the eluting solution. Then, 15-ml centrifugal tubes were placed under the columns, eluting solution was added to the two columns to release bound sugars, and the eluates representing galactose and GalNAc enriched fraction were collected and stored at -20°C until use (Fig. 5.1).

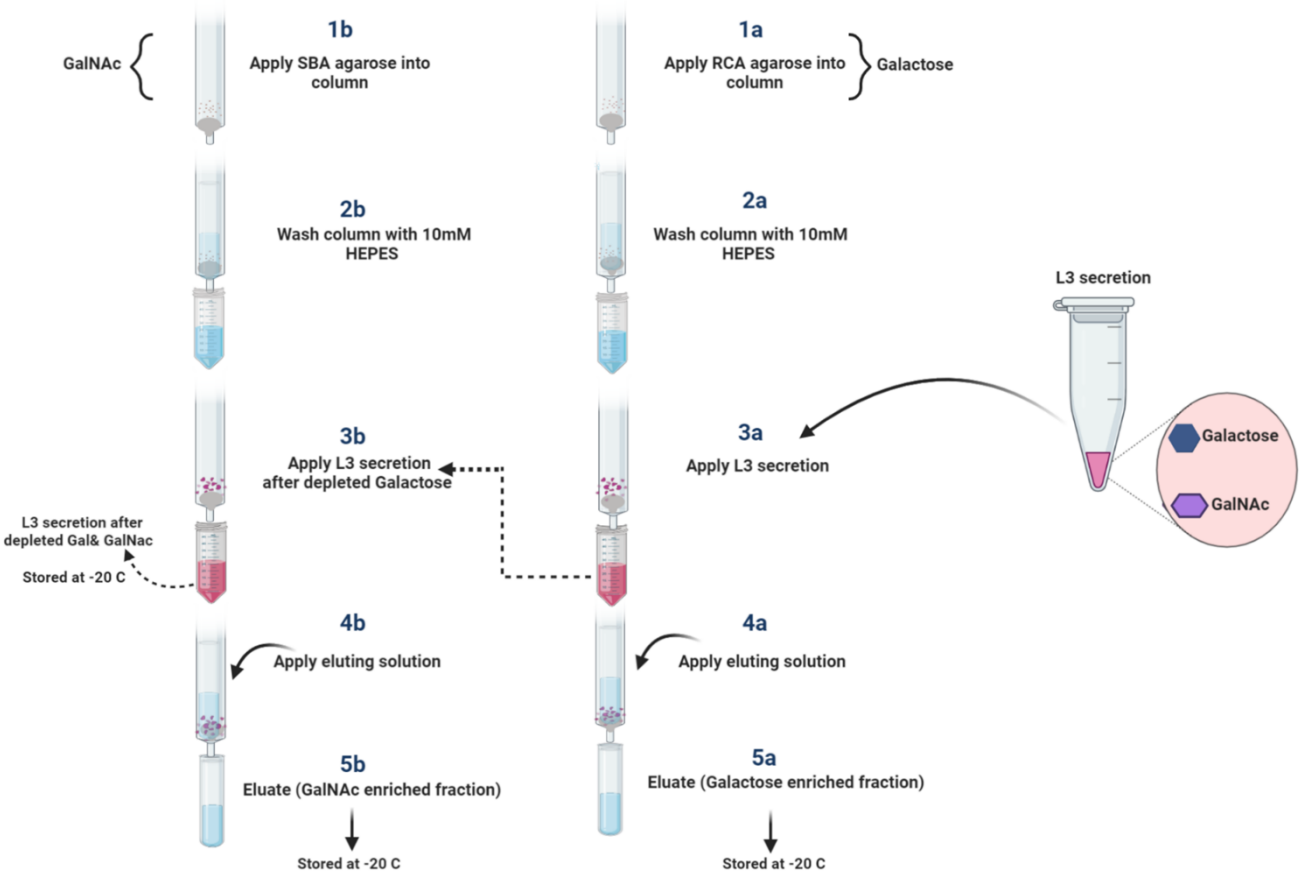

Figure 5.1: Illustration of galactose and N-acetylgalactosamine (GalNAc) depletion from larval secretions. 1a & 1b) Two disposable columns were prepared by inserting filter discs inside the columns, then applying RCA and SBA agarose lectins. **2a & 2b)** The columns were washed with 10-mM HEPES buffer and the buffer was allowed to drain by gravity. **3a)** Larval secretions were added to the column containing RCA agarose lectin and the larval secretions were allowed to drain through the column by gravity. **3b)** The flow-through from the 3a column was added and the larval secretions were allowed to drain by gravity. The flow-through from this column was stored as 'galactose- and GalNAc-depleted larval secretions. **4a & 4b)** columns were washed with 10 mM HEPES and eluting solution was applied. The elutes of galactose and GalNAc were stored at -20°C until use.

5.2.3 Characterisation of depleted sugars using SDS-PAGE, silver staining, and Western blot

As previously mentioned in Chapter 4 section 4.3.5 whole larval secretions, galactose and GalNAc enriched fractions from the secretion, and larval secretions after glycoprotein depletion were run in Mini-Protein Precast Gel 4–15% (Bio-Rad, UK). The gel was stained with silver stain (Vector laboratories, UK). To perform Western blotting, unstained SDS-PAGE gel was transferred onto a PVDF nitrocellulose membrane. The nitrocellulose membrane was stained with RCA and SBA biotinylated labelled lectin antibodies (Vector Laboratories, UK), according to the manufacturer's protocol. Finally, the membrane was incubated with chemiluminescent fluorescent substrate and imaged using a chemiluminescent imaging system.

5.2.4 Dendritic cell generation and naïve T-cell isolation

Monocytes were isolated from the buffy coat of healthy donors following approval of the ethics committee (National Blood Service, Sheffield, UK). DCs were generated from the monocytes, while naïve T cells were isolated from monocytes, as previously described in Chapter 3 section 3.2.2.

5.2.5 Dendritic cell-depleted sugar co-culture

iDCs (2.5×10^5 cells/well) were seeded in a 24-well plate in complete RPMI 1640 medium and treated with 20 ug/ml of each depleted sugar in the presence or absence of LPS. iDCs were also treated with 20 ug/ml of sugar-depleted larval secretions in the presence and absence of LPS. For the positive control, iDCs were stimulated with LPS from *E. coli* (10 ng/ml), while unstimulated DCs were used as the negative control. Cells were incubated for 24 hours at 37°C with 5% CO_2.

5.2.6 Analytical flow cytometry and cytokine measurement

Following 24 hours of culture, cells were harvested from the well plate to FACS tubes and centrifuged at 350 g for 5 minutes, acc/dec=3. Cell supernatants were collected and analysed for cytokine content. Cell pellets were washed with PBA (PBS with 0.5% bovine serum albumin and 0.1% sodium azide), followed by incubation with labelled antibodies (CD209 FIT-C, CD206 PerCP, CD86 PE, CD80 APC, HLA-DR PerCP, or CD40 PE) in the dark at 4°C for 20 minutes. Cells were then washed with PBA

and fixed with 4% paraformaldehyde until analysis. The samples were measured using the FC500 flow cytometer (Beckman Coulter, UK), and the resulting data were analysed using Kaluza software.

5.2.7 Quantification of dendritic cell viability assay

As described in Chapter 2, cell viability assessment was performed using LIVE/DEAD stain (Thermo Fisher Scientific) according to the manufacturer's protocol. Briefly, cell supernatants were removed, stained with 250 µl of LIVE/DEAD stain, and incubated for 20 minutes in the dark at 37°C before analysis. Cells were imaged using the Fluorescent Cell Imager (Etaluma) and data analysis was conducted by counting fluorescent cells using ImageJ software.

5.2.8 Dendritic cell-T-cell co-culture

Autologous naïve T cells were co-cultured with DCs primed by enriched glycoproteins at a ratio of 1:10 (DC:T cell) in RPMI media supplemented with 5% human AB serum, 100 U/ml penicillin, 100 mg/ml streptomycin, and 2 mM L-glutamine (all from Sigma-Aldrich). On day 3 after co-culture, fresh media supplemented with 2 ng/ml of IL-2 was added to the co-culture. On day 6, cells were harvested, counted, re-stimulated with 2 ug/ml of anti-CD3 and anti-CD28, then seeded in a flat-bottom 96-well plate (1×10^5 cells/well) and incubated for 24 hours. The cells were then stained for phenotypic identification using T-cell markers CD4 (clone REA623), CD25 (clone) and FOXP3 (clone 236AE7) (all from Miltenyi Biotec, UK), non-reactive isotype-matched antibodies were used as controls, while cell supernatants were collected for cytokine analysis.

5.2.9 RNA isolation and cDNA synthesis

As described in Chapter 3 section 3.2.10, RNA extraction was carried out using the RNeasy kit (QIAGEN), while cDNA synthesis was carried out using the PCRBIO synthesis kit, according to the manufacturer's instructions.

5.2.10 End-point PCR and real-time quantitative PCR

Endpoint-PCR and real-time PCR were carried out using Taq mix and SYBR Green qPCR Master Mix, respectively, as described in Chapter 3 section 3.2.10.

5.2.11 Statistical analysis

Data were analysed and evaluated using GraphPad Prism version 7.02 (GraphPad Software, San Diego, CA). Values are presented as mean ± SEM and statistical significance was determined by one-way ANOVA when comparing two groups. A p-value <0.05 was considered statistically significant.

5.3 Results

5.3.1 Characterising the galactose and N-acetylgalactosamine depleted from larval secretions

Following depletion of galactose and GalNAc from larval secretions using agarose bound lectins, the eluted enriched glycoproteins were separated via protein gel electrophoresis followed and the gel was stained with silver stain. Fig. 5.2 shows galactose and GalNAc enriched fractions, represented by the presence of bands between 62 kDa and 83 kDa. The data also showed the absence of those bands from larval secretions after depletion of galactose and GalNAc, as compared with whole larval secretions. To verify this result, unstained protein gel was transferred onto a PVDF nitrocellulose membrane and Western blotting was performed. After Western blotting, each of membrane lanes were stained separately with either RCA or SBA lectins. Figure 5.3 shows that galactose enriched fraction positively reacted with RCA lectin, while SBA lectin positively reacted with GalNAc enriched fraction, compared with the galactose/GalNAc-depleted larval secretions, which did not react with RCA and SBA lectins. These results confirm that galactose and GalNAc enriched fraction from larval secretions could be used for further experiments.

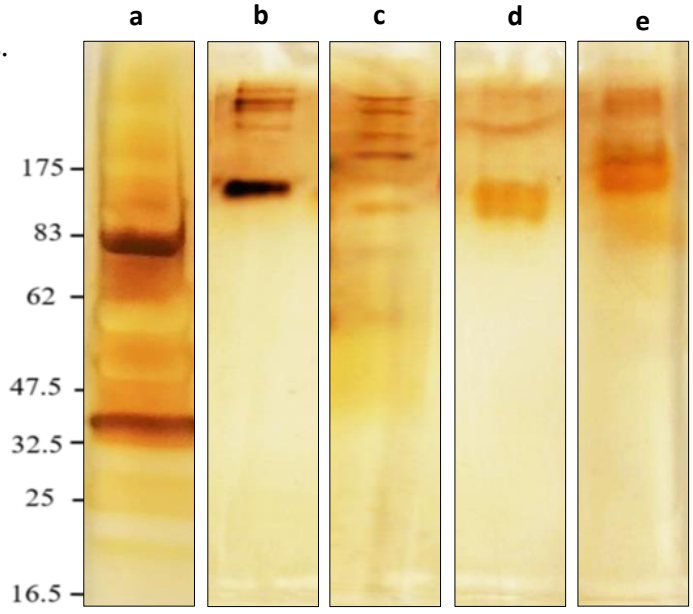

Figure 5.2: Separation of galactose and GalNAc enriched larval secretion on SDS-PAGE gel. After gel electrophoresis, the gel was silver stained. **a)** Protein ladder molecular weight 16.5–175 kDa. **b)** Whole larval secretions. **c)** Galactose/GalNAc-depleted larval secretions. **d)** Galactose enriched. **e)** GalNAc enriched. Data shown are from two independent experiments (n=2).

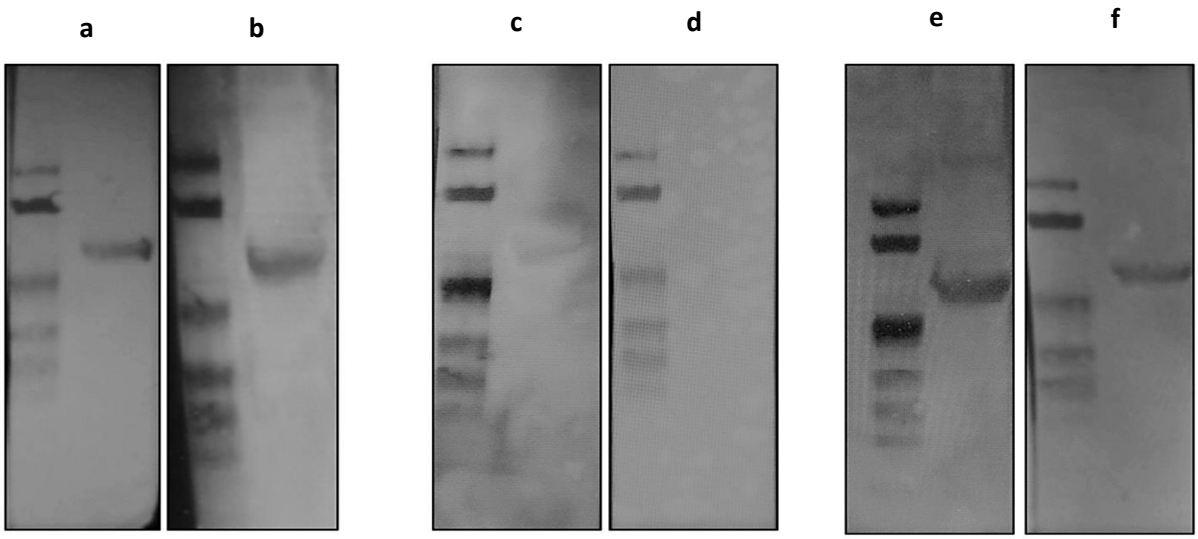

Figure 5.3: Analysis of galactose and GalNAc enriched fractions using biotinylated lectins. a) & b) Whole L3 secretions positively reacted with RCA and SBA lectins that recognised galactose and GalNAc containing glycoproteins, respectively. **c) & d)** Galactose/GalNAc-enriched fractions did not react with SBA and RCA lectins. **e)** Galactose enriched positively reacted with RCA lectin. **f)** GalNAc enriched positively reacted with SBA lectin. Data shown are from two independent experiments (n=2).

5.3.2 Effect of galactose and N-acetylgalactosamine on dendritic cell phenotype and function

To investigate the effect of galactose and GalNAc isolated from L3 secretion on immature and mature DCs, unstimulated and LPS-stimulated DCs were cultured with 20 ug/ml of either galactose or GalNAc enriched fractions. After 24-hour culture, flow cytometric analysis was performed to identify DC phenotype changes using surface markers, and cytokine production was measured in cell supernatants. The data showed that galactose and GalNAc enriched fractions alone did not induce any changes in DC phenotype compared with unstimulated DCs; the DCs maintained an immature phenotype, as evidenced by a lack of upregulation of maturation markers (supplementary figure 11). In contrast, galactose and GalNAc enriched fractions could modulate DC phenotype in LPS-stimulated DCs, as evidenced by a significant decrease in maturation marker expression, including HLA-DR, CD80, CD86, and a decrease in expression of the co-stimulatory marker CD40; there was an increase in PDL-1 expression compared to LPS stimulated cells as shown in flow cytometry data (Fig. 5.4), suggesting a bias towards an anti-inflammatory phenotype in DCs stimulated with either galactose or GalNAc enriched. This observation is also reflected in the cytokine profile, where IL-12p70 production was decreased and IL-10 production

was increased (Fig. 5.5), supporting our previously observed changes in DC surface phenotype. This data clearly shows that galactose and GalNAc isolated from larval secretions have an immunomodulatory effect on DCs. DC viability was also monitored following these experiments using LIVE/DEAD staining, and >90% of cells were viable after co-culture with isolated carbohydrates (Fig. 5.6).

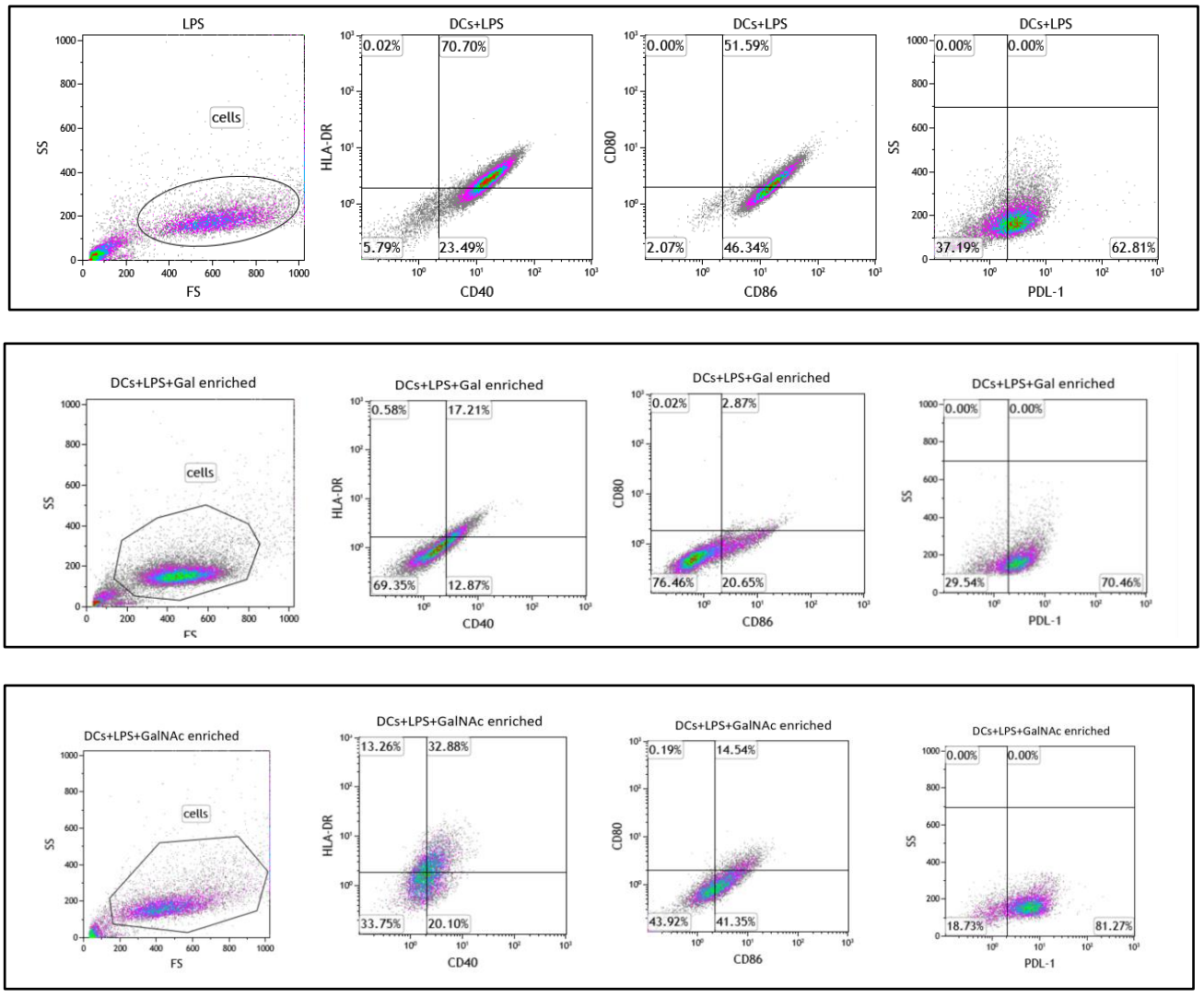

Figure 5.4: Phenotypic analysis of galactose and GalNAc enriched fractions on mature DCs. DCs were analysed for expression of maturation markers (HLA-DR, CD86 and CD80), a co-stimulation marker (CD40), and inhibitory marker (PDL-1). The data showed that galactose and GalNAc enriched fractions in the presence of LPS, were able to modulate DC phenotype compared with stimulation with LPS only. Data are from three independent experiments using DCs from three different donors (n=3).

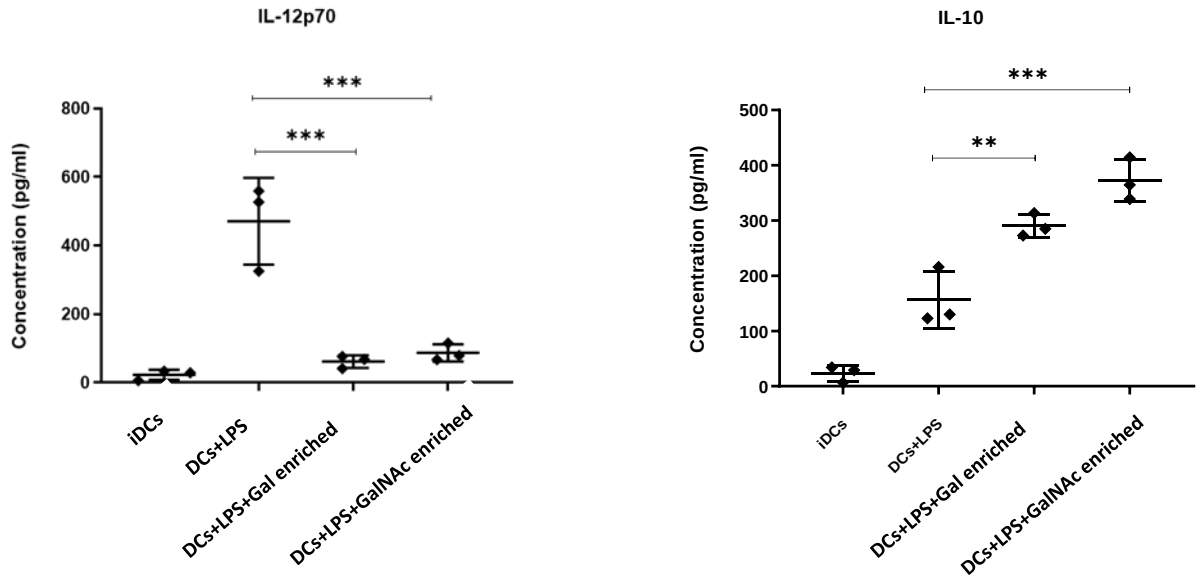

Figure 5.5. Cytokine profile of dendritic cells treated with galactose and GalNAc enriched fractions in the presence of a TLR4 ligand (LPS). Galactose and GalNAc enriched fractions induced a significant increase in IL-10 production and suppression of IL-12 in DCs stimulated with LPS compared with LPS stimulation alone. Data are shown as mean ± SD for three independent donors (n = 3). *p<0.05, **p<0.01, ***p< 0.001, ****p <0.0001. Data are from three independent experiments using DCs from three different donors (n=3).

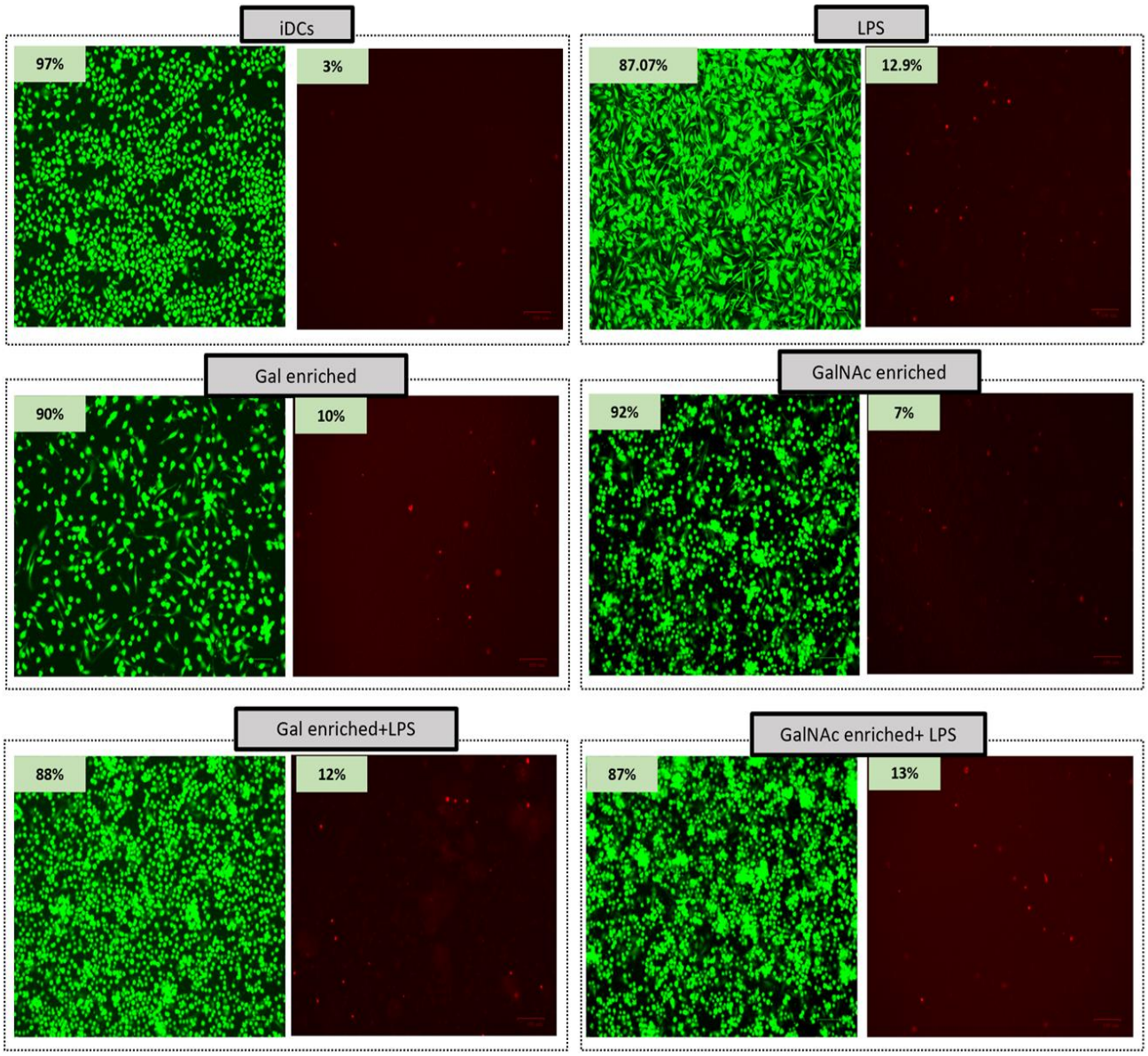

Figure 5.6: The viability of DCs 24 hours after treatment with galactose and GalNAc enriched fractions. DCs treated with Galactose and GalNAc enriched glycoproteins showed 90% viability. Data are from three independent experiments using DCs from three different donors (n=3).

5.3.3 Dendritic cells conditioned by galactose or N-acetylgalactosamine promoted T-cell differentiation towards IL-10-producing cells in autologous dendritic cell-T-cell co-cultures

Our previous findings showed that glycoproteins isolated from larval products, including galactose and GalNAc enriched, produced high levels of IL-10 while suppressing induction of IL-12 in the presence of LPS. Therefore, we next aimed to understand the downstream effect of these glycoproteins-primed DCs on T-cell differentiation through DC-T-cell co-culture studies. The co-culture experiment was performed as described previously using autologous naïve T-cells and DCs. Briefly, autologous naïve $CD45RA^+$ T cells were isolated from PBMCs, as described previously; the purity of the purified naïve T-cell population was assessed for expression of CD45RA. Our data confirmed that 96% of the isolated cells expressed CD45RA, indicating the purity of the naïve cells (supplementary figure 12). These cells can be used for co-culture study to investigate the effect of galactose- and GalNAc-primed DCs on T-cell activation and immune system modulation. Then, purified naïve T cells were preserved in liquid nitrogen for 7 days until the co-culture experiment was prepared. On co-culture day 1, thawed naïve T cells were tested for viability and activation status using a Trypan blue automated cell counter and testing for expression of CD25, respectively. Our data demonstrated that liquid nitrogen preservation did not affect naïve T-cell viability, as 94% of the cells were alive after storage, compared with cell viability after isolation (supplementary figure 13). Moreover, the naïve T cells did not express CD25 activation marker, indicating that the cells were not activated, and they were able to interact with DCs (supplementary figure 14).

Galactose and GalNAc enriched fractions induced high levels of IL-10 production while suppressing IL-12 production in LPS-stimulated DCs. The DCs were treated with 20 μg/ml of either galactose or GalNAc in the presence or absence of LPS for 24 hours. The DCs were then harvested and co-cultured with naïve T cells for 7 days; co-culture cells were supplemented with IL-2 on day 3, and on day 6 the T cells were restimulated with anti-CD3 and anti-CD28 for 24 hours. After co-culture, the T cells were assessed for phenotype and cytokine profile. Phenotypic analysis of T cells assessed the presence of CD3 as a general marker for T cells. In addition, we assessed expression of CD4 within the $CD3^+$ population and the presence of FOXP3 and CD25 populations within the $CD4^+$ T-cell population using

flow cytometry. Our data confirmed the expression of CD3 on the naïve T-cell population under all conditions (supplementary figure 15). The data also confirmed the presence of $CD4^+$ T cells within T-cell population, and the presence of FOXP3 and CD25 expression within the $CD4^+$ cell population under depleted carbohydrate conditions, as compared with LPS alone (Fig. 5.7). We assessed the levels of key cytokines in co-culture supernatant, including IL-10 and TGF-β, to investigate downstream of the T-cell phenotype. Fig. 5.8 shows a significant increase in IL-10 and TGF-β production by naïve T cells with galactose and GalNAc in the presence of LPS compared with LPS alone. This observation is in line with our previous T-cell phenotype analysis data. Overall, the co-culture results indicated that glycoproteins modulated DC function, which led to the induction of $CD4^+FOXP3^+CD25^{high}$ Tregs.

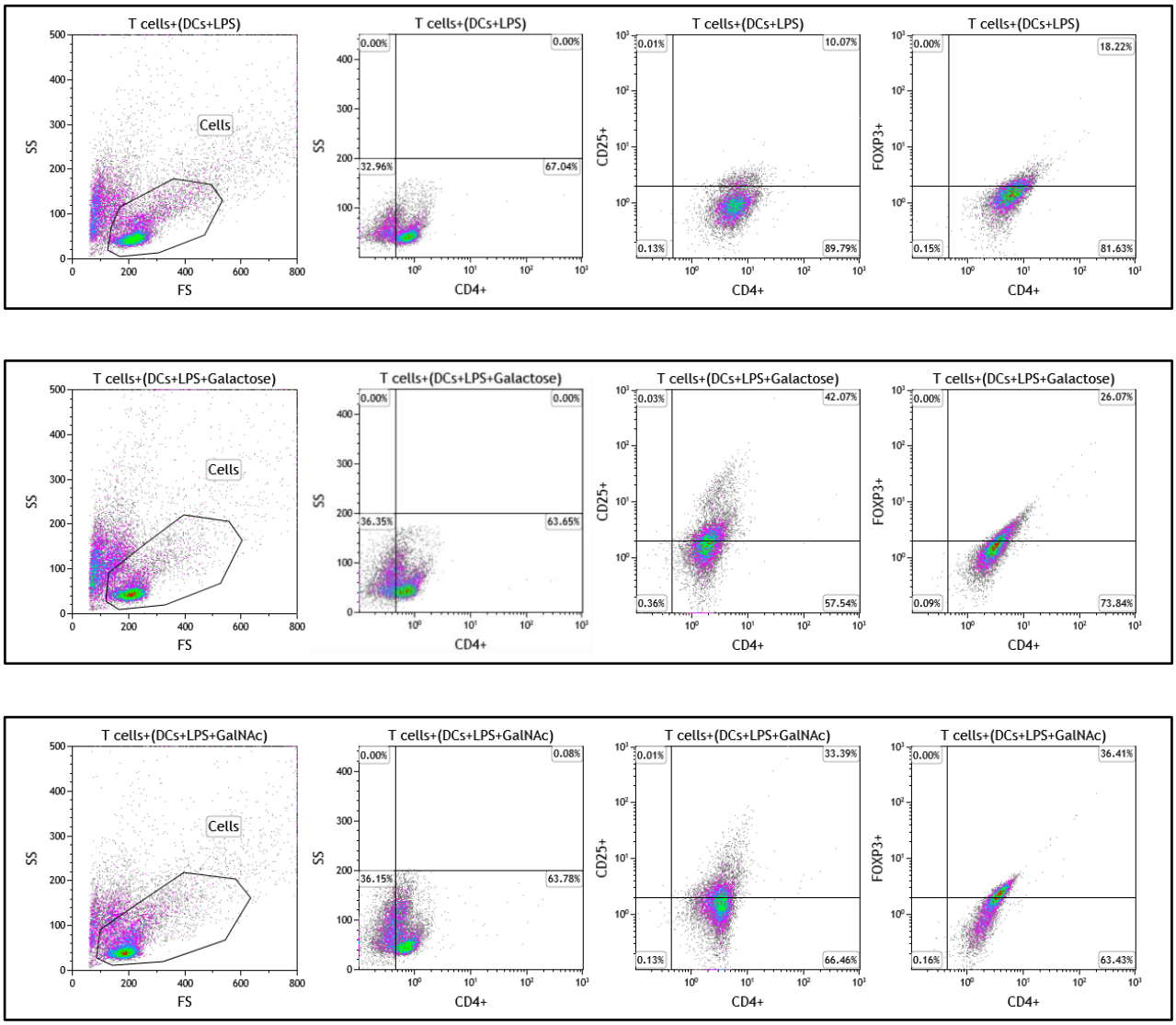

Figure 5.7: Flow cytometry phenotypic analysis of naïve T cells co-cultured with galactose- and GalNAc-primed DCs. Dot plot data confirm the expression of CD4 in the cell population in all conditions. The presence of CD25 and FOXP3 in the $CD4^+$ T-cell population was higher with galactose and GalNAc enriched fractions in the presence of LPS compared with LPS alone. Data are from independent experiments using naïve T cells from three different donors (n=3).

.

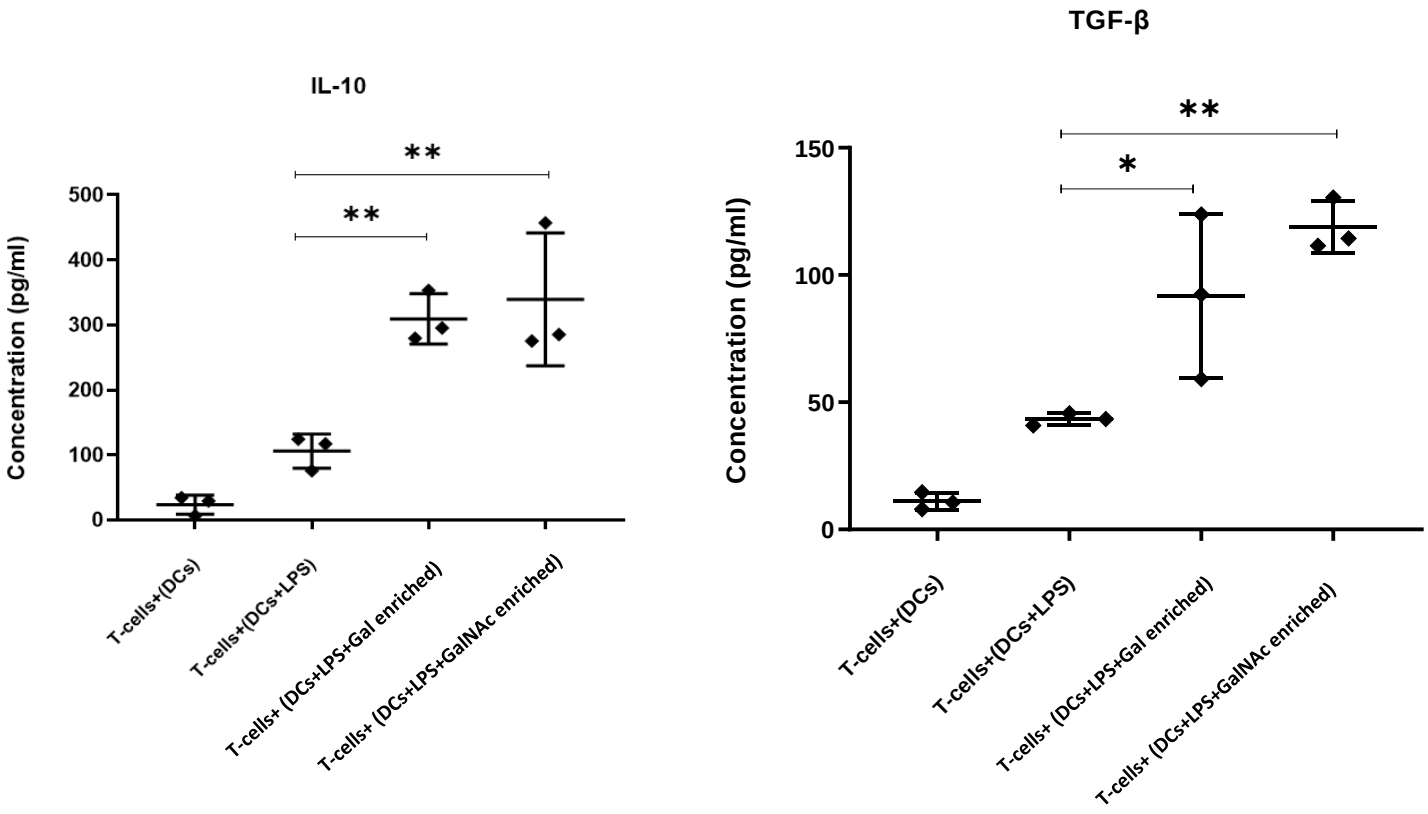

Figure 5.8: Naïve T-cell cytokine profile after co-culture with galactose- and GalNAc-conditioned DCs. An increase in IL-10 and TGF-β production was observed with galactose and GalNAc compared with LPS alone. Data shown are mean values ± S.D of three independent experiments using cells supernatants from three different donors (n=3).

5.3.4 Dendritic cells conditioned with galactose or N-acetylgalactosamine promoted T-cell differentiation towards a T-reg phenotype in dendritic cell-T-cell co-cultures

From our previous data, we hypothesised that naïve T cells co-cultured with galactose- or GalNAc-treated DCs acquired an anti-inflammatory phenotype. To confirm the phenotype of these cells, we investigated the expression of FOXP3 transcription factor using end-point PCR and RT-PCR. The data obtained from end-point PCR indicated the expression of FOXP3 in T cells co-cultured with galactose- or GalNAc-primed DCs in the presence or absence of LPS (Fig. 5.9A). Our RT-PCR results were consistent with the end-point PCR results, which showed a significant increase in FOXP3 expression under these conditions compared with LPS alone (Fig. 5.9B).

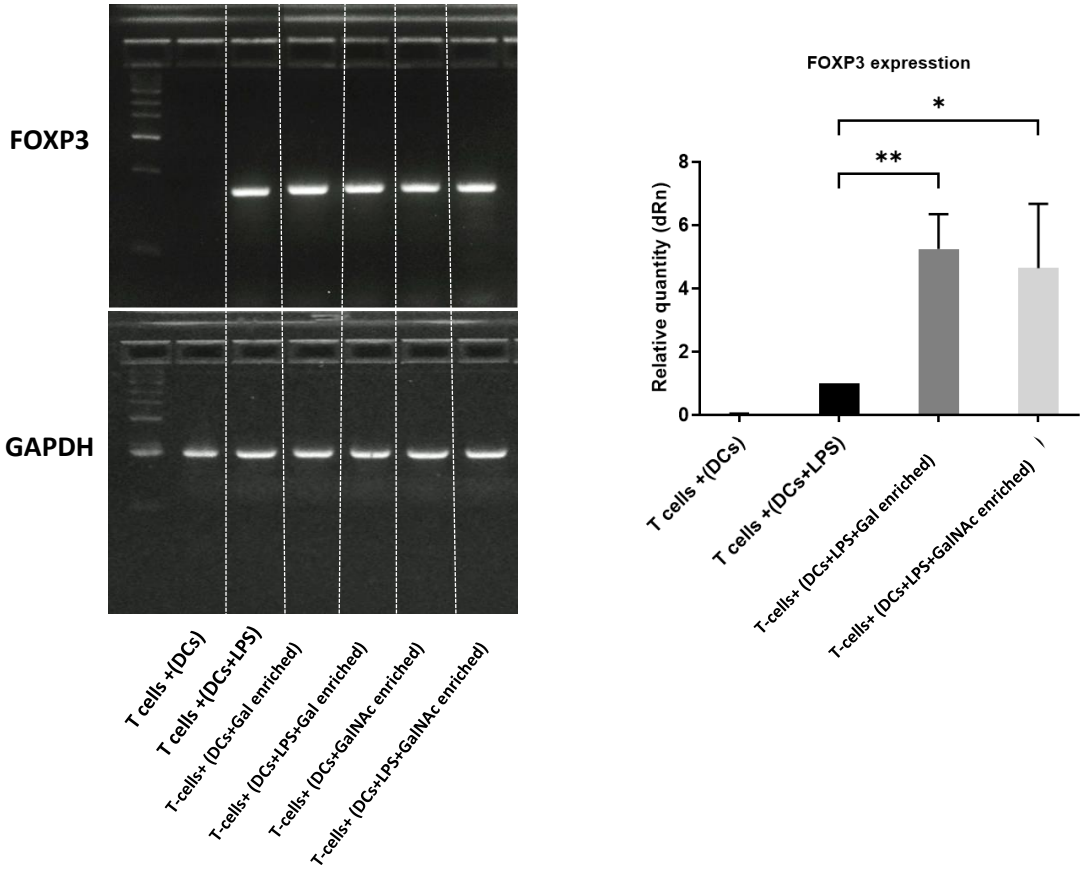

Figure 5.9: PCR data obtained from DC-T-cell co-culture. A) End-point PCR data showed the induction of FOXP3 in galactose and GalNAc fractions in the presence or absence of LPS (n=2). B) The RT-PCR data was also consistent with end-point PCR data showing significant increases in FOXP3 gene expression compared with LPS alone, indicating the generation of a Treg phenotype under galactose and GalNAc fractions conditions. Data are shown as mean ± SD of three independent donors (n=3).

5.4 Discussion

There is increasing interest in identifying parasite-derived immunomodulatory molecules can modulate immune responses for use as therapeutic agents in autoimmune diseases [306]. There are promising data from the use of parasite-derived immunomodulatory molecules that are able to modulate immune responses and protect the host against inflammation, thereby inhibiting progression of autoimmune diseases [307,308]. However, despite the significance of being able to use parasite secretions as immunomodulators for the host immune response, the immunomodulatory properties of carbohydrates depleted from larval secretions has remained unexplored. Therefore, we aimed to investigate the influence of carbohydrates isolated from larval products on human DC phenotype and function, particularly regarding cell surface marker expression, cytokine production, and downstream effects on T-cell polarisation.

The initial examination of galactose and GalNAc enriched fractions from *N. brasiliensis* larval products by electrophoretic separation demonstrated the presence of bands within a molecular weight between 60–83 kDa. This observation is in line with a study that showed that galactose and GalNAc from mucin in bovine milk were located between 60–75 kDa [291]. This band did not appear in larval secretions after depletion of galactose and GalNAc, successfully confirming depletion of the target carbohydrates from the larval secretions. Galactose and GalNAc enriched glycoproteins were examined using RCA and SBA biotinylated labelled lectins to confirm the depletion of these carbohydrates. Galactose and GalNAc enriched were detected as dark bands between 62–83 kDa against a clear background; these bands were missing from the carbohydrate-depleted larval secretions when the membrane was stained with RCA or SBA, compared with the whole larval secretion.

DCs are consider an ideal target for immune modulation or immunotherapy, including the treatment of autoimmune diseases or cancers, as they have a central role in shaping the adaptive immune response [309-311]. Some tumour cells can suppress immune responses by skewing DC function from an inflammatory phenotype to a tolerogenic phenotype. For example, it has been shown that Tn and sTn

antigens, which are overexpressed on tumour cells that contain galactose and GalNAc enriched, are able to suppress DC function and thus evade the immune system [272, 312].

Furthermore, some carbohydrates decorating pathogens or synthetic carbohydrates have been known to inhibit immune responses by modulating DC function, which in turn suppresses the immune system. For example, it was shown that *E. histolytica* expressed galactose and GalNAc on its surface. These carbohydrates are important for parasite survival, allowing evasion of the host immune system by promoting degradation of the mucin layer in the intestine and generation of a cyst where the parasite can survive and the infection can persist [313-315]. It has been shown that immobilised galactose has immunoregulatory properties, with the ability to induce differentiation of DCs towards a tolerogenic phenotype, which in turn supports naïve T-cell differentiation towards a Treg phenotype [302]. This finding is in line with our data, which showed that galactose and GalNAc enriched from larval secretions were able to induce a regulatory phenotype in LPS-challenged DCs, as evidenced by a significant reduction in the expression of co-stimulatory molecules HLA-DR, CD80, CD86, and CD40, and an increase in expression of tolerogenic CD274 (PDL-1).

The maturation status of DCs plays a key role in their ability to initiate T-cell activation. Other co-stimulatory molecules found on DCs, such as CD40, have been shown to play an important role in priming of Th1 cell differentiations through binding with CD40L on T cells, resulting in production of IL-12, which is a known key pro-inflammatory cytokine [316,317]. However, the lack of upregulation of DC co-stimulatory molecules, such as CD80/86, prevents the effective activation of T cells, as these molecules bind to TCR and CD28 [253]. Furthermore, a lack of HLA-DR upregulation in response to foreign antigens prevents further activation of Th cells and the production of antibodies against pathogen [254]. PDL-1 (CD274) is an inhibitory ligand for T-cell activation and proliferation and plays a role in the development of Tregs [318]. This function is consistent with how some parasite-derived molecules that contain carbohydrates can modulate the immune system. For example, studies showed that soluble egg antigens (SEAs) from *S. mansoni* inhibited DC maturation in the presence of LPS by decreasing co-stimulatory molecule expression, presumably contributing to parasite survival [250,320].

Interestingly, our data also showed that parasite-derived molecules that contained carbohydrates were able to suppress maturation of LPS-challenged DCs.

Phenotype changes in galactose- and GalNAc-conditioned DCs are also reflected in their cytokine profiles. Specifically, galactose or GalNAc cultured with LPS-stimulated DCs showed a significant increase in IL-10 production and decrease in IL-12 production. This observation is in line with how glycoantigens produced by some pathogens can modulate DC function. For example, glycoantigens produced by *F. hepatica*, such as GalNAc decorated glycoproteins, are involve in the modulation of DC function through promotion of the production of IL-10 [320]. IL-10 is an anti-inflammatory cytokine that prevents excessive immune response through influencing the differentiation of Treg cells; IL-12 is a pro-inflammatory cytokine that plays a key role in skewing the immune response towards Th1-cell differentiation [321]. Together, these data strongly suggest that the galactose- and GalNAc-primed DCs acquired a tolerogenic phenotype; to confirm our findings, these conditions were applied in DC-T-cell co-cultures.

To better understand the immunomodulatory effect of galactose and GalNAc isolated from larval products on the immune response, we decided to investigate the influence of these carbohydrates on T-cell differentiation in DC-T-cell co-cultures. The data show that galactose and GalNAc enhanced expression of CD25 and FOXP3 in the $CD4^+$ T-cell population, suggesting the differentiation of naïve T cells towards Tregs. This finding is consistent with our cytokine profile data, which showed increased IL-10 and TGF-β production under galactose and GalNAc conditions. Finally, we investigated FOXP3 gene expression to confirm the ability of galactose and GalNAc to generate a Treg phenotype. The data showed that DCs conditioned with galactose or GalNAc could induce the regulatory gene FOXP3. This supports the consistency of our results and confirms the presence of regulatory T-cell phenotype under these conditions. Our findings are in line with a previous study that showed that carbohydrates, such as GalNAc, secreted by *Aspergillus fumigatus* had immunosuppressive activity and were believed to induce a Treg response, which in turn promoted fungal development [322,323]. Furthermore, the Tn antigen of *F. hepatica* contains GalNAc that can participate in inhibition of the upregulation of DC-

maturation marker expression, which in turn favours expansion of regulatory T cells [320]. A study showed that glycans containing GalNAc from the soluble products of *Trichuris suis* contributed to modulation of human DC function and were believed to induce Treg cells that favoured survival of parasite in the host [324,325].

Interestingly, various studies have shown that infection with parasitic helminths can suppress inflammation in a variety of inflammatory conditions. An example, clinical trials have shown that treatment with *T. suis* eggs could improve active Crohn's disease and ulcerative colitis outcomes [326,327]. The treatment of MS patients with *T. suis* eggs reduced the amount of newly detected MS lesions and significantly lower magnetic resonance imaging (MRI) activity compared with uninfected MS subjects [328,329]. However, using parasitic helminths in the treatment of some inflammatory diseases or allergic conditions did not result in suppression or significant improvement of disease activity; for example, using *T. suis* to treat patients with allergic rhinitis or using *N. americanus* to treat patients with asthma [330,331]. This discrepancy indicates that more studies are necessary to understand the underlying mechanisms of how helminths can induce immunomodulation. Therefore, the data in this chapter may give insights into the mechanism of how parasites can modulate host immune responses and how these immunomodulator molecules can be applied to develop immunotherapeutic strategies to treat inflammatory diseases.

5.5 Conclusion

The data presented in this chapter demonstrated the biological relevance of galactose and GalNAc enriched from *N. brasiliensis* larval secretions and that they could modulate DC immune responses towards anti-inflammatory phenotypes. Furthermore, the data illustrated the immunomodulatory effects of galactose- and GalNAc-primed DCs in modulating adaptive immune responses to induce Treg populations (Fig. 5.10). These data provide new insight as to how non-infectious parasite derived products modulate the immune system and could potentially pave the way for the development of new therapies for inflammatory diseases using these carbohydrates.

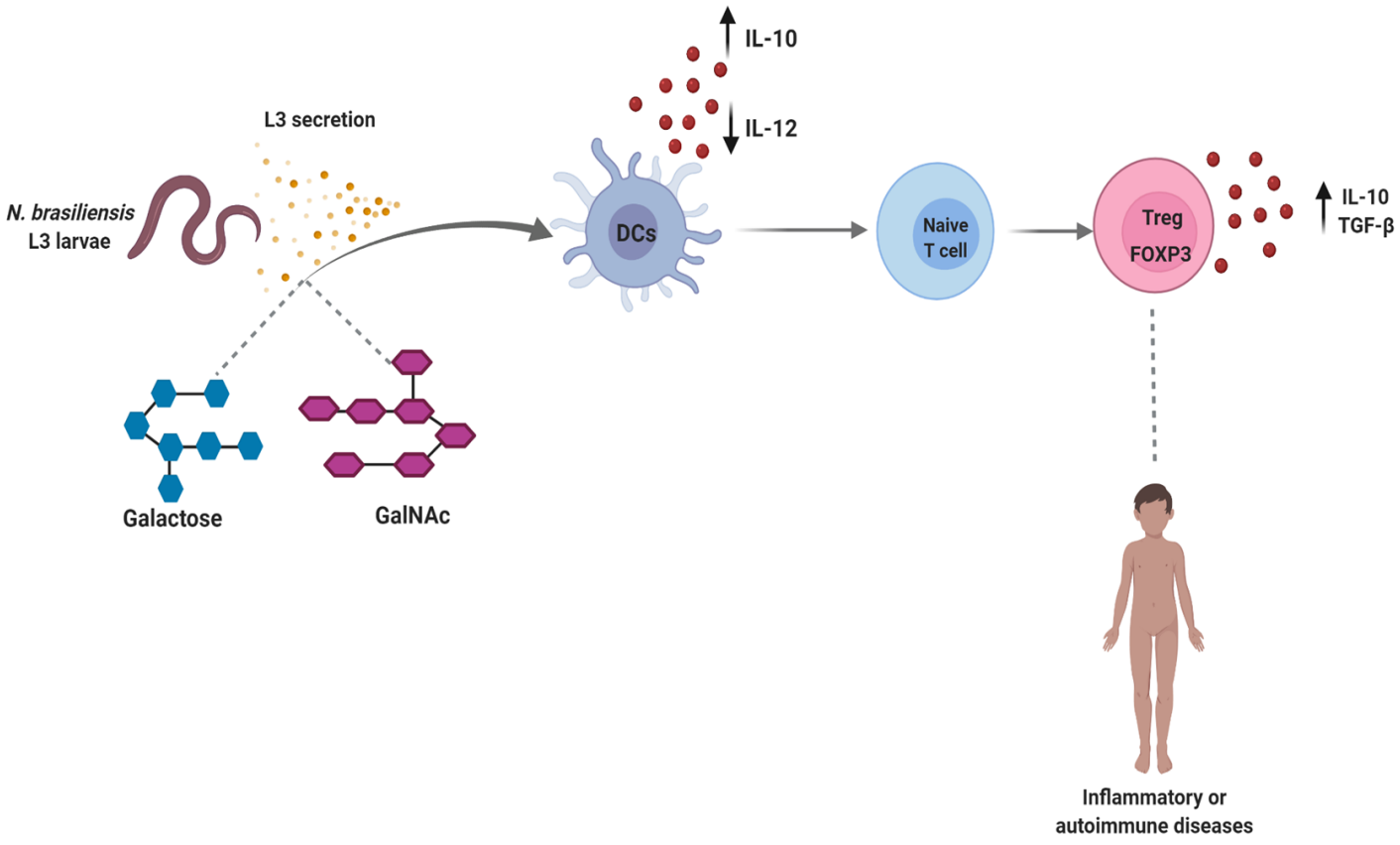

Figure 5.10: Schematic illustration summarising the effects of galactose and GalNAc depleted from *N. brasiliensis* larval secretions on innate and adaptive immune responses.

Chapter 6:

General discussion

The immune system consists of immune cells and a diverse group of proteins that are programmed to respond to changes in the microenvironment to protect the host against different invaders without causing extensive tissue damage [332]. APCs act as link between the innate and adaptive arms of the immune system to initiate a specific immune response for efficient elimination of pathogen [333]. DCs are professional APCs that act as sentinels of the immune system and sense their surrounding environment using PRRs, such as TLRs and CLRs [334]. Carbohydrates act as ligands for CLRs and different CLRs recognise different carbohydrate moieties. The interaction between a specific CLR and its ligand can influence DC phenotype, thereby influencing T-cell differentiation [242,335]. Numerous investigations have suggested that carbohydrates and glycoconjugates have the potential to modulate immune responses [336]. Tumour cells have been reported to express aberrant glycosylation patterns that interact with immune cells, be involved in modulation of these cells, and enhance tumour metastasis [337]. Necatoriasis is a neglected tropical disease caused by *N. americanus* that is considered a significant public health concern, particularly in developing countries. Despite the chronicity of *N. americanus* infections, little is known about how this parasite interacts with the host immune system to arrive in the gut and survive long-term besides the complex immune responses it generates [276]. Despite relative success with drugs used to treat hookworm infections, there is a high rate of re-infection, and the immune response against hookworms is typically not protective [180,181]. Therefore, there is a need to better understand the early events involved in the interface between hookworms and the immune system to pave the way for the development of more effective therapies and vaccines.

The main aim of the current study was to evaluate the effectiveness of *N. brasiliensis* infective larvae as a model system to investigate the immunomodulatory properties of *N. americanus*. *N. brasiliensis* was selected because it had previously been used as a model GI parasite in the study of nematode infection and immunity. Furthermore, this parasite has a similar life cycle to *N. americanus*. Unlike *N. americanus*, it can be easily and inexpensively maintained in the laboratory; it has a short life cycle, and large quantities of worms can be easily obtained. In this context, we investigated the immunomodulatory properties of *N. brasiliensis* infective larvae and their secretions on immune cells with the goal of possibly using this parasite as a model system for *N. americanus* larvae. Understanding

how this parasite or its secretions influences and modulates the immune system and successfully identifying immunomodulatory carbohydrates on the larval cuticle and within their secretions could pave the way for the development of autoimmune therapies and improved strategies for the development of effective vaccines against hookworms.

A previous study described how *N. americanus* infective larvae induced exsheathment to evade immunity upon initial interaction with human DCs. The data suggested that a difference in chemical signatures between the *N. americanus* larval sheath and its cuticle could play a role in its immune evasiveness, although this mechanism has yet to be established [201]. In Chapter 2, we described the physical interaction between human DCs and *N. brasiliensis* infective larvae in the presence and absence of the larval sheath: the DCs aggregated on the ensheathed larvae, triggered larval exsheathing, and exhibited negligible interactions with the exposed larvae. These findings are consistent with the physical interactions previously observed with *N. americanus*, indicating that *N. brasiliensis* larvae behave in a similar manner to *N. americanus* larvae and could represent a good experimental model for investigating the immunomodulatory response of the human hookworm. Interestingly, our data showed that DCs exhibited no preference to interacting with the larval cuticle in the absence of the cuticle sheath after a 24-hour incubation period. These data suggested that the chemical structures of the larval sheath and its cuticle were fundamentally different. To confirm this hypothesis, we investigated the chemical signatures of the L3 cuticle and its sheath using TOF-SIMS. The data showed that the larval sheath contained ions assigned to sulphur-containing compounds and heparan sulphate while the larval cuticle contained ions assigned to lipids (e.g., phosphatidylglycerol), monosaccharides (e.g., galactose, GalNAc, fucose, and L-rhamnose), and amino acids (e.g., cysteine). A previous study showed that expression of heparan sulphate on endothelial cells played an important role in the recruitment of DCs from peripheral tissues, while decreased expression of heparan sulphate reduced recruitment of DCs [223]. In contrast, an in vitro study showed that the presence of phosphatidylglycerol lipid on respiratory epithelial cells could inhibit aggregation and attachment of *Pseudomonas aeruginosa* [216]. Therefore, our findings provided a rationale for why DCs bound to and sequestered the larval sheath but not the L3 cuticle.

To investigate the immunomodulatory properties of the L3 larvae on immune cells and whether the chemical signatures of monosaccharides expressed on the larval cuticle had a role in modulating the immune response, we co-cultured the *N. brasiliensis* L3 larva with DCs and investigated the downstream effects of the larval cuticle on modulating the adaptive immune response (see Chapter 3). The data for DCs co-cultured with L3 larvae showed no significant increase in expression of maturation markers and co-costimulatory markers, such as CD80, CD86, HLA-DR, and CD40; however, there was an increase in tolerogenic PDL-1 expression in the conditioned cells compared with the untreated cells. To confirm the tolerogenic phenotype, we analysed the cytokine profiles of the cells under these conditions. Our data showed a significant increase in anti-inflammatory IL-10 and no significant change in IL-12 production in the larval cuticle-conditioned DCs compared with the untreated cells. Interestingly, DCs conditioned with the larval cuticle were able to modulate DC phenotype and cytokine profile in LPS-stimulated cells. These findings suggest that the *N. brasiliensis* larval cuticle alone maintained an immature DC phenotype and has the potential to significantly reduce inflammation in the presence of LPS through modulation of TLR–CLR crosstalk. Our findings were consistent with studies showing that *N. americanus* infective larvae had similar effects on modulating DC function, suggesting that *N. brasiliensis* induced immunomodulatory effects similar to the human hookworm [201]. Furthermore, previous studies have shown the carbohydrates coating pathogens and parasites have an immunomodulatory effect on DC function. For example, the *Mycobacterium tuberculosis* cell wall contains ManLam, a glycoconjugate containing mannose that can target DC-SIGN on DCs, thereby impairing DC maturation and inducing the production of the anti-inflammatory cytokine IL-10. This process promotes immunosuppression and can contribute to the survival of *M. tuberculosis* [168]. Another example is *H. pylori*, which contains fucose that can cause tolerogenic DC, which in turn suppresses the adaptive immune response and promotes bacterial persistence [338].

IDO is an enzyme involved in immune cell activation and stimulation that has a direct relationship with the DC inflammatory condition [339]. In Chapter 3, we described how larval cuticle-conditioned DCs showed no significant increase in IDO activity compared with untreated cells, while that condition showed a significant reduction in IDO activity in LPS-stimulated DCs compared with LPS alone. These

findings were consistent with the previously observed phenotypic and cytokine profile changes. A reduction in CD40, increase in CD274, and reduction in IDO activity would suggest a tolerogenic DC phenotype. Similar findings were observed by Shih Ling et al., who reported that inhibition of IDO activity suppressed the DC inflammatory response to LPS [339]. Collectively, our findings support the hypothesis that the *N. brasiliensis* larval cuticle has immunomodulatory effects on DC function.

To understand the ability of the *N. brasiliensis* larval cuticle to modulate the adaptive immune response, DC-T-cell co-cultures were used to determine immune response outcomes. Data obtained from co-culture of the *N. brasiliensis* larval cuticle and naïve T cells revealed the presence of $CD25^{+}FOXP3^{+}$ cells within the $CD4^{+}$ T-cell population under infective larval conditions in the presence and absence of LPS compared with untreated cells or LPS-stimulated cells, respectively. Therefore, we hypothesised the presence of a Treg cell population; to confirm our findings, we analysed the cytokine profile. Cytokine profiling revealed a significant increase in the anti-inflammatory cytokines IL-10 and TGF-β in T cells co-cultured with DCs primed with infective larvae. Similar findings were observed by Matoso et al., who reported that *N. americanus* infection was associated with induction of Treg cells, which in turn enhanced pathogen survival and promoted long-term persistence [270]. Furthermore, our findings were consistent with studies showing that some pathogens coated with carbohydrates could modulate the outcome of immune responses. For example, *Mycobacterium* cell walls coated with mannose and Fasciola *hepatica* coated with both mannose and fucose have been shown to induce DCs to a tolerogenic phenotype, leading to increased IL-10 production in T cells [221,340,341]. In addition, research has shown that some tumour cells overexpress Tn antigens that contain galactose and GalNAc and can cause immune suppression [272]. To confirm the presence of a Treg population, we performed end-point and real-time PCR targeting the FOXP3 gene, which is expressed in Tregs. The PCR data showed increased FOXP3 levels under larval conditions. These data confirmed the T-cell phenotype and cytokine profile that were previously observed and represent *N. brasiliensis* larval cuticle-mediated generation of a Treg cell population. Our findings were consistent with studies showing that *N. americanus* larvae had similar effects on the generation of FOXP3 regulatory T cells, suggesting that *N. brasiliensis* could induce an immunomodulatory effect similar to that of the human hookworm [271].

N. americanus larvae are believed to infect the human not only mechanically during penetration, but also by secreting a wide range of immune modulatory molecules [152,218]. These secretions are mostly glycosylated in nature and can influence the immune response [106,154]. However, the mechanism by which these secretions interfere with the immune response, particularly DC function, is still under intensive research and is far from being completely understood [250]. Despite our observation in the lack of any stable physical interaction between DCs and the *N. brasiliensis* larval cuticle. These evasion strategies are believed to be related to the secretions of the infective larvae. These secretions might contain immuno-regulatory molecules that can interfere with the induction of sufficient immunity against the parasite; it is thus reasonable to suggest that the larval cuticle could have an immunomodulatory effect via its secretions. Therefore, in Chapter 4, we aimed to investigate the impact of *N. brasiliensis* larval secretions on DC function and its downstream effects on adaptive immune response. In addition, we aimed to characterise this secretion and also identify whether galactose and GalNAc which previously identified on surface of larval cuticle could be found in larval secretions. Data obtained from larval secretion-conditioned DCs showed that DCs maintained an immature phenotype, as evidenced by an absence of significant expression of maturation and co-stimulatory markers. Furthermore, larval secretion-conditioned DCs showed a significant increase anti-inflammatory IL-10, decrease in IL-12, and no significant induction of IDO activity compared with untreated DCs. Interestingly, *N. brasiliensis* larval secretions were able to modulate DC phenotype, cytokine production, and IDO activity patterns in LPS-stimulated DCs through modulation of TLR–CTL crosstalk. These findings provide enough evidence to confirm that larval secretions possess similar immunomodulatory potential for suppressing the DC inflammatory response to TLR4 activation as infective L3. Research has shown the link between CTLs and TLRs, and that pathogen binding through these receptors can modulate the immune system [74]. Our findings are consistent with research that showed that *Heligmosomoides polygyrus* (Hp) nematode secretions alone failed to induce DC maturation, while these secretions were able to modulate DC activation in the presence of a TLR4 ligand [342]. *Trypanosoma cruzi* secretions have been shown to impair maturation of DCs in the presence of LPS, with marked reduction in pro-inflammatory cytokine secretion [296].

Glycosylated antigens are a known ligand for CLRs, which are expressed on the surface of APCs, such as DCs [137]. As mentioned previously, most parasitic secretions are glycosylated in nature and have an immunomodulatory effect on the immune response. It has been shown that *Toxocara canis* secretions containing O-methylated glycans, such as fucose and galactose, that mimic mammalian blood group antigen H are able to interact with DC-SIGN on DCs and modulate immune responses [278]. *S. mansoni* secretions contain fucosylated glycoprotein, which can interact with DC-SIGN on DCs and subsequently inhibit maturation of DCs that drives such a response from T cells [279]. To determine whether *N. brasiliensis* larval secretions target CLRs on DCs, blocking antibodies, including DC-SIGN and MR, have been used to block CLRs. Data obtained from these experiments showed a significant decrease in IL-10 production with an increase in IL-12p70 production in L3 secretion-conditioned DCs compared with unblocked DCs. This finding suggests that *N. brasiliensis* larval secretions target CLRs on DCs to modulate the immune response. To confirm the presence of glycosylated molecules within larval secretions, we examined larval secretions for the presence of different sugars using biotinylated labelled lectin. Data obtained from glycosylation analysis showed that larval secretions contained different monosaccharide moieties, including galactose, GalNAc, fucose, and mannose glycoproteins. These data are in line with our previous findings (see Chapter 2), where these carbohydrates were present on the larval cuticle and provided sufficient evidence that *N. brasiliensis* larvae contained glycosylated molecules in their secretions that could interfere with immune responses previously observed. Furthermore, our findings were consistent with research that showed that glycosylated antigens were abundant in some parasitic secretions and had a role in modulating host immunity [152,289,290].

To understand the effect of larval secretion-conditioned DCs on T-cell polarisation, DC-T-cell co-cultures were used to determine the outcomes of the adaptive immune response. The data obtained from our co-culture experiments showed that larval secretion conditions in the presence and absence of LPS compared with untreated cells or LPS-stimulated cells, respectively, exhibited the presence of a $CD25^{+}FOXP3^{+}$ Treg cell population within the $CD4^{+}$ T-cell population. In addition, cytokine profiling data showed a remarkable increase in anti-inflammatory IL-10 and TGF-β in naïve T cells primed with

larval secretion-conditioned DCs compared with the control, confirming our previous findings and the presence of Tregs. To further confirm the presence of Tregs, we performed PCR to evaluate FOXP3 gene expression in these cells. The PCR data showed increased levels of the regulatory gene FOXP3 under larval secretion conditions, which confirmed the previously observed T-cell phenotype and cytokine analysis findings and provides sufficient evidence for the presence of Treg cells in our T-cell population. These findings were consistent with research that showed that the secretions of some GI nematodes, including *H. polygyrus* and *Teladorsagia circumcincta*, were capable of directly inducing $FOXP3^+$ Treg cells that played a role in regulating host immunity [343]. Furthermore, these findings were in line with research showing that parasites, such as *Entamoeba histolytica*, relied on galactose and GalNAc for survival via modulation of host immunity [295]. Another study showed that a protein containing galactose from *T. cruzi* bound to human erythrocytes and mediated host cell invasion [296].

There is a particular focus on understanding the products released by parasites and how these products are responsible for regulating the host immune system [152]. It has been shown that O-methylated glycans in *Toxocara canis* containing fucose and galactose mimic mammalian blood group antigen H and are able to interact with DC-SIGN on DCs to regulate immune responses [278]. Fucosylated *Schistosoma mansoni* glycoproteins can interact with DC-SIGN on DCs and subsequently inhibit maturation of DCs [279]. We showed the immunomodulatory effect of *N. brasiliensis* infective larvae and their secretions on human immune cells and the presence of immunoregulatory monosaccharides that might play role in skewing DC immune responses to an anti-inflammatory phenotype and modulating adaptive immune responses. Chapter 5 describes how we aimed to deplete immunoregulatory glycoproteins and glycoconjugates from larval secretions and investigate the biological relevance of these glcoproteins on DCs to understand their ability to modulate the adaptive immune response.

Initial experiments involved analysis of the immunomodulatory properties of enriched glycoproteins, including galactose and GalNAc, on DC phenotype and function. Through assessment of co-stimulatory molecule (CD80, CD86, HLA-DR, and CD40) expression on conditioned DCs, our data showed that

these monosaccharides were able to modulate DC phenotype in the presence of LPS. This observation was similar to how infective larvae and their secretions were able to modulate the effects of DCs.

This modulation is also reflected in changes in the cytokine profile, where IL-12p70 was decreased and IL-10 was increased in LPS-stimulated DCs. These data clearly showed that depleted galactose and GalNAc had an immunomodulatory effect on DCs with a bias towards inducing an anti-inflammatory phenotype. These findings were consistent with a study that showed that expression of galactose and galactosamine in *E, histolytica* played a role in evading innate immune cells and thus enhanced infection and promoted parasite survival [313]. The findings were also in line with a study that showed that immobilised galactose could modulate DC phenotype and function, which in turn modulated the outcome of the adaptive immune response [302].

The biological relevance of galactose and GalNAc enriched fractions from *N. brasiliensis* larval secretion-conditioned DCs and the downstream effects of galactose and GalNAc enriched fractions depends on their ability to modulate adaptive immune responses. This process is represented by cell-to-cell communication between conditioned DCs and naïve T cells. The in vitro co-culture approach has been used to understand in vivo cell-to-cell interactions and to determine immune response outcomes [344]. We aimed to understand the influence of galactose and GalNAc enriched glycoproteins from larval secretions on T-cell polarisation. Data obtained from co-culture of galactose- or GalNAc-conditioned DCs and naïve T cells showed that galactose and GalNAc enriched secretions enhanced expression of CD25 and FOXP3 in the $CD4^+$ T-cell population in addition to remarkable changes in their cytokine profile compared with the control. Naïve T cells showed increased anti-inflammatory IL-10 and TGF-β production under galactose and GalNAc conditioning, indicating the presence of tolerogenic DCs that drove such a response from T cells. To confirm our findings, we analysed expression of FOXP3 in these T cells. PCR data showed that the FOXP3 was induced in DCs conditioned with galactose or GalNAc. This finding supports the consistency of our T-cell phenotype findings and cytokine data and provides sufficient evidence for presence of a regulatory T-cell population under these conditions. Our findings are in line with research showing that glycoproteins

secreted by pathogens plays a role in modulating the immune system. For example, GalNAc secreted by *Aspergillus fumigatus* has been shown to have immunosuppressive activity and is believed to induce a Treg response, which in turn promotes fungal development [323,324]. In addition, the secretory products of *Trichinella spiralis* composed of GalNAc can induce immunomodulation and enhance generation of a Treg response [345].

In conclusion, we were able to demonstrate that *N. brasiliensis* modulate human Dc functional properties similar to *N. americanus*, supporting the suitability of *N. brasiliensis* as a model system for investigating the interface of hookworms with immune cells in early stages. Interestingly, we were able to elucidate different surface chemistries between the *N. brasiliensis* larval cuticle and its sheath that could be of biological significance. In addition, we have shown that *N. brasiliensis* infective larvae and their secretions have potent immunomodulatory effects which are, at least partly, due to carbohydrates released by the worm, which could be potentially utilised as a promising tool in autoimmune therapy. The beneficial effects of using parasite-derived products or parasite larvae in the treatment of autoimmune, allergic, and malignant diseases have been shown in various studies. Therefore, future work on utilising either *N. brasiliensis* larvae or their products for the design of more efficient therapies in the treatment of inflammatory or autoimmune diseases is needed.

Supplementary materials

Supplementary video 1: physical interaction of human DCs with *N. brasiliensis* ensheathed larvae

Ensheathed L3 larvae with DCs. Mp4

Supplementary video 2: physical interaction of human DCs with *N. brasiliensis* exsheathed larvae (L3 cuticle)

L3 cuticle and DCs.mp4

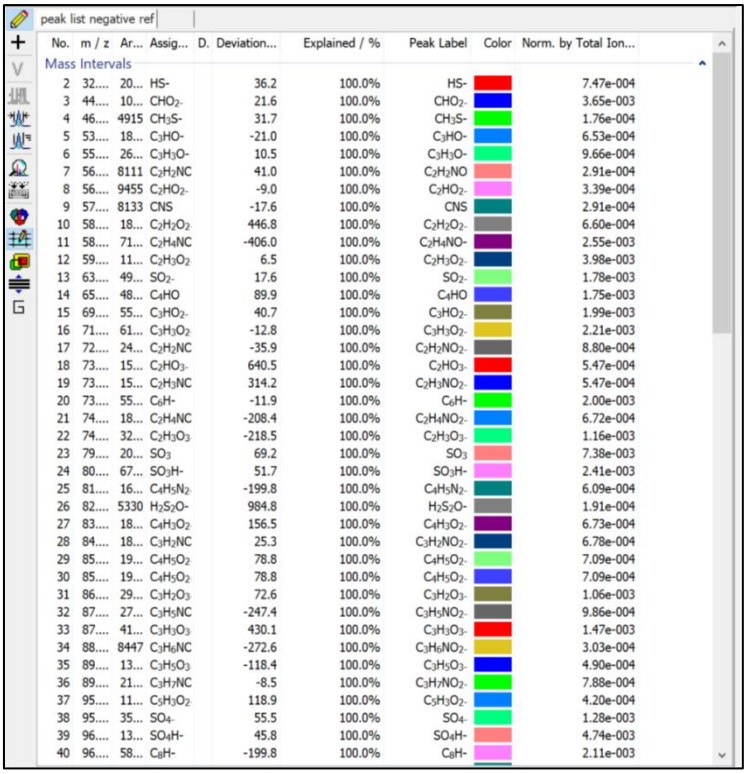

peak list negative ref

No.	m / z	Ar...	Assig...	D.	Deviation...	Explained / %	Peak Label	Color	Norm. by Total Ion...
Mass Intervals									
2	32....	20...	HS-		36.2	100.0%	HS-		7.47e-004
3	44....	10...	CHO_2-		21.6	100.0%	CHO_2-		3.65e-003
4	46....	4915	CH_3S-		31.7	100.0%	CH_3S-		1.76e-004
5	53....	18...	C_3HO-		-21.0	100.0%	C_3HO-		6.53e-004
6	55....	26...	C_3H_3O-		10.5	100.0%	C_3H_3O-		9.66e-004
7	56....	8111	C_2H_2NC		41.0	100.0%	C_2H_2NO		2.91e-004
8	56....	9455	C_2HO_2-		-9.0	100.0%	C_2HO_2-		3.39e-004
9	57....	8133	CNS		-17.6	100.0%	CNS		2.91e-004
10	58....	18...	$C_2H_2O_2$		446.8	100.0%	$C_2H_2O_2$-		6.60e-004
11	58....	71...	C_2H_4NC		-406.0	100.0%	C_2H_4NO-		2.55e-003
12	59....	11...	$C_2H_3O_2$		6.5	100.0%	$C_2H_3O_2$-		3.98e-003
13	63....	49...	SO_2-		17.6	100.0%	SO_2-		1.78e-003
14	65....	48...	C_4HO		89.9	100.0%	C_4HO		1.75e-003
15	69....	55...	C_3HO_2-		40.7	100.0%	C_3HO_2-		1.99e-003
16	71....	61...	$C_3H_3O_2$		-12.8	100.0%	$C_3H_3O_2$-		2.21e-003
17	72....	24...	C_2H_2NC		-35.9	100.0%	$C_2H_2NO_2$-		8.80e-004
18	73....	15...	C_2HO_3-		640.5	100.0%	C_2HO_3-		5.47e-004
19	73....	15...	C_2H_3NC		314.2	100.0%	$C_2H_3NO_2$-		5.47e-004
20	73....	55...	C_6H-		-11.9	100.0%	C_6H-		2.00e-003
21	74....	18...	C_2H_4NC		-208.4	100.0%	$C_2H_4NO_2$-		6.72e-004
22	74....	32...	$C_2H_3O_3$		-218.5	100.0%	$C_2H_3O_3$-		1.16e-003
23	79....	20...	SO_3		69.2	100.0%	SO_3		7.38e-003
24	80....	67...	SO_3H-		51.7	100.0%	SO_3H-		2.41e-003
25	81....	16...	C_4HS_N-		-199.8	100.0%	C_4HS_N-		6.09e-004
26	82....	5330	H_2S_2O-		984.8	100.0%	H_2S_2O-		1.91e-004
27	83....	18...	$C_4H_3O_2$		156.5	100.0%	$C_4H_3O_2$-		6.73e-004
28	84....	18...	C_3H_2NC		25.3	100.0%	$C_3H_2NO_2$-		6.78e-004
29	85....	19...	$C_4HS_O_2$		78.8	100.0%	$C_4HS_O_2$-		7.09e-004
30	85....	19...	$C_4HS_O_2$		78.8	100.0%	$C_4HS_O_2$-		7.09e-004
31	86....	29...	$C_3H_2O_3$		72.6	100.0%	$C_3H_2O_3$-		1.06e-003
32	87....	27...	C_3HS_NC		-247.4	100.0%	$C_3HS_NO_2$-		9.86e-004
33	87....	41...	$C_3H_3O_3$		430.1	100.0%	$C_3H_3O_3$-		1.47e-003
34	88....	8447	C_3H_6NC		-272.6	100.0%	$C_3H_6NO_2$-		3.03e-004
35	89....	13...	$C_3H_5O_3$		-118.4	100.0%	$C_3H_5O_3$-		4.90e-004
36	89....	21...	C_3H_7NC		-8.5	100.0%	$C_3H_7NO_2$-		7.88e-004
37	95....	11...	$C_5H_3O_2$		118.9	100.0%	$C_5H_3O_2$-		4.20e-004
38	95....	35...	SO_4-		55.5	100.0%	SO_4-		1.28e-003
39	96....	13...	SO_4H-		45.8	100.0%	SO_4H-		4.74e-003
40	96....	58...	C_8H-		-199.8	100.0%	C_8H-		2.11e-003

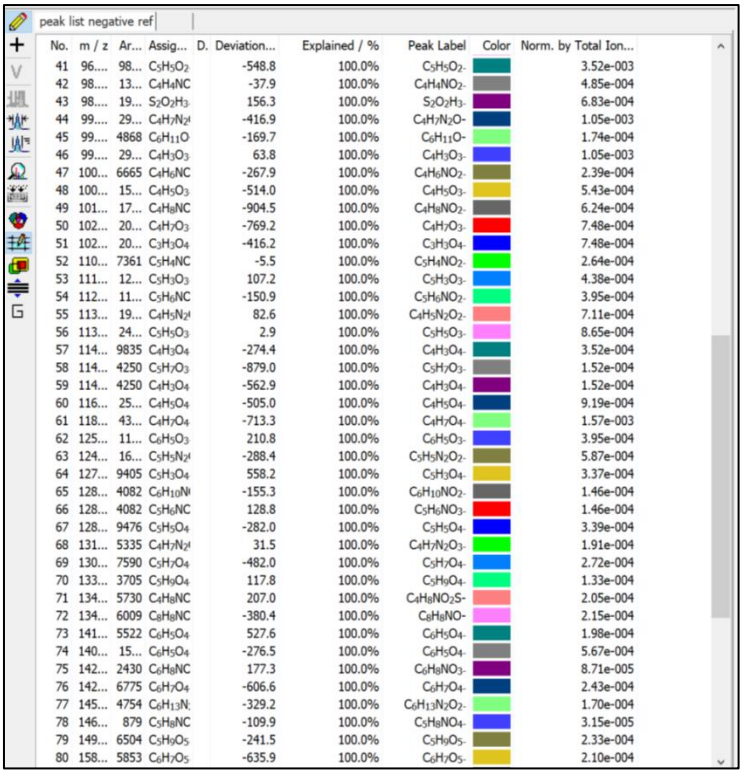

peak list negative ref

No.	m / z	Ar...	Assig...	D.	Deviation...	Explained / %	Peak Label	Color	Norm. by Total Ion...
41	96....	98...	$C_5H_5O_2$		-548.8	100.0%	$C_5H_5O_2$-		3.52e-003
42	98....	13...	C_4H_4NC		-37.9	100.0%	$C_4H_4NO_2$-		4.85e-004
43	98....	19...	$S_2O_2H_3$		156.3	100.0%	$S_2O_2H_3$		6.83e-004
44	99....	29...	$C_4H_7N_2$		-416.9	100.0%	$C_4H_7N_2O$-		1.05e-003
45	99....	4868	$C_6H_{11}O$		-169.7	100.0%	$C_6H_{11}O$-		1.74e-004
46	99....	29...	$C_4H_3O_3$		63.8	100.0%	$C_4H_3O_3$-		1.05e-003
47	100....	6665	C_4H_6NC		-267.9	100.0%	$C_4H_6NO_2$-		2.39e-004
48	100....	15...	$C_4H_5O_3$		-514.0	100.0%	$C_4H_5O_3$-		5.43e-004
49	101....	17...	C_4H_8NC		-904.5	100.0%	$C_4H_8NO_2$-		6.24e-004
50	102....	20...	$C_4H_7O_3$		-769.2	100.0%	$C_4H_7O_3$-		7.48e-004
51	102....	20...	$C_3H_3O_4$		-416.2	100.0%	$C_3H_3O_4$-		7.48e-004
52	110....	7361	C_5H_4NC		-5.5	100.0%	$C_5H_4NO_2$-		2.64e-004
53	111....	12...	$C_5H_3O_3$		107.2	100.0%	$C_5H_3O_3$-		4.38e-004
54	112....	11...	C_5H_6NC		-150.9	100.0%	$C_5H_6NO_2$-		3.95e-004
55	113....	19...	$C_4H_5N_2$		82.6	100.0%	$C_4H_5N_2O_2$-		7.11e-004
56	113....	24...	$C_5H_5O_3$		2.9	100.0%	$C_5H_5O_3$-		8.65e-004
57	114....	9835	$C_4H_3O_4$		-274.4	100.0%	$C_4H_3O_4$-		3.52e-004
58	114....	4250	$C_5H_7O_3$		-879.0	100.0%	$C_5H_7O_3$-		1.52e-004
59	114....	4250	$C_4H_3O_4$		-562.9	100.0%	$C_4H_3O_4$-		1.52e-004
60	116....	25...	$C_4H_5O_4$		-505.0	100.0%	$C_4H_5O_4$-		9.19e-004
61	118....	43...	$C_4H_7O_4$		-713.3	100.0%	$C_4H_7O_4$-		1.57e-003
62	125....	11...	$C_6H_5O_3$		210.8	100.0%	$C_6H_5O_3$-		3.95e-004
63	124....	16...	$C_5H_5N_2$		-288.4	100.0%	$C_5H_5N_2O_2$-		5.87e-004
64	127....	9405	$C_5H_3O_4$		558.2	100.0%	$C_5H_3O_4$-		3.37e-004
65	128....	4082	$C_6H_{10}N$		-155.3	100.0%	$C_6H_{10}NO_2$-		1.46e-004
66	128....	4082	C_5H_6NC		128.8	100.0%	$C_5H_6NO_3$-		1.46e-004
67	128....	9476	$C_5H_5O_4$		-282.0	100.0%	$C_5H_5O_4$-		3.39e-004
68	131....	5335	$C_4H_7N_2$		31.5	100.0%	$C_4H_7N_2O_3$-		1.91e-004
69	130....	7590	$C_5H_7O_4$		-482.0	100.0%	$C_5H_7O_4$-		2.72e-004
70	133....	3705	$C_5H_9O_4$		117.8	100.0%	$C_5H_9O_4$-		1.33e-004
71	134....	5730	C_4H_8NC		207.0	100.0%	$C_4H_8NO_2S$-		2.05e-004
72	134....	6009	C_8H_8NC		-380.4	100.0%	C_8H_8NO-		2.15e-004
73	141....	5522	$C_6H_5O_4$		527.6	100.0%	$C_6H_5O_4$-		1.98e-004
74	140....	15...	$C_6H_5O_4$		-276.5	100.0%	$C_6H_5O_4$-		5.67e-004
75	142....	2430	C_6H_8NC		177.3	100.0%	$C_6H_8NO_3$-		8.71e-005
76	142....	6775	$C_6H_7O_4$		-606.6	100.0%	$C_6H_7O_4$-		2.43e-004
77	145....	4754	$C_6H_{13}N$		-329.2	100.0%	$C_6H_{13}N_2O_2$-		1.70e-004
78	146....	879	C_5H_8NC		-109.9	100.0%	$C_5H_8NO_4$-		3.15e-005
79	149....	6504	$C_5H_9O_5$		-241.5	100.0%	$C_5H_9O_5$-		2.33e-004
80	158....	5853	$C_6H_7O_5$		-635.9	100.0%	$C_6H_7O_5$-		2.10e-004

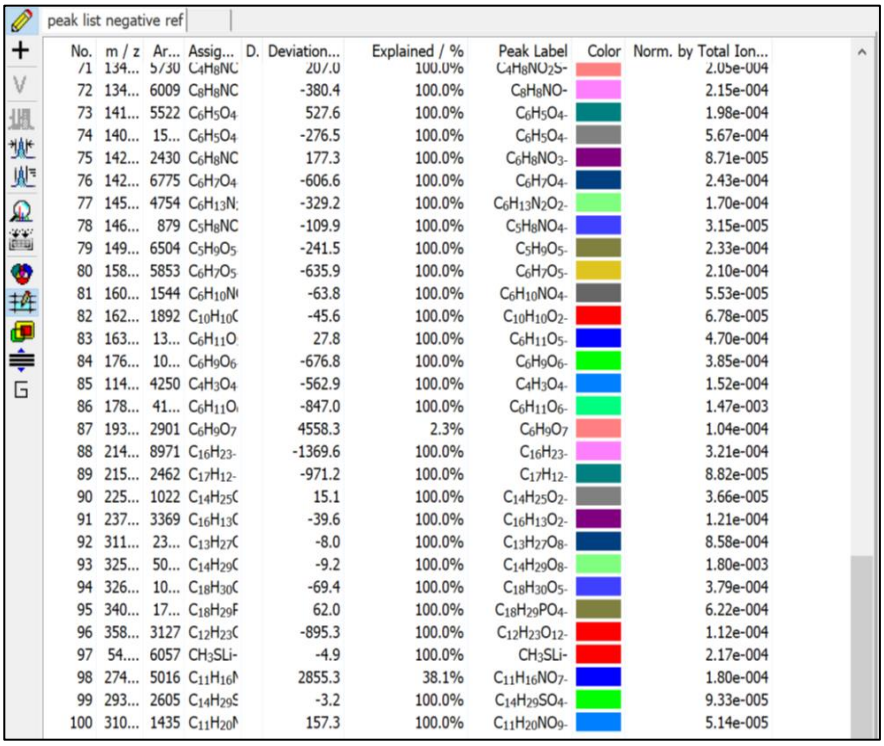

peak list negative ref

No.	m / z	Ar...	Assig...	D.	Deviation...	Explained / %	Peak Label	Color	Norm. by Total Ion...
71	134...	5730	C_4H_8NC		207.0	100.0%	$C_4H_8NO_2S$-		2.05e-004
72	134...	6009	C_8H_8NC		-380.4	100.0%	C_8H_8NO-		2.15e-004
73	141...	5522	$C_6H_5O_4$		527.6	100.0%	$C_6H_5O_4$-		1.98e-004
74	140...	15...	$C_6H_5O_4$		-276.5	100.0%	$C_6H_5O_4$-		5.67e-004
75	142...	2430	C_6H_8NC		177.3	100.0%	$C_6H_8NO_3$-		8.71e-005
76	142...	6775	$C_6H_7O_4$		-606.6	100.0%	$C_6H_7O_4$-		2.43e-004
77	145...	4754	$C_6H_{13}N$		-329.2	100.0%	$C_6H_{13}N_2O_2$-		1.70e-004
78	146...	879	C_5H_8NC		-109.9	100.0%	$C_5H_8NO_4$-		3.15e-005
79	149...	6504	$C_5H_9O_5$		-241.5	100.0%	$C_5H_9O_5$-		2.33e-004
80	158...	5853	$C_6H_7O_5$		-635.9	100.0%	$C_6H_7O_5$-		2.10e-004
81	160...	1544	$C_6H_{10}N$		-63.8	100.0%	$C_6H_{10}NO_4$-		5.53e-005
82	162...	1892	$C_{10}H_{10}$		-45.6	100.0%	$C_{10}H_{10}O_2$-		6.78e-005
83	163...	13...	$C_6H_{11}O$		27.8	100.0%	$C_6H_{11}O_5$-		4.70e-004
84	176...	10...	$C_6H_9O_6$		-676.8	100.0%	$C_6H_9O_6$-		3.85e-004
85	114...	4250	$C_4H_3O_4$		-562.9	100.0%	$C_4H_3O_4$-		1.52e-004
86	178...	41...	$C_6H_{11}O$		-847.0	100.0%	$C_6H_{11}O_6$-		1.47e-003
87	193...	2901	$C_6H_9O_7$		4558.3	2.3%	$C_6H_9O_7$		1.04e-004
88	214...	8971	$C_{16}H_{23}$-		-1369.6	100.0%	$C_{16}H_{23}$-		3.21e-004
89	215...	2462	$C_{17}H_{12}$-		-971.2	100.0%	$C_{17}H_{12}$-		8.82e-005
90	225...	1022	$C_{14}H_{25}$		15.1	100.0%	$C_{14}H_{25}O_2$-		3.66e-005
91	237...	3369	$C_{16}H_{13}$		-39.6	100.0%	$C_{16}H_{13}O_2$-		1.21e-004
92	311...	23...	$C_{13}H_{27}$		-8.0	100.0%	$C_{13}H_{27}O_8$-		8.58e-004
93	325...	50...	$C_{14}H_{29}$		-9.2	100.0%	$C_{14}H_{29}O_8$-		1.80e-003
94	326...	10...	$C_{18}H_{30}$		-69.4	100.0%	$C_{18}H_{30}O_5$-		3.79e-004
95	340...	17...	$C_{18}H_{29}F$		62.0	100.0%	$C_{18}H_{29}PO_4$-		6.22e-004
96	358...	3127	$C_{12}H_{23}$		-895.3	100.0%	$C_{12}H_{23}O_{12}$-		1.12e-004
97	54....	6057	CH_3SLi-		-4.9	100.0%	CH_3SLi-		2.17e-004
98	274...	5016	$C_{11}H_{16}$		2855.3	38.1%	$C_{11}H_{16}NO_7$-		1.80e-004
99	293...	2605	$C_{14}H_{29}$		-3.2	100.0%	$C_{14}H_{29}SO_4$-		9.33e-005
100	310...	1435	$C_{11}H_{20}$		157.3	100.0%	$C_{11}H_{20}NO_9$-		5.14e-005

Supplementary figure 1: Peak list generated for larval cuticle and larval sheath.

Larval cuticle

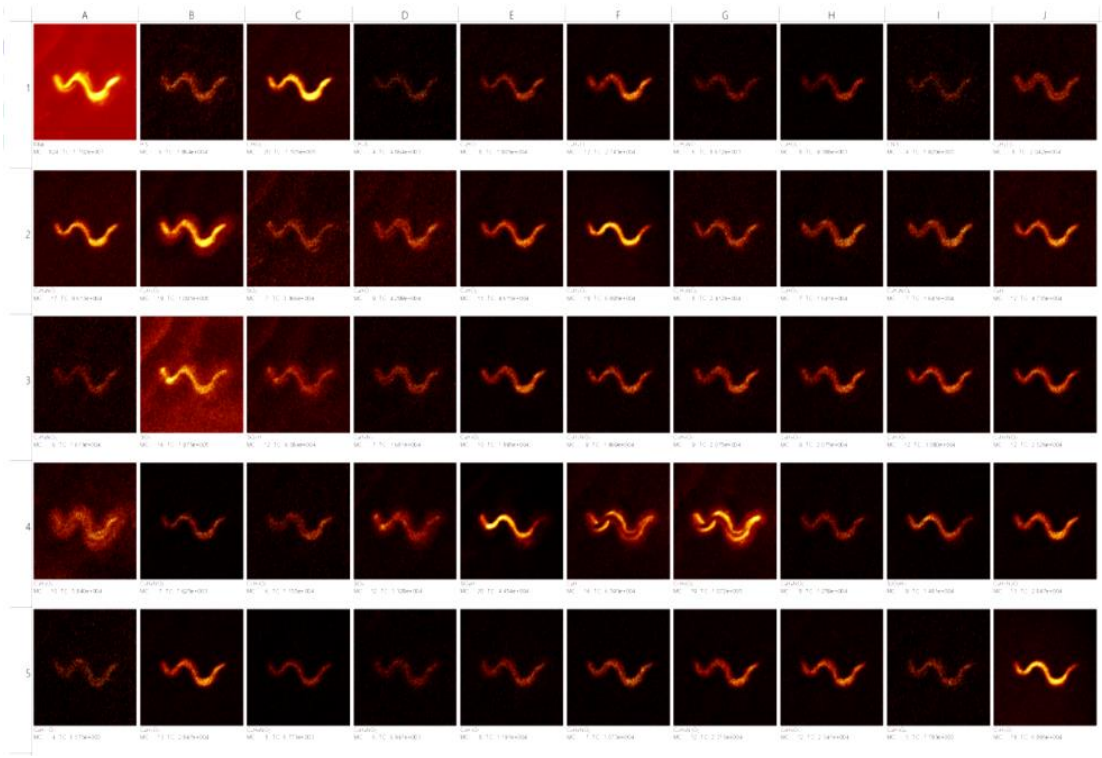

Larval sheath

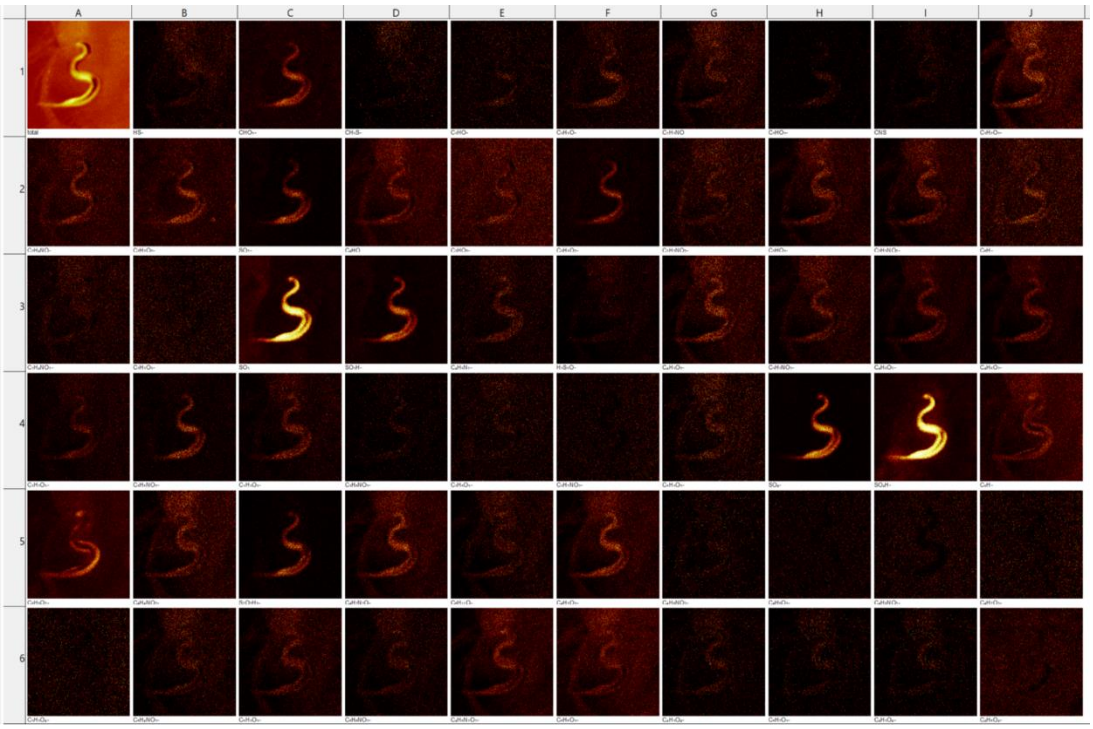

Supplementary figure 2: Total loaded ions expressed on larval cuticle vs larval sheath.

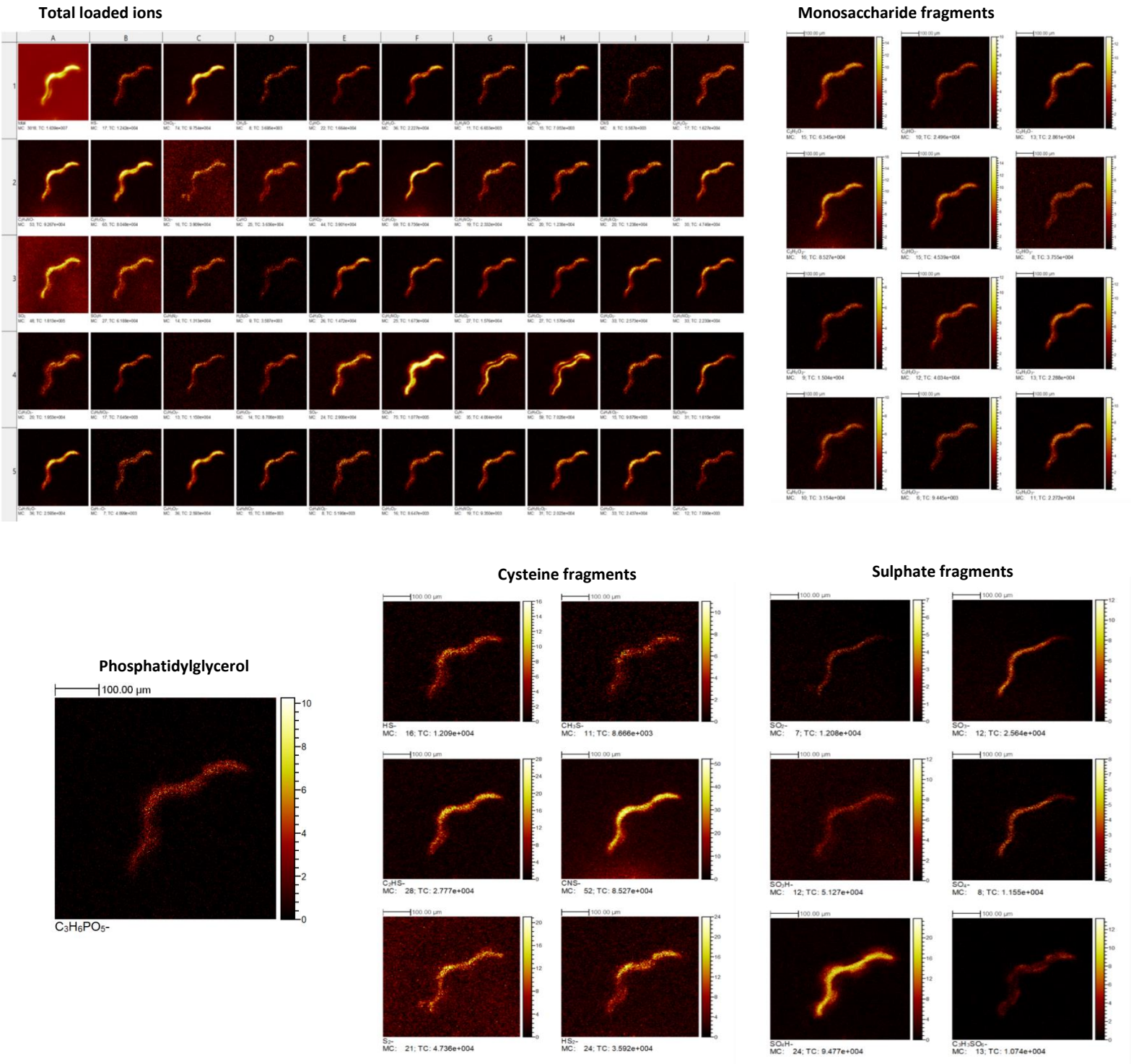

Supplementary figure 3: Total loaded ions images expressed on the L3 cuticle (second worm). The L3 cuticle surface exhibited monosaccharide secondary ions. Also, it contains phosphatidylglycerol head group. In addition, the L3 cuticle surface elucidate expression of secondary ions associated with cysteine amino acid. However, The L3 cuticle contained probable sulphate compounds, but not heparan sulphate.

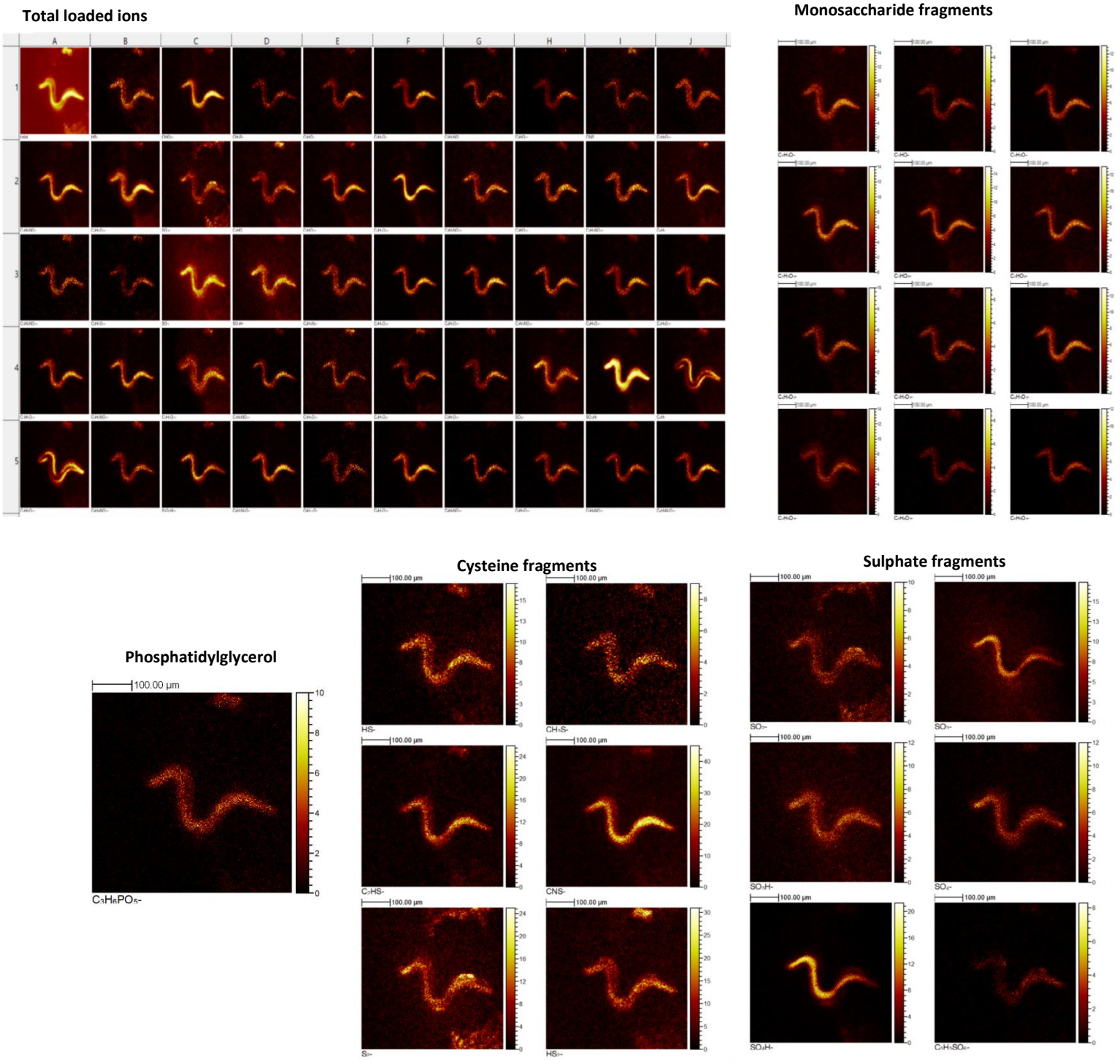

Supplementary figure 4: Total loaded ions images expressed on the L3 cuticle (third worm). The L3 cuticle surface exhibited monosaccharide secondary ions. Also, it contains phosphatidylglycerol head group. In addition, the L3 cuticle surface elucidate expression of secondary ions associated with cysteine amino acid. However, The L3 cuticle contained probable sulphate compounds, but not heparan sulphate.

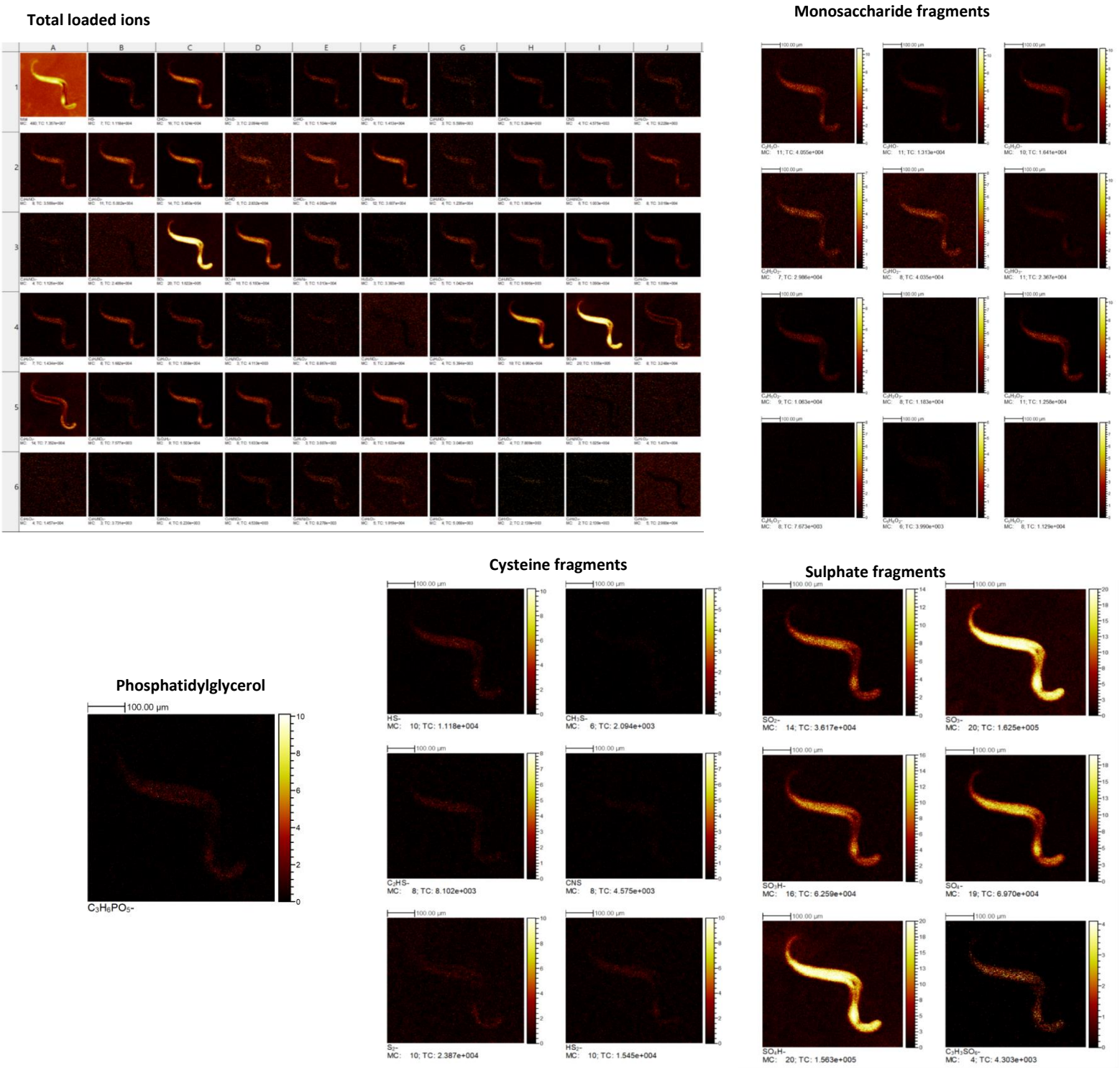

Supplementary figure 5: Total loaded ions images expressed on the L3 sheath (second worm). The L3 cuticle surface exhibited monosaccharide secondary ions. Also, it contains phosphatidylglycerol head group. In addition, the L3 cuticle surface elucidate expression of secondary ions associated with cysteine amino acid. However, The L3 cuticle contained probable sulphate compounds, but not heparan sulphate.

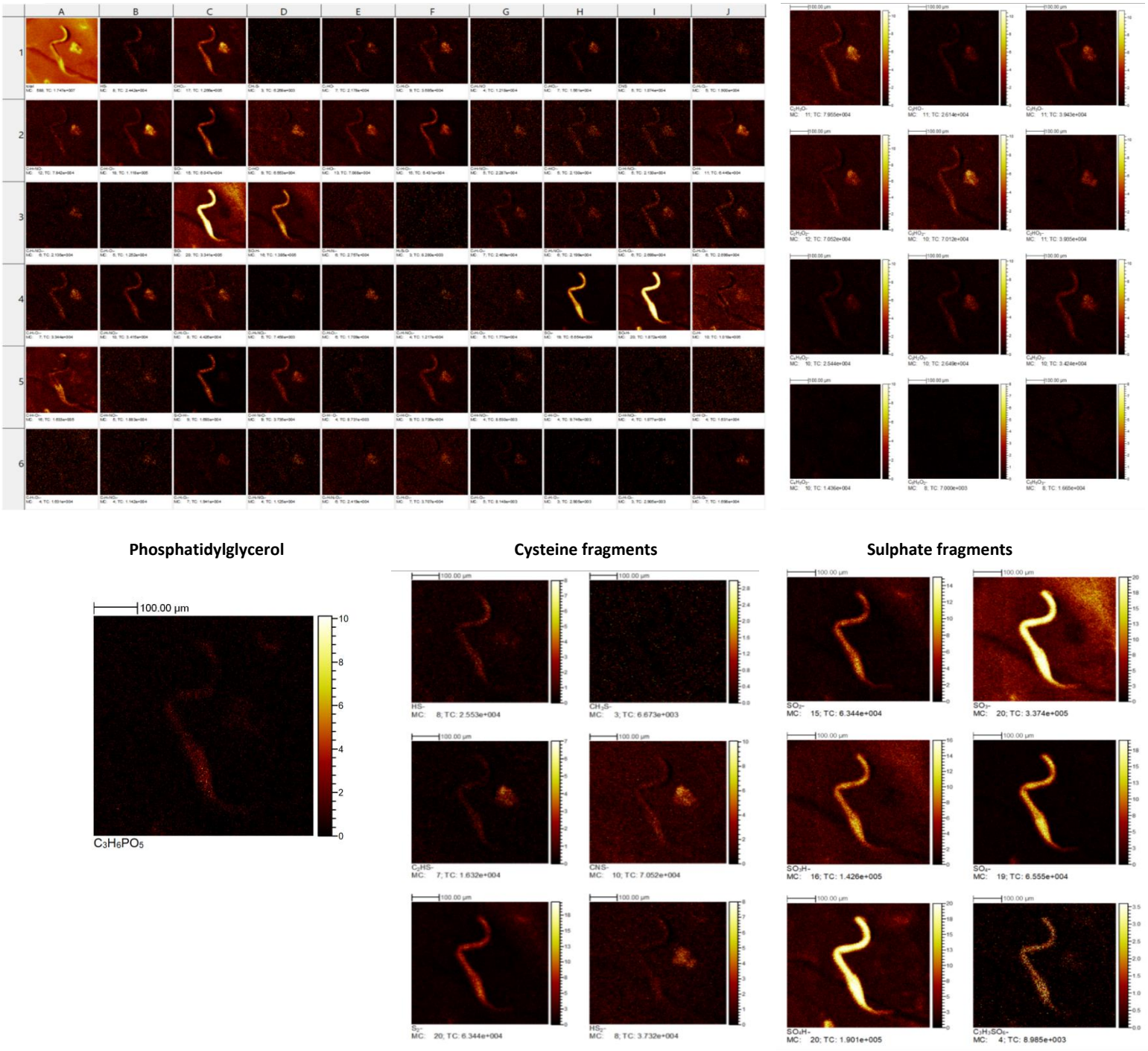

Supplementary figure 6: Total loaded ions images expressed on the L3 sheath (third worm). The L3 cuticle surface exhibited monosaccharide secondary ions. Also, it contains phosphatidylglycerol head group. In addition, the L3 cuticle surface elucidate expression of secondary ions associated with cysteine amino acid. However, The L3 cuticle contained probable sulphate compounds, but not heparan sulphate.

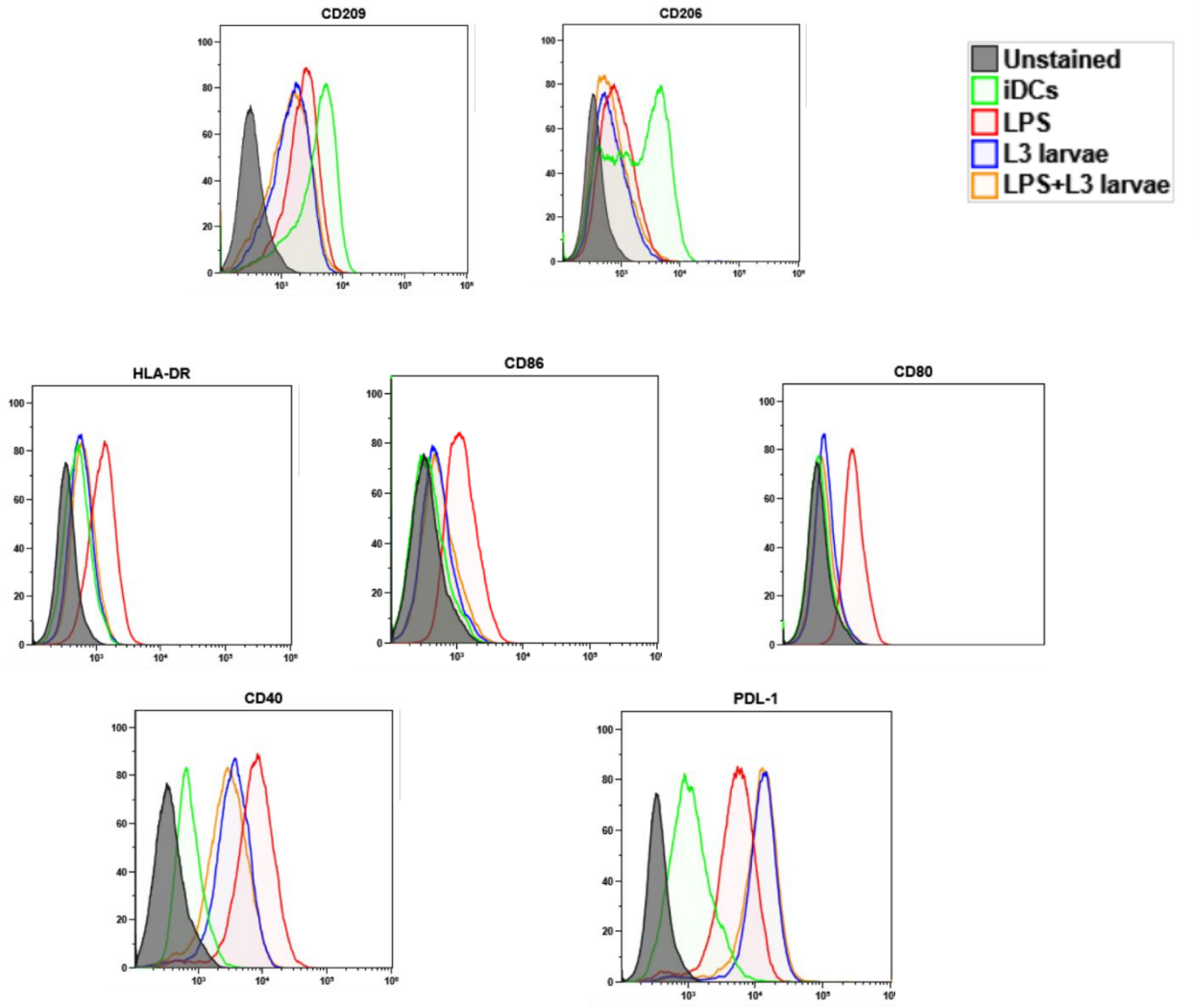

Supplementary figure 7: Phenotypic analysis of L3 larvae conditioned iDCs and mDCs. DCs were analysed for expression of MR and DC-SIGN. In addition, they analysed for maturation and co-stimulation markers (HLA-DR, CD86, CD80 and CD40) and inhibitory markers (PDL-1). Data shows no significant increase in the expression of maturation markers in L3-treated cells in its own and in presence of LP. In addition, MR (CD206) and DC-SIGN (CD209) expression were significantly downregulated in DCs primed with infective larvae. Interestingly, expression of programmed death-ligand-1 (PDL-1) was significantly increased following exposure to L3 larvae in presence or absence of LPS.

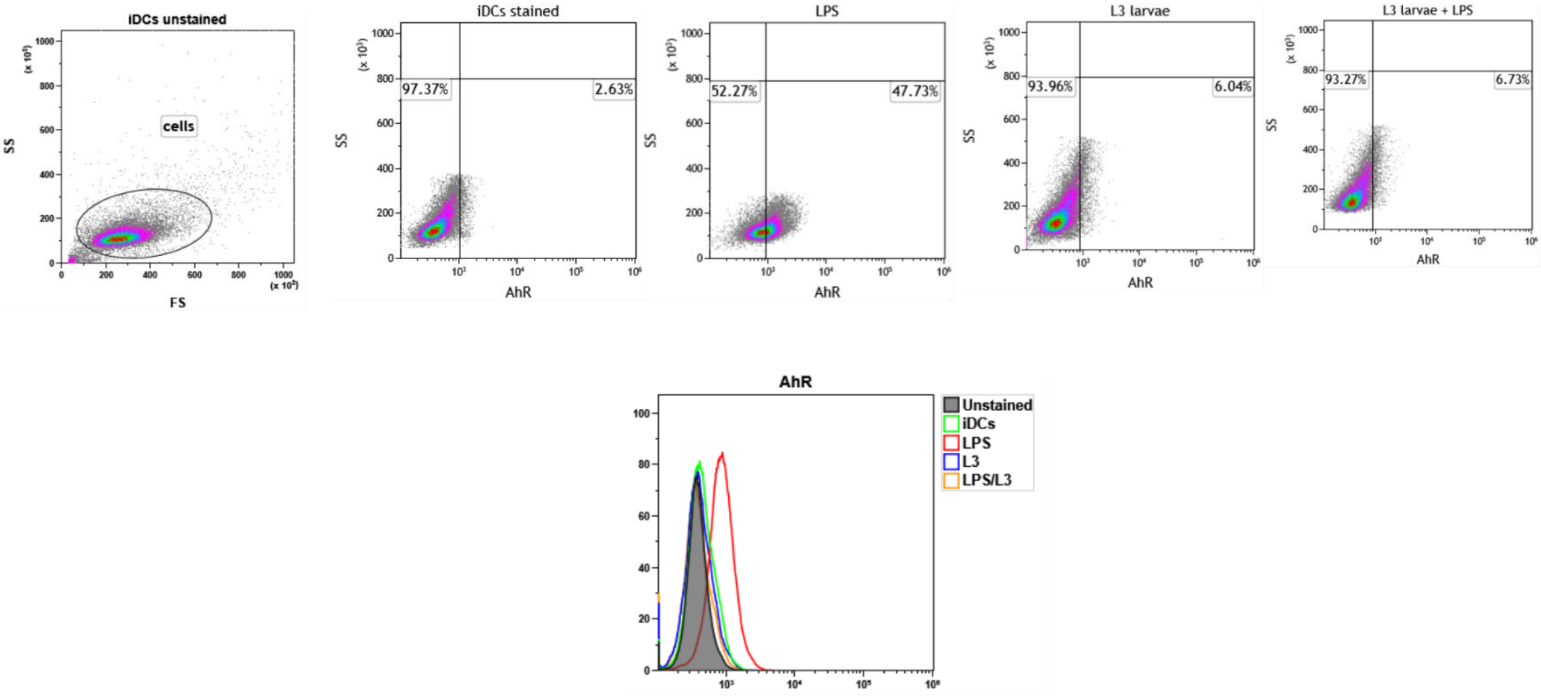

Supplementary figure 8: **Expression of aryl hydrocarbon receptor (AhR) in DCs stimulated with either LPS or L3 larvae in presence and absence of LPS.** Dot plot and histogram data show no expression of AhR in DCs stimulated with L3 larvae in presence and absence of LPS.

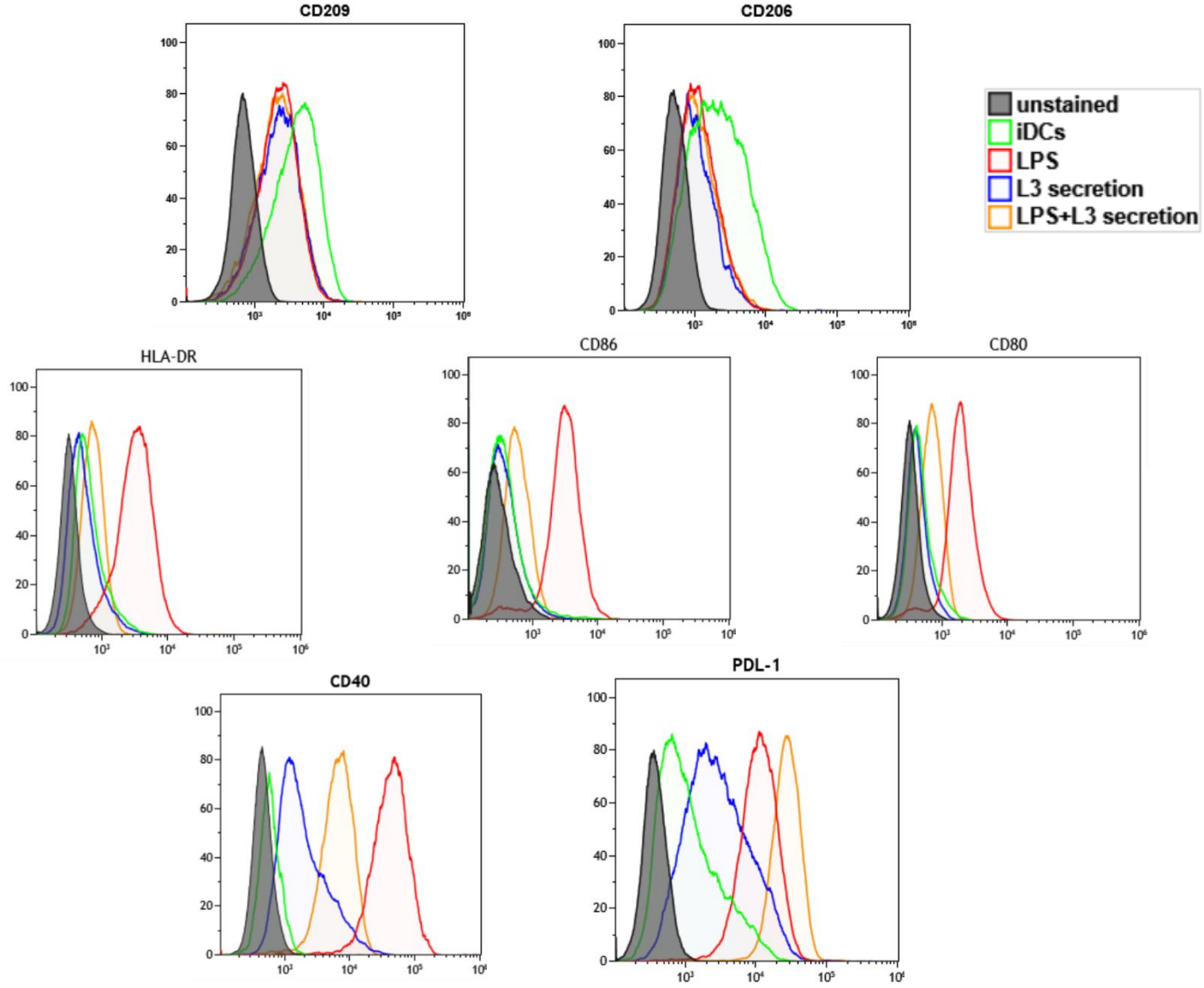

Supplementary figure 9: Phenotypic analysis of L3 secretion conditioned iDCs and mDCs. DCs were analysed for expression of MR and DC-SIGN. In addition, they analysed for maturation and co-stimulation markers (HLA-DR, CD86, CD80 and CD40) and inhibitory markers (PDL-1). Data shows no significant increase in the expression of maturation markers in L3 secretion -treated cells in its own and in presence of LP. In addition, MR (CD206) and DC-SIGN (CD209) expression were significantly downregulated in DCs primed with infective larvae. Interestingly, expression of programmed death-ligand-1 (PDL-1) was significantly increased following exposure to L3 secretion in presence or absence of LPS.

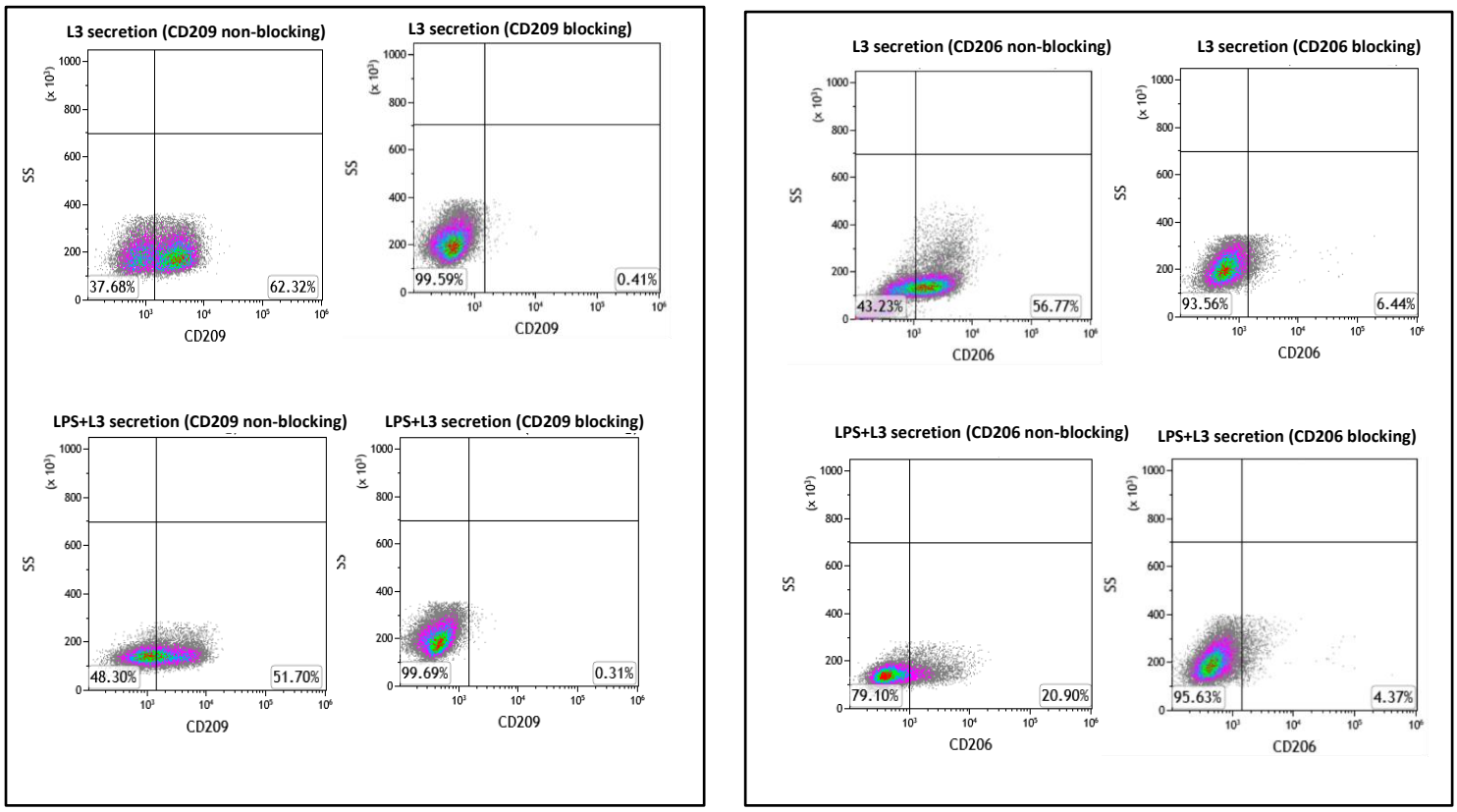

Supplementary figure 10: Expression of MR and DC-SIGN after their blocking in cells stimulated by L3 secretions in the presence or absence of LPS. Data show significant reduction in the expression of either DCs MR or DC-SIGN after their blocking compared to non-blocked cells.

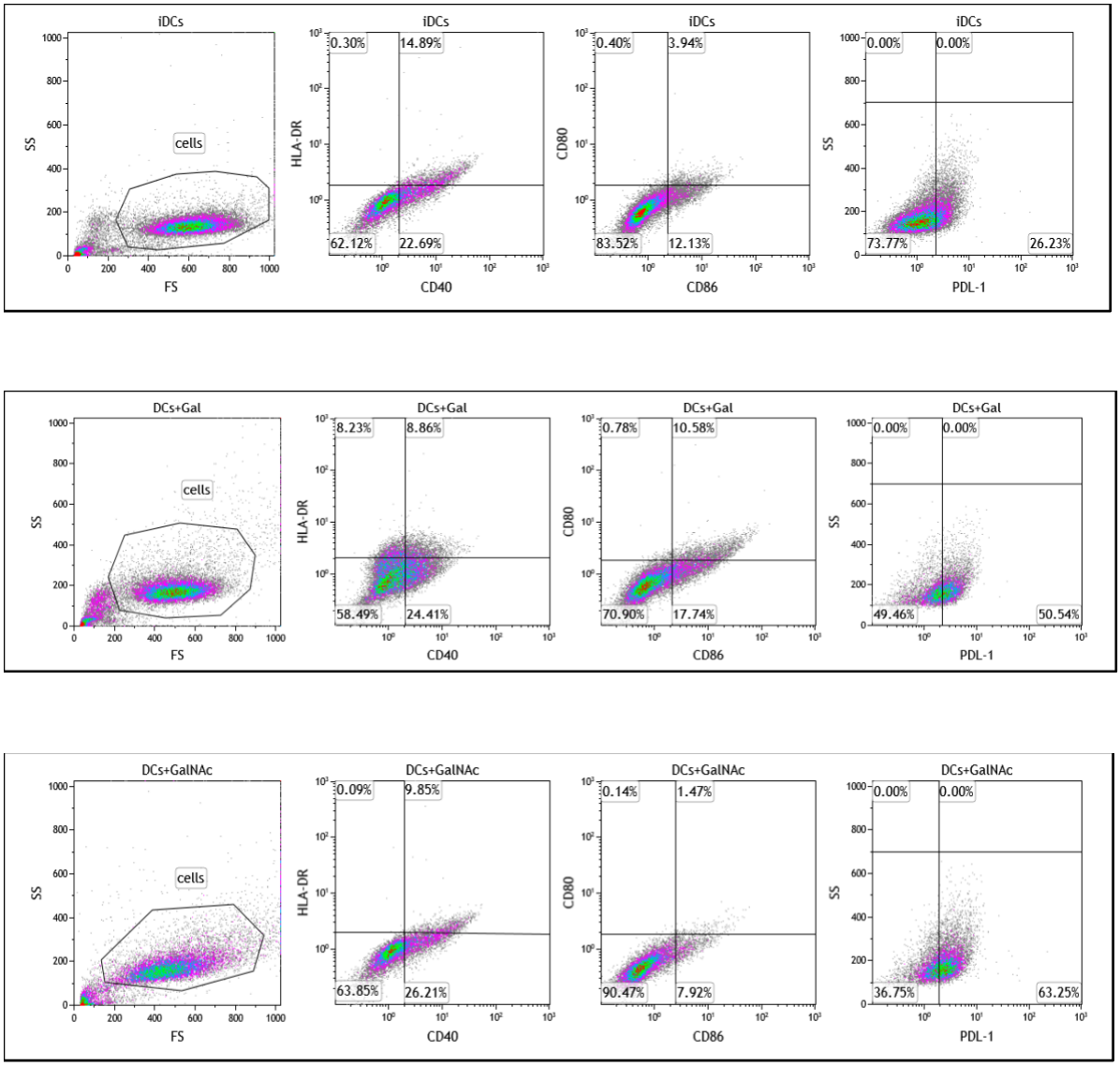

Supplementary figure 11: Phenotypic analysis of galactose and GalNAc on iDCs. DCs were analysed for expression of maturation markers including (HLA-DR, CD86 and CD80), co-stimulation markers (CD40) and inhibitory markers (PDL-1). Data show no significant phenotype changes on DCs conditioned with galactose or GalNAc in the absence of LPS compared to immature DCs.

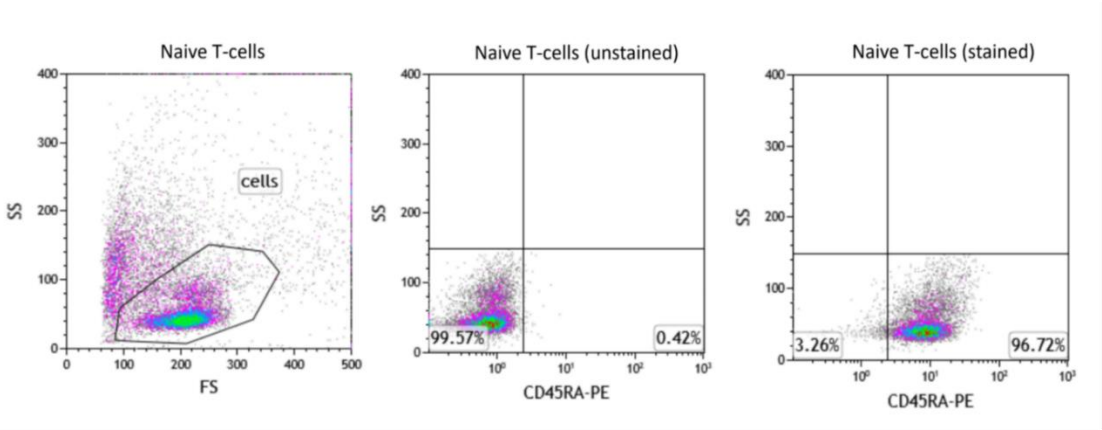

Supplementary figure 12: Analysis of isolated naïve T cells using flow cytometry. The population of naïve T-cells shown 91% expression of CD45RA which successfully indicating isolation of target cells.

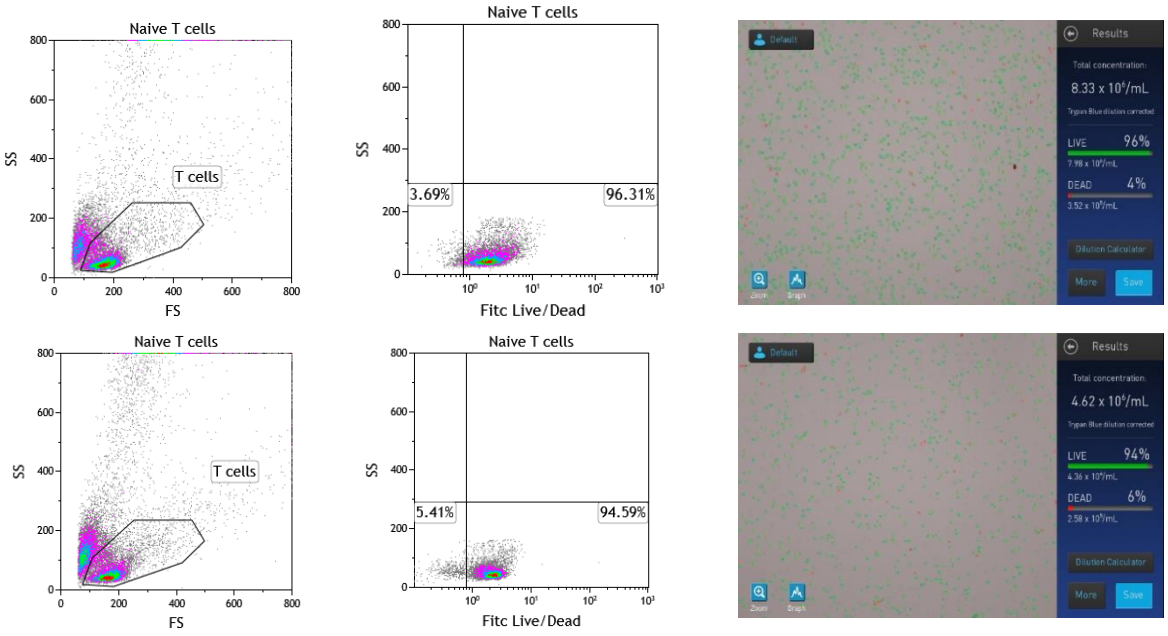

Supplementary figure 13: Viability of naïve T-cells using live/dead flow cytometry staining Countess™ II FL Automated Cell Counter after isolation and liquid nitrogen preservation methods. **A)** Data shown 95% of naïve T cells are live after isolation from PBMCs by using live/dead flow staining also showing similar viability using trypan blue automated counter. B) Naïve T cells viability show no marked reduction in live cells number after liquid nitrogen thawing comparing to naïve T cells number after isolation process

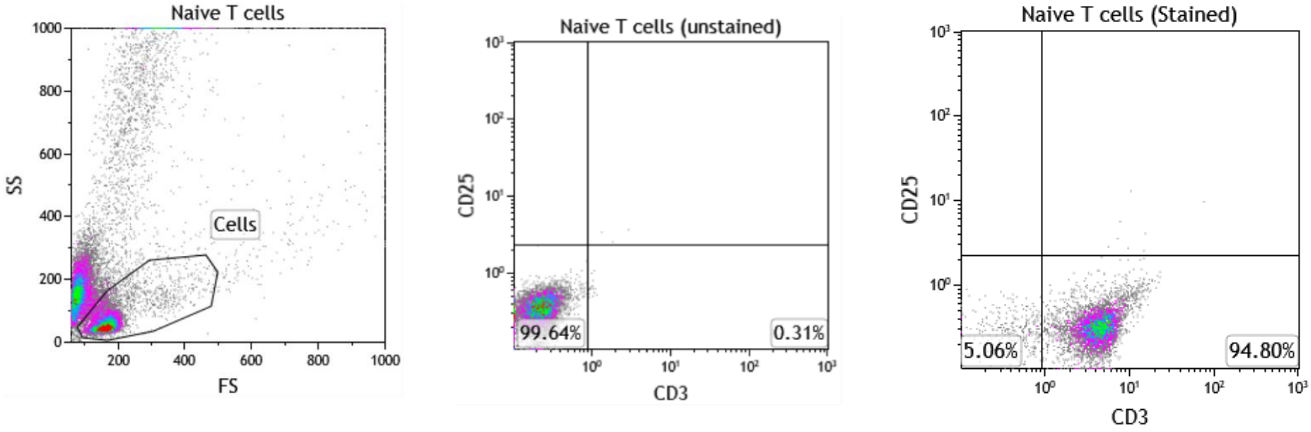

Supplementary figure 14: Showing CD25 expression in CD3 T cells after preservation in liquid nitrogen. Naïve T cells show no expression of CD25 activation marker after stored in liquid nitrogen.

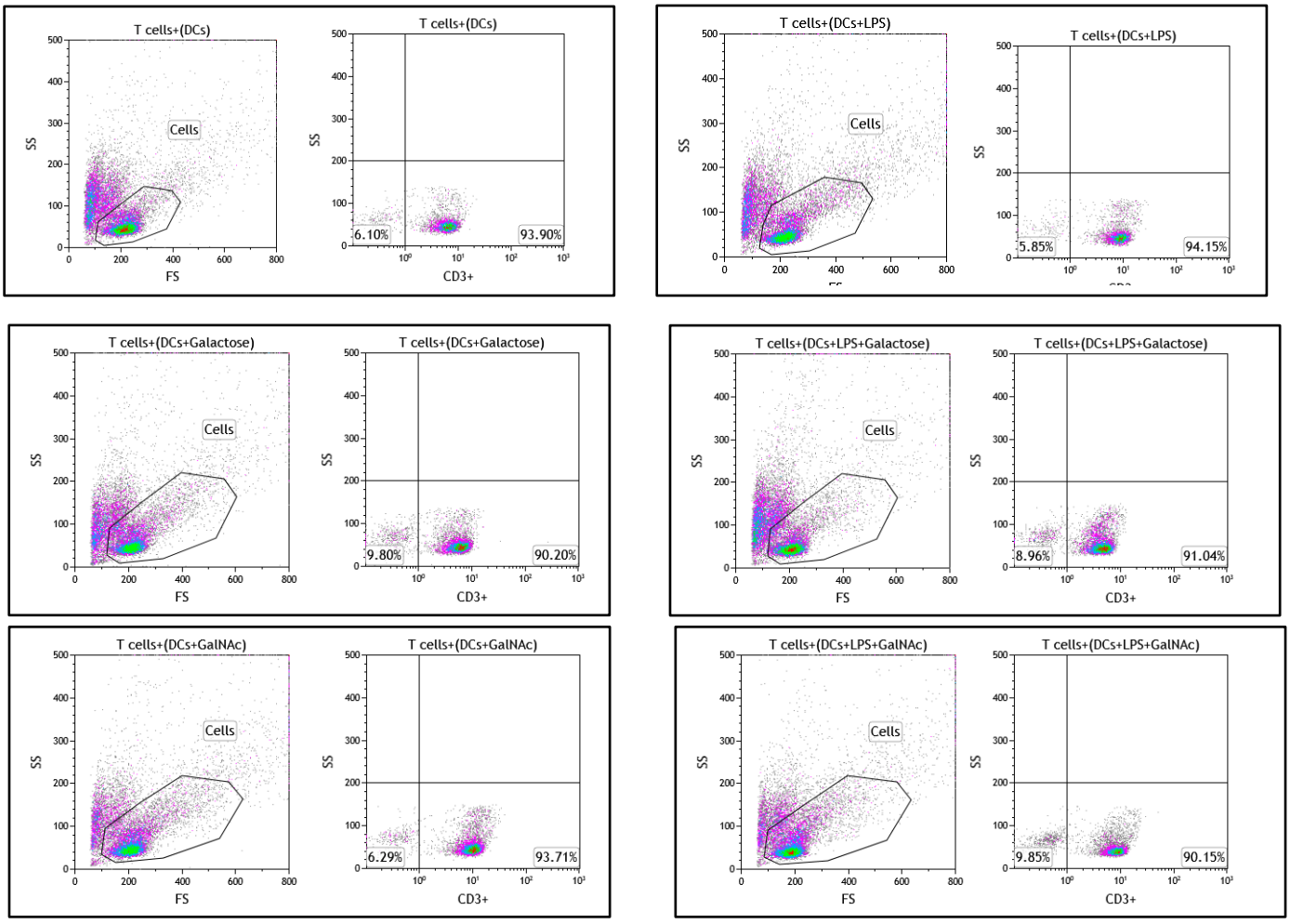

Supplementary figure 15: Showing CD3 expression in naïve T cell co-cultured with galactose and GalNAc primed DCs. Naïve T cells show expression of CD3 in all conditions indicating presence of naïve T cells population in all condition.

References

1. Smith, D.A. and Germolec, D.R., 1999. Introduction to immunology and autoimmunity. Environmental health perspectives, 107(suppl 5), pp.661-665.
2. Chaplin, D.D. Overview of the immune response. Journal of Allergy and Clinical Immunology, 2010, 125(2), pp. S3-S23.
3. Soares, M.P., Teixeira, L. and Moita, L.F., 2017. Disease tolerance and immunity in host protection against infection. *Nature Reviews Immunology*, *17*(2), pp.83-96.
4. Roberts, K., Alberts, B., Johnson, A., Walter, P. and Hunt, T., 2002. Molecular biology of the cell. *New York: Garland Science*, *32*(2).
5. Medzhitov, R. and Janeway Jr, C., 2000. Innate immunity. New England Journal of Medicine, 343(5), pp.338-344.
6. Abbas, A.K., Lichtman, A.H. and Pillai, S., 2019. *Basic immunology e-book: functions and disorders of the immune system*. Elsevier Health Sciences.
7. Rosales, C., 2018. Neutrophil: a cell with many roles in inflammation or several cell types?. *Frontiers in physiology*, *9*, p.113.
8. Richards, D.M. and Endres, R.G., 2014. The mechanism of phagocytosis: two stages of engulfment. *Biophysical journal*, ***107***(7), pp.1542-1553.
9. Underhill, D.M. and Goodridge, H.S., 2012. Information processing during phagocytosis. *Nature Reviews Immunology*, ***12***(7), pp.492-502.
10. Boltjes, A. and Van Wijk, F., 2014. Human dendritic cell functional specialization in steady-state and inflammation. *Frontiers in immunology*, *5*, p.131.
11. Hoebe, K., Janssen, E. and Beutler, B., 2004. The interface between innate and adaptive immunity. *Nature immunology*, *5*(10), pp.971-974.
12. Cruvinel, W.D.M., Mesquita Júnior, D., Araújo, J.A.P., Catelan, T.T.T., Souza, A.W.S.D., Silva, N.P.D. and Andrade, L.E.C., 2010. Immune system: Part I. Fundamentals of innate immunity with emphasis on molecular and cellular mechanisms of inflammatory response. Revista brasileira de reumatologia, 50, pp.434-447.
13. Bonilla, F.A. and Oettgen, H.C., 2010. Adaptive immunity. Journal of Allergy and Clinical Immunology, 125(2), pp.S33-S40.
14. Randolph, G.J., Jakubzick, C. and Qu, C., 2008. Antigen presentation by monocytes and monocyte-derived cells. *Current opinion in immunology*, *20*(1), pp.52-60.
15. Chen, X. and Jensen, P.E., 2008. The role of B lymphocytes as antigen-presenting cells. *Archivum immunologiae et therapiae experimentalis*, *56*(2), pp.77-83.
16. Miyazaki, T., Suzuki, G. and Yamamura, K.I., 1993. The role of macrophages in antigen presentation and T cell tolerance. *International immunology*, *5*(9), pp.1023-1033.

17. Collin, M., McGovern, N. and Haniffa, M., 2013. Human dendritic cell subsets. *Immunology*, ***140***(1), pp.22-30.
18. Collin, M. and Bigley, V., 2018. Human dendritic cell subsets: an update. *Immunology*, ***154***(1), pp.3-20.
19. Patente, T.A., Pinho, M.P., Oliveira, A.A., Evangelista, G., Bergami-Santos, P.C. and Barbuto, J.A., 2019. Human dendritic cells: their heterogeneity and clinical application potential in cancer immunotherapy. *Frontiers in immunology*, *9*, p.3176.
20. Dalod, M., Chelbi, R., Malissen, B. and Lawrence, T., 2014. Dendritic cell maturation: functional specialization through signaling specificity and transcriptional programming. *The EMBO journal*, *33*(10), pp.1104-1116.
21. Alonso, M.N., Wong, M.T., Zhang, A.L., Winer, D., Suhoski, M.M., Tolentino, L.L., Gaitan, J., Davidson, M.G., Kung, T.H., Galel, D.M. and Nadeau, K.C., 2011. TH1, TH2, and TH17 cells instruct monocytes to differentiate into specialized dendritic cell subsets. *Blood, The Journal of the American Society of Hematology*, *118*(12), pp.3311-3320.
22. Sousa, C.R., 2004. Activation of dendritic cells: translating innate into adaptive immunity. *Current opinion in immunology*, *16*(1), pp.21-25.
23. Nace, G., Evankovich, J., Eid, R. and Tsung, A., 2012. Dendritic cells and damage-associated molecular patterns: endogenous danger signals linking innate and adaptive immunity. *Journal of innate immunity*, *4*(1), pp.6-15.
24. Roche, P.A. and Furuta, K., 2015. The ins and outs of MHC class II-mediated antigen processing and presentation. *Nature Reviews Immunology*, *15*(4), pp.203-216.
25. Inaba, K. and Inaba, M., 2005. Antigen recognition and presentation by dendritic cells. *International journal of hematology*, *81*(3), pp.181-187.
26. Blum, J.S., Wearsch, P.A. and Cresswell, P., 2013. Pathways of antigen processing. *Annual review of immunology*, *31*, pp.443-473.
27. Ten Broeke, T., Wubbolts, R. and Stoorvogel, W., 2013. MHC class II antigen presentation by dendritic cells regulated through endosomal sorting. Cold Spring Harbor perspectives in biology, 5(12), p.a016873. Villadangos, J.A. and Schnorrer, P., 2007. Intrinsic and cooperative antigen-presenting functions of dendritic-cell subsets in vivo. *Nature Reviews Immunology*, *7*(7), pp.543-555.
28. Krishnaswamy, J.K., Chu, T. and Eisenbarth, S.C., 2013. Beyond pattern recognition: NOD-like receptors in dendritic cells. *Trends in immunology*, *34*(5), pp.224-233.
29. Devi, S., Rajakumara, E. and Ahmed, N., 2015. Induction of Mincle by Helicobacter pylori and consequent anti-inflammatory signaling denote a bacterial survival strategy. *Scientific reports*, *5*(1), pp.1-13.
30. Ramirez-Ortiz, Z.G. and Means, T.K., 2012. The role of dendritic cells in the innate recognition of pathogenic fungi (A. fumigatus, C. neoformans and C. albicans). *Virulence*, *3*(7), pp.635-646.
31. O'neill, L.A., Golenbock, D. and Bowie, A.G., 2013. The history of Toll-like receptors—redefining innate immunity. *Nature Reviews Immunology*, *13*(6), pp.453-460.

32. Kawasaki, T. and Kawai, T., 2014. Toll-like receptor signaling pathways. *Frontiers in immunology*, *5*, p.461.
33. Kawai, T. and Akira, S., 2010. The role of pattern-recognition receptors in innate immunity: update on Toll-like receptors. *Nature immunology*, *11*(5), pp.373-384.
34. Akira, S., Uematsu, S. and Takeuchi, O., 2006. Pathogen recognition and innate immunity. *Cell*, *124*(4), pp.783-801.
35. Regan, T., Nally, K., Carmody, R., Houston, A., Shanahan, F., MacSharry, J. and Brint, E., 2013. Identification of TLR10 as a key mediator of the inflammatory response to Listeria monocytogenes in intestinal epithelial cells and macrophages. *The Journal of Immunology*, *191*(12), pp.6084-6092.
36. Lee, S.M., Kok, K.H., Jaume, M., Cheung, T.K., Yip, T.F., Lai, J.C., Guan, Y., Webster, R.G., Jin, D.Y. and Peiris, J.M., 2014. Toll-like receptor 10 is involved in induction of innate immune responses to influenza virus infection. *Proceedings of the National Academy of Sciences*, *111*(10), pp.3793-3798.
37. Zhang, S.Y., Jouanguy, E., Ugolini, S., Smahi, A., Elain, G., Romero, P., Segal, D., Sancho-Shimizu, V., Lorenzo, L., Puel, A. and Picard, C., 2007. TLR3 deficiency in patients with herpes simplex encephalitis. *science*, *317*(5844), pp.1522-1527.
38. Bernard, J.J., Cowing-Zitron, C., Nakatsuji, T., Muehleisen, B., Muto, J., Borkowski, A.W., Martinez, L., Greidinger, E.L., Benjamin, D.Y. and Gallo, R.L., 2012. Ultraviolet radiation damages self noncoding RNA and is detected by TLR3. *Nature medicine*, *18*(8), pp.1286-1290.
39. Mancuso, G., Gambuzza, M., Midiri, A., Biondo, C., Papasergi, S., Akira, S., Teti, G. and Beninati, C., 2009. Bacterial recognition by TLR7 in the lysosomes of conventional dendritic cells. *Nature immunology*, *10*(6), pp.587-594.
40. Kawai, T. and Akira, S., 2006. Innate immune recognition of viral infection. *Nature immunology*, *7*(2), pp.131-137.
41. O'Neill, L.A. and Bowie, A.G., 2007. The family of five: TIR-domain-containing adaptors in Toll-like receptor signalling. *Nature Reviews Immunology*, *7*(5), pp.353-364.
42. Mogensen, T.H., 2009. Pathogen recognition and inflammatory signaling in innate immune defenses. *Clinical microbiology reviews*, *22*(2), pp.240-273.
43. Burns, K., Martinon, F., Esslinger, C., Pahl, H., Schneider, P., Bodmer, J.L., Di Marco, F., French, L. and Tschopp, J., 1998. MyD88, an adapter protein involved in interleukin-1 signaling. *Journal of biological chemistry*, *273*(20), pp.12203-12209.
44. Kawai, T. and Akira, S., 2007. Signaling to NF-κB by Toll-like receptors. *Trends in molecular medicine*, *13*(11), pp.460-469.
45. Yamamoto, M., Sato, S., Hemmi, H., Hoshino, K., Kaisho, T., Sanjo, H., Takeuchi, O., Sugiyama, M., Okabe, M., Takeda, K. and Akira, S., 2003. Role of adaptor TRIF in the MyD88-independent toll-like receptor signaling pathway. *Science*, *301*(5633), pp.640-643.

46. Yamamoto, M., Sato, S., Hemmi, H., Sanjo, H., Uematsu, S., Kaisho, T., Hoshino, K., Takeuchi, O., Kobayashi, M., Fujita, T. and Takeda, K., 2002. Essential role for TIRAP in activation of the signalling cascade shared by TLR2 and TLR4. *Nature*, *420*(6913), pp.324-329.
47. Yamamoto, M., Sato, S., Hemmi, H., Uematsu, S., Hoshino, K., Kaisho, T., Takeuchi, O., Takeda, K. and Akira, S., 2003. TRAM is specifically involved in the Toll-like receptor 4–mediated MyD88-independent signaling pathway. *Nature immunology*, *4*(11), pp.1144-1150.
48. Hoebe, K., Janssen, E.M., Kim, S.O., Alexopoulou, L., Flavell, R.A., Han, J. and Beutler, B., 2003. Upregulation of costimulatory molecules induced by lipopolysaccharide and double-stranded RNA occurs by Trif-dependent and Trif-independent pathways. *Nature immunology*, *4*(12), pp.1223-1229.
49. Horng, T., Barton, G.M., Flavell, R.A. and Medzhitov, R., 2002. The adaptor molecule TIRAP provides signalling specificity for Toll-like receptors. *Nature*, *420*(6913), pp.329-333.
50. Ozinsky, A., Underhill, D.M., Fontenot, J.D., Hajjar, A.M., Smith, K.D., Wilson, C.B., Schroeder, L. and Aderem, A., 2000. The repertoire for pattern recognition of pathogens by the innate immune system is defined by cooperation between toll-like receptors. *Proceedings of the National Academy of Sciences*, *97*(25), pp.13766-13771.
51. Lin, S.C., Lo, Y.C. and Wu, H., 2010. Helical assembly in the MyD88–IRAK4–IRAK2 complex in TLR/IL-1R signalling. *Nature*, *465*(7300), pp.885-890.
52. Kollewe, C., Mackensen, A.C., Neumann, D., Knop, J., Cao, P., Li, S., Wesche, H. and Martin, M.U., 2004. Sequential autophosphorylation steps in the interleukin-1 receptor-associated kinase-1 regulate its availability as an adapter in interleukin-1 signaling. *Journal of Biological Chemistry*, *279*(7), pp.5227-5236.
53. Jiang, Z., Ninomiya-Tsuji, J., Qian, Y., Matsumoto, K. and Li, X., 2002. Interleukin-1 (IL-1) receptor-associated kinase-dependent IL-1-induced signaling complexes phosphorylate TAK1 and TAB2 at the plasma membrane and activate TAK1 in the cytosol. *Molecular and cellular biology*, *22*(20), pp.7158-7167.
54. Li, S., Strelow, A., Fontana, E.J. and Wesche, H., 2002. IRAK-4: a novel member of the IRAK family with the properties of an IRAK-kinase. *Proceedings of the National Academy of Sciences*, *99*(8), pp.5567-5572.
55. Kanayama, A., Seth, R.B., Sun, L., Ea, C.K., Hong, M., Shaito, A., Chiu, Y.H., Deng, L. and Chen, Z.J., 2004. TAB2 and TAB3 activate the NF-κB pathway through binding to polyubiquitin chains. *Molecular cell*, *15*(4), pp.535-548.
56. Yamamoto, M., Sato, S., Mori, K., Hoshino, K., Takeuchi, O., Takeda, K. and Akira, S., 2002. Cutting edge: a novel Toll/IL-1 receptor domain-containing adapter that preferentially activates the IFN-β promoter in the Toll-like receptor signaling. *The Journal of Immunology*, *169*(12), pp.6668-6672.
57. Hacker, H. and Karin, M., 2006. Regulation and function of IKK and IKK-related kinases. Science's STKE, 2006(357), pp.re13-re13.

58. Mercurio, F., Zhu, H., Murray, B.W., Shevchenko, A., Bennett, B.L., Wu Li, J., Young, D.B., Barbosa, M., Mann, M., Manning, A. and Rao, A., 1997. IKK-1 and IKK-2: cytokine-activated IκB kinases essential for NF-κB activation. Science, 278(5339), pp.860-866.
59. Rothwarf, D.M., Zandi, E., Natoli, G. and Karin, M., 1998. IKK-γ is an essential regulatory subunit of the IκB kinase complex. Nature, 395(6699), pp.297-300.
60. Zandi, E., Rothwarf, D.M., Delhase, M., Hayakawa, M. and Karin, M., 1997. The IkB kinase complex (IKK) contains two kinase subunits, IKKa and IKKb, necessary for IkB phosphorylation and NF-kB activation. Cell, 91(2), pp.243-252.
61. Ullah, M.O., Sweet, M.J., Mansell, A., Kellie, S. and Kobe, B., 2016. TRIF-dependent TLR signaling, its functions in host defense and inflammation, and its potential as a therapeutic target. *Journal of leukocyte biology*, *100*(1), pp.27-45.
62. Oganesyan, G., Saha, S.K., Guo, B., He, J.Q., Shahangian, A., Zarnegar, B., Perry, A. and Cheng, G., 2006. Critical role of TRAF3 in the Toll-like receptor-dependent and-independent antiviral response. *Nature*, *439*(7073), pp.208-211.
63. Salazar, F., Sewell, H.F., Shakib, F. and Ghaemmaghami, A.M., 2013. The role of lectins in allergic sensitization and allergic disease. *Journal of allergy and clinical immunology*, *132*(1), pp.27-36.
64. Bermejo-Jambrina, M., Eder, J., Helgers, L.C., Hertoghs, N., Nijmeijer, B.M., Stunnenberg, M. and Geijtenbeek, T.B., 2018. C-type lectin receptors in antiviral immunity and viral escape. *Frontiers in immunology*, *9*, p.590.
65. Guo, Y., Feinberg, H., Conroy, E., Mitchell, D.A., Alvarez, R., Blixt, O., Taylor, M.E., Weis, W.I. and Drickamer, K., 2004. Structural basis for distinct ligand-binding and targeting properties of the receptors DC-SIGN and DC-SIGNR. *Nature structural & molecular biology*, *11*(7), pp.591-598.
66. Kerrigan, A.M. and Brown, G.D., 2009. C-type lectins and phagocytosis. *Immunobiology*, *214*(7), pp.562-575.
67. Figdor, C.G., van Kooyk, Y. and Adema, G.J., 2002. C-type lectin receptors on dendritic cells and Langerhans cells. *Nature Reviews Immunology*, *2*(2), pp.77-84.
68. Martinez-Pomares, L., 2012. The mannose receptor. *Journal of leukocyte biology*, *92*(6), pp.1177-1186.
69. Cummings, R.D. and McEver, R.P., 2009. C-type lectins. *Essentials of Glycobiology. 2nd edition*
70. van Kooyk, Y. and Geijtenbeek, T.B., 2003. DC-SIGN: escape mechanism for pathogens. *Nature Reviews Immunology*, *3*(9), pp.697-709.
71. Lee, R.T., Hsu, T.L., Huang, S.K., Hsieh, S.L., Wong, C.H. and Lee, Y.C., 2011. Survey of immune-related, mannose/fucose-binding C-type lectin receptors reveals widely divergent sugar-binding specificities. Glycobiology, 21(4), pp.512-520.
72. Gringhuis, S.I., Den Dunnen, J., Litjens, M., Van Der Vlist, M. and Geijtenbeek, T.B., 2009. Carbohydrate-specific signaling through the DC-SIGN signalosome tailors immunity to Mycobacterium tuberculosis, HIV-1 and Helicobacter pylori. Nature immunology, 10(10), pp.1081-1088.

73. Geijtenbeek, T.B. and Gringhuis, S.I., 2009. Signalling through C-type lectin receptors: shaping immune responses. Nature Reviews Immunology, 9(7), pp.465-479.
74. Gringhuis, S.I., den Dunnen, J., Litjens, M., van Het Hof, B., van Kooyk, Y. and Geijtenbeek, T.B., 2007. C-type lectin DC-SIGN modulates Toll-like receptor signaling via Raf-1 kinase-dependent acetylation of transcription factor NF-κB. *Immunity*, *26*(5), pp.605-616.
75. Gringhuis, S.I., Kaptein, T.M., Wevers, B.A., Mesman, A.W. and Geijtenbeek, T.B., 2014. Fucose-specific DC-SIGN signalling directs T helper cell type-2 responses via IKKε-and CYLD-dependent Bcl3 activation. *Nature communications*, *5*(1), pp.1-13.
76. Palucka, K. and Banchereau, J., 2002. How dendritic cells and microbes interact to elicit or subvert protective immune responses. *Current opinion in immunology*, *14*(4), pp.420-431.
77. Goyal, S., Klassert, T.E. and Slevogt, H., 2016. C-type lectin receptors in tuberculosis: what we know. *Medical microbiology and immunology*, *205*(6), pp.513-535.
78. Salazar, F., Hall, L., Negm, O.H., Awuah, D., Tighe, P.J., Shakib, F. and Ghaemmaghami, A.M., 2016. The mannose receptor negatively modulates the Toll-like receptor 4–aryl hydrocarbon receptor–indoleamine 2, 3-dioxygenase axis in dendritic cells affecting T helper cell polarization. *Journal of Allergy and Clinical Immunology*, *137*(6), pp.1841-1851.
79. Von Bubnoff, D., Scheler, M., Wilms, H., Fimmers, R. and Bieber, T., 2011. Identification of IDO-positive and IDO-negative human dendritic cells after activation by various proinflammatory stimuli. *The Journal of Immunology*, *186*(12), pp.6701-6709.
80. Eminel, S., Jin, N., Rostami, M., Dibbert, S., Mrowietz, U. and Suhrkamp, I., 2017. Dimethyl-and monomethylfumarate regulate indoleamine 2, 3-dioxygenase (IDO) activity in human immune cells. *Experimental dermatology*, *26*(8), pp.685-690.
81. Meireson, A., Devos, M. and Brochez, L., 2020. IDO expression in cancer: Different compartment, different functionality?. *Frontiers in immunology*, *11*, p.2340.
82. Romani, L., Zelante, T., De Luca, A., Bozza, S., Bonifazi, P., Moretti, S., D'Angelo, C., Giovannini, G., Bistoni, F., Fallarino, F. and Puccetti, P., 2009. Indoleamine 2, 3-dioxygenase (IDO) in inflammation and allergy to Aspergillus. *Medical mycology*, *47*(Supplement_1), pp.S154-S161.
83. Von Bubnoff, D. and Bieber, T., 2012. The indoleamine 2, 3-dioxygenase (IDO) pathway controls allergy. *Allergy*, *67*(6), pp.718-725.
84. Munn, D.H. and Mellor, A.L., 2013. Indoleamine 2, 3 dioxygenase and metabolic control of immune responses. *Trends in immunology*, *34*(3), pp.137-143.
85. Von Bubnoff, D., Scheler, M., Wilms, H., Fimmers, R. and Bieber, T., 2011. Identification of IDO-positive and IDO-negative human dendritic cells after activation by various proinflammatory stimuli. *The Journal of Immunology*, *186*(12), pp.6701-6709.
86. Braun, D., Longman, R.S. and Albert, M.L., 2005. A two-step induction of indoleamine 2, 3 dioxygenase (IDO) activity during dendritic-cell maturation. *Blood*, *106*(7), pp.2375-2381.

87. Knubel, C.P., Martínez, F.F., Fretes, R.E., Lujan, C.D., Theumer, M.G., Cervi, L. and Motrán, C.C., 2010. Indoleamine 2, 3-dioxigenase (IDO) is critical for host resistance against Trypanosoma cruzi. *The FASEB Journal*, *24*(8), pp.2689-2701.
88. Kumar, B.V., Connors, T.J. and Farber, D.L., 2018. Human T cell development, localization, and function throughout life. *Immunity*, *48*(2), pp.202-213.
89. Pennock, N.D., White, J.T., Cross, E.W., Cheney, E.E., Tamburini, B.A. and Kedl, R.M., 2013. T cell responses: naive to memory and everything in between. *Advances in physiology education*, *37*(4), pp.273-283.
90. Castro, G.A., 2011. Helminths: Structure, classification, growth, and development.
91. Smyth, J.D. and Wakelin, D., 1994. *Introduction to animal parasitology*. Cambridge university press.
92. Dorris, M., De Ley, P. and Blaxter, M.L., 1999. Molecular analysis of nematode diversity and the evolution of parasitism. *Parasitology today*, *15*(5), pp.188-193.
93. Blaxter, M.L., De Ley, P., Garey, J.R., Liu, L.X., Scheldeman, P., Vierstraete, A., Vanfleteren, J.R., Mackey, L.Y., Dorris, M., Frisse, L.M. and Vida, J.T., 1998. A molecular evolutionary framework for the phylum Nematoda. *Nature*, *392*(6671), pp.71-75.
94. Montaño, K.J., Cuéllar, C. and Sotillo, J., 2021. Rodent Models for the Study of Soil-Transmitted Helminths: A Proteomics Approach. *Frontiers in Cellular and Infection Microbiology*, *11*, p.309.
95. Loukas, A., Constant, S.L. and Bethony, J.M., 2005. Immunobiology of hookworm infection. FEMS Immunology & Medical Microbiology, 43(2), pp.115-124.
96. Hotez, P.J., Brooker, S., Bethony, J.M., Bottazzi, M.E., Loukas, A. and Xiao, S., 2004. Hookworm infection. New England Journal of Medicine, 351(8), pp.799-807.
97. Brooker, S., Bethony, J. and Hotez, P.J., 2004. Human hookworm infection in the 21st century. Advances in parasitology, 58, p.197.
98. Loukas, A., Hotez, P.J., Diemert, D., Yazdanbakhsh, M., McCarthy, J.S., Correa-Oliveira, R., Croese, J. and Bethony, J.M., 2016. Hookworm infection. *Nature Reviews Disease Primers*, *2*(1), pp.1-18.
99. Quinnell, R.J., Bethony, J. and Pritchard, D.I., 2004. The immunoepidemiology of human hookworm infection. *Parasite immunology*, *26*(11-12), pp.443-454.
100. Hotez, P.J., Bethony, J., Bottazzi, M.E., Brooker, S. and Buss, P., 2005. Hookworm:"the great infection of mankind". *PLoS medicine*, *2*(3), p.e67.
101. Hawdon, J.M., Volk, S.W., Rose, R., Pritchard, D.I., Behnke, J.M. and Schad, G.A., 1993. Observations on the feeding behaviour of parasitic third-stage hookworm larvae. Parasitology, 106(2), pp.163-169.
102. Bethony, J., Brooker, S., Albonico, M., Geiger, S.M., Loukas, A., Diemert, D. and Hotez, P.J., 2006. Soil-transmitted helminth infections: ascariasis, trichuriasis, and hookworm. The lancet, 367(9521), pp.1521-1532.
103. Jian, X., Shu-Hua, X., Hui-Qing, Q., Sen, L., Hotez, P., Bing-Gui, S., Hai-Chou, X., Tie-Hua, L. and Bin, Z., 2003. Necator americanus: maintenance through one hundred generations in golden hamsters

(Mesocricetus auratus). II. Morphological development of the adult and its comparison with humans. *Experimental parasitology*, *105*(3-4), pp.192-200.

104. Hoagland, K.E. and Schad, G.A., 1978. Necator americanus and Ancylostoma duodenale: life history parameters and epidemiological implications of two sympatric hookworms of humans. *Experimental parasitology*, *44*(1), pp.36-49.
105. Pritchard, D.I., Quinnell, R.J., Slater, A.F.G., McKean, P.G., Dale, D.D.S., Raiko, A. and Keymer, A.E., 1990. Epidemiology and immunology of Necator americanus infection in a community in Papua New Guinea: humoral responses to excretory-secretory and cuticular collagen antigens. *Parasitology*, *100*(2), pp.317-326.
106. Loukas, A. and Prociv, P., 2001. Immune responses in hookworm infections. *Clinical microbiology reviews*, *14*(4), pp.689-703.
107. Udonsi, J.K. and Atata, G., 1987. Necator americanus: temperature, pH, light, and larval development, longevity, and desiccation tolerance. *Experimental Parasitology*, *63*(2), pp.136-142.
108. Schad, G.A., Chowdhury, A.B., Dean, C.G., Kochar, V.K., Nawalinski, T.A., Thomas, J. and Tonascia, J.A., 1973. Arrested development in human hookworm infections: an adaptation to a seasonally unfavorable external environment. *Science*, *180*(4085), pp.502-504.
109. Hotez, P.J. and Pritchard, D.I., 1995. Hookworm infection. *Scientific American*, *272*(6), pp.68-74.
110. Haas, W., Haberl, B., Idris, I. and Kersten, S., 2005. Infective larvae of the human hookworms Necator americanus and Ancylostoma duodenale differ in their orientation behaviour when crawling on surfaces. Parasitology research, 95(1), pp.25-29.
111. Salafsky, B., Fusco, A.C. and Siddiqui, A., 1990. Necator americanus: factors influencing skin penetration by larvae. *Hookworm disease-current status and new directions.*, pp.329-339.
112. Matthews, B.E., 1982. Skin penetration by Necator americanus larvae. Zeitschrift für Parasitenkunde, 68(1), pp.81-86.
113. Matthews, B.E., 1975. Mechanism of skin penetration by Ancylostoma tubaeforme larvae. Parasitology, 70(1), pp.25-38.
114. Kumar, S. and Pritchard, D.I., 1992. Skin penetration by ensheathed third-stage infective larvae of Negator americanus, and the host's immune response to larval antigens. International journal for parasitology, 22(5), pp.573-579.
115. Behnke, J.M., Paul, V. and Rajasekariah, G.R., 1986. The growth and migration of Necator americanus following infection of neonatal hamsters. Transactions of the Royal Society of Tropical Medicine and Hygiene, 80(1), pp.146-149.
116. Devaney, E., 2005. The end of the line for hookworm? An update on vaccine development. PLoS medicine, 2(10), p.e327.
117. Haldeman, M.S., Nolan, M.S. and Ng'habi, K.R., 2020. Human hookworm infection: Is effective control possible? A review of hookworm control efforts and future directions. *Acta tropica*, *201*, p.105214.

118. Pritchard, D.I. and Brown, A., 2001. Is Necator americanus approaching a mutualistic symbiotic relationship with humans?. *Trends in Parasitology*, *17*(4), pp.169-172.
119. Wright, V. and Bickle, Q., 2005. Immune responses following experimental human hookworm infection. *Clinical & Experimental Immunology*, *142*(2), pp.398-403.
120. Fujiwara, R.T., Cançado, G.G., Freitas, P.A., Santiago, H.C., Massara, C.L., Carvalho, O.D.S., Corrêa-Oliveira, R., Geiger, S.M. and Bethony, J., 2009. Necator americanus infection: a possible cause of altered dendritic cell differentiation and eosinophil profile in chronically infected individuals. *PLoS Neglected Tropical Diseases*, *3*(3), p.e399.
121. Urb, M. and Sheppard, D.C., 2012. The role of mast cells in the defence against pathogens. *PLoS pathogens*, *8*(4), p.e1002619.
122. Muller, W.A., 2011. Mechanisms of leukocyte transendothelial migration. *Annual Review of Pathology: Mechanisms of Disease*, *6*, pp.323-344.
123. Nourshargh, S. and Alon, R., 2014. Leukocyte migration into inflamed tissues. *Immunity*, *41*(5), pp.694-707.
124. Janeway Jr, C.A., Travers, P., Walport, M. and Shlomchik, M.J., 2001. The components of the immune system. In *Immunobiology: The Immune System in Health and Disease. 5th edition*. Garland Science.
125. Ramírez-Toloza, G., Aguilar-Guzmán, L., Valck, C., Ferreira, V.P. and Ferreira, A., 2020. The interactions of parasite calreticulin with initial complement components: consequences in immunity and virulence. *Frontiers in Immunology*, *11*, p.1561.
126. Shao, S., Sun, X., Chen, Y., Zhan, B. and Zhu, X., 2019. Complement evasion: an effective strategy that parasites utilize to survive in the host. *Frontiers in microbiology*, *10*, p.532.
127. Kasper, G., Brown, A., Eberl, M., Vallar, L., Kieffer, N., Berry, C., Girdwood, K., Eggleton, P., Quinnell, R. and Pritchard, D.I., 2001. A calreticulin-like molecule from the human hookworm Necator americanus interacts with C1q and the cytoplasmic signalling domains of some integrins. *Parasite immunology*, *23*(3), pp.141-152.
128. White, C.J., Maxwell, C.J. and Gallin, J.I., 1986. Changes in the structural and functional properties of human eosinophils during experimental hookworm infection. *Journal of Infectious Diseases*, *154*(5), pp.778-783.
129. Desakorn, V.A.R.U.N.E.E., Suntharasamai, P.R.A.V.A.N., Pukrittayakamee, S.A.S.I.T.H.O.N., Migasena, S.R.I.C.H.A.R.O.E.N. and Bunnag, D.A.N.A.I., 1987. Adherence of human eosinophils to infective filariform larvae of Necator americanus in vitro. *The Southeast Asian journal of tropical medicine and public health*, *18*(1), pp.66-72.
130. Daub, J., Loukas, A., Pritchard, D.I. and Blaxter, M., 2000. A survey of genes expressed in adults of the human hookworm, Necator americanus. *Parasitology*, *120*(2), pp.171-184.

131. Tang, Y.T., Gao, X., Rosa, B.A., Abubucker, S., Hallsworth-Pepin, K., Martin, J., Tyagi, R., Heizer, E., Zhang, X., Bhonagiri-Palsikar, V. and Minx, P., 2014. Genome of the human hookworm Necator americanus. *Nature genetics*, *46*(3), pp.261-269.
132. Pritchard, D.I., 1995. The survival strategies of hookworms. *Parasitology Today*, *11*(7), pp.255-259.
133. Tormo, N., del Remedio Guna, M., Teresa Fraile, M., Dolores Ocete, M., Garcia, A., Navalpotro, D., Chanzá, M., Luis Ramos, J. and Gimeno, C., 2011. Immunity to Parasites. *Current Immunology Reviews*, *7*(1), pp.25-43.
134. Hubo, M., Trinschek, B., Kryczanowsky, F., Tuettenberg, A., Steinbrink, K. and Jonuleit, H., 2013. Costimulatory molecules on immunogenic versus tolerogenic human dendritic cells. *Frontiers in immunology*, *4*, p.82.
135. Howard, C.J., Charleston, B., Stephens, S.A., Sopp, P. and Hope, J.C., 2004. The role of dendritic cells in shaping the immune response. *Animal health research reviews*, *5*(2), pp.191-195.
136. Schülke, S., 2018. Induction of interleukin-10 producing dendritic cells as a tool to suppress allergen-specific T helper 2 responses. *Frontiers in immunology*, *9*, p.455.
137. Van Die, I. and Cummings, R.D., 2010. Glycan gimmickry by parasitic helminths: a strategy for modulating the host immune response?. *Glycobiology*, *20*(1), pp.2-12.
138. Okano, M., Satoskar, A.R., Nishizaki, K., Abe, M. and Harn, D.A., 1999. Induction of Th2 responses and IgE is largely due to carbohydrates functioning as adjuvants on Schistosoma mansoni egg antigens. *The Journal of Immunology*, *163*(12), pp.6712-6717.
139. Okano, M., Satoskar, A.R., Nishizaki, K. and Harn, D.A., 2001. Lacto-N-fucopentaose III found on Schitosoma mansoni egg antigens functions as adjuvant for proteins by inducing Th2-type response. *The Journal of Immunology*, *167*(1), pp.442-450.
140. Faveeuw, C., Mallevaey, T., Paschinger, K., Wilson, I.B., Fontaine, J., Mollicone, R., Oriol, R., Altmann, F., Lerouge, P., Capron, M. and Trottein, F., 2003. Schistosome N-glycans containing core α3-fucose and core β2-xylose epitopes are strong inducers of Th2 responses in mice. *European journal of immunology*, *33*(5), pp.1271-1281.
141. Thomas, P.G. and Harn Jr, D.A., 2004. Immune biasing by helminth glycans. *Cellular microbiology*, *6*(1), pp.13-22.
142. Tawill, S., Le Goff, L., Ali, F., Blaxter, M. and Allen, J.E., 2004. Both free-living and parasitic nematodes induce a characteristic Th2 response that is dependent on the presence of intact glycans. *Infection and immunity*, *72*(1), pp.398-407.
143. Hokke, C.H. and Yazdanbakhsh, M., 2005. Schistosome glycans and innate immunity. *Parasite immunology*, *27*(7-8), pp.257-264.
144. Gómez-García, L., Rivera-Montoya, I., Rodríguez-Sosa, M. and Terrazas, L.I., 2006. Carbohydrate components of Taenia crassiceps metacestodes display Th2-adjuvant and anti-inflammatory properties when co-injected with bystander antigen. *Parasitology Research*, *99*(4), pp.440-448.

145. Teixeira-Carvalho, A., Fujiwara, R.T., Stemmy, E.J., Olive, D., Damsker, J.M., Loukas, A., Corrêa-Oliveira, R., Constant, S.L. and Bethony, J.M., 2008. Binding of excreted and/or secreted products of adult hookworms to human NK cells in Necator americanus-infected individuals from Brazil. Infection and immunity, 76(12), pp.5810-5816.
146. Pit, D., Polderman, A., Baeta, S., Schulz-Key, H. and Soboslay, P., 2001. Parasite-specific antibody and cellular immune responses in humans infected with Necator americanus and Oesophagostomum bifurcum. Parasitology research, 87(9), pp.722-729.
147. MacDonald, A.S. and Maizels, R.M., 2008. Alarming dendritic cells for Th2 induction. *Journal of Experimental Medicine*, *205*(1), pp.13-17.
148. Kane, C.M., Cervi, L., Sun, J., McKee, A.S., Masek, K.S., Shapira, S., Hunter, C.A. and Pearce, E.J., 2004. Helminth antigens modulate TLR-initiated dendritic cell activation. *The Journal of Immunology*, *173*(12), pp.7454-7461.
149. Geiger, S.M., Caldas, I.R., Mc Glone, B.E., Campi-Azevedo, A.C., De Oliveira, L.M., Brooker, S., Diemert, D., CORRÊA-OLIVEIRA, R. and Bethony, J.M., 2007. Stage-specific immune responses in human Necator americanus infection. *Parasite Immunology*, *29*(7), pp.347-358.
150. Everts, B., Smits, H.H., Hokke, C.H. and Yazdanbakhsh, M., 2010. Helminths and dendritic cells: sensing and regulating via pattern recognition receptors, Th2 and Treg responses. *European journal of immunology*, *40*(6), pp.1525-1537.
151. Harnett, W., 2014. Secretory products of helminth parasites as immunomodulators. *Molecular and biochemical parasitology*, *195*(2), pp.130-136.
152. Hewitson, J.P., Grainger, J.R. and Maizels, R.M., 2009. Helminth immunoregulation: the role of parasite secreted proteins in modulating host immunity. *Molecular and biochemical parasitology*, *167*(1), pp.1-11.
153. Brown, A., Girod, N., Billett, E.E. and Pritchard, D.I., 1999. Necator americanus (human hookworm) aspartyl proteinases and digestion of skin macromolecules during skin penetration. *The American journal of tropical medicine and hygiene*, *60*(5), pp.840-847.
154. Carr, A. and Pritchard, D.I., 1986. Identification of hookworm (Necator americanus) antigens and their translation in vitro. *Molecular and biochemical parasitology*, *19*(3), pp.251-258.
155. Moyle, M., Foster, D.L., McGrath, D.E., Brown, S.M., Laroche, Y., De Meutter, J., Stanssens, P., Bogowitz, C.A., Fried, V.A. and Ely, J.A., 1994. A hookworm glycoprotein that inhibits neutrophil function is a ligand of the integrin CD11b/CD18. *Journal of Biological Chemistry*, *269*(13), pp.10008-10015.
156. Brophy, P.M., Patterson, L.H., Brown, A. and Pritchard, D.I., 1995. Glutathione S-transferase (GST) expression in the human hookworm Necator americanus: potential roles for excretory-secretory forms of GST. *Acta tropica*, *59*(3), pp.259-263.

157. Williamson, A.L., Lecchi, P., Turk, B.E., Choe, Y., Hotez, P.J., McKerrow, J.H., Cantley, L.C., Sajid, M., Craik, C.S. and Loukas, A., 2004. A multi-enzyme cascade of hemoglobin proteolysis in the intestine of blood-feeding hookworms. *Journal of Biological Chemistry*, *279*(34), pp.35950-35957.
158. Williamson, A.L., Brindley, P.J. and Loukas, A., 2003. Hookworm cathepsin D aspartic proteases: contributing roles in the host-specific degradation of serum proteins and skin macromolecules. *Parasitology*, *126*(2), pp.179-185.
159. Williamson, A.L., Lecchi, P., Turk, B.E., Choe, Y., Hotez, P.J., McKerrow, J.H., Cantley, L.C., Sajid, M., Craik, C.S. and Loukas, A., 2004. A multi-enzyme cascade of hemoglobin proteolysis in the intestine of blood-feeding hookworms. *Journal of Biological Chemistry*, *279*(34), pp.35950-35957.
160. Souadkia, N., Brown, A., Leach, L. and Pritchard, D.I., 2010. Hookworm (Necator americanus) larval enzymes disrupt human vascular endothelium. *The American journal of tropical medicine and hygiene*, *83*(3), p.549.
161. Abuzeid, A.M., Zhou, X., Huang, Y. and Li, G., 2020. Twenty-five-year research progress in hookworm excretory/secretory products. *Parasites & vectors*, *13*(1), pp.1-18.
162. Smith, J.M., 1976. Comparative ultrastructure of the oesophageal glands of third stage larval hookworms. *International journal for parasitology*, *6*(1), pp.9-13.
163. Culley, F.J., Brown, A., Conroy, D.M., Sabroe, I., Pritchard, D.I. and Williams, T.J., 2000. Eotaxin is specifically cleaved by hookworm metalloproteases preventing its action in vitro and in vivo. *The Journal of Immunology*, *165*(11), pp.6447-6453.
164. Ranjit, N., Zhan, B., Hamilton, B., Stenzel, D., Lowther, J., Pearson, M., Gorman, J., Hotez, P. and Loukas, A., 2009. Proteolytic degradation of hemoglobin in the intestine of the human hookworm Necator americanus. *The Journal of infectious diseases*, *199*(6), pp.904-912.
165. Caffrey, C.R., Goupil, L., Rebello, K.M., Dalton, J.P. and Smith, D., 2018. Cysteine proteases as digestive enzymes in parasitic helminths. *PLoS neglected tropical diseases*, *12*(8), p.e0005840.
166. KUMAR, S. and PRITCHARD, D.I., 1992. Distinction of human hookworm larvae based on lectin-binding characteristics. *Parasite immunology*, *14*(2), pp.233-237.
167. Chieppa, M., Bianchi, G., Doni, A., Del Prete, A., Sironi, M., Laskarin, G., Monti, P., Piemonti, L., Biondi, A., Mantovani, A. and Introna, M., 2003. Cross-linking of the mannose receptor on monocyte-derived dendritic cells activates an anti-inflammatory immunosuppressive program. *The Journal of Immunology*, *171*(9), pp.4552-4560.
168. Geijtenbeek, T.B., Van Vliet, S.J., Koppel, E.A., Sanchez-Hernandez, M., Vandenbroucke-Grauls, C.M., Appelmelk, B. and Van Kooyk, Y., 2003. Mycobacteria target DC-SIGN to suppress dendritic cell function. *The Journal of experimental medicine*, *197*(1), pp.7-17.
169. Bergman, M.P., Engering, A., Smits, H.H., Van Vliet, S.J., Van Bodegraven, A.A., Wirth, H.P., Kapsenberg, M.L., Vandenbroucke-Grauls, C.M., Van Kooyk, Y. and Appelmelk, B.J., 2004. Helicobacter

pylori modulates the T helper cell 1/T helper cell 2 balance through phase-variable interaction between lipopolysaccharide and DC-SIGN. *Journal of Experimental Medicine*, *200*(8), pp.979-990.

170. Van Kooyk, Y. and Rabinovich, G.A., 2008. Protein-glycan interactions in the control of innate and adaptive immune responses. *Nature immunology*, *9*(6), pp.593-601.
171. Meyer-Wentrup, F., Cambi, A., Joosten, B., Looman, M.W., de Vries, I.J.M., Figdor, C.G. and Adema, G.J., 2009. DCIR is endocytosed into human dendritic cells and inhibits TLR8-mediated cytokine production. *Journal of leukocyte biology*, *85*(3), pp.518-525.
172. World Health Organization, 2006. *Preventive chemotherapy in human helminthiasis. Coordinated use of anthelminthic drugs in control interventions: a manual for health professionals and programme managers*. World Health Organization.
173. Keiser, J. and Utzinger, J., 2008. Efficacy of current drugs against soil-transmitted helminth infections: systematic review and meta-analysis. *Jama*, *299*(16), pp.1937-1948.
174. Xiao, S.H., Hui-Ming, W., Tanner, M., Utzinger, J. and Chong, W., 2005. Tribendimidine: a promising, safe and broad-spectrum anthelmintic agent from China. *Acta tropica*, *94*(1), pp.1-14.
175. Wu, Z.X., Fang, Y.Y. and Liu, Y.S., 2006. Effect of a novel drug--enteric coated tribendimidine in the treatment of intestinal nematode infections. *Zhongguo ji sheng chong xue yu ji sheng chong bing za zhi= Chinese journal of parasitology & parasitic diseases*, *24*(1), pp.23-26.
176. Cline, B.L., Little, M.D., Bartholomew, R.K. and Halsey, N.A., 1984. Larvicidal activity of albendazole against Necator americanus in human volunteers. *The American journal of tropical medicine and hygiene*, *33*(3), pp.387-394.
177. Albonico, M., Ramsan, M., Wright, V., Jape, K., Haji, H.J., Taylor, M., Savioli, L. and Bickle, Q., 2002. Soil-transmitted nematode infections and mebendazole treatment in Mafia Island schoolchildren. *Annals of Tropical Medicine & Parasitology*, *96*(7), pp.717-726.
178. Albonico, M., Bickle, Q., Ramsan, M., Montresor, A., Savioli, L. and Taylor, M., 2003. Efficacy of mebendazole and levamisole alone or in combination against intestinal nematode infections after repeated targeted mebendazole treatment in Zanzibar. *Bulletin of the World Health Organization*, *81*, pp.343-352.
179. Horton, J., 2003. Human gastrointestinal helminth infections: are they now neglected diseases?. *Trends in parasitology*, *19*(11), pp.527-531.
180. Quinnell, R.J., Slater, A.F.G., Tighe, P., Walsh, E.A., Keymer, A.E. and Pritchard, D.I., 1993. Reinfection with hookworm after chemotherapy in Papua New Guinea. *Parasitology*, *106*(4), pp.379-385.
181. Albonico, M., Smith, P.G., Ercole, E., Hall, A., Chwaya, H.M., Alawi, K.S. and Savioli, L., 1995. Rate of reinfection with intestinal nematodes after treatment of children with mebendazole or albendazole in a highly endemic area. *Transactions of the Royal Society of Tropical Medicine and Hygiene*, *89*(5), pp.538-541.
182. McSorley, H.J. and Loukas, A., 2010. The immunology of human hookworm infections. *Parasite immunology*, *32*(8), pp.549-559.

183. Navarro, S., Ferreira, I. and Loukas, A., 2013. The hookworm pharmacopoeia for inflammatory diseases. *International journal for parasitology*, *43*(3-4), pp.225-231.
184. Weinstock, J.V. and Elliott, D.E., 2009. Helminths and the IBD hygiene hypothesis. *Inflammatory bowel diseases*, *15*(1), pp.128-133.
185. Altmann, D.M., 2009. Review series on helminths, immune modulation and the hygiene hypothesis: nematode coevolution with adaptive immunity, regulatory networks and the growth of inflammatory diseases. *Immunology*, *126*(1), p.1.
186. Jackson, J.A., Friberg, I.M., Little, S. and Bradley, J.E., 2009. Review series on helminths, immune modulation and the hygiene hypothesis: immunity against helminths and immunological phenomena in modern human populations: coevolutionary legacies?. *Immunology*, *126*(1), pp.18-27.
187. Gaze, S.T., 2016. Experimental human hookworm infection: therapeutic potential. *Reports in Parasitology*, *5*, pp.35-41.
188. Palmer, E.D., 1955. Course of Egg Output Over a 15 Year Period in a Case of experimentally induced Neoatoriasis amerioanus, in the absenoe of Hyperinfection. *American Journal of Tropical Medicine and Hygiene*, *4*(4), pp.756-7.
189. Mortimer, K., Brown, A., Feary, J., Jagger, C., Lewis, S., Antoniak, M., Pritchard, D. and Britton, J., 2006. Dose-ranging study for trials of therapeutic infection with Necator americanus in humans. *The American journal of tropical medicine and hygiene*, *75*(5), pp.914-920.
190. Blount, D., Hooi, D., Feary, J., Venn, A., Telford, G., Brown, A., Britton, J. and Pritchard, D., 2009. Immunologic profiles of persons recruited for a randomized, placebo-controlled clinical trial of hookworm infection. *The American journal of tropical medicine and hygiene*, *81*(5), pp.911-916.
191. Feary, J.R., Venn, A.J., Mortimer, K., Brown, A.P., Hooi, D., Falcone, F.H., Pritchard, D.I. and Britton, J.R., 2010. Experimental hookworm infection: a randomized placebo-controlled trial in asthma. *Clinical & Experimental Allergy*, *40*(2), pp.299-306.
192. Croese, J., O'neil, J., Masson, J., Cooke, S., Melrose, W., Pritchard, D. and Speare, R., 2006. A proof of concept study establishing Necator americanus in Crohn's patients and reservoir donors. *Gut*, *55*(1), pp.136-137.
193. Moore, J.K., West, S.R. and Robins, G., 2011. Advances in celiac disease. *Current opinion in gastroenterology*, *27*(2), pp.112-118.
194. McSorley, H.J., Gaze, S., Daveson, J., Jones, D., Anderson, R.P., Clouston, A., Ruyssers, N.E., Speare, R., McCarthy, J.S., Engwerda, C.R. and Croese, J., 2011. Suppression of inflammatory immune responses in celiac disease by experimental hookworm infection. *PloS one*, *6*(9), p.e24092.
195. Correale, J., 2014. Helminth/Parasite treatment of multiple sclerosis. *Current treatment options in neurology*, *16*(6), pp.1-12.
196. Smallwood, T.B., Giacomin, P.R., Loukas, A., Mulvenna, J.P., Clark, R.J. and Miles, J.J., 2017. Helminth immunomodulation in autoimmune disease. *Frontiers in immunology*, *8*, p.453.

197. Correale, J. and Farez, M., 2007. Association between parasite infection and immune responses in multiple sclerosis. *Annals of Neurology: Official Journal of the American Neurological Association and the Child Neurology Society*, *61*(2), pp.97-108.
198. Kassai, T., 1982. Handbook of Nippostrongylus brasiliensis (nematode). *Handbook of Nippostrongylus brasiliensis (nematode).*
199. Nair, M.G. and Herbert, D.B.R., 2016. Immune polarization by hookworms: taking cues from T helper type 2, type 2 innate lymphoid cells and alternatively activated macrophages. *Immunology*, *148*(2), pp.115-124.
200. Ogilvie, B.M. and Jones, V.E., 1971. Nippostrongylus brasiliensis: a review of immunity and the host/parasite relationship in the rat. *Experimental parasitology*, *29*(1), pp.138-177.
201. Hassan, A., Pritchard, D.I. and Ghaemmaghami, A.M., 2018. Human dendritic cell sequestration onto the Necator americanus larval sheath during ex-sheathing: a possible mechanism for immune privilege. *Parasitology*, *145*(9), pp.1183-1190
202. Camberis, M., Le Gros, G. and Urban Jr, J., 2003. Animal model of Nippostrongylus brasiliensis and Heligmosomoides polygyrus. *Current protocols in immunology*, *55*(1), pp.19-12.
203. Awuah, D., Alobaid, M., Latif, A., Salazar, F., Emes, R.D. and Ghaemmaghami, A.M., 2019. The cross-talk between miR-511-3p and C-type lectin receptors on dendritic cells affects dendritic cell function. *The Journal of Immunology*, *203*(1), pp.148-157.
204. Trindade, G.F., Abel, M.L. and Watts, J.F., 2018. simsMVA: A tool for multivariate analysis of ToF-SIMS datasets. *Chemometrics and Intelligent Laboratory Systems*, *182*, pp.180-187.
205. Kawecki, M. and Bernard, L., 2018. Database of proteinogenic amino acid reference spectra for Bismuth-cluster ToF-SIMS. I. Negative polarity. *Surface Science Spectra*, *25*(1), p.015001.
206. Bernard, L., Crockett, R. and Kawecki, M., 2019. Monosaccharides: A ToF-SIMS reference spectra database. I. Negative polarity. *Surface Science Spectra*, *26*(2), p.025001.
207. Scurr, D.J., Horlacher, T., Oberli, M.A., Werz, D.B., Kroeck, L., Bufali, S., Seeberger, P.H., Shard, A.G. and Alexander, M.R., 2010. Surface characterization of carbohydrate microarrays. *Langmuir*, *26*(22), pp.17143-17155.
208. Pearson, M.S., Tribolet, L., Cantacessi, C., Periago, M.V., Valerio, M.A., Jariwala, A.R., Hotez, P., Diemert, D., Loukas, A. and Bethony, J., 2012. Molecular mechanisms of hookworm disease: stealth, virulence, and vaccines. *Journal of allergy and clinical immunology*, *130*(1), pp.13-21.
209. Albonico, M., Engels, D. and Savioli, L., 2004. Monitoring drug efficacy and early detection of drug resistance in human soil-transmitted nematodes: a pressing public health agenda for helminth control. *International journal for parasitology*, *34*(11), pp.1205-1210.
210. Pasuralertsakul, S. and Ngrenngarmlert, W., 2006. The exsheathment of Necator americanus infective larvae. *Southeast Asian journal of tropical medicine and public health*, *37*, p.28.

211. Huang, S.C.C., Chan, D.T.Y., Smyth, D.J., Ball, G., Gounaris, K. and Selkirk, M.E., 2010. Activation of Nippostrongylus brasiliensis infective larvae is regulated by a pathway distinct from the hookworm Ancylostoma caninum. *International journal for parasitology*, *40*(14), pp.1619-1628.
212. Agrawal, S., Gupta, S. and Agrawal, A., 2010. Human dendritic cells activated via dectin-1 are efficient at priming Th17, cytotoxic CD8 T and B cell responses. *PloS one*, *5*(10), p.e13418.
213. Ronchese, F., Hilligan, K.L. and Mayer, J.U., 2020. Dendritic cells and the skin environment. *Current opinion in immunology*, *64*, pp.56-62.
214. Lumb, F.E., Doonan, J., Bell, K.S., Pineda, M.A., Corbet, M., Suckling, C.J., Harnett, M.M. and Harnett, W., 2017. Dendritic cells provide a therapeutic target for synthetic small molecule analogues of the parasitic worm product, ES-62. *Scientific reports*, *7*(1), pp.1-13.
215. Chauhan, V.M., Scurr, D.J., Christie, T., Telford, G., Aylott, J.W. and Pritchard, D.I., 2017. The physicochemical fingerprint of Necator americanus. *PLoS neglected tropical diseases*, *11*(12), p.e0005971.
216. Bajolet-Laudinat, O., Girod-de Bentzmann, S., Tournier, J.M., Madoulet, C., Plotkowski, M.C., Chippaux, C. and Puchelle, E., 1994. Cytotoxicity of Pseudomonas aeruginosa internal lectin PA-I to respiratory epithelial cells in primary culture. *Infection and immunity*, *62*(10), pp.4481-4487.
217. Numata, M., Kandasamy, P., Nagashima, Y., Fickes, R., Murphy, R.C. and Voelker, D.R., 2015. Phosphatidylinositol inhibits respiratory syncytial virus infection. *Journal of lipid research*, *56*(3), pp.578-587.
218. Kumar, S. and Pritchard, D.I., 1992. The partial characterization of proteases present in the excretory/secretory products and exsheathing fluid of the infective (L3) larva of Necator americanus. *International journal for parasitology*, *22*(5), pp.563-572.
219. Baba, T., Yoshida, T., Yoshida, T. and Cohen, S., 1979. Suppression of cell-mediated immune reactions by monosaccharides. *The Journal of Immunology*, *122*(3), pp.838-841.
220. Moran, A.P., 2008. Relevance of fucosylation and Lewis antigen expression in the bacterial gastroduodenal pathogen Helicobacter pylori. *Carbohydrate research*, *343*(12), pp.1952-1965.
221. Rodríguez, E., Kalay, H., Noya, V., Brossard, N., Giacomini, C., van Kooyk, Y., García-Vallejo, J.J. and Freire, T., 2017. Fasciola hepatica glycoconjugates immuneregulate dendritic cells through the Dendritic Cell-Specific Intercellular adhesion molecule-3-Grabbing Non-integrin inducing T cell anergy. *Scientific reports*, *7*(1), pp.1-10.
222. Kim, T.H., Hwang, S.B., Jeong, P.Y., Lee, J. and Cho, J.W., 2005. Requirement of tyrosylprotein sulfotransferase-A for proper cuticle formation in the nematode C. elegans. *FEBS letters*, *579*(1), pp.53-58.
223. Bao, X., Moseman, E.A., Saito, H., Petryanik, B., Thiriot, A., Hatakeyama, S., Ito, Y., Kawashima, H., Yamaguchi, Y., Lowe, J.B. and von Andrian, U.H., 2010. Endothelial heparan sulfate controls chemokine

presentation in recruitment of lymphocytes and dendritic cells to lymph nodes. *Immunity*, *33*(5), pp.817-829.

224. Steinman, R.M. and Banchereau, J., 2007. Taking dendritic cells into medicine. *Nature*, *449*(7161), pp.419-426.
225. Guermonprez, P., Valladeau, J., Zitvogel, L., Théry, C. and Amigorena, S., 2002. Antigen presentation and T cell stimulation by dendritic cells. *Annual review of immunology*, *20*(1), pp.621-667.
226. Merad, M., Sathe, P., Helft, J., Miller, J. and Mortha, A., 2013. The dendritic cell lineage: ontogeny and function of dendritic cells and their subsets in the steady state and the inflamed setting. *Annual review of immunology*, *31*, pp.563-604.
227. Savina, A. and Amigorena, S., 2007. Phagocytosis and antigen presentation in dendritic cells. *Immunological reviews*, *219*(1), pp.143-156.
228. Keir, M.E., Francisco, L.M. and Sharpe, A.H., 2007. PD-1 and its ligands in T-cell immunity. *Current opinion in immunology*, *19*(3), pp.309-314.
229. Höpken, U.E., Lehmann, I., Droese, J., Lipp, M., Schüler, T. and Rehm, A., 2005. The ratio between dendritic cells and T cells determines the outcome of their encounter: proliferation versus deletion. *European journal of immunology*, *35*(10), pp.2851-2863.
230. Sittig, S.P., Bakdash, G., Weiden, J., Sköld, A.E., Tel, J., Figdor, C.G., de Vries, I.J.M. and Schreibelt, G., 2016. A comparative study of the T cell stimulatory and polarizing capacity of human primary blood dendritic cell subsets. *Mediators of inflammation*, *2016*.
231. Curato, C., Bernshtein, B., Zupancič, E., Dufner, A., Jaitin, D., Giladi, A., David, E., Chappell-Maor, L., Leshkowitz, D., Knobeloch, K.P. and Amit, I., 2019. DC respond to cognate T cell interaction in the antigen-challenged lymph node. *Frontiers in immunology*, *10*, p.863.
232. Kim, B. and Kim, T.H., 2018. Fundamental role of dendritic cells in inducing Th2 responses. *The Korean journal of internal medicine*, *33*(3), p.483.
233. Kumar, S., Jeong, Y., Ashraf, M.U. and Bae, Y.S., 2019. Dendritic cell-mediated Th2 immunity and immune disorders. *International journal of molecular sciences*, *20*(9), p.2159.
234. Na, H., Cho, M. and Chung, Y., 2016. Regulation of Th2 cell immunity by dendritic cells. *Immune network*, *16*(1), pp.1-12.
235. Salazar, F., Sewell, H.F., Shakib, F. and Ghaemmaghami, A.M., 2013. The role of lectins in allergic sensitization and allergic disease. *Journal of allergy and clinical immunology*, *132*(1), pp.27-36.
236. Singh, S., Almuhanna, Y., Alshahrani, M.Y., Lowman, D.W., Rice, P.J., Gell, C., Ma, Z., Graves, B., Jackson, D., Lee, K. and Juarez, R., 2021. Carbohydrates from Pseudomonas aeruginosa biofilms interact with immune C-type lectins and interfere with their receptor function. *npj Biofilms and Microbiomes*, *7*(1), pp.1-14.
237. Drickamer, K., 1999. C-type lectin-like domains. *Current opinion in structural biology*, *9*(5), pp.585-590.

238. Poget, S.F., Legge, G.B., Proctor, M.R., Butler, P.J.G., Bycroft, M. and Williams, R.L., 1999. The structure of a tunicate C-type lectin from Polyandrocarpa misakiensis complexed with D-galactose. *Journal of molecular biology*, *290*(4), pp.867-879.
239. Kolatkar, A.R., Leung, A.K., Isecke, R., Brossmer, R., Drickamer, K. and Weis, W.I., 1998. Mechanism of N-acetylgalactosamine binding to a C-type animal lectin carbohydrate-recognition domain. *Journal of Biological Chemistry*, *273*(31), pp.19502-19508.
240. Kolatkar, A.R. and Weis, W.I., 1996. Structural Basis of Galactose Recognition by C-type Animal Lectins (∗). *Journal of Biological Chemistry*, *271*(12), pp.6679-6685.
241. Engering, A., Geijtenbeek, T.B., van Vliet, S.J., Wijers, M., van Liempt, E., Demaurex, N., Lanzavecchia, A., Fransen, J., Figdor, C.G., Piguet, V. and van Kooyk, Y., 2002. The dendritic cell-specific adhesion receptor DC-SIGN internalizes antigen for presentation to T cells. *The Journal of Immunology*, *168*(5), pp.2118-2126
242. Martínez, J.D., Valverde, P., Delgado, S., Romanò, C., Linclau, B., Reichardt, N.C., Oscarson, S., Ardá, A. and Jiménez-Barbero, J., 2019. Unraveling sugar binding modes to DC-SIGN by employing fluorinated carbohydrates. *Molecules*, *24*(12), p.2337.
243. Schmidt, S.K., Ebel, S., Keil, E., Woite, C., Ernst, J.F., Benzin, A.E., Rupp, J. and Däubener, W., 2013. Regulation of IDO activity by oxygen supply: inhibitory effects on antimicrobial and immunoregulatory functions. *PloS one*, *8*(5), p.e63301.
244. Salazar, F., Hall, L., Negm, O.H., Awuah, D., Tighe, P.J., Shakib, F. and Ghaemmaghami, A.M., 2016. The mannose receptor negatively modulates the Toll-like receptor 4–aryl hydrocarbon receptor–indoleamine 2, 3-dioxygenase axis in dendritic cells affecting T helper cell polarization. *Journal of Allergy and Clinical Immunology*, *137*(6), pp.1841-1851.
245. Gupta, S.L., Carlin, J.M., Pyati, P., Dai, W., Pfefferkorn, E.R. and Murphy Jr, M.J., 1994. Antiparasitic and antiproliferative effects of indoleamine 2, 3-dioxygenase enzyme expression in human fibroblasts. *Infection and immunity*, *62*(6), pp.2277-2284.
246. MacKenzie, C.R., Hadding, U. and Däubener, W., 1998. Interferon-γ-induced activation of indoleamine 2, 3-dioxygenase in cord blood monocyte-derived macrophages inhibits the growth of group B streptococci. *Journal of Infectious Diseases*, *178*(3), pp.875-878.
247. Nigou, J., Zelle-Rieser, C., Gilleron, M., Thurnher, M. and Puzo, G., 2001. Mannosylated lipoarabinomannans inhibit IL-12 production by human dendritic cells: evidence for a negative signal delivered through the mannose receptor. *The Journal of Immunology*, *166*(12), pp.7477-7485.
248. Hong, P.W.P., Nguyen, S., Young, S., Su, S.V. and Lee, B., 2007. Identification of the optimal DC-SIGN binding site on human immunodeficiency virus type 1 gp120. *Journal of virology*, *81*(15), pp.8325-8336.
249. Hirbod, T., Bailey, R.C., Agot, K., Moses, S., Ndinya-Achola, J., Murugu, R., Andersson, J., Nilsson, J. and Broliden, K., 2010. Abundant expression of HIV target cells and C-type lectin receptors in the foreskin tissue of young Kenyan men. *The American journal of pathology*, *176*(6), pp.2798-2805.

250. Terrazas, C.A., Terrazas, L.I. and Gómez-García, L., 2010. Modulation of dendritic cell responses by parasites: a common strategy to survive. *Journal of Biomedicine and Biotechnology*, *2010*.
251. Kruse, M., Meinl, E., Henning, G., Kuhnt, C., Berchtold, S., Berger, T., Schuler, G. and Steinkasserer, A., 2001. Signaling lymphocytic activation molecule is expressed on mature CD83+ dendritic cells and is up-regulated by IL-1β. *The Journal of Immunology*, *167*(4), pp.1989-1995.
252. Elgueta, R., Benson, M.J., De Vries, V.C., Wasiuk, A., Guo, Y. and Noelle, R.J., 2009. Molecular mechanism and function of CD40/CD40L engagement in the immune system. *Immunological reviews*, *229*(1), pp.152-172.
253. Vasilevko, V., Ghochikyan, A., Holterman, M.J. and Agadjanyan, M.G., 2002. CD80 (B7-1) and CD86 (B7-2) are functionally equivalent in the initiation and maintenance of CD4+ T-cell proliferation after activation with suboptimal doses of PHA. *DNA and cell biology*, *21*(3), pp.137-149.
254. McLellan, A.D., Heiser, A. and Hart, D.N.J., 1999. Induction of dendritic cell costimulator molecule expression is suppressed by T cells in the absence of antigen-specific signalling: role of cluster formation, CD40 and HLA-class II for dendritic cell activation. *Immunology*, *98*(2), p.171.
255. Blanco, P., Palucka, A.K., Pascual, V. and Banchereau, J., 2008. Dendritic cells and cytokines in human inflammatory and autoimmune diseases. *Cytokine & growth factor reviews*, *19*(1), pp.41-52.
256. Couper, K.N., Blount, D.G. and Riley, E.M., 2008. IL-10: the master regulator of immunity to infection. *The Journal of Immunology*, *180*(9), pp.5771-5777.
257. Miro, F., Nobile, C., Blanchard, N., Lind, M., Filipe-Santos, O., Fieschi, C., Chapgier, A., Vogt, G., de Beaucoudrey, L., Kumararatne, D.S. and Le Deist, F., 2006. T cell-dependent activation of dendritic cells requires IL-12 and IFN-γ signaling in T cells. *The Journal of Immunology*, *177*(6), pp.3625-3634.
258. Royer, P.J., Emara, M., Yang, C., Al-Ghouleh, A., Tighe, P., Jones, N., Sewell, H.F., Shakib, F., Martinez-Pomares, L. and Ghaemmaghami, A.M., 2010. The mannose receptor mediates the uptake of diverse native allergens by dendritic cells and determines allergen-induced T cell polarization through modulation of IDO activity. *The Journal of Immunology*, *185*(3), pp.1522-1531.
259. tan Deslée, G., Charbonnier, A.S., Hammad, H., Angyalosi, G., Tillie-Leblond, I., Mantovani, A. and Pestel, J., 2002. Involvement of the mannose receptor in the uptake of Der p 1, a major mite allergen, by human dendritic cells. *Journal of Allergy and Clinical Immunology*, *110*(5), pp.763-770.
260. Emara, M., Royer, P.J., Mahdavi, J., Shakib, F. and Ghaemmaghami, A.M., 2012. Retagging identifies dendritic cell-specific intercellular adhesion molecule-3 (ICAM3)-grabbing non-integrin (DC-SIGN) protein as a novel receptor for a major allergen from house dust mite. *Journal of Biological Chemistry*, *287*(8), pp.5756-5763.
261. Harden, J.L. and Egilmez, N.K., 2012. Indoleamine 2, 3-dioxygenase and dendritic cell tolerogenicity. *Immunological investigations*, *41*(6-7), pp.738-764.
262. Munn, D.H. and Mellor, A.L., 2013. Indoleamine 2, 3 dioxygenase and metabolic control of immune responses. *Trends in immunology*, *34*(3), pp.137-143.

263. Brenk, M., Scheler, M., Koch, S., Neumann, J., Takikawa, O., Häcker, G., Bieber, T. and von Bubnoff, D., 2009. Tryptophan deprivation induces inhibitory receptors ILT3 and ILT4 on dendritic cells favoring the induction of human CD4+ CD25+ Foxp3+ T regulatory cells. *The Journal of Immunology*, *183*(1), pp.145-154.
264. Hoshi, M., Saito, K., Hara, A., Taguchi, A., Ohtaki, H., Tanaka, R., Fujigaki, H., Osawa, Y., Takemura, M., Matsunami, H. and Ito, H., 2010. The absence of IDO upregulates type I IFN production, resulting in suppression of viral replication in the retrovirus-infected mouse. *The Journal of Immunology*, *185*(6), pp.3305-3312.
265. Terness, P., Bauer, T.M., Röse, L., Dufter, C., Watzlik, A., Simon, H. and Opelz, G., 2002. Inhibition of allogeneic T cell proliferation by indoleamine 2, 3-dioxygenase–expressing dendritic cells: mediation of suppression by tryptophan metabolites. *The Journal of experimental medicine*, *196*(4), pp.447-457.
266. Van Vliet, S.J., den Dunnen, J., Gringhuis, S.I., Geijtenbeek, T.B. and van Kooyk, Y., 2007. Innate signaling and regulation of dendritic cell immunity. *Current opinion in immunology*, *19*(4), pp.435-440.
267. Zahorchak, A.F., Macedo, C., Hamm, D.E., Butterfield, L.H., Metes, D.M. and Thomson, A.W., 2018. High PD-L1/CD86 MFI ratio and IL-10 secretion characterize human regulatory dendritic cells generated for clinical testing in organ transplantation. *Cellular immunology*, *323*, pp.9-18.
268. Unger, W.W., Laban, S., Kleijwegt, F.S., van der Slik, A.R. and Roep, B.O., 2009. Induction of Treg by monocyte-derived DC modulated by vitamin D3 or dexamethasone: differential role for PD-L1. *European journal of immunology*, *39*(11), pp.3147-3159.
269. Kushwah, R. and Hu, J., 2011. Role of dendritic cells in the induction of regulatory T cells. *Cell & bioscience*, *1*(1), pp.1-10.
270. Matoso, R.R.C.D.M., Geiger, S.M., Correa-Oliveira, R., Gazzinelli, A., Bartholomeu, D.C. and Fujiwara, R.T., 2011. Induction of CD4 CD25 FOXP3 Regulatory T Cells during Human Hookworm Infection Modulates Antigen-Mediated Lymphocyte Proliferation.
271. Ricci, N.D., Fiúza, J.A., Bueno, L.L., Cançado, G.G.L., Gazzinelli-Guimarães, P.H., Martins, V.G., Matoso, L.F., Miranda, R.R.C.D., Geiger, S.M., Correa-Oliveira, R. and Gazzinelli, A., 2011. Induction of CD4+ CD25+ FOXP3+ regulatory T cells during human hookworm infection modulates antigen-mediated lymphocyte proliferation. *PLoS neglected tropical diseases*, *5*(11), p.e1383.
272. Pirro, M., Schoof, E., van Vliet, S.J., Rombouts, Y., Stella, A., de Ru, A., Mohammed, Y., Wuhrer, M., van Veelen, P.A. and Hensbergen, P.J., 2018. Glycoproteomic analysis of MGL-binding proteins on acute T-cell leukemia cells. *Journal of proteome research*, *18*(3), pp.1125-1132.
273. Maizels, R.M., Bundy, D.A., Selkirk, M.E., Smith, D.F. and Anderson, R.M., 1993. Immunological modulation and evasion by helminth parasites in human populations. *Nature*, *365*(6449), pp.797-805.
274. Gershon, R.K. and Kondo, K., 1971. Infectious immunological tolerance. *Immunology*, *21*(6), p.903.
275. Gershon, R.K. and Kondo, K., 1970. Cell interactions in the induction of tolerance: the role of thymic lymphocytes. *Immunology*, *18*(5), p.723.

276. Hsieh, G.C.F., Loukas, A., Wahl, A.M., Bhatia, M., Wang, Y., Williamson, A.L., Kehn, K.W., Maruyama, H., Hotez, P.J., Leitenberg, D. and Bethony, J., 2004. A secreted protein from the human hookworm Necator americanus binds selectively to NK cells and induces IFN-γ production. *The Journal of Immunology*, *173*(4), pp.2699-2704
277. van Kooyk, Y., Engering, A., Lekkerkerker, A.N., Ludwig, I.S. and Geijtenbeek, T.B., 2004. Pathogens use carbohydrates to escape immunity induced by dendritic cells. *Current opinion in immunology*, *16*(4), pp.488-493.
278. Schabussova, I., Amer, H., van Die, I., Kosma, P. and Maizels, R.M., 2007. O-methylated glycans from Toxocara are specific targets for antibody binding in human and animal infections. *International journal for parasitology*, *37*(1), pp.97-109
279. van Die, I., van Vliet, S.J., Nyame, A.K., Cummings, R.D., Bank, C.M., Appelmelk, B., Geijtenbeek, T.B. and van Kooyk, Y., 2003. The dendritic cell–specific C-type lectin DC-SIGN is a receptor for Schistosoma mansoni egg antigens and recognizes the glycan antigen Lewis x. *Glycobiology*, *13*(6), pp.471-478.
280. Loukas, A. and Maizels, R.M., 2000. Helminth C-type lectins and host–parasite interactions. *Parasitology Today*, *16*(8), pp.333-339
281. Salazar, F., Hall, L., Negm, O.H., Awuah, D., Tighe, P.J., Shakib, F. and Ghaemmaghami, A.M., 2016. The mannose receptor negatively modulates the Toll-like receptor 4–aryl hydrocarbon receptor–indoleamine 2, 3-dioxygenase axis in dendritic cells affecting T helper cell polarization. *Journal of Allergy and Clinical Immunology*, *137*(6), pp.1841-1851
282. Wang, J., Roderiquez, G. and Norcross, M.A., 2012. Control of Adaptive Immune Responses by Staphylococcus aureus through IL-10, PD-L1 and TLR2. *Scientific reports*, *2*(1), pp.1-11.
283. Liu, H., Bakthavatsalam, R., Meng, Z., Li, Z., Li, W., Perkins, J.D. and Reyes, J., 2013, June. PD-L1 signal on liver dendritic cells is critical for Foxp3+ CD4+ CD25+ Treg and liver tolerance induction in mice. In *Transplantation proceedings* (Vol. 45, No. 5, pp. 1853-1855). Elsevier.
284. Schülke, S., 2018. Induction of interleukin-10 producing dendritic cells as a tool to suppress allergen-specific T helper 2 responses. *Frontiers in immunology*, *9*, p.455.
285. Jonuleit, H., Schmitt, E., Steinbrink, K. and Enk, A.H., 2001. Dendritic cells as a tool to induce anergic and regulatory T cells. *Trends in immunology*, *22*(7), pp.394-400.
286. Richmond, J.M., Lee, J., Green, D.S., Kornfeld, H. and Cruikshank, W.W., 2012. Mannose-capped lipoarabinomannan from Mycobacterium tuberculosis preferentially inhibits sphingosine-1-Phosphate–induced migration of Th1 cells. *The Journal of Immunology*, *189*(12), pp.5886-5895.
287. Gringhuis, S.I., Kaptein, T.M., Wevers, B.A., Mesman, A.W. and Geijtenbeek, T.B., 2014. Fucose-specific DC-SIGN signalling directs T helper cell type-2 responses via IKKε-and CYLD-dependent Bcl3 activation. *Nature communications*, *5*(1), pp.1-13.
288. van Liempt, E., van Vliet, S.J., Engering, A., Vallejo, J.J.G., Bank, C.M., Sanchez-Hernandez, M., van Kooyk, Y. and van Die, I., 2007. Schistosoma mansoni soluble egg antigens are internalized by human

dendritic cells through multiple C-type lectins and suppress TLR-induced dendritic cell activation. *Molecular immunology*, *44*(10), pp.2605-2615.

289. Khoo, K.H. and Dell, A., 2001. Glycoconjugates from parasitic helminths: structure diversity and immunobiological implications. *The Molecular Immunology of Complex Carbohydrates—2*, pp.185-205.
290. Cummings, R.D. and Nyame, A.K., 1996. Glycobiology of schistosomiasis. *The FASEB journal*, *10*(8), pp.838-848.
291. Pallesen, L.T., Pedersen, L.R.L., Petersen, T.E. and Rasmussen, J.T., 2007. Characterization of carbohydrate structures of bovine MUC15 and distribution of the mucin in bovine milk. *Journal of dairy science*, *90*(7), pp.3143-3152.
292. Waespy, M., Gbem, T.T., Elenschneider, L., Jeck, A.P., Day, C.J., Hartley-Tassell, L., Bovin, N., Tiralongo, J., Haselhorst, T. and Kelm, S., 2015. Carbohydrate recognition specificity of trans-sialidase lectin domain from Trypanosoma congolense. *PLoS neglected tropical diseases*, *9*(10), p.e0004120.
293. Houser, J., Komarek, J., Kostlanova, N., Cioci, G., Varrot, A., Kerr, S.C., Lahmann, M., Balloy, V., Fahy, J.V., Chignard, M. and Imberty, A., 2013. A soluble fucose-specific lectin from Aspergillus fumigatus conidia-structure, specificity and possible role in fungal pathogenicity. *PloS one*, *8*(12), p.e83077.
294. McSorley, H.J., Harcus, Y.M., Murray, J., Taylor, M.D. and Maizels, R.M., 2008. Expansion of Foxp3+ regulatory T cells in mice infected with the filarial parasite Brugia malayi. *The Journal of Immunology*, *181*(9), pp.6456-6466
295. Frederick, J.R. and Petri Jr, W.A., 2005. Roles for the galactose-/N-acetylgalactosamine-binding lectin of Entamoeba in parasite virulence and differentiation. *Glycobiology*, *15*(12), pp.53R-59R.
296. Silber, A.M., Marcipar, I.S., Roodveldt, C., Meckert, P.C., Laguens, R. and Marcipar, A.J., 2002. Trypanosoma cruzi: identification of a galactose-binding protein that binds to cell surface of human erythrocytes and is involved in cell invasion by the parasite. *Experimental parasitology*, *100*(4), pp.217-225.
297. Belkaid, Y., 2003. The role of CD4+ CD25+ regulatory T cells in Leishmania infection. *Expert opinion on biological therapy*, *3*(6), pp.875-885.
298. Lam, S.K. and Ng, T.B., 2011. Lectins: production and practical applications. *Applied microbiology and biotechnology*, *89*(1), pp.45-55.
299. Hollmig, S.T., Ariizumi, K. and Cruz Jr, P.D., 2009. Recognition of non-self-polysaccharides by C-type lectin receptors dectin-1 and dectin-2. *Glycobiology*, *19*(6), pp.568-575.
300. Kerrigan, A.M. and Brown, G.D., 2009. C-type lectins and phagocytosis. *Immunobiology*, *214*(7), pp.562-575.
301. Szczykutowicz, J., Tkaczuk-Włach, J. and Ferens-Sieczkowska, M., 2021. Glycoproteins Presenting Galactose and N-Acetylgalactosamine in Human Seminal Plasma as Potential Players Involved in Immune Modulation in the Fertilization Process. *International journal of molecular sciences*, *22*(14), p.7331.

302. Alobaid, M.A., Richards, S.J., Alexander, M.R., Gibson, M.I. and Ghaemmaghami, A.M., 2020. Developing immune-regulatory materials using immobilized monosaccharides with immune-instructive properties. *Materials Today Bio*, *8*, p.100080.
303. Hamilton, C.M., Dowling, D.J., Loscher, C.E., Morphew, R.M., Brophy, P.M. and O'Neill, S.M., 2009. The Fasciola hepatica tegumental antigen suppresses dendritic cell maturation and function. *Infection and immunity*, *77*(6), pp.2488-2498.
304. Versini, M., Jeandel, P.Y., Bashi, T., Bizzaro, G., Blank, M. and Shoenfeld, Y., 2015. Unraveling the hygiene hypothesis of helminthes and autoimmunity: origins, pathophysiology, and clinical applications. *BMC medicine*, *13*(1), pp.1-16.
305. Rodgers, D.T., McGrath, M.A., Pineda, M.A., Al-Riyami, L., Rzepecka, J., Lumb, F., Harnett, W. and Harnett, M.M., 2015. The parasitic worm product, ES-62 targets MyD88-dependent effector mechanisms to suppress ANA production and proteinuria in MRL/Lpr mice. *Arthritis and Rheumatology*, *67*(4), pp.1023-1035.
306. Wu, Z., Wang, L., Tang, Y. and Sun, X., 2017. Parasite-derived proteins for the treatment of allergies and autoimmune diseases. *Frontiers in Microbiology*, *8*, p.2164.
307. Zhu, B., Trikudanathan, S., Zozulya, A.L., Sandoval-Garcia, C., Kennedy, J.K., Atochina, O., Norberg, T., Castagner, B., Seeberger, P., Fabry, Z. and Harn, D., 2012. Immune modulation by Lacto-N-fucopentaose III in experimental autoimmune encephalomyelitis. *Clinical immunology*, *142*(3), pp.351-361.
308. Elliott, D.E. and Weinstock, J.V., 2017. Nematodes and human therapeutic trials for inflammatory disease. *Parasite Immunology*, *39*(5), p.e12407.
309. Zhang, Y., Fu, J., Shi, Y., Peng, S., Cai, Y., Zhan, X., Song, N., Liu, Y., Wang, Z., Yu, Y. and Wang, Y., 2018. A new cancer immunotherapy via simultaneous DC-mobilization and DC-targeted IDO gene silencing using an immune-stimulatory nanosystem. *International Journal of Cancer*, *143*(8), pp.2039-2052.
310. Wang, F., Xiao, W., Elbahnasawy, M.A., Bao, X., Zheng, Q., Gong, L., Zhou, Y., Yang, S., Fang, A., Farag, M. and Wu, J., 2018. Optimization of the linker length of mannose-cholesterol conjugates for enhanced mRNA delivery to dendritic cells by liposomes. *Frontiers in pharmacology*, *9*, p.980.
311. Keselowsky, B.G. and Lewis, J.S., 2017, February. Dendritic cells in the host response to implanted materials. In *Seminars in immunology* (Vol. 29, pp. 33-40). Academic Press.
312. Fu, C., Zhao, H., Wang, Y., Cai, H., Xiao, Y., Zeng, Y. and Chen, H., 2016. Tumor-associated antigens: Tn antigen, sTn antigen, and T antigen. *Hla*, *88*(6), pp.275-286.
313. Petri Jr, W.A., Joyce, M.P., Broman, J., Smith, R.D., Murphy, C.F. and Ravdin, J.I., 1987. Recognition of the galactose-or N-acetylgalactosamine-binding lectin of Entamoeba histolytica by human immune sera. *Infection and immunity*, *55*(10), pp.2327-2331.
314. Frederick, J.R. and Petri Jr, W.A., 2005. Roles for the galactose-/N-acetylgalactosamine-binding lectin of Entamoeba in parasite virulence and differentiation. *Glycobiology*, *15*(12), pp.53R-59R.

315. Campos-Rodríguezp, R. and Jarillo-Luna, A., 2005. The pathogenicity of Entamoeba histolytica is related to the capacity of evading innate immunity. *Parasite immunology*, *27*(1-2), pp.1-8.
316. Morgado, P., Sudarshana, D.M., Gov, L., Harker, K.S., Lam, T., Casali, P., Boyle, J.P. and Lodoen, M.B., 2014. Type II Toxoplasma gondii induction of CD40 on infected macrophages enhances interleukin-12 responses. *Infection and immunity*, *82*(10), pp.4047-4055.
317. Ghaemmaghami, A.M., Gough, L., Sewell, H.F. and Shakib, F., 2002. The proteolytic activity of the major dust mite allergen Der p 1 conditions dendritic cells to produce less interleukin-12: allergen-induced Th2 bias determined at the dendritic cell level. *Clinical & Experimental Allergy*, *32*(10), pp.1468-1475.
318. Habib, S., El Andaloussi, A., Elmasry, K., Handoussa, A., Azab, M., Elsawey, A., Al-Hendy, A. and Ismail, N., 2018. PDL-1 blockade prevents T cell exhaustion, inhibits autophagy, and promotes clearance of Leishmania donovani. *Infection and immunity*, *86*(6), pp.e00019-18.
319. Kane, C.M., Cervi, L., Sun, J., McKee, A.S., Masek, K.S., Shapira, S., Hunter, C.A. and Pearce, E.J., 2004. Helminth antigens modulate TLR-initiated dendritic cell activation. *The Journal of Immunology*, *173*(12), pp.7454-7461.
320. Rodríguez, E., Noya, V., Cervi, L., Chiribao, M.L., Brossard, N., Chiale, C., Carmona, C., Giacomini, C. and Freire, T., 2015. Glycans from Fasciola hepatica modulate the host immune response and TLR-induced maturation of dendritic cells. *PLoS neglected tropical diseases*, *9*(12), p.e0004234.
321. Ma, X., Yan, W., Zheng, H., Du, Q., Zhang, L., Ban, Y., Li, N. and Wei, F., 2015. Regulation of IL-10 and IL-12 production and function in macrophages and dendritic cells. *F1000Research*, *4*.
322. Fontaine, T., Delangle, A., Simenel, C., Coddeville, B., van Vliet, S.J., van Kooyk, Y., Bozza, S., Moretti, S., Schwarz, F., Trichot, C. and Aebi, M., 2011. Galactosaminogalactan, a new immunosuppressive polysaccharide of Aspergillus fumigatus. *PLoS pathogens*, *7*(11), p.e1002372.
323. Bozza, S., Clavaud, C., Giovannini, G., Fontaine, T., Beauvais, A., Sarfati, J., D'Angelo, C., Perruccio, K., Bonifazi, P., Zagarella, S. and Moretti, S., 2009. Immune sensing of Aspergillus fumigatus proteins, glycolipids, and polysaccharides and the impact on Th immunity and vaccination. *The Journal of immunology*, *183*(4), pp.2407-2414.
324. Klaver, E.J., Kuijk, L.M., Laan, L.C., Kringel, H., van Vliet, S.J., Bouma, G., Cummings, R.D., Kraal, G. and van Die, I., 2013. Trichuris suis-induced modulation of human dendritic cell function is glycan-mediated. *International journal for parasitology*, *43*(3-4), pp.191-200.
325. Haak, S., Gyülveszi, G. and Becher, B., 2009. Th17 cells in autoimmune disease: changing the verdict.
326. Summers, R.W., Elliott, D.E., Urban, J.F., Thompson, R.O.B.I.N. and Weinstock, J., 2005. Trichuris suis therapy in Crohn's disease. *Gut*, *54*(1), pp.87-90.
327. Weinstock, J.V. and Elliott, D.E., 2009. Helminths and the IBD hygiene hypothesis. *Inflammatory bowel diseases*, *15*(1), pp.128-133.
328. Correale, J. and Farez, M.F., 2011. The impact of parasite infections on the course of multiple sclerosis. *Journal of neuroimmunology*, *233*(1-2), pp.6-11.

329. Fleming, J.O., Isaak, A., Lee, J.E., Luzzio, C.C., Carrithers, M.D., Cook, T.D., Field, A.S., Boland, J. and Fabry, Z., 2011. Probiotic helminth administration in relapsing–remitting multiple sclerosis: a phase 1 study. *Multiple Sclerosis Journal*, *17*(6), pp.743-754.
330. Bager, P., Arnved, J., Rønborg, S., Wohlfahrt, J., Poulsen, L.K., Westergaard, T., Petersen, H.W., Kristensen, B., Thamsborg, S., Roepstorff, A. and Kapel, C., 2010. Trichuris suis ova therapy for allergic rhinitis: a randomized, double-blind, placebo-controlled clinical trial. *Journal of allergy and clinical immunology*, *125*(1), pp.123-130.
331. Experimental hookworm infection: a randomized placebo-controlled trial in asthma. *Clinical & Experimental Allergy*,
332. Rankin, L.C. and Artis, D., 2018. Beyond host defense: emerging functions of the immune system in regulating complex tissue physiology. *Cell*, *173*(3), pp.554-567.
333. Gaudino, S.J. and Kumar, P., 2019. Cross-talk between antigen presenting cells and T cells impacts intestinal homeostasis, bacterial infections, and tumorigenesis. *Frontiers in immunology*, *10*, p.360.
334. Dakappagari, N., Maruyama, T., Renshaw, M., Tacken, P., Figdor, C., Torensma, R., Wild, M.A., Wu, D., Bowdish, K. and Kretz-Rommel, A., 2006. Internalizing antibodies to the C-type lectins, L-SIGN and DC-SIGN, inhibit viral glycoprotein binding and deliver antigen to human dendritic cells for the induction of T cell responses. *The Journal of Immunology*, *176*(1), pp.426-440.
335. Chiffoleau, E., 2018. C-type lectin-like receptors as emerging orchestrators of sterile inflammation represent potential therapeutic targets. *Frontiers in Immunology*, *9*, p.227.
336. Baum, L.G. and Cobb, B.A., 2017. The direct and indirect effects of glycans on immune function. *Glycobiology*, *27*(7), pp.619-624.
337. Häuselmann, I. and Borsig, L., 2014. Altered tumor-cell glycosylation promotes metastasis. *Frontiers in oncology*, *4*, p.28.
338. Kao, J.Y., Zhang, M., Miller, M.J., Mills, J.C., Wang, B., Liu, M., Eaton, K.A., Zou, W., Berndt, B.E., Cole, T.S. and Takeuchi, T., 2010. Helicobacter pylori immune escape is mediated by dendritic cell–induced Treg skewing and Th17 suppression in mice. *Gastroenterology*, *138*(3), pp.1046-1054.
339. Hwang, S.L., Chung, N.P.Y., Chan, J.K.Y. and Lin, C.L.S., 2005. Indoleamine 2, 3-dioxygenase (IDO) is essential for dendritic cell activation and chemotactic responsiveness to chemokines. *Cell research*, *15*(3), pp.167-175.
340. Ravidà, A., Aldridge, A.M., Driessen, N.N., Heus, F.A., Hokke, C.H. and O'Neill, S.M., 2016. Fasciola hepatica surface coat glycoproteins contain mannosylated and phosphorylated N-glycans and exhibit immune modulatory properties independent of the mannose receptor. *PLoS Neglected Tropical Diseases*, *10*(4), p.e0004601.
341. Torrelles, J.B., Azad, A.K. and Schlesinger, L.S., 2006. Fine discrimination in the recognition of individual species of phosphatidyl-myo-inositol mannosides from Mycobacterium tuberculosis by C-type lectin pattern recognition receptors. *The Journal of immunology*, *177*(3), pp.1805-1816.

342. Segura, M., Su, Z., Piccirillo, C. and Stevenson, M.M., 2007. Impairment of dendritic cell function by excretory-secretory products: a potential mechanism for nematode-induced immunosuppression. *European journal of immunology*, *37*(7), pp.1887-1904.
343. Grainger, J.R., Smith, K.A., Hewitson, J.P., McSorley, H.J., Harcus, Y., Filbey, K.J., Finney, C.A., Greenwood, E.J., Knox, D.P., Wilson, M.S. and Belkaid, Y., 2010. Helminth secretions induce de novo T cell Foxp3 expression and regulatory function through the TGF-β pathway. *Journal of Experimental Medicine*, *207*(11), pp.2331-2341.
344. Märten, A., Greten, T., Ziske, C., Renoth, S., Schöttker, B., Buttgereit, P., Schakowski, F., von Rücker, A., Sauerbruch, T. and Schmidt-Wolf, I.G., 2002. Generation of activated and antigen-specific T cells with cytotoxic activity after co-culture with dendritic cells. Cancer Immunology, Immunotherapy, 51(1), pp.25-32.
345. Sofronic-Milosavljevic, L., Ilic, N., Pinelli, E. and Gruden-Movsesijan, A., 2015. Secretory products of Trichinella spiralis muscle larvae and immunomodulation: implication for autoimmune diseases, allergies, and malignancies. *Journal of Immunology Research*, *2015*.